

**University of Alberta**

**Development of Intermittent Electrical Stimulation for the Prevention of  
Deep Tissue Injury**

by

**Leandro Rafael Solis Aguilar**

A thesis submitted to the Faculty of Graduate Studies and Research  
in partial fulfillment of the requirements for the degree of

**Doctor of Philosophy**

in

**Rehabilitation Science**

**Faculty of Rehabilitation Medicine**

©Leandro Rafael Solis Aguilar

Fall 2013

Edmonton, Alberta

Permission is hereby granted to the University of Alberta Libraries to reproduce single copies of this thesis and to lend or sell such copies for private, scholarly or scientific research purposes only. Where the thesis is converted to, or otherwise made available in digital form, the University of Alberta will advise potential users of the thesis of these terms.

The author reserves all other publication and other rights in association with the copyright in the thesis and, except as herein before provided, neither the thesis nor any substantial portion thereof may be printed or otherwise reproduced in any material form whatsoever without the author's prior written permission.

## **DEDICATION**

A Dios por llenarme siempre de bendiciones y ayudarme a salir adelante en los momentos más difíciles de este proyecto. A mi amada esposa Brenda por tener el amor, la paciencia, y la comprensión para soportar el tiempo que tuvimos que estar lejos debido a mis estudios, así como las lagrimas y sacrificios que tuvimos que superar una vez juntos, sin nunca dejar de apoyarme y darme ánimos a seguir adelante, recordándome que Dios nos acompañaba a cada paso, ayudándome a mantener la fé. Finalmente a mis padres por su apoyo incondicional durante toda mi vida, en especial durante este ultimo año en el cual sin su ayuda jamás hubiera podido completar este sueño.

## **ACKNOWLEDGEMENTS**

To my supervisor Dr. Mushahwar and co-supervisor Dr. Ferguson-Pell for their guidance and support throughout my graduate studies. To my thesis committee members for their invaluable input and feedback to improve my research projects. To Dr. Tammy Hopper for her help and support with the thesis revisions. To Peter Seres as well as my lab coworkers Enid Pehowich, Adrian Liggins, Yahya Kinyogo, Jason Tong, and Mark Diaz, as well as the staff of HSLAS and SMRI for their assistance in the multiple experiments conducted for this thesis.

## **ABSTRACT**

The main goal of this thesis was to develop a novel intervention named Intermittent Electrical Stimulation (IES) to prevent the formation of deep tissue injury (DTI) in immobilized individuals, in particular those with spinal cord injury. Deep tissue injury is a type of pressure ulcer that originates at the deep bone-muscle interface due to the prolonged entrapment of soft tissue between a bony prominence and an external surface. Intermittent electrical stimulation is applied to muscles at risk of developing DTI and works by eliciting periodic muscle contractions in cycles of 10 seconds “ON” followed by a period of 10 minutes “OFF”, replicating the subconscious repositioning performed by able bodied individuals in response to sitting discomfort. These periodic IES-elicited muscle contractions are able to counteract both the mechanical and vascular factors leading to DTI. Four studies were conducted to test the effects of IES within the muscle and its effectiveness to prevent DTI. In able-bodied volunteers the use of IES reduced and redistributed superficial pressure around the ischial tuberosities. In addition, it increased the level of muscle oxygenation immediately after the IES-induced muscle contraction, and kept it elevated throughout the entire duration of each IES “OFF” phase. In studies conducted in adult pigs both intact and with spinal cord injury, the results of this thesis showed that peak internal pressures due to external loading was localized within a 2cm area centered around the ischial tuberosities. Peak internal pressures were approximately 2 times higher than peak superficial pressures. The use of IES effectively reduced internal pressure levels around the ischial tuberosities and

redistributed internal pressure levels away from the ischial tuberosities during each IES-induced contraction. The effectiveness of IES was demonstrated in a study in adult pigs with injured spinal cords and atrophied muscles. An external load equivalent to 25% of body weight was applied to the paralyzed limb of each animal every day for 4hrs a day for 1 month. In the group of pigs that received the application of IES the extent of DTI was significantly less (8%) compared to the extent of DTI in the control group (48%).

# TABLE OF CONTENTS

<b>INTRODUCTION</b>	1
Incidence of pressure ulcers	1
Pressure ulcer classification	3
Detection of pressure ulcers	7
Mechanisms of Deep Tissue Injury	8
Ischemia/reperfusion	8
Ischemia	10
Reperfusion	12
Mechanical deformation	16
Interaction between vascular and mechanical pathways of injury	21
Prevention of pressure ulcers	22
Repositioning	23
Specialized cushions and bed mattresses	24
Non-powered cushions and bed mattresses	25
Powered cushions and bed mattresses	27
Summary of conventional preventative interventions	28
Electrical stimulation	28
Intermittent electrical stimulation (IES)	29
Specific objectives of thesis	30
References	31

<b>CHAPTER 1. Effects of intermittent electrical stimulation on superficial pressure, tissue oxygenation, and discomfort levels, for the prevention of deep tissue injury</b>	<b>41</b>
1.2 Introduction	41
1.3 Methods	44
1.3.1 Overview	44
1.3.2 Application of IES	45
1.3.3 IES protocols and testing conditions	45
1.3.4 Measurements of superficial pressure	47
1.3.5 Measurements of tissue oxygenation	48
1.3.6 Volunteers' perception of discomfort due to sitting	53
1.3.7 Statistical Analyses	54
1.4 Results	55
1.4.1 Pressure Reduction due to IES	55
1.4.1.1 Effectiveness of different IES protocols in reducing pressure at the ischial tuberosities	55
1.4.1.2 Effectiveness of IES in reducing pressure under increased loading conditions	59
1.4.2 Increase in Tissue Oxygenation due to IES	61
1.4.2.1 Effectiveness of IES protocols in increasing oxygenation in the gluteus maximus muscles	62

1.4.2.2	Effectiveness of IES in increasing tissue oxygenation under increased loading conditions	63
1.4.2.3	Perception of Discomfort due to Sitting Pressure and IES	68
1.5	Discussion	71
1.5.1	Overview	71
1.5.2	IES decreases pressure around bony prominences	72
1.5.3	IES increases tissue oxygenation in compressed Muscles	76
1.5.4	IES reduces perceived discomfort due to sitting	78
1.5.5	Conclusion	80
1.6	References	81

## **CHAPTER 2. Distribution of Internal Pressure around Bony**

### **Prominences: Implications to Deep Tissue Injury and**

### **Effectiveness of Intermittent Electrical Stimulation** 85

2.2	Introduction	85
2.3	Methods	87
2.3.1	Overview	87
2.3.2	Spinal Cord Hemi-transection and Palliative Care	88
2.3.3	Animal Preparation and Magnetic Resonance Imaging	89

2.3.4	External Loading and Internal Pressure Mapping	91
2.3.5	Internal Pressure Mapping during Intermittent Electrical Stimulation	94
2.3.6	Data Acquisition	95
2.3.7	Data Analysis and Statistics	96
2.4	Results	98
2.4.1	Appropriateness of the Yucatan Minipig as an Animal Model	98
2.4.2	Distribution of Interfacial Pressure	100
2.4.3	Distribution of Internal Pressure in Spinally Intact Pigs	102
2.4.4	Distribution of Internal Pressure following Chronic Spinal Cord Injury	107
2.4.5	Effects of IES on the Distribution of Internal Pressure	114
2.5	Discussion	121
2.5.1	Overview	121
2.5.2	Internal Pressure is Highly Concentrated around the Bone	121
2.5.3	Intermittent Electrical Stimulation Effectively Redistributes Internal Pressure	125
2.5.4	Study Limitations	127
2.5.5	Conclusion	128

2.6	References	129
-----	------------	-----

## **CHAPTER 3. Distribution of Internal Strains around Bony**

<b>Prominences in Pigs</b>	133
3.2 INTRODUCTION	133
3.3 METHODS	136
3.3.1 Overview	136
3.3.2 Test subjects	136
3.3.3 Development of DTI in one pig with spinal cord injury	137
3.3.4 Experimental setup	138
3.3.5 Application of external loading	139
3.3.6 MRI tagging sequence	140
3.3.7 Measurement of strain magnitudes	146
3.3.8 Application of intermittent electrical stimulation	147
3.3.9 Statistical Analysis	148
3.4 RESULTS	149
3.4.1 Tissue loading	149
3.4.2 Distribution of strain magnitudes in pigs with intact spinal cords	150
3.4.3 Degree of atrophy due to SCI	157
3.4.4 Distribution of strain magnitudes in	

	pigs with SCI	157
	3.4.5 Effects of IES	162
3.5	DISCUSSION	164
	3.5.1 Overview	164
	3.5.2 Strain measurements	165
	3.5.3 Effects of IES	169
	3.5.4 Study Limitations	171
	3.5.5 Conclusions	173
3.6	REFERENCES	174

**CHAPTER 4. Prevention of Deep Tissue Injury by inducing muscle contractions using Intermittent Electrical Stimulation after Spinal Cord Injury in Pigs**

		179
	4.2 INTRODUCTION	179
	4.3 METHODS	182
	4.3.1 Spinalization surgery	182
	4.3.2 Post-surgical recovery and palliative care	183
	4.3.3 Daily loading procedure	184
	4.3.4 Application of IES	187
	4.3.5 Assessment of DTI through MRI	188
	4.3.6 Analysis of MR images	190
	4.3.7 Histological assessment of tissue	193
	4.3.8 Statistical analyses	194

4.4 RESULTS	196
4.4.1 Assessment of muscle injury	197
4.4.2 Changes to intracellular and extracellular muscle components by DTI	199
4.4.3 Assessment of cellular necrosis	202
4.4.4 Summary of results	205
4.5 DISCUSSION	206
4.5.1 Skin is a poor indicator of DTI	206
4.5.2 MRI techniques are sensitive measures of edema formation and associated DTI	207
4.5.3 IES may be effective in preventing the formation of DTI	208
4.5.4 Comparison of IES to other interventions for preventing pressure ulcers	211
4.6 CONCLUSION	212
4.6.1 ACKNOWLEDGEMENTS	213
4.7 REFERENCES	214
<b>CHAPTER 5. CONCLUSIONS AND FUTURE DIRECTIONS</b>	<b>218</b>

# LIST OF TABLES AND FIGURES

## CHAPTER 1

Figure 1	52
Figure 2	57
Figure 3	59
Figure 4	60
Figure 5	63
Figure 6	65
Figure 7	67
Figure 8	69

## CHAPTER 2

Figure 1	93
Figure 2	100
Figure 3	101
Figure 4	104
Figure 5	106
Figure 6	109
Figure 7	111
Figure 8	113
Figure 9	115
Figure 10	117
Figure 11	120

## **CHAPTER 3**

Figure 1	140
Figure 2	142
Figure 3	143
Figure 4	145
Figure 5	147
Figure 6	151
Figure 7	153
Figure 8	154
Table 1	158
Figure 9	159
Figure 10	161
Figure 11	163

## **CHAPTER 4**

Figure 1	186
Figure 2	188
Figure 3	192
Figure 4	198
Figure 5	199
Figure 6	201
Figure 7	203
Figure 8	204

# **LIST OF SYMBOLS, NOMENCLATURE AND ABBREVIATIONS**

*ANOVA*: Analysis of variance

*BW*: Percentage of body weight

*DTI*: Deep tissue injury

*EPUAP*: European pressure ulcer advisory panel

*IES*: Intermittent electrical simulation

*MRI*: Magnetic resonance imaging

*NIRS*: Near infrared spectroscopy

*NPUPAP*: National pressure ulcer advisory panel

*SCI*: Spinal cord injury

# INTRODUCTION

## *Overview*

Pressure ulcers, commonly known as bed sores or pressure sores, are a major complication associated with people with reduced mobility and/or loss of sensation, and constitute a severe health care concern. Pressure ulcers develop as a result of skin breakdown due to continuous surface abrasion, moisture and poor hygiene, or as a consequence of deep muscle necrosis due to localized and sustained external pressure. The estimated annual cost of only treating those pressure ulcers that develop during a hospital stay is \$11 billion in the United States [1-2].

## **Incidence of Pressure Ulcers**

Populations at risk of developing pressure ulcers are primarily those who are confined to a bed or are dependent on a wheelchair for daily mobility. They include the elderly; residents of long-term care facilities and nursing homes; patients in acute and critical care units; patients who undergo lengthy surgeries; people with bone and joint disease, vasculopathies associated with diabetes, or cardiovascular failure; and those with neurological insults such as spinal cord injury, stroke or multiple sclerosis [3-8]. Although the risk of pressure ulcers increases with age reaching an incidence rate of 85% in the elderly [9], pressure ulcers can also develop in immobilized infants and children. The incidence rates of pressure ulcers in pediatric intensive care units are reported to be as high as 27% [10].

Pressure ulcers can develop within a few hours of immobilization [11]; their incidence rate due to long surgeries and in acute and critical care settings are as high as 40% [7-8]. Individuals with spinal cord injury are among those most at risk of developing pressure ulcers due to their impaired sensation and atrophied muscles. Impaired sensation compromises judgment regarding the state of muscles and skin [12], and atrophied muscles reduce the tissue's natural cushioning abilities [13]. Twenty nine (29%) to 80% of individuals with spinal cord injury develop pressure ulcers [6], with incidence rates varying depending on the level and completeness of injury [14-16].

Treating deep pressure ulcers is a difficult process; severe ulcers require an average hospital stay of 2 months and cost \$15,800 to \$72,680 per ulcer to heal [17-18]. After their discharge, patients are at higher risk of developing a recurring ulcer primarily due to scar formation and compromised tissue integrity [7]. Deep scars act as promoters for pressure ulcer development because of their mismatched mechanical properties with the surrounding muscle; this results in heightened pressures between the tissue layers and increased tendencies for inducing ischemia in the adjoining soft tissue. Niazi et al. [19] reported a pressure ulcer recurrence rate of 91% in wheelchair-dependent individuals with spinal cord injury.

In addition to the financial consequences, pressure ulcers lead to further debilitation in individuals whose physical abilities are already compromised,

further reducing general independence and productivity, and lowering self-esteem and self-worth [20]. Overall, the physical and psychological toll of pressure ulcers results in a considerable decrease in the quality of life.

### **Pressure ulcer classifications**

Pressure ulcers can develop in two forms: either developing at the level of the skin and progressing to affect the underlying fat, muscle and bone tissue, or in deep muscle tissue and progress towards the skin after destroying the surrounding tissue. Candidate factors for ulcers originating at the skin are friction between skin and an external surface, tissue hygiene, moisture, temperature, circulatory integrity, and nutrition [21]. This class of ulcers has long been recognized clinically and a staging system has been developed to assess the state of progression of these ulcers. The most frequently used staging system in North America is set forth by the National Pressure Ulcer Advisory Panel (NPUAP) in the United States. Detected ulcers are classified into different stages, ranging from discoloration of intact skin to full-thickness skin loss and tissue damage that extends to the underlying bone, muscle and fat [22]. The classified stages are as follow:

#### **Category/Stage I: Non-blanchable erythema**

Intact skin with non-blanchable redness of a localized area usually over a bony prominence. Darkly pigmented skin may not have visible blanching; its color may differ from the surrounding area. The area may be painful, firm, soft,

warmer or cooler as compared to adjacent tissue. Category I may be difficult to detect in individuals with dark skin tones. May indicate “at risk” persons.

### **Category/Stage II: Partial thickness**

Partial thickness loss of dermis presenting as a shallow open ulcer with a red pink wound bed, without slough. May also present as an intact or open/ruptured serum-filled or sero-sanguinous filled blister. Presents as a shiny or dry shallow ulcer without slough or bruising\*. This category should not be used to describe skin tears, tape burns, incontinence associated dermatitis, maceration or excoriation.

\*Bruising indicates deep tissue injury.

### **Category/Stage III: Full thickness skin loss**

Full thickness tissue loss. Subcutaneous fat may be visible but bone, tendon or muscle are *not* exposed. Slough may be present but does not obscure the depth of tissue loss. *May* include undermining and tunneling. The depth of a Category/Stage III pressure ulcer varies by anatomical location. The bridge of the nose, ear, occiput and malleolus do not have (adipose) subcutaneous tissue and Category/Stage III ulcers can be shallow. In contrast, areas of significant adiposity can develop extremely deep Category/Stage III pressure ulcers. Bone/tendon is not visible or directly palpable.

#### **Category/Stage IV: Full thickness tissue loss**

Full thickness tissue loss with exposed bone, tendon or muscle. Slough or eschar may be present. Often includes undermining and tunneling. The depth of a Category/Stage IV pressure ulcer varies by anatomical location. The bridge of the nose, ear, occiput and malleolus do not have (adipose) subcutaneous tissue and these ulcers can be shallow. Category/Stage IV ulcers can extend into muscle and/or supporting structures (e.g., fascia, tendon or joint capsule) making osteomyelitis or osteitis likely to occur. Exposed bone/muscle is visible or directly palpable.

#### **Unstageable/Unclassified: Full thickness skin or tissue loss – depth unknown**

Full thickness tissue loss in which actual depth of the ulcer is completely obscured by slough (yellow, tan, gray, green or brown) and/or eschar (tan, brown or black) in the wound bed. Until enough slough and/or eschar are removed to expose the base of the wound, the true depth cannot be determined; but it will be either a Category/Stage III or IV. Stable (dry, adherent, intact without erythema or fluctuance) eschar on the heels serves as “the body’s natural (biological) cover” and should not be removed.

#### **Suspected Deep Tissue Injury – depth unknown**

Purple or maroon localized area of discolored intact skin or blood-filled blister due to damage of underlying soft tissue from pressure and/or shear. The

area may be preceded by tissue that is painful, firm, mushy, boggy, warmer or cooler as compared to adjacent tissue. Deep tissue injury may be difficult to detect in individuals with dark skin tones. Evolution may include a thin blister over a dark wound bed. The wound may further evolve and become covered by thin eschar. Evolution may be rapid exposing additional layers of tissue even with optimal treatment.

A similar system set forth by the European Pressure Ulcer Advisory Panel (EPUAP) is utilized in Europe. These systems help to assess and classify those who have developed a pressure ulcer in order to prescribe the best treatment for them.

The leading factor for the formation of ulcers of deep origin is the entrapment and compression of tissue between a bony prominence and an external hard surface for extended periods of time [7, 13, 21, 23-25]. This class of ulcers has only been recently acknowledged clinically, and it was not until 2001 that the NPUAP defined this type of pressure ulcer as “deep tissue injury” (DTI). Ulcers of deep origin are the more perilous ulcers as they are difficult to detect and cause severe damage in bone, ligament, muscle, and fat tissue prior to exhibiting obvious skin signs. The most susceptible location for DTI formation in wheelchair-dependent individuals is the tissue over the ischial tuberosities where muscle-bone interface forces are greatest [26-28]. Ischial ulcers represent 24% of the total incidence of pressure ulcers in all groups at risk [29].

## **Detection of pressure ulcers**

Current clinically available techniques to detect and assess pressure ulcers focus mainly on the condition of the skin and are insensitive to the breakdown of the underlying muscle tissue [30]. Skin inspections of the body regions commonly susceptible to pressure ulcer development are performed routinely to identify signs of skin discoloration or breakdown in a timely manner. Although this detection method has some limitations to properly detect ulcers of superficial origin, particularly in individuals with darkly pigmented skin [31], it is completely insensitive to the early development of DTI.

Due to the absence of clinical detection methods of DTI, it is difficult to differentiate between the incidence rates of ulcers due to DTI and those due to superficial skin injury in the literature. Different methods have been attempted in research studies with the goal of developing early detection techniques for DTI. These methods include measuring different biochemical markers present in sweat [32-33] or blood [34], either directly, or through the use of indirect methods like near infra-red spectroscopy [35]. Imaging techniques like magnetic resonance imaging (MRI) [36-38] and ultrasound [39] have also been utilized. In spite of varying degrees of success at detecting early signs of DTI in controlled studies, none of these methods are currently feasible as clinical detection tools for DTI.

## **Mechanisms of Deep Tissue Injury**

An understanding of the underlying factors resulting in the development of the different classes of pressure ulcers is essential for devising effective methods for risk assessment and prevention of these ulcers [25]. Numerous studies have been conducted over the past 50 years with the goal of understanding the mechanism by which sustained pressure leads to the formation of a pressure ulcer. One of the most studied pathways is that of ischemia and subsequent reperfusion, which arises when the pressure levels applied to soft tissue interrupt blood flow through the capillaries for prolonged durations. Another pathway, studied to a lesser extent, is that of the direct effect of mechanical deformation on soft tissue. This section discusses the manner in which ischemia/reperfusion and mechanical deformation contribute to the onset of DTI.

### *Ischemia/Reperfusion*

In order to maintain sufficient energy stores, and thus cell health, tissue requires a steady supply of oxygen and nutrients as well as constant removal of metabolic wastes. Capillaries subjected to pressures greater than their perfusion pressures become occluded, halting this necessary exchange [21]. Extended loading of the tissue, causing prolonged ischemia of the surrounding region, renders cells unable to function properly [40-42]. Restoring blood flow to this injured tissue, while necessary, can paradoxically further the tissue damage [43-46]. In fact, cellular damage following ischemia-reperfusion injury is more severe than the damage incurred after ischemia alone, and is a primary factor in pressure

ulcer development [43].

The duration of cell survival under limited blood flow varies with cell type. Due to its high energy demands, muscle tissue is extensively vascularized, and in turn, is especially sensitive to interruptions in blood flow [28, 47-48]. This sensitivity renders muscle more susceptible to ischemic injury than skin, which has a lower metabolic rate, and accordingly, is less vascularized.

Normally, cells maintain homeostasis by creating, storing and utilizing energy in the form of adenosine triphosphate (ATP). Under aerobic conditions, glycolysis and oxidative phosphorylation work consecutively to generate ATP by completely oxidizing glucose. Glycolysis creates 2 moles of ATP by breaking glucose down to pyruvate. In the presence of oxygen, pyruvate undergoes a sequence of enzyme-assisted conversions, known as the citric acid cycle. These reactions generate NADH or NADPH which are electron carriers in their reduced forms that are shunted to a respiratory complex in the mitochondria. Here, the electrons move through a series of enzyme complexes, transferring large amounts of energy that is harnessed by the cell to create 34 moles of ATP per cycle. Aerobic conditions are necessary for the post-glycolysis process of oxidative phosphorylation, as molecular oxygen is the final electron acceptor within the respiratory complex. The final products are CO<sub>2</sub> and water.

## *Ischemia*

In the absence of oxygen, cells are forced to give up the high yielding oxidative phosphorylation cycle, for the much less effective anaerobic process. ATP can be generated anaerobically for a short period of time, by using creatine phosphate as an ATP substrate or through glycolysis. Creatine phosphate combines with adenosine diphosphate (ADP) to form ATP. In the first three hours of ischemia, this pathway produces enough ATP to compensate the effects of losing oxidative phosphorylation. Beyond this window, creatine phosphate stores are exhausted and only glycolysis is available for ATP formation. Depletion of energy levels is accelerated as the rate of energy production by these pathways cannot meet the rate of consumption [49-50]. After 4 hours of ischemia, there is a 96% drop in ATP levels in muscle cells [51].

In the absence of ATP, the  $\text{Na}^+\text{K}^+$ -ATPase ion pumps cannot maintain the necessary ion gradients across the cell membrane.  $\text{K}^+$  diffuses out of the cell while  $\text{Na}^+$ ,  $\text{Ca}^{2+}$  and water accumulate inside the cell [52] leading to swelling and eventual rupture of the cell membrane. It is also proposed that ischemic conditions force the mitochondrial permeability transition pore (MPTP) open. This pore extends through the outer and inner mitochondrial matrix, connecting the inner mitochondrial matrix to the cytosol. As a potent signaling molecule,  $\text{Ca}^{2+}$  is carefully compartmentalized within the mitochondria. Inappropriate opening of the MPTP allows  $\text{Ca}^{2+}$  to move from the mitochondria into the cell [53-55]. Unexpected surges in  $\text{Ca}^{2+}$  damage the mitochondrial electron transport

chain - increasing free radical production, as well as activate  $\text{Ca}^{2+}$ -dependent proteases and nucleases, triggering apoptosis directly [55-60].

Additionally, without blood flow, glycolysis products rise to cytotoxic levels. Under anaerobic conditions, the pyruvate created from glycolysis is converted into lactate in the cytoplasm, instead of being transported into the mitochondria for further oxidation. The conversion of pyruvate to lactate generates hydrogen ions as lactate reconfigures in the cytosol to lactic acid, and therefore prolonged ischemia can result in cellular acidosis. Lactic acid levels increase 10-fold over 4 hours of ischemia [61-63], compromising cellular function by inducing clumping of nuclear chromatin, and inactivation of DNA and enzymes [43, 62]. The Cori cycle, the metabolic pathway by which lactate is converted back into glucose by the liver is also interrupted with the lack of blood flow, contributing to the accumulation of lactate within the ischemic region.

Skeletal muscle death is highly correlated to ATP depletion, which is associated to the duration of ischemia. In fact, the relationship between the duration of ischemia and extent of tissue necrosis approaches an exponential curve. Labbe et al. [64] found that after 3, 4, and 5 hours of ischemia the proportion of skeletal muscle affected by necrosis increased from 2 to 30 to 90%, respectively. The earlier-described depletion of substrates as alternate methods of ATP production explain how the damage progresses from mild at 3 hours (2% necrosis) to extensive within 5 hours (90% necrosis).

The extent of damage is also dependent on the tissue's ability to restore ATP levels following ischemia. Skeletal muscle can quickly reestablish pre-ischemic levels of ATP following ischemic periods of less than an hour, allowing the cell to resume normal function. However, tissues subjected to ischemia for longer than 4 hours take much longer to regenerate their energy supply as ATP formation itself costs energy, and cellular ATP levels is scarce after 4 hours of ischemia [63].

### *Reperfusion*

While the restoration of blood flow is critical for cell and tissue survival, reperfusion following prolonged periods of ischemia can further cellular injury [43, 65]. In fact, reperfusion based events, including activation of inflammation cascades, infiltration of leukocytes, generation of reactive oxygen species, and  $\text{Ca}^{2+}$  overload, make ischemia-reperfusion injury more detrimental than ischemia alone [5, 43-44, 61, 63, 66] .

The hypoxic environment resulting from interrupted blood flow stimulates blood vessel dilation. Upon reperfusion, the induced vasodilation allows for increased blood flow and oxygen to the ischemic area, a phenomenon known as reactive hyperemia. The peak and duration of the reactive hyperemia is inversely proportional to the duration of ischemia [67]. Oxygen in the returning blood is a primary cause of reperfusion injury [68] as it combines with free radical substrates that have accumulated during ischemia. Accordingly, longer periods of

ischemia generate higher levels of reactive free radicals, resulting in greater damage during reperfusion. Significant reduction in cell damage and skeletal muscle necrosis is observed by using deoxygenated blood or reintroducing oxygen gradually into the reperfusate post-ischemia [68]. Additionally, using free radical scavengers with deoxygenated blood resulted in further reductions in post-ischemic necrosis [69], directly linking free radicals as primary causes of damage.

The formation of these free radicals is initiated by the original ischemic conditions. Without oxygen, the cell's ability to convert ADP to ATP is significantly reduced. The increasing levels of ADP are broken down into hypoxanthine. However, under ischemic conditions the enzyme that normally breaks down hypoxanthine, xanthine dehydrogenase (XDH), is converted to xanthine oxidase (XO), causing hypoxanthine to build up during ischemia [44, 70]. Although not entirely understood, this conversion has been found to be modulated in varying degrees by the levels of NADPH oxidase, nitric oxide (NO), hydrogen peroxide ( $H_2O_2$ ), and calcium ( $Ca^{2+}$ ). [71-72]

Post-ischemia, the reintroduced oxygen reacts with hypoxanthine and xanthine. Both reactions are catalyzed by XO and form reactive oxygen species, notably superoxide, hydrogen peroxide and the hydroxyl radical. In prolonged ischemia, the reactive oxygen species overwhelm the cell's free radical scavengers [73-74], leading to oxidative damage. The reactive oxygen species attack lipids, enzymes, proteins and DNA. Injury to the lipid-based membranes

within and surrounding the cell results in leakage of autolytic enzymes, apoptotic factors, reactive compounds and ions (like  $\text{Ca}^{2+}$ ) into the extra-cellular environment [75-77]. Oxidative stress to structural proteins, enzymes and DNA renders the cell unable to undergo tasks essential to cell survival. Collectively, the structural and functional damage resulting from reperfusion reactive oxygen species directs the cell towards death [5, 43-44, 63, 66].

Another significant factor resulting in cell and tissue death in reperfusion injury is damage to the vasculature itself. The endothelium is a single layer of cells lining all blood vessels in the body. It is in direct contact with the blood cells and the vasculature, and intensively regulates both environments, maintaining both vascular and total internal homeostasis [78-79]. Damage to the endothelium results in microvasculature dysfunction, heightening the effects of ischemic-reperfusion injury [80]. Distressing stimuli, such as ischemia-based release of cytotoxic compounds, shifts the endothelium from a 'resting' condition to a proinflammatory state[68]. Leukocytes and platelets migrate to the distressed site and adhere to the endothelium [81-83]. The cytotoxic compounds released by dying cells activate leukocytes, which release their own toxic substances. The autolytic enzymes and reactive oxygen species released in this cycle damage healthy cells in the microvasculature and surrounding environment [84-86]. Structural damage to the endothelial cell layer allows large proteins and molecules to leak out, resulting in interstitial edema [87-89]. The increased permeability of the microvasculature further propagates the inflammatory

cascade, resulting in an extremely detrimental cycle.

One established phenomenon of the inflammatory response to ischemia-reperfusion injury is the ‘no-reflow’ effect [90], in which even after reperfusion has been established, areas of tissue remain ischemic. Similar to other mechanisms of injury within the reperfusion phase, the duration and severity of ischemia determine the extent of no-reflow induced damage [91]. A number of factors are interposed to create this phenomenon. During reperfusion, endothelial cell swelling reduces the diameter of the capillary lumen. Due to the expression of adhesion molecules, activated leukocytes travel slowly through these capillaries, and accumulate easily in the capillary, hindering reperfusion [92-93]. Furthermore, the slow speed of the migrating leukocytes allows for more interaction with platelets, increasing the incidence of microvascular thrombosis [94]. Coagulation and thrombosis within the microvasculature can restrict delivery of nutrients and removal of waste products despite reperfusion [95]. The improvement in tissue viability observed by administering blood thinners such as heparin following ischemia [96-97] provide evidence for the role of coagulation and thrombosis in post-ischemic damage.

Endothelial cells express two ligands particularly involved in ischemia-reperfusion injury: intercellular cell adhesion molecules (ICAMs) and selectins [98]. Both ligands propagate inflammatory events [99]. For example, selectin facilitates adhesion allowing for leukocyte rolling [98] and neutrophil aggregation

within the microvasculature. Selectin-mediated adhesion, and ICAM-1 expression correspond with changes in intracellular  $\text{Ca}^{2+}$  levels [100], illustrating that  $\text{Ca}^{2+}$  plays a critical role in both stages of ischemic and reperfusion injury. The literature shows that ischemia-reperfusion injury is significantly reduced when selectin activation and ICAM expression is blocked [101-103].

Another signaling molecule important in ischemia-reperfusion is nitric oxide (NO). NO is a short lived free radical, formed within the endothelium, and produced by the nitric oxide synthase enzyme. In early ischemia-reperfusion injury, it contributes reactive nitrogen species, which damage the endothelium directly and indirectly [104]. For example, peroxynitrate, an NO based free radical, can promote thrombosis in the vasculature. Peroxynitrate also reacts with oxygen free radicals to inhibit NO production [105]. NO has a variety of functions that protect against microvascular dysfunctions such as leukocyte adhesion and platelet aggregation. NO also promotes vasodilation [106], inhibits lipid peroxidation [107], the expression of pro-inflammatory genes [108] and apoptosis [109]. NO has also been found to have an antioxidant effect, inhibiting the conversion of XDH to XO. Therefore, the inhibition of NO by reactive nitrogen species impede the cell's capacity to combat injury.

### *Mechanical deformation*

Mechanical loading of tissue can result in friction, shear stresses and strain, as well as compressive and tensile stress and strain being generated within the

loaded tissue. Friction is the force that resists movement between two surfaces, and is generated when the individual is moved across a surface without completely lifting the affected area of the body. Repeated exposure to friction can cause tearing of the skin and lead to damage of the superficial layers of the tissue [110-111]. Shear stress is generated by the parallel force vector from the external loading applied to the tissue, which in turns creates shear strain as tissue moves in a parallel but opposite direction to the supporting surface. Shear stresses have been associated with the onset of superficial pressure ulcers [110-113] and are also believed to contribute to the onset of DTI [114-115]. Both compression and tension are the stress and strain components resulting from the normal (perpendicular) force vector resulting due to the external loading. When only the compression component is evaluated, typically at the skin-surface interface, this is often simply referred to as pressure. This has been the most studied mechanical factor in understanding the etiology of pressure ulcers.

Several studies agree that there exists an inverse relationship between the level of pressure required to develop DTI and the duration of pressure application [41, 111, 116-117]; however, there is no consensus regarding a threshold level of pressure or duration beyond which an injury is certain to happen, nor can the extent of injury be accurately predicted. Historically, pressures exceeding that of capillary pressure (32mmHg) have been considered as being conducive to damage in clinical medicine, however, this measurement is not a reliable predictor under all conditions. Traditionally, pressure has been measured at the skin-surface

interface to predict the risk of developing a pressure ulcer; however, there is growing evidence that to predict the onset of DTI, surface pressure measurements are inadequate on their own [115, 118-121]. From a purely mechanical perspective, one reason behind the difficulty in establishing threshold levels is the heterogeneous composition of soft tissue compressed between a bony prominence and an external surface. While soft tissue in general can be considered a viscoelastic material capable of withstanding some degree of deformation without suffering irreversible damage, the degree of soft tissue deformation in response to mechanical loading depends on the mechanical properties of the particular tissue layer. At the macroscopic level, the soft tissues involved in pressure ulcers are typically composed of skin, fat, and muscle cells organized in layers from bone to skin level. At the microscopic level, each type of cell possesses its own mechanical properties. In addition to the inherent mechanical properties of the different cells, the stress-strain relationship of tissue can be affected by the cells' arrangement, location and orientation with respect to bone, as well as their physical integrity. This combination of factors determines the stresses and strains experienced by different areas in the tissue and determine whether the induced deformation will lead to the onset of DTI [28]. The manner in which excessive deformation can lead to DTI in the muscle can be better understood by studying its effect at the cellular level. In vitro studies in single muscle cells [122-124] were performed to investigate the cells' stress-strain relationship and viability under different levels of compression. It was observed that single cells subjected to compressive stress experience some deformation and as the stress level

increases, blebs begin to form around the membrane, which eventually ruptures. As more cells die from excessive deformation the integrity of the muscle as a whole becomes affected. A recent study by Slmoka et al [125] demonstrated that at the cellular level, tensile strains exceeding 3% can cause significant permeability changes in the cell membrane, which might play a role in the likelihood of developing DTI.

It is believed that during loading, the stress and strain levels around the bony prominences are higher than those experienced at the skin level [47, 115, 118, 120, 126], however, in-vivo measurements of deep pressure are lacking. To obtain a better understanding of the forces experienced in the deep tissue, finite element models of the buttocks have been developed with the goal of predicting the amount of stress and strain generated across the different layers of tissue, in particular around the bony prominences, in seated individuals. These models incorporate the mechanical properties of different types of tissue to estimate the propagation of stress and strain based on external pressure measurements. The degree of complexity of published models varies tremendously. Initially models were 2 dimensional and utilized generic dimensions [115]. More recent models are 3 dimensional and use personalized dimensions obtained mostly from MRI scans [121, 127-131]. Although there is variability in the magnitude of the stresses and strains obtained from the different models, one common denominator among all is that the tissue around the bony prominences always experiences higher levels of stress and strain than more superficial tissue. Incorporating real

life bone and tissue dimensions has shown that individuals with sharper ischial tuberosities experience higher strain levels around the bone, compared to individuals with more blunt tuberosities [132]. In addition to bone shape, muscle mass and body composition has also been found to be a factor affecting the levels of internal strain and stress [131]. Individuals with paraplegia have been found to experience higher stress and strain levels than intact individuals due to the atrophied state of their muscles [133], highlighting the higher risk of developing DTI among the spinal cord injury population.

One confounding factor in predicting the onset of DTI due to mechanical deformation is that exposure to prolonged periods of high stress induces changes in the muscle's mechanical properties, whereby the muscle becomes stiffer during the development of injury. The increase in stiffness of injured muscles can increase the stress levels of adjacent and previously uninjured muscle [47, 126], thus propagating an expansion of muscle volume subjected to high levels of mechanical stress. In addition to this, atrophied muscles, typical of individuals with spinal cord injury, exhibit a decrease in muscle stiffness, which increases the levels of strain experienced by muscles during loading periods [134]. These changes in muscle stiffness due to atrophy or ongoing DTI create a perpetual risk of DTI development, which if not addressed properly will develop into an open ulcer.

With today's technology it is not possible to measure directly the amount of stress generated in the deep tissue in a non-invasive manner, therefore, a limitation of computer models is that the stress levels predicted for the deep layers of tissue have not been validated with in-vivo measurements. One study where external pressure was compared against internal pressure was performed by Dodd and Gross in Yorkshire pigs [135]. In it, an external load was applied to the spinous process and to the wings of the ilium to obtain a correlation between external pressure and interstitial pressure. Interstitial pressure was measured through a needle-wick catheter inserted into the subcutaneous tissue directly under the indenter utilized to compress the tissue. Their results showed that the interstitial pressure at the ilium and spinous process was only about 28% and 42 – 43% respectively, of the total pressure measured at the skin-indenter interface. This result contradicts the notion that the deeper tissue experiences higher levels of stress; however, the interstitial pressure measurements in this study were obtained from subcutaneous tissue directly under the skin, in a body location where there is no muscle between the bone and the skin, therefore a direct comparison to a location like the ischial tuberosities of humans can not be made.

#### *Interaction between Vascular and Mechanical Pathways of Injury*

The independent contribution of ischemia/reperfusion and mechanical deformation to DTI is currently unknown. A study conducted by Stekelenburg et al [136] compared the effects of mechanical deformation against those of ischemia on the onset of DTI in leg muscles of Brown-Norway rats. The authors

found that when the muscle is externally loaded with an indenter for 2 hours (~150 kPa), irreversible injury to the tissue could be detected through magnetic resonance imaging, as well as by histological assessments of the tissue. In comparison, a 2-hour period of ischemia induced by the application of a tourniquet (~140 kPa) only generated reversible changes in the tissue. In a parallel set of experiments [136], the authors quantified the strain throughout the muscle using magnetic resonance imaging when the muscle was compressed in short bursts. The results showed a good correlation between the areas where the highest strains were measured and the areas with damaged tissue due to a 2-hour compression period. Another study by Loerakker et al [137] showed that the degree of muscle deformation determines whether or not injury occurs, while the duration of the deformation determines the extent of injury.

While there is evidence to indicate that mechanical deformation alone can injure tissue, in in-vivo situations it is difficult to dissociate the effects of ischemia/reperfusion on the development of DTI. It is likely that the initial onset of DTI is caused by the mechanical deformation of the tissue, and as time progresses the amount of damage is compounded with injury caused by the ischemia/reperfusion cascade.

### **Prevention of Pressure Ulcers**

Preventing the initial onset of pressure ulcers is critical to avoid the exceptionally arduous and expensive interventions for treating them. To date, no

intervention strategy has succeeded in reducing the incidence of pressure ulcers consistently and reproducibly [6, 138]. In people with spinal cord injury, incidence rates of pressure ulcers have not changed significantly from those reported since the late 1940's during which they ranged from 57 to 85% [139]. While these comparisons should be interpreted with caution given the differences in detection and assessment techniques as well as changes in terminology and definitions over the years, they do suggest that the interventions may not be fully in step with the mechanisms leading to the formation of pressure ulcers, especially those originating from DTI.

Given the vascular and mechanical pathways leading to DTI, the ultimate prevention of this class of pressure ulcers lies in invoking frequent postural adjustments to relieve internal pressure, emulating the constant subconscious adjustments performed by able-bodied individuals in reaction to discomfort when seated or lying down.

### *Repositioning*

The staff at hospitals and nursing homes plays a pivotal role in repositioning patients or residents unable to move independently for preventing the development of pressure ulcers. While there is no conclusive evidence for an ideal repositioning frequency [140-143], it is traditionally recommended that patients are repositioned every two hours [144]. This time, however, can vary for each individual, with some people requiring more frequent repositioning [140-141,

144]. In practice, institutions establish their own pressure ulcer prevention program [145-146], and repositioning frequency is determined by the patient's condition, staff's availability, and costs associated with the time needed for repositioning procedures [140, 144, 147].

For wheelchair users, rehabilitation therapists train people to adjust their posture. People with paraplegia are trained to perform wheelchair push-ups and those with quadriplegia are trained to perform side leans and front-to-back rocking to relieve ischial tuberosity pressure [17, 148-149]. In these cases, the effectiveness in preventing DTI and the formation of pressure ulcers is largely dependent on 1) patient compliance, 2) the ease with which the exercises can be performed, and very importantly 3) adequate relief of internal pressure at bone-muscle interfaces. Unfortunately, none of the behaviors recommended during inpatient rehabilitation significantly contribute to reduction in the incidence of pressure ulcers [138, 150].

### *Specialized Cushions and Bed Mattresses*

Specialized wheelchair cushions, bed mattresses and overlays are often used to reduce the pressure at the interface between the skin and the chair/bed [151-155]. Although the use of these special surfaces does not eliminate the need for periodical repositioning, reductions in interfacial pressures generally lead to a reduction in internal pressure around bony prominences and longer intervals between repositioning procedures may be tolerated without compromising the

integrity of deep tissue. Based on their operating mode, support surfaces can be divided into non-powered and powered systems. Non-powered systems provide static relief of pressure while powered systems provide dynamic relief of pressure by inducing periodical redistribution of superficial pressure.

### *Non-powered Cushions and Bed Mattresses*

Non-powered cushions and bed mattresses are designed to maximize the support surface area in contact with the skin, thus reducing the pressure at the skin-surface interface. The devices are generally composed of high-density, viscoelastic, elastic closed-cell or open-cell foams, elastomers, or sacks filled with air, water or viscous fluids. Their compliant surface allows regions of high pressure under bony prominences to sink into the surface, thus diffusing the pressure to surrounding areas [7]. The support surface is made of a single component or a combination of different components. For wheelchair users, specialized wheelchair cushions are currently the only devices available for providing pressure relief while sitting, and are routinely prescribed by physical and occupational therapists.

Air-filled cushions are composed of multiple cells that are inflated to a desired air pressure. The amount of pressure reduction provided by air filled cushions is affected by variables such as the size, shape, material, air capacity, and air pressure of the inflated cushion. Varying the inflation pressure changes the amount of pressure relief provided by the cushion. Pitfalls of this type of cushion

include difficulties in adjusting the air pressure by the user and/or caregiver [156]. In the absence of adequate air pressure the user can “bottom out” in the cushion, thus eliminating the pressure relief around bony prominences [157-158]. Moreover, air cushions do not account for users’ postural imbalance and could compromise their stability in the wheelchair [3, 26, 159]. Gel-filled cushions provide better support than air-filled devices; however, changes in the viscous properties of the gel occur over time, reducing the effectiveness of the cushion in relieving interfacial pressure. The properties of gel-filled cushions can also be altered by temperature. In cold weather conditions, gel cushions may lose some of their pressure relief capabilities, and they can become a hazard if the gel freezes, exposing the user to the risk of frost bite and extreme cold injuries[160].

Viscoelastic foam cushions and mattresses are made of heat-sensitive foam that allows them to mold to the contour of the body, providing a reduction in the interfacial pressures, friction and shear forces [161]. One study showed their use reduced the incidence of pressure ulcers from 3.5–4% to less than 1% in an acute care setting [161]. Different studies have compared the use of standard hospital mattresses and cushions against mattresses and cushions made from viscoelastic foam in the same population. The results indicate that the use of these surfaces offers better pressure reduction [162], and significantly reduces the incidence of blanchable erythema compared to standard devices; however, in the cases where blanchable erythema developed, the progression of the lesion seemed to be unaffected by the type of support surface utilized [163]. One of the pitfalls

associated with foam-based surfaces is their propensity to increase skin temperature, thereby increasing the susceptibility to ulcer formation due to skin breakdown [164].

### *Powered Cushions and Bed Mattresses*

Dynamic wheelchair cushions, mattresses and overlays are available wherein alternating interfacial pressure is achieved [165]. These systems require an external source of power and are based on pumping air or water through the cells of the support surface in adjustable cycles. Other alternating pressure air systems use variable density foam within the air cells; this makes the flow of air through the cells more subtle, and reduces the unpleasant sensations that some alternating pressure air systems can generate [165]. Some drawbacks of alternating air pressure mattresses are that: 1) they can cause the sensation of “seasickness” in some people; 2) they are noisy which makes sleeping more difficult; 3) they can get damaged easily [161]; and 4) they are hard to keep clean especially between patients where they become a vehicle for bacterial spread.

Because the operation of powered pressure reduction devices is dependent on compressors and power supplies, these systems can limit the person’s mobility and level of activity [3]. Reclining and “tilt-in-space” wheelchairs provide an alternative approach for periodical alternation in interfacial pressure [166-167]. These wheelchairs are designed for individuals who lack the upper body strength needed to perform periodical wheelchair push-ups and side leans for pressure

relief [167]. The wheelchairs are equipped with a motor that tilts the backrest of the wheelchair to different angles. The change in inclination shifts the weight of the body from the ischial tuberosities to the sacrum, thus redistributing the pressure with each setting [167]. Drawbacks of this type of chair include the risk of generating shear forces [166], malpositioning for some individuals [166-167], high cost, and the larger size than regular wheelchairs which limits the mobility and encumbers transportation of the wheelchair [167].

#### *Summary of conventional preventative interventions*

Static and dynamic pressure relief systems undoubtedly play a vital role in preventing the formation of DTI and subsequent pressure ulcers. Due to the absence of early detection and assessment methods of DTI as well as the absence of non-invasive measurement approaches of internal pressure, it is unclear how effective the currently available systems are in reducing pressure at deep bone-muscle interfaces. The continued prevalence of pressure ulcers and the mounting medical costs warrant the search for additional interventions that could be used in addition to existing pressure relief surfaces to counteract the vascular and mechanical pathways of DTI.

#### **Electrical Stimulation**

An alternative prevention technique entails the use of functional electrical stimulation. Levine et al. [168-170] first proposed the use of electrical stimulation for preventing the formation of pressure ulcers in people with spinal cord injury.

Their studies showed that electrical stimulation applied to the motor point of the gluteus maximus muscles overlying the ischial tuberosities generated changes in muscle shape [170], redistribution of pressure at the seating interface [168], and increases in blood flow [169]. More recent studies showed that frequent use of electrical stimulation increased muscle mass, which could allow wheelchair users to remain seated for longer periods of time [18, 171] [172-174]. Increases in transcutaneous oxygen levels have also been reported in a long-term study with a single subject [175]. Collectively, these studies suggest that the benefits obtained through the daily use of functional electrical stimulation (i.e., increased blood flow and larger muscle mass) could lead to long-term improvements in soft tissue health and the reduction in the formation of pressure ulcers.

### **Intermittent Electrical Stimulation (IES)**

The main goal of my PhD thesis is to develop a functional electrical stimulation technique for the prevention of deep tissue injury. The proof of principle studies were completed in 2007 as part of my MSc degree, with results indicating that the use of IES could significantly reduce the formation of DTI in rats [38, 176]. Intermittent electrical stimulation consists on applying short bouts (~10 seconds) of electrical stimulation to the motor point of muscles overlying bony prominences to relieve pressure in a manner that mimics the subconscious adjustments in posture conducted by able-bodied individuals in response to discomfort due to increases in internal pressure. This pattern of stimulation is then repeated once every 5 to 10 minutes to induce muscle contractions [38, 176].

While long-term application of IES could lead to increases in muscle mass and improvement in the cushioning capacity of atrophied muscles, the mechanism of action of IES does not directly depend on muscle mass. Instead, the periodical contractions induced by IES in muscles compressed by external pressure reconfigure the shape of the muscle, thereby altering the distribution of internal stress and strain in the deep tissue surrounding bony prominences. The muscle contractions also could periodically increase tissue oxygenation in the compressed region, thus providing nutrients and removing metabolic waste products from areas susceptible to ischemia.

#### *Specific objectives of thesis*

In order to accomplish the main goal of this thesis, four studies with specific objectives were conducted.

1. Identify IES paradigms that provide the best surface pressure redistribution, deep tissue oxygenation, and reduction of sitting discomfort effects in humans with intact spinal cords. The basic IES duty cycle is based on the frequency at which able bodied people reposition themselves, which is on average every 6 to 7 minutes. The remaining IES parameters are adjusted for each individual to those that better generate a full muscle contraction.
2. Assess changes in internal strain levels around bony prominences due to varying levels of external loading in adult miniature pigs with and without paralyzed muscles.

3. Assess changes in internal stress levels around bony prominences due to varying levels of external loading in adult miniature pigs with and without paralyzed muscles.
4. Test the effectiveness of IES for the prevention of deep tissue injury in paralyzed muscles of miniature pigs subjected to external loading on a daily basis for one month.

These objectives were addressed in four studies which became four separate published papers. Each study is presented in a chapter of this thesis.

## References

- [1] I. Bales and A. Padwojski, "Reaching for the moon: achieving zero pressure ulcer prevalence.," *Journal of Wound Care*, vol. 18, pp. 137 - 144, 2009.
- [2] C. A. Russo, C. Steiner, and W. Spector, "Statistical Brief #64: Hospitalizations Related to Pressure Ulcers among Adults 18 Years and Older, 2006," Agency for Healthcare Research and Quality: Healthcare Cost and Utilization Project (HCUP), 2008.
- [3] T. A. Conine, A. K. Choi, and R. Lim, "The user-friendliness of protective support surfaces in prevention of pressure sores," *Rehabilitation Nursing*, vol. 14, pp. 261-3, 1989.
- [4] R. F. Edlich, K. L. Winters, C. R. Woodard, R. M. Buschbacher, W. B. Long, J. H. Gebhart, and E. K. Ma, "Pressure ulcer prevention," *Journal of Long-term Effects of Medical Implants*, vol. 14, pp. 285-304, 2004.
- [5] R. Labbe, T. Lindsay, and P. M. Walker, "The extent and distribution of skeletal muscle necrosis after graded periods of complete ischemia," *Journal of Vascular Surgery*, vol. 6, pp. 152-7, 1987.
- [6] C. A. Salzberg, D. W. Byrne, C. G. Cayten, P. van Niewerburgh, J. G. Murphy, and M. Viehbeck, "A new pressure ulcer risk assessment scale for individuals with spinal cord injury," *American Journal of Physical Medicine & Rehabilitation*, vol. 75, pp. 96-104, 1996.
- [7] R. M. Woolsey and J. D. McGarry, "The cause, prevention, and treatment of pressure sores," *Neurologic Clinics.*, vol. 9, pp. 797-808, 1991.
- [8] J. M. Zanca, D. M. Brienza, D. Berlowitz, R. G. Bennett, C. H. Lyder, and N. P. U. A. Panel., "Pressure ulcer research funding in America: creation and analysis of an on-line database," *Advances in Skin & Wound Care*, vol. 16, pp. 190-7, 2003.
- [9] N. P. U. A. Panel, "Pressure ulcers in America: prevalence, incidence, and implications for the future. An executive summary of the National Pressure Ulcer Advisory Panel monograph.," *Advances in Skin & Wound Care*, vol. 14, pp. 208-215, 2001.
- [10] M. A. Curley, S. M. Quigley, and M. Lin, "Pressure ulcers in pediatric intensive care: incidence and associated factors.," *Pediatric Critical Care Medicine*, vol. 4, pp. 284-290, 2003.
- [11] S. A. Aronovitch, "Intraoperatively acquired pressure ulcers: are there common risk factors?," *Ostomy Wound Management*, vol. 53, pp. 57-69, 2007.
- [12] C. Thiyagarajan and J. R. Silver, "Aetiology of pressure sores in patients with spinal cord injury," *British Medical Journal*, vol. 289, pp. 1487-90, 1984.
- [13] R. H. Guthrie and D. Goulian, "Decubitus ulcers: Prevention and Treatment," *Geriatrics*, vol. 28, pp. 67-71, 1973.

- [14] R. R. Richardson and P. R. Meyer, Jr., "Prevalence and incidence of pressure sores in acute spinal cord injuries," *Paraplegia*, vol. 19, pp. 235-47, 1981.
- [15] a. B. P. E. Young J.S., "Pressure sores and the spinal cord injured: Part II, Model Systems," *SCI Digest*, vol. 3, pp. 11-26, 1981.
- [16] S. L. Garber and D. H. Rintala, "Pressure ulcers in veterans with spinal cord injury: a retrospective study," *Journal of Rehabilitation Research & Development*, vol. 40, pp. 433-41, 2003.
- [17] J. C. Grip and C. T. Merbitz, "Wheelchair-based mobile measurement of behavior for pressure sore prevention," *Computer Methods & Programs in Biomedicine*, vol. 22, pp. 137-44, 1986.
- [18] H. Rischbieth, M. Jelbart, and R. Marshall, "Neuromuscular electrical stimulation keeps a tetraplegic subject in his chair: a case study," *Spinal Cord.*, vol. 36, pp. 443-5, 1998.
- [19] Z. B. Niazi, C. A. Salzberg, D. W. Byrne, and M. Viehbeck, "Recurrence of initial pressure ulcer in persons with spinal cord injuries," *Advances in Wound Care*, vol. 10, pp. 38-42, 1997.
- [20] T. A. Krouskop, P. C. Noble, S. L. Garber, and W. A. Spencer, "The effectiveness of preventive management in reducing the occurrence of pressure sores," *Journal of Rehabilitation Research & Development*, vol. 20, pp. 74-83, 1983.
- [21] R. Salcido, S. B. Fisher, J. C. Donofrio, M. Bieschke, C. Knapp, R. Liang, E. K. LeGrand, and J. M. Carney, "An animal model and computer-controlled surface pressure delivery system for the production of pressure ulcers," *Journal of Rehabilitation Research & Development*, vol. 32, pp. 149-61, 1995.
- [22] C. H. Lyder, "Pressure ulcer prevention and management," *Journal of the American Medical Association*, vol. 289, pp. 223-6, 2003.
- [23] A. E. Swarts, T. A. Krouskop, and D. R. Smith, "Tissue pressure management in the vocational setting," *Archives of Physical Medicine & Rehabilitation*, vol. 69, pp. 97-100, 1988.
- [24] D. Fennegan, "Positive living or negative existence?," *Nursing Times*, vol. 15, pp. 51-54, 1983.
- [25] D. R. Berlowitz and D. M. Brienza, "Are all pressure ulcers the result of deep tissue injury? A review of the literature.," *Ostomy Wound Management*, vol. 53, pp. 34 - 38, 2007.
- [26] D. S. Drummond, R. G. Narechania, A. N. Rosenthal, A. L. Breed, T. A. Lange, and D. K. Drummond, "A study of pressure distributions measured during balanced and unbalanced sitting," *Journal of Bone and Joint Surgery*, vol. 64, pp. 1034-1039, 1982.
- [27] M. W. Ferguson-Pell, "Design criteria for the measurement of pressure at body support interfaces," *Engineering in Medicine*, vol. 9, pp. 209-214, 1980.
- [28] R. G. M. Breuls, C. V. Bouten, C. W. Oomens, D. L. Bader, and F. P. Baaijens, "A theoretical analysis of damage evolution in skeletal muscle tissue with reference to pressure ulcer development," *Journal of Biomedical Engineering*, vol. 125, pp. 902-909, 2003.
- [29] M. H. Liu, D. R. Grimm, V. Teodorescu, S. J. Kronowitz, and W. A. Bauman, "Transcutaneous oxygen tension in subjects with tetraplegia with and without pressure ulcers: a preliminary report," *Journal of Rehabilitation Research & Development*, vol. 36, pp. 202-6, 1999.
- [30] E. M. H. Bosboom, C. V. Bouten, C. W. Oomens, F. P. Baaijens, and K. Nicolay, "Quantifying pressure sore-related muscle damage using high-resolution MRI," *Journal of Applied Physiology*, vol. 95, pp. 2235-2240, 2003.
- [31] J. Rosen, Mittal, V., H. Degenholtz, N. Castle, B. H. Mulsant, D. Nace, and F. H. Rubin, "Pressure ulcer prevention in black and white nursing home residents: A QI initiative of enhanced ability, incentives, and management feedback.," *Advances in Skin & Wound Care*, vol. 19, pp. 262-268, 2006.
- [32] A. Polliack, R. Taylor, and D. Bader, "Analysis of sweat during soft tissue breakdown following pressure ischaemia.," *Journal of Rehabilitation Research & Development*, vol. 30, pp. 250-259, 1993.

- [33] A. Polliack, R. Taylor, and D. Bader, "Sweat analysis following pressure ischaemia in a group of debilitated subjects.," *Journal of Rehabilitation Research & Development.*, vol. 34, pp. 303-308, 1997.
- [34] S. Hagnosisawa, M. W. Ferguson-Pell, V. R. Palmieri, and G. V. Cochran, "Pressure sores: a biochemical test for early detection of tissue damage," *Archives of Physical Medicine & Rehabilitation*, vol. 69, pp. 668-71, 1988.
- [35] B. P. Keller, J. P. Schuurman, and C. van der Werken, "Can near infrared spectroscopy measure the effect of pressure on oxygenation of sacral soft tissue?," *Journal of Wound Care*, vol. 15, pp. 213 - 217, 2006.
- [36] A. Stekelenburg, C. W. Oomens, G. J. Strijkers, K. Nicolay, and D. L. Bader, "Compression-induced deep tissue injury examined with magnetic resonance imaging and histology.," *Journal of Applied Physiology*, vol. 100, pp. 1946-1954, 2006.
- [37] B. J. van Nierop, A. Stekelenburg, S. Loerakker, C. W. Oomens, D. Bader, G. J. Strijkers, and K. Nicolay, "Diffusion of water in skeletal muscle tissue is not influenced by compression in a rat model of deep tissue injury.," *Journal of Biomechanics*, vol. 43, pp. 570 - 575, 2010.
- [38] L. R. Solis, D. P. Hallihan, R. R. Uwiera, R. B. Thompson, E. D. Pehowich, and V. K. Mushahwar, "Prevention of pressure-induced deep tissue injury using intermittent electrical stimulation.," *Journal of Applied Physiology*, vol. 102, pp. 1992-2001, 2007.
- [39] J. F. Deprez, E. Brusseau, J. Fromageau, G. Cloutier, and O. Basset, "On the potential of ultrasound elastography for pressure ulcer early detection.," *Medical Physics*, vol. 38, pp. 1943 - 1950, 2011.
- [40] M. Kosiak, "Etiology and pathology of ischemic ulcers," *Archives of Physical Medicine & Rehabilitation*, vol. 40, pp. 62-9, 1959.
- [41] M. Kosiak, "Etiology of decubitus ulcers," *Archives of Physical Medicine & Rehabilitation*, vol. 42, pp. 19-29, 1961.
- [42] M. Kosiak, W. G. Kubicek, M. Olson, J. N. Danz, and F. J. Kottke, "Evaluation of pressure as factor in production of ischial ulcers," *Archives of Physical Medicine & Rehabilitation*, vol. 39, pp. 623-629, 1958.
- [43] P. A. Grace, "Ischaemia-reperfusion injury," *British Journal of Surgery*, vol. 81, pp. 637-47, 1994.
- [44] D. C. Gute, T. Ishida, K. Yarimizu, and R. J. Korthuis, "Inflammatory responses to ischemia and reperfusion in skeletal muscle," *Molecular & Cellular Biochemistry*, vol. 179, pp. 169-87, 1998.
- [45] S. M. Peirce, T. C. Skalak, and G. T. Rodeheaver, "Ischemia-reperfusion injury in chronic pressure ulcer formation: a skin model in the rat," *Wound Repair and Regeneration*, vol. 8, pp. 68-76, 2000.
- [46] S. Tsuji, S. Ichioka, N. Sekiya, and T. Nakatsuka, "Analysis of ischemia-reperfusion injury in a microcirculatory model of pressure ulcers," *Wound Repair and Regeneration*, vol. 13, pp. 209-215, 2005.
- [47] A. Gefen, N. Gefen, E. Linder-Ganz, and S. S. Margulies, "In vivo muscle stiffening under bone compression promotes deep pressure sores," *Journal of Biomechanical Engineering*, vol. 127, pp. 512-524, 2005.
- [48] E. Linder-Ganz, S. Engelberg, M. Scheinowitz, and A. Gefen, "Pressure-time cell death threshold for albino rat skeletal muscles as related to pressure sore biomechanics.," *Journal of Biomechanics*, vol. 39, pp. 2725-2732, 2006.
- [49] K. Harris, P. M. Walker, D. A. Mickle, R. Harding, R. Gatley, G. J. Wilson, B. Kuzon, N. McKee, and A. D. Romaschin, "Metabolic response of skeletal muscle to ischemia.," *The American Journal of Physiology*, vol. 250, pp. H213 - H220, 1986.
- [50] H. Haljamäe and E. Enger, "Human skeletal muscle energy metabolism during and after complete tourniquet ischemia.," *Annals of Surgery*, vol. 182, pp. 9 - 14, 1975.
- [51] R. Tupling, H. Green, G. Senisterra, J. Lepock, and N. McKee, "Effects of 4-h ischemia and 1-h reperfusion on rat muscle sarcoplasmic reticulum function.," *American Journal of Physiology. Endocrinology & Metabolism*, vol. 281, pp. E867 - E877, 2001.

- [52] J. L. Farber, "Biology of disease: membrane injury and calcium homeostasis in the pathogenesis of coagulative necrosis.," *Laboratory Investigation*, vol. 47, pp. 114 - 123, 1982.
- [53] L. Schild, F. Plumeyer, and G. Reiser, "Ca(2+) rise within a narrow window of concentration prevents functional injury of mitochondria exposed to hypoxia/reoxygenation by increasing antioxidative defence.," *The FEBS Journal*, vol. 272, pp. 5844 - 5852, 2005.
- [54] A. P. Halestrap, "Calcium, mitochondria and reperfusion injury: a pore way to die.," *Biochemical Society Transactions*, vol. 34, pp. 232 - 237, 2006.
- [55] A. M. Byrne, J. J. Lemasters, and A. L. Nieminen, "Contribution of increased mitochondrial free Ca<sup>2+</sup> to the mitochondrial permeability transition induced by tert-butylhydroperoxide in rat hepatocytes," *Hepatology*, vol. 29, pp. 1523-31, 1999.
- [56] N. Ueda and S. V. Shah, "Role of intracellular calcium in hydrogen peroxide-induced renal tubular cell injury," *Am J Physiol*, vol. 263, pp. F214-21, 1992.
- [57] J. V. Gerasimenko, O. V. Gerasimenko, A. Palejwala, A. V. Tepikin, O. H. Petersen, and A. J. Watson, "Menadione-induced apoptosis: roles of cytosolic Ca(2+) elevations and the mitochondrial permeability transition pore," *J Cell Sci*, vol. 115, pp. 485-97, 2002.
- [58] Y. Hara, M. Wakamori, M. Ishii, E. Maeno, M. Nishida, T. Yoshida, H. Yamada, S. Shimizu, E. Mori, J. Kudoh, N. Shimizu, H. Kurose, Y. Okada, K. Imoto, and Y. Mori, "LTRPC2 Ca<sup>2+</sup>-permeable channel activated by changes in redox status confers susceptibility to cell death," *Mol Cell*, vol. 9, pp. 163-73, 2002.
- [59] A. K. Stout, H. M. Raphael, B. I. Kanterewicz, E. Klann, and I. J. Reynolds, "Glutamate-induced neuron death requires mitochondrial calcium uptake," *Nat Neurosci*, vol. 1, pp. 366-73, 1998.
- [60] L. Virag, G. S. Scott, P. Antal-Szalmas, M. O'Connor, H. Ohshima, and C. Szabo, "Requirement of intracellular calcium mobilization for peroxynitrite-induced poly(ADP-ribose) synthetase activation and cytotoxicity," *Mol Pharmacol*, vol. 56, pp. 824-33, 1999.
- [61] R. Tupling, H. Green, G. Senisterra, J. Lepock, and N. McKee, "Effects of ischemia on sarcoplasmic reticulum Ca(2+) uptake and Ca(2+) release in rat skeletal muscle," *American Journal of Physiology Endocrinology & Metabolism*, vol. 281, pp. E224-232, 2001.
- [62] R. Tupling, H. Green, G. Senisterra, J. Lepock, and N. McKee, "Ischemia-induced structural change in SR Ca<sup>2+</sup>-ATPase is associated with reduced enzyme activity in rat muscle," *American Journal of Physiology Regulatory Integrative & Comparative Physiology*, vol. 281, pp. R1681-88, 2001.
- [63] A. Kabaroudis, T. Gerassimidis, D. Karamanos, B. Papaziogas, V. Antonopoulos, and A. Sakantamis, "Metabolic alterations of skeletal muscle tissue after prolonged acute ischemia and reperfusion," *Journal of Investigative Surgery*, vol. 16, pp. 219-28, 2003.
- [64] R. Labbe, T. Lindsay, and P. M. Walker, "The extent and distribution of skeletal muscle necrosis after graded periods of complete ischemia.," *Journal of Vascular Surgery*, vol. 6, pp. 152 - 157, 1987.
- [65] K. A. Reimer, R. B. Jennings, and A. H. Tatum, "Pathobiology of acute myocardial ischemia: metabolic, functional and ultrastructural studies.," *The American Journal of Cardiology*, vol. 52, pp. 72A - 81A, 1983.
- [66] H. J. Appell, S. Glöser, J. M. C. Soares, and J. A. Duarte, "Structural alterations of skeletal muscle induced by ischemia and reperfusion.," *Basic Appl. Myol.*, vol. 9, pp. 263-268, 1999.
- [67] I. Forrest, T. Lindsay, A. Romaschin, and P. Walker, "The rate and distribution of muscle blood flow after prolonged ischemia.," *Journal of Vascular Surgery*, vol. 10, pp. 83 - 88, 1989.
- [68] R. J. Korthuis, J. K. Smith, and D. L. Carden, "Hypoxic reperfusion attenuates postischemic microvascular injury.," *The American Journal of Physiology*, vol. 256, pp. H315 - H319, 1989.

- [69] P. M. Walker, T. F. Lindsay, R. Labbe, D. A. Mickle, and A. D. Romaschin, "Salvage of skeletal muscle with free radical scavengers.," *Journal of Vascular Surgery*, vol. 5, pp. 68 - 75, 1987.
- [70] K. A. Kaminski, T. A. Bonda, J. Korecki, and W. J. Musial, "Oxidative stress and neutrophil activation--the two keystones of ischemia/reperfusion injury.," *International Journal of Cardiology*, vol. 86, pp. 41 - 59, 2002.
- [71] J. S. McNally, A. Saxena, H. Cai, S. Dikalov, and D. G. Harrison, "Regulation of xanthine oxidoreductase protein expression by hydrogen peroxide and calcium.," *Arteriosclerosis, Thrombosis, and Vascular Biology.*, vol. 25, pp. 1623 - 1628, 2005.
- [72] J. S. McNally, M. E. Davis, D. P. Giddens, A. Saha, J. Hwang, S. Dikalov, H. Jo, and D. G. Harrison, "Role of xanthine oxidoreductase and NAD(P)H oxidase in endothelial superoxide production in response to oscillatory shear stress.," *American Journal of Physiology. Heart and Circulatory Physiology.*, vol. 285, pp. H2290 - H2297, 2003.
- [73] A. Meneshian and G. B. Bulkley, "The physiology of endothelial xanthine oxidase: from urate catabolism to reperfusion injury to inflammatory signal transduction.," *Microcirculation*, vol. 9, pp. 161 - 175, 2002.
- [74] J. M. McCord, "Oxygen-derived free radicals in postischemic tissue injury.," *New England Journal of Medicine*, vol. 312, pp. 159 - 163, 1985.
- [75] T. Lindsay, P. M. Walker, D. A. Mickle, and A. D. Romaschin, "Measurement of hydroxy-conjugated dienes after ischemia-reperfusion in canine skeletal muscle.," *The American Journal of Physiology*, vol. 254, pp. H578 - H583, 1988.
- [76] S. Hoshino, Y. Kikuchi, M. Nakajima, H. Kimura, S. Tsuyama, K. Uemura, and K. Yoshida, "Endothelial NO Synthase (eNOS) phosphorylation regulates coronary diameter during ischemia-reperfusion in association with oxidative stress.," *Free Radical Research*, vol. 39, pp. 481 - 489, 2005.
- [77] J. H. Kramer, V. Misík, and W. B. Weglicki, "Lipid peroxidation-derived free radical production and postischemic myocardial reperfusion injury.," *Annals of the New York Academy of Sciences*, vol. 723, pp. 180 - 196, 1994.
- [78] M. G. Davies and P. O. Hagen, "The vascular endothelium. A new horizon.," *Annals of Surgery*, vol. 218, pp. 593 - 609, 1993.
- [79] D. B. Cines, E. S. Pollak, C. A. Buck, J. Loscalzo, G. A. Zimmerman, R. P. McEver, J. S. Pober, T. M. Wick, B. A. Konkle, B. S. Schwartz, E. S. Barnathan, K. R. McCrae, B. A. Hug, A. M. Schmidt, and D. M. Stern, "Endothelial cells in physiology and in the pathophysiology of vascular disorders.," *Blood*, vol. 19, pp. 3527 - 3561, 1998.
- [80] H. R. Girn, S. Ahilathirunayagam, A. Mavor, and S. Homer-Vanniasinkam, "Reperfusion syndrome: cellular mechanisms of microvascular dysfunction and potential therapeutic strategies.," *Vascular and Endovascular Surgery*, vol. 41, pp. 277 - 293, 2007.
- [81] L. Yang, R. M. Froio, T. E. Sciuto, A. M. Dvorak, R. Alon, and F. W. Luscinskas, "ICAM-1 regulates neutrophil adhesion and transcellular migration of TNF-alpha-activated vascular endothelium under flow.," *Blood*, vol. 106, pp. 584 - 592, 2005.
- [82] W. A. Muller, "Migration of leukocytes across endothelial junctions: some concepts and controversies.," *Microcirculation*, vol. 8, pp. 181 - 193, 2001.
- [83] P. R. Kvietys and M. Sandig, "Neutrophil diapedesis: paracellular or transcellular?," *News in Physiological Sciences*, vol. 16, pp. 15 - 19, 2001.
- [84] M. Braide, B. Amundson, S. Chien, and U. Bagge, "Quantitative studies on the influence of leukocytes on the vascular resistance in a skeletal muscle preparation.," *Microvascular Research*, vol. 27, pp. 331 - 352, 1984.
- [85] S. J. Weiss, "Tissue destruction by neutrophils.," *New England Journal of Medicine*, vol. 320, pp. 365 - 376, 1989.
- [86] R. J. Korthuis, D. N. Granger, M. I. Townsley, and A. E. Taylor, "The role of oxygen-derived free radicals in ischemia-induced increases in canine skeletal muscle vascular permeability.," *Circulation Research*, vol. 57, pp. 599 - 604, 1985.
- [87] M. C. Mazzoni, P. Borgström, K. C. Warnke, T. C. Skalak, M. Intaglietta, and K. E. Arfors, "Mechanisms and implications of capillary endothelial swelling and luminal narrowing in low-flow ischemias.," *International Journal of Microcirculation, Clinical and Experimental*, vol. 15, pp. 265 - 270, 1995.

- [88] A. G. Harris, M. Steinbauer, R. Leiderer, and K. Messmer, "Role of leukocyte plugging and edema in skeletal muscle ischemia-reperfusion injury.," *The American Journal of Physiology*, vol. 273, pp. H989 - H996, 1997.
- [89] I. Kurose, D. C. Anderson, M. Miyasaka, T. Tamatani, J. C. Paulson, R. F. Todd, J. R. Rusche, and D. N. Granger, "Molecular determinants of reperfusion-induced leukocyte adhesion and vascular protein leakage.," *Circulation Research*, vol. 74, pp. 336 - 343, 1995.
- [90] M. D. Menger, D. Steiner, and K. Messmer, "Microvascular ischemia-reperfusion injury in striated muscle: significance of "no reflow".," *The American Journal of Physiology*, vol. 263, pp. H1892 - H1900, 1992.
- [91] S. C. Hardy, S. Homer-Vanniasinkam, and M. J. Gough, "The triphasic pattern of skeletal muscle blood flow in reperfusion injury: an experimental model with implications for surgery on the acutely ischaemic lower limb.," *European Journal of Vascular Surgery*, vol. 4, pp. 587 - 590, 1990.
- [92] R. L. Engler, M. D. Dahlgren, M. A. Peterson, A. Dobbs, and G. W. Schmid-Schönbein, "Accumulation of polymorphonuclear leukocytes during 3-h experimental myocardial ischemia.," *The American Journal of Physiology*, vol. 251, pp. H93 - H100, 1986.
- [93] G. W. Schmid-Schönbein, "Capillary plugging by granulocytes and the no-reflow phenomenon in the microcirculation.," *Federation Proceedings*, vol. 46, pp. 2397 - 2401, 1987.
- [94] D. Cooper, J. Russell, K. D. Chitman, M. C. Williams, R. E. Wolf, and D. N. Granger, "Leukocyte dependence of platelet adhesion in postcapillary venules.," *American Journal of Physiology. Heart and Circulatory Physiology*, vol. 286, pp. H1895 - H1900, 2004.
- [95] L. A. Hartsock, A. V. Seaber, and J. R. Urbaniak, "Intravascular thrombosis in skeletal muscle microcirculation after ischemia.," *Microsurgery*, vol. 10, pp. 161 - 166, 1989.
- [96] M. Belkin, C. R. Valeri, and R. W. n. Hobson, "Intraarterial urokinase increases skeletal muscle viability after acute ischemia.," *Journal of Vascular Surgery*, vol. 9, pp. 161 - 168, 1989.
- [97] R. W. n. Hobson, J. G. Wright, D. Fox, and J. C. Kerr, "Heparinization reduces endothelial permeability and hydrogen ion accumulation in a canine skeletal muscle ischemia-reperfusion model.," *Journal of Vascular Surgery*, vol. 7, pp. 585 - 591, 1988.
- [98] T. A. Springer, "Traffic signals for lymphocyte recirculation and leukocyte emigration: the multistep paradigm.," *Cell*, vol. 76, pp. 301 - 314, 1994.
- [99] R. J. Korthuis, J. K. Smith, and D. L. Carden, "Hypoxic reperfusion attenuates postischemic microvascular injury.," *The American Journal of Physiology*, vol. 256, pp. H315 - H319, 1989.
- [100] J. Greenwood, C. L. Amos, C. E. Walters, P. O. Couraud, R. Lyck, B. Engelhardt, and P. Adamson, "Intracellular domain of brain endothelial intercellular adhesion molecule-1 is essential for T lymphocyte-mediated signaling and migration.," *Journal of Immunology*, vol. 171, pp. 2099 - 2108, 2003.
- [101] S. S. Yadav, D. N. Howell, W. Gao, D. A. Steeber, R. C. Harland, and P. A. Clavien, "L-selectin and ICAM-1 mediate reperfusion injury and neutrophil adhesion in the warm ischemic mouse liver.," *The American Journal of Physiology*, vol. 275, pp. G1341 - G1352, 1998.
- [102] I. Singh, G. B. Zibari, H. Zizzi, D. N. Granger, L. Cruz, E. Gonsales, J. C. McDonald, and M. F. Brown, "Anti-P-selectin antibody protects against hepatic ischemia-reperfusion injury.," *Transplantation Proceedings*, vol. 30, pp. 2324 - 2326, 1998.
- [103] Y. Nishimura, Y. Takei, S. Kawano, M. Goto, K. Nagano, S. Tsuji, H. Nagai, A. Ohmae, H. Fusamoto, and T. Kamada, "The F(ab')<sub>2</sub> fragment of an anti-ICAM-1 monoclonal antibody attenuates liver injury after orthotopic liver transplantation.," *Transplantation*, vol. 61, pp. 99 - 104, 1996.
- [104] L. Virág, E. Szabó, P. Gergely, and C. Szabó, "Peroxyxynitrite-induced cytotoxicity: mechanism and opportunities for intervention.," *Toxicology Letters*, vol. 140 - 141, pp. 113 - 124, 2003.

- [105] A. Khanna, P. A. Cowled, and R. A. Fitridge, "Nitric oxide and skeletal muscle reperfusion injury: current controversies (research review)." *The Journal of Surgical Research*, vol. 128, pp. 98 - 107, 2005.
- [106] P. Vallance and J. Collier, "Biology and clinical relevance of nitric oxide.," *BMJ (Clinical Research Edition)*, vol. 309, pp. 453 - 457, 1994.
- [107] H. Rubbo, R. Radi, M. Trujillo, R. Telleri, B. Kalyanaraman, S. Barnes, M. Kirk, and B. A. Freeman, "Nitric oxide regulation of superoxide and peroxynitrite-dependent lipid peroxidation. Formation of novel nitrogen-containing oxidized lipid derivatives.," *The Journal of Biological Chemistry*, vol. 269, pp. 26066-26075, 1994.
- [108] A. Mantovani, C. Garlanda, M. Introna, and A. Vecchi, "Regulation of endothelial cell function by pro- and anti-inflammatory cytokines.," *Transplantation Proceedings*, vol. 30, pp. 4239 - 4243, 1998.
- [109] L. Rössig, B. Fichtlscherer, K. Breitschopf, J. Haendeler, A. M. Zeiher, A. Mülsch, and S. Dimmeler, "Nitric oxide inhibits caspase-3 by S-nitrosation in vivo.," *The Journal of Biological Chemistry*, vol. 274, pp. 6823 - 6826, 1999.
- [110] S. M. Dinsdale, "Decubitus ulcers in swine: light and electron microscopy study of pathogenesis," *Archives of Physical Medicine & Rehabilitation*, vol. 54, pp. 51-6, 1973.
- [111] S. M. Dinsdale, "Decubitus ulcers: role of pressure and friction in causation.," *Archives of Physical Medicine and Rehabilitation*, vol. 55, pp. 147-152, 1974.
- [112] B. Goldstein and J. Sanders, "Skin response to repetitive mechanical stress: a new experimental model in pig," *Archives of Physical Medicine & Rehabilitation.*, vol. 79, pp. 265-72, 1998.
- [113] J. Vidal and M. Sarrias, "An analysis of the diverse factors concerned with the development of pressure sores in spinal cord injured patients," *Paraplegia.*, vol. 29, pp. 261-7, 1991.
- [114] E. Linder-Ganz and A. Gefen, "The effects of pressure and shear on capillary closure in the microstructure of skeletal muscles.," *Annals of Biomedical Engineering*, vol. 35, pp. 2095 - 2107, 2007.
- [115] C. W. Oomens, O. F. Bressers, E. M. Bosboom, C. V. Bouten, and D. L. Blader, "Can loaded interface characteristics influence strain distributions in muscle adjacent to bony prominences?," *Computer Methods in Biomechanics & Biomedical Engineering*, vol. 6, pp. 171-80, 2003.
- [116] R. K. Daniel, D. L. Priest, and D. C. Wheatley, "Etiologic factors in pressure sores: an experimental model," *Archives of Physical Medicine & Rehabilitation*, vol. 62, pp. 492-8, 1981.
- [117] J. B. Reswick and J. E. Rogers, "Experience at Rancho Los Amigos Hospital with devices and techniques to prevent pressure sores.," in *Bedsore Biomechanics*, R. M. Kenedi, J. M. Cowden, and J. T. Scales, Eds. London: Macmillan, 1976, pp. 301 - 310.
- [118] A. Gefen and J. Levine, "The false premise in measuring body-support interface pressures for preventing serious pressure ulcers.," *Journal of Medical Engineering & Technology*, vol. 31, pp. 375 - 380, 2007.
- [119] L. Agam and A. Gefen, "Pressure ulcers and deep tissue injury: a bioengineering perspective.," *Journal of Wound Care.*, vol. 16, pp. 336 - 342, 2007.
- [120] C. V. Bouten, C. W. Oomens, F. P. Baaijens, and D. L. Bader, "The etiology of pressure ulcers: skin deep or muscle bound?," *Archives of Physical Medicine and Rehabilitation*, vol. 84, pp. 616-619, 2003.
- [121] D. Lim, F. Lin, R. W. Hendrix, B. Moran, C. Fasanati, and M. Makhsous, "Evaluation of a new sitting concept designed for prevention of pressure ulcer on the buttock using finite element analysis.," *Medical & Biological Engineering & Computing*, vol. 45 pp. 1074 - 1089, 2007.
- [122] E. A. Peeters, C. V. Bouten, C. W. Oomens, D. L. Bader, L. H. Snoeckx, and F. P. Baaijens, "Anisotropic, three-dimensional deformation of single attached cells under compression.," *Annals of Biomedical Engineering*, vol. 32, pp. 1443 - 1452, 2004.
- [123] Y. N. Wang, C. V. Bouten, D. A. Lee, and D. L. Bader, "Compression-induced damage in a muscle cell model in vitro.," *Proceedings of the Institution of Mechanical Engineers. Part H Journal of Engineering in Medicine*, vol. 219, pp. 1 - 12, 2005.

- [124] E. A. Peeters, C. W. Oomens, C. V. Bouten, D. L. Bader, and F. P. Baaijens, "Viscoelastic properties of single attached cells under compression.," *Journal of Biomechanical Engineering*, vol. 127, pp. 237 - 243, 2005.
- [125] N. Slomka and A. Gefen, "Relationship Between Strain Levels and Permeability of the Plasma Membrane in Statically Stretched Myoblasts.," *Annals of Biomedical Engineering*, vol. Epub ahead of print, 2011.
- [126] E. Linder-Ganz and A. Gefen, "Mechanical compression-induced pressure sores in rat hindlimb: muscle stiffness, histology, and computational models," *Journal of Applied Physiology*, vol. 96, pp. 2034-49, 2004.
- [127] N. Shabshin, G. Zoizner, A. Herman, V. Ougortsin, and A. Gefen, "Use of weight-bearing MRI for evaluating wheelchair cushions based on internal soft-tissue deformations under ischial tuberosities.," *Journal of Rehabilitation Research and Development*, vol. 47, pp. 31 - 42, 2010.
- [128] E. Linder-Ganz, N. Shabshin, Y. Itzchak, and A. Gefen, "Assessment of mechanical conditions in sub-dermal tissues during sitting: A combined experimental-MRI and finite element approach.," *Journal of Biomechanics*, 2006.
- [129] M. Makhsous, D. Lim, R. Hendrix, J. Bankard, W. Z. Rymer, and F. Lin, "Finite element analysis for evaluation of pressure ulcer on the buttock: development and validation.," *IEEE Transactions on Neural Systems and Rehabilitation Engineering*, vol. 15, pp. 517 - 525, 2007.
- [130] E. L. Wagnac, C. E. Aubin, and J. Dansereau, "A new method to generate a patient-specific finite element model of the human buttocks.," *IEEE Transactions on Biomedical Engineering*, vol. 55, pp. 774 - 783, 2008.
- [131] R. Sopher, J. Nixon, C. Gorecki, and A. Gefen, "Exposure to internal muscle tissue loads under the ischial tuberosities during sitting is elevated at abnormally high or low body mass indices.," *Journal of Biomechanics*, vol. 43, pp. 280 - 286, 2010.
- [132] E. Linder-Ganz, N. Shabshin, Y. Itzchak, and A. Gefen, "Assessment of mechanical conditions in sub-dermal tissues during sitting: A combined experimental-MRI and finite element approach.," *Journal of Biomechanics*, vol. 40, pp. 1443 - 1454, 2007.
- [133] E. Linder-Ganz, N. Shabshin, Y. Itzchak, Z. Yizhar, I. Siev-Ner, and A. Gefen, "Strains and stresses in sub-dermal tissues of the buttocks are greater in paraplegics than in healthy during sitting.," *Journal of Biomechanics*, vol. 41, pp. 567 - 580, 2008.
- [134] S. Loerakker, L. R. Solis, D. L. Bader, F. P. Baaijens, V. K. Mushahwar, and C. W. Oomens, "How does muscle stiffness affect the internal deformations within the soft tissue layers of the buttocks under constant loading?," *Computer Methods in Biomechanics and Biomedical Engineering*, vol. Epub ahead of print, 2012.
- [135] K. T. Dodd and D. R. Gross, "Three-dimensional tissue deformation in subcutaneous tissues overlying bony prominences may help to explain external load transfer to the interstitium," *Journal of Biomechanics*, vol. 24, pp. 11-9, 1991.
- [136] A. Stekelenburg, G. J. Strijkers, H. Parusel, D. L. Bader, K. Nicolay, and C. W. Oomens, "Role of ischemia and deformation in the onset of compression-induced deep tissue injury: MRI-based studies in a rat model.," *Journal of Applied Physiology*, vol. 102, pp. 2002-2011, 2007.
- [137] S. Loerakker, A. Stekelenburg, G. J. Strijkers, J. J. Rijpkema, F. P. Baaijens, D. L. Bader, K. Nicolay, and C. W. Oomens, "Temporal effects of mechanical loading on deformation-induced damage in skeletal muscle tissue.," *Annals of Biomedical Engineering*, vol. 38, pp. 2577 - 2587, 2010.
- [138] D. R. Thomas, "Are all pressure ulcers avoidable?," *Journal of the American Medical Directors Association*, vol. 4, pp. S43-S48, 2003.
- [139] E. S. Marks and C. L. Cogbill, "Surgical Therapy of Decubitus Ulcers in the Paraplegic Patient," *Annals of Surgery*, vol. 132, pp. 994 - 1002, 1950.
- [140] D. R. Thomas, "Prevention and treatment of pressure ulcers.," *Journal of the American Medical Directors Association*, vol. 7, pp. 46-59, 2006.
- [141] D. R. Thomas, "Prevention and treatment of pressure ulcers:what works?what doesn't?," *Cleveland Clinic Journal of Medicine*, vol. 68, pp. 704-7, 710-14, 717-22, 2001.

- [142] K. Vanderwee, M. H. Grypdonck, D. De Bacquer, and T. Defloor, "Effectiveness of turning with unequal time intervals on the incidence of pressure ulcer lesions.," *Journal of Advanced Nursing*, vol. 57, pp. 59-68, 2007.
- [143] T. Defloor, D. De Bacquer, and M. H. Grypdonck, "The effect of various combinations of turning and pressure reducing devices on the incidence of pressure ulcers.," *International Journal of Nursing Studies*, vol. 42, pp. 37-46, 2005.
- [144] S. Baranoski, "Raising Awareness of Pressure Ulcer Prevention and Treatment," *Advances in Skin & Wound Care*, vol. 19, pp. 398-405, 2006.
- [145] K. Catania, C. Huang, P. James, M. Madison, M. Moran, and M. Ohr, "PUPP: The Pressure Ulcer Prevention Protocol Interventions," *The American Journal of Nursing*, vol. 107, pp. 44-52, 2007.
- [146] E. H. de Laat, P. Pickkers, L. Schoonhoven, A. L. Verbeek, T. Feuth, and T. van Achterberg, "Guideline implementation results in a decrease of pressure ulcer incidence in critically ill patients.," *Critical Care Medicine*, vol. 35, pp. 815-820, 2007.
- [147] G. C. Xakellis, R. A. Frantz, A. Lewis, and P. Harvey, "Translating pressure ulcer guidelines into practice: it's harder than it sounds.," *Advances in Skin & Wound Care*, vol. 14, pp. 249-256, 2001.
- [148] G. W. White, R. M. Mathews, and S. B. Fawcett, "Reducing risk of pressure sores: effects of watch prompts and alarm avoidance on wheelchair push-ups," *Journal of Applied Behavior Analysis*, vol. 22, pp. 287-95, 1989.
- [149] C. T. Merbitz, R. B. King, J. Bleiberg, and J. C. Grip, "Wheelchair push-ups: measuring pressure relief frequency," *Archives of Physical Medicine & Rehabilitation*, vol. 66, pp. 433-8, 1985.
- [150] J. S. Krause and L. Broderick, "Patterns of recurrent pressure ulcers after spinal cord injury: identification of risk and protective factors 5 or more years after onset," *Archives of Physical Medicine & Rehabilitation*, vol. 85, pp. 1257-64, 2004.
- [151] S. L. Garber, "A classification of wheelchair seating," *American Journal of Occupational Therapy*, vol. 33, pp. 652-4, 1979.
- [152] S. L. Garber, "Wheelchair cushions for spinal cord-injured individuals," *American Journal of Occupational Therapy*, vol. 39, pp. 722-5, 1985.
- [153] S. L. Garber, "Wheelchair cushions: a historical review," *American Journal of Occupational Therapy*, vol. 39, pp. 453-9, 1985.
- [154] M. Ferguson-Pell, G. V. B. Cochran, V. R. Palmieri, and J. B. Brunski, "Development of a modular wheelchair cushion for spinal cord injured persons," *Journal of Rehabilitation Research and Development*, vol. 23, pp. 63-76, 1986.
- [155] M. Marshall and P. Overstall, "Pressure sores, 2. Mattresses to prevent pressure sores," *Nursing Times*, vol. 79, pp. 54, 56, 57, 1983.
- [156] K. Hamanami, A. Tokuhira, and H. Inoue, "Finding the optimal setting of inflated air pressure for a multi-cell air cushion for wheelchair patients with spinal cord injury.," *Acta Medica Okayama*, vol. 58, pp. 37-44, 2004.
- [157] T. A. Krouskop, R. Williams, P. Noble, and J. Brown, "Inflation pressure effect on performance of air-filled wheelchair cushions," *Archives of Physical Medicine & Rehabilitation*, vol. 67, pp. 126-8, 1986.
- [158] P. Werner and I. Perlash, "Warning mat to signal air seat cushion failure," *Archives of Physical Medicine and Rehabilitation*, vol. 63, pp. 188-190, 1982.
- [159] S. L. Garber and T. A. Krouskop, "Body build and its relationship to pressure distribution in the seated wheelchair patient," *Archives of Physical Medicine & Rehabilitation*, vol. 63, pp. 17-20, 1982.
- [160] I. R. Odderson, K. M. Jaffe, C. A. Sleicher, R. Price, and R. J. Kropp, "Gel wheelchair cushions: a potential cold weather hazard," *Archives of Physical Medicine & Rehabilitation*, vol. 72, pp. 1017-20, 1991.
- [161] P. Beldon, "Transfoam Visco: evaluation of a viscoelastic foam mattress.," *British Journal of Nursing*, vol. 11, pp. 651-655, 2002.
- [162] S. Hampton and F. Collins, "Reducing pressure ulcer incidence in a long-term setting.," *British Journal of Nursing*, vol. 14, pp. S6-S12, 2005.

- [163] L. J. Russell, T. M. Reynolds, C. Park, S. Rithalia, M. Gonsalkorale, J. Birch, D. Torgerson, and C. Iglesias, "Randomized clinical trial comparing 2 support surfaces: results of the prevention of pressure ulcers study.," *Advances in Skin & Wound Care*, vol. 16, pp. 317-327, 2003.
- [164] R. J. Seymour and W. E. Lacefield, "Wheelchair cushion effect on pressure and skin temperature," *Archives of Physical Medicine & Rehabilitation*, vol. 66, pp. 103-8, 1985.
- [165] D. Gray, "Pressure ulcer prevention and treatment: the Transair range.," *British Journal of Nursing*, vol. 8, pp. 454-458, 1999.
- [166] R. A. Cooper, M. J. Dvorznak, A. J. Rentschler, and M. L. Boninger, "Displacement between the seating surface and hybrid test dummy during transitions with a variable configuration wheelchair: a technical note.," *Journal of Rehabilitation Research & Development*, vol. 37, pp. 297 - 303, 2000.
- [167] S. P. Burns and K. L. Betz, "Seating pressures with conventional and dynamic wheelchair cushions in tetraplegia.," *Archives of Physical Medicine & Rehabilitation*, vol. 80, pp. 566 - 571, 1999.
- [168] S. P. Levine, R. L. Kett, P. S. Cederna, L. D. Bowers, and S. V. Brooks, "Electrical muscle stimulation for pressure variation at the seating interface," *Journal of Rehabilitation Research & Development*, vol. 26, pp. 1-8, 1989.
- [169] S. P. Levine, R. L. Kett, M. D. Gross, B. A. Wilson, P. S. Cederna, and J. E. Juni, "Blood flow in the gluteus maximus of seated individuals during electrical muscle stimulation," *Archives of Physical Medicine & Rehabilitation*, vol. 71, pp. 682-6, 1990.
- [170] S. P. Levine, R. L. Kett, P. S. Cederna, and S. V. Brooks, "Electric muscle stimulation for pressure sore prevention: tissue shape variation," *Archives of Physical Medicine & Rehabilitation*, vol. 71, pp. 210-5, 1990.
- [171] K. M. Bogie, S. I. Reger, S. P. Levine, and V. Sahgal, "Electrical stimulation for pressure sore prevention and wound healing," *Assistive Technology*, vol. 12, pp. 50-66, 2000.
- [172] L. Q. Liu, G. P. Nicholson, S. L. Knight, R. Chelvarajah, A. Gall, F. R. Middleton, M. W. Ferguson-Pell, and M. D. Craggs, "Pressure changes under the ischial tuberosities of seated individuals during sacral nerve root stimulation.," *Journal of Rehabilitation Research & Development*, vol. 43, pp. 209 - 218, 2006.
- [173] L. Q. Liu, G. P. Nicholson, S. L. Knight, R. Chelvarajah, A. Gall, F. R. Middleton, M. W. Ferguson-Pell, and M. D. Craggs, "Interface pressure and cutaneous hemoglobin and oxygenation changes under ischial tuberosities during sacral nerve root stimulation in spinal cord injury.," *Journal of Rehabilitation Research & Development*, vol. 43, pp. 553 - 564, 2006.
- [174] K. M. Bogie and R. J. Triolo, "Effects of regular use of neuromuscular electrical stimulation on tissue health," *Journal of Rehabilitation Research & Development*, vol. 40, pp. 469-75, 2003.
- [175] K. M. Bogie, X. Wang, and R. J. Triolo, "Long-term prevention of pressure ulcers in high-risk patients: a single case study of the use of gluteal neuromuscular electric stimulation," *Archives of Physical Medicine & Rehabilitation*, vol. 87, pp. 585-591, 2006.
- [176] V. K. Mushahwar and L. R. Solis, "Mitigation of pressure ulcers using electrical stimulation," vol. Patent Pending, 2008.

## CHAPTER 1

# Effects of intermittent electrical stimulation on superficial pressure, tissue oxygenation, and discomfort levels for the prevention of deep tissue injury.

### 1.2. Introduction

Pressure ulcers are a severe type of soft tissue injury commonly prevalent in individuals who have reduced mobility and/or sensation. Populations at risk of developing pressure ulcers are those confined to a bed or dependent on wheelchair use for daily mobility. They include the elderly, patients in intensive care units, individuals in long-term care, and people with spinal cord injury (SCI) [1-3].

A developed ulcer can severely affect the quality of life of the person, limiting their comfort, mobility, and ability to participate in daily life activities [4]. If infected, pressure ulcers can lead to death due to sepsis [5-6]. Treating advanced stage ulcers can require surgery and lengthy hospital stays [7-8]. In developed countries, the annual costs of treating pressure ulcers are estimated to be in the billions of dollars [2, 9-10].

Pressure ulcers can originate at the level of the skin and progress inwards. These ulcers start as a red or discolored area on the skin and progress inwards to deeper layers of tissue. Contributing factors to these ulcers are excessive friction, shear, and poor skin hygiene [11]. Pressure ulcers can also originate at deep bone-

muscle interfaces and progress outwards [12-13]. The main factor contributing to the development of these ulcers, which are termed deep tissue injury (DTI), is the prolonged compression of soft tissue between a bony prominence (e.g., ischial tuberosities or sacrum) and a surface (e.g., wheelchair or bed) [1, 11, 14-17]. The compression leads to tissue injury by two mechanisms: 1) Excessive mechanical deformation leading to rupture of cell membranes [18-21]. 2) Blood vessel occlusion leading to prolonged ischemia [22-24] and accumulation of metabolic waste [25], the effects of which are further exacerbated during reperfusion [26-28]. Muscle is more susceptible to breakdown than skin due to mechanical deformation and ischemia/reperfusion stress [18, 29]; therefore, DTI presents a very perilous form of pressure ulcers that develops without exhibiting obvious skin signs.

The gluteal muscles over the ischial tuberosities are among the most susceptible locations for DTI in wheelchair users [17, 30][31]. Conventional preventative interventions focus on reducing superficial pressure through the use of specialized wheelchair cushions [32-33]; however, most wheelchair cushions provide static reduction of pressure. Moreover, the effectiveness of pressure reduction depends on the type of cushion used, degree of muscle atrophy, and geometry of the ischial tuberosities [17, 30] among other factors. For dynamic relief of pressure, wheelchair users are encouraged to perform back and forth, and side-to-side leans as well as wheelchair push-ups [8, 34-35]. The effectiveness of these exercises in preventing DTI is limited by the ability of the individual to

perform them, and the extent to which they reduce pressure at deep bone-muscle interfaces.

We suggested previously the use of intermittent electrical stimulation (IES) as a method for preventing pressure ulcers of deep origin [36]. In this approach, electrical stimulation is applied for a short duration (on the order of seconds) with several minutes of recovery between stimulations. The muscle contractions produced by the intermittent bursts of stimulation mimic the natural repositioning movements subconsciously performed by able-bodied individuals in response to discomfort while sitting. Each IES-induced muscle contraction redistributes pressure over the ischial tuberosities and increases tissue oxygenation, effectively counteracting the two pathways that lead to DTI [36].

In rat experiments we demonstrated the effectiveness of IES in reducing the amount of DTI in a compressed muscle [36]. More recently, IES was tested in human volunteers with SCI, and the capacity of IES-elicited contractions in highly atrophied muscles to distribute superficial pressure and increase tissue oxygenation was assessed [37]. The results demonstrated that IES produced significant reductions in pressure over the ischial tuberosities and increased oxygenation in the stimulated muscles, suggesting that the IES effects were independent of muscle mass.

The present study was performed in able-bodied volunteers and had three

main goals: 1) to test the effects of four different IES protocols and identify those that were more likely to prevent DTI; 2) to compare the IES effects against those produced by voluntary contractions and conventional pressure relief maneuvers such as chair push-ups; and 3) to identify if the effects of IES are dependent on the amount of superficial pressure experienced at the sitting interface since, for wheelchair users, superficial pressure can vary greatly depending on factors such as muscle mass and type of cushion utilized.

### **1.3. METHODS**

#### *1.3.1 Overview*

All experimental protocols were approved by the University of Alberta Human Ethics committee. Experiments were performed in two groups of adult able-bodied volunteers with six participants in each. Volunteers provided informed consent prior to their participation. Each volunteer participated in two testing sessions held on two separate days. The first session involved the assessment of changes in superficial pressure due to IES, voluntary contractions or a conventional pressure relief maneuver (chair push-up). The second session involved the assessment of changes in tissue oxygenation throughout the gluteus maximus muscles induced by the same testing parameters.

In the first group of volunteers (3 F, 3 M, 20 – 42 yrs old) the effects of four IES protocols were tested, as well as the effects of voluntary contractions. In the second group (3 F, 3 M, 21 – 32 yrs old) the effects of the two best IES

protocols identified in the first group were tested under two loading levels, and were compared to the effects of conventional relief of pressure (chair push-ups). Superficial pressure, deep tissue oxygenation levels, and perceived changes in the level of muscle discomfort due to sitting were assessed in both groups. Each test trial consisted of applying one IES protocol, a voluntary contraction, or a chair-push up, and each trial was replicated three times. The order in which trials were acquired was randomized.

### *1.3.2. Application of IES*

The application of IES was performed through rectangular (50x100mm) self adhesive electrodes (*Pure Care, Sherwood Park, Alberta, Canada*) placed bilaterally on the surface of the skin, over the motor points of the gluteus maximus muscles. A commercially available stimulator (*BioStim NMS+, BioMedical Life Systems, California, U.S.A.*) was used. Stimulation pulses were square, biphasic and charge balanced. Stimulation frequency and pulse width were held constant at 40Hz and 250 $\mu$ s, respectively. Pulse amplitude was set to the level required to elicit a strong fused contraction in each volunteer. The required stimulator intensity level ranged from levels 3 – 8 (out of 10 levels) depending on the volunteer.

### *1.3.3 IES protocols and testing conditions*

The four IES protocols tested were: 1) **Bilateral Continuous**. This consisted of a 10 sec bout of stimulation (“ON” phase) applied to both the left and

right gluteus maximus muscles simultaneously in order to elicit a strong contraction in both sides of the buttocks. The “ON” phase was followed by a 7 minute no stimulation period (“OFF” phase). 2) **Bilateral Bursting**. In this protocol, the “ON” phase was composed of three short bouts (3 sec) of stimulation applied simultaneously to both the left and right gluteus muscles, with two short periods (2 sec) of rest between each bout to elicit three bilateral short contractions in near succession. This “ON” phase was followed by a 7 minute “OFF” phase. 3) **Alternating Continuous** and 4) **Alternating Bursting**. These were similar to the bilateral continuous and bilateral bursting protocols, respectively, with the exception that the “ON” phase of IES was first applied to one side of the buttocks, followed by the other. This generated contractions in one side followed immediately by contractions in the other. The bilateral and alternating protocols were chosen because their action was expected to mimic the effect of wheelchair push-ups and side-to-side leans performed by wheelchair users, respectively. The continuous IES protocols were expected to cause an influx of blood after each muscle contraction as a result of reactive hyperemia, even while seated, which would cause large, transient increases in tissue oxygenation. The bursting IES protocols were expected to act as blood pumps, generating cumulative increases in blood flow and tissue oxygenation after each brief contraction.

For trials that required a voluntary contraction, the volunteers were asked to contract both left and right gluteus muscles simultaneously and hold the

contraction for 10 sec, followed by a 7-minute rest period.

To determine whether the effects of IES could be limited by the level of superficial pressure at the ischial tuberosities, two loading conditions were used. The natural bodyweight (BW) condition was tested by asking the volunteers to sit upright on an office chair. The increased loading condition (BW + 30%) was implemented by asking the volunteers to wear a weighted vest. The weight of the vest was equivalent to 30% of each person's body weight.

The effects of IES were also compared to conventional pressure relief involving complete lifting of the buttocks off the chair (chair push-up). The volunteers held the push-up position for 10 sec, followed by a 7-minute rest period.

#### *1.3.4 Measurements of superficial pressure*

The first testing session involved the assessment of changes in superficial pressure around the ischial tuberosities. All volunteers sat upright on a standard office chair with their feet flat on the ground and their arms rested on the chair's armrests. The chair had a thin (~1 in), regular foam padding over the seating area. Once the experimental session began the volunteers were not allowed to stand up or move their legs between trials. Superficial pressure was measured utilizing an XSensor pressure sensing mattress (*XSensor, Calgary, Alberta, Canada*), composed of an array of 36x36 capacitive pressure sensors 1cm<sup>2</sup> each. The

mattress was placed between the volunteers' buttocks and the chair. Pressure measurements were acquired at three different periods during each trial: **1)** A 5 sec period before the application of IES (baseline), **2)** during the IES-elicited or voluntary contraction, and **3)** a 5 sec period immediately after the cessation of contraction. Data were acquired using XSensor software, X3 Pro V5, at a sampling rate of 10 frames per second. Recordings from each sensor were subsequently exported into Matlab (*Mathworks, Massachusetts, U.S.A.*) for analysis using custom-written scripts. Half a second worth of data (5 pressure readings) from the start and end of each period were discarded to remove fluctuations in pressure occurring at the beginning and end of contraction. The pressure readings from all 3 trials within a protocol were grouped, and sensors that experienced a significant change in their pressure readings were identified, and a protocol-specific spatial representation of pressure changes was obtained for each volunteer.

#### *1.3.5 Measurements of tissue oxygenation*

The second testing session assessed the changes in tissue oxygenation throughout the gluteal muscles induced by the different test protocols. The testing took place in the Peter S Allen MR Research Centre (University of Alberta) within a week of the first session. A full-body 1.5T Magnet (Siemens Sonata) was utilized. Because subjects were limited to supine positions inside the magnet, a device was built to compress the gluteus muscles in a manner that resembled sitting (**figure 1A, top**). An indenter was used to apply pressure to the ischial

tuberosities in a near perpendicular alignment to emulate sitting compression. A neoprene garment with adjustable Velcro® straps placed over the volunteer's thighs and hips was used to compress the buttocks and adjust the level of pressure measured around the ischial tuberosities. The load applied to the gluteus muscles through this device was adjusted to match that measured while sitting (with or without the weight vest) for each volunteer (**figure 1A, bottom plots**). Each experimental trial consisted of a 30 sec baseline period, followed by a 10 sec IES-induced/voluntary contraction ("ON" phase), and a 7 min rest period ("OFF" phase).

To obtain an assessment of changes in tissue oxygenation in the gluteal muscles, a  $T_2^*$ -weighted magnetic resonance imaging (MRI) sequence was utilized, which provides blood oxygen level dependent (BOLD) image contrast [38-40]. An echo-planar imaging sequence was used with the following parameters: echo time = 37 ms, repetition time = 1.33 s, flip angle = 75°, bandwidth = 1500 Hz/pixel, field of view = 275 \* 400 mm, acquisition matrix = 88 x 128 pixel, and in-plane resolution = 3.125 x 3.125 mm. Fifteen 6 mm thick slices with no gap between were acquired to provide full coverage of the buttocks. A total of 343 stacks of images were obtained for each trial over 7.6 minutes, with full three-dimensional coverage every 1.33 seconds.

Analysis of acquired images was conducted using custom-written Matlab scripts that allowed for the quantification of changes in tissue oxygenation due to

the different protocols. Similar analysis procedures as those used in functional MRI were utilized [41-43]. Within a trial the gluteus maximus muscles were delineated bilaterally in each MR slice starting at the first time point of the baseline period (**figure 1B, left image**). The signal intensity of each pixel contained within the delineated regions was obtained and the average signal intensity throughout the regions was calculated. The same template of the delineated muscles was subsequently applied to the images acquired at every time point throughout the baseline period and post-stimulation periods, and the average signal intensity for each muscle was calculated. Signal intensity was not measured during the contraction period because the change in the shape of the muscle (**figure 1B, middle image**) causes the signal to be measured from tissue outside the region of interest. Because muscle returns to its original shape following the contraction (**figure 1B, right image**), changes in signal intensity measured before and after contraction can be compared, as they are obtained from the same tissue. This process was repeated for all slices within a trial, and changes in signal intensity post IES-induced or voluntary contraction were calculated as a percent change from baseline.

The effect of chair push-ups on tissue oxygenation was assessed using another setup inside the magnet. The volunteers lay down in a prone position and a portable wooden surface with handles was placed over the gluteus muscles to compress the buttocks against the sacrum. Bags filled with sand were placed on

the surface to further compress the gluteus muscles to levels equivalent to those measured when the person laid in a supine position. Two assistants standing on opposite ends of the MRI scanner lifted the loaded surface when needed to simulate chair push-ups. To compare the effects of this conventional pressure relief strategy to IES, the bilateral continuous IES protocol was tested with this loading setup. When IES was applied, the load was not lifted by the assistants. The analysis of the images obtained from the “chair push-up” setup was conducted in the same manner as the one described for the IES/voluntary contraction protocols.

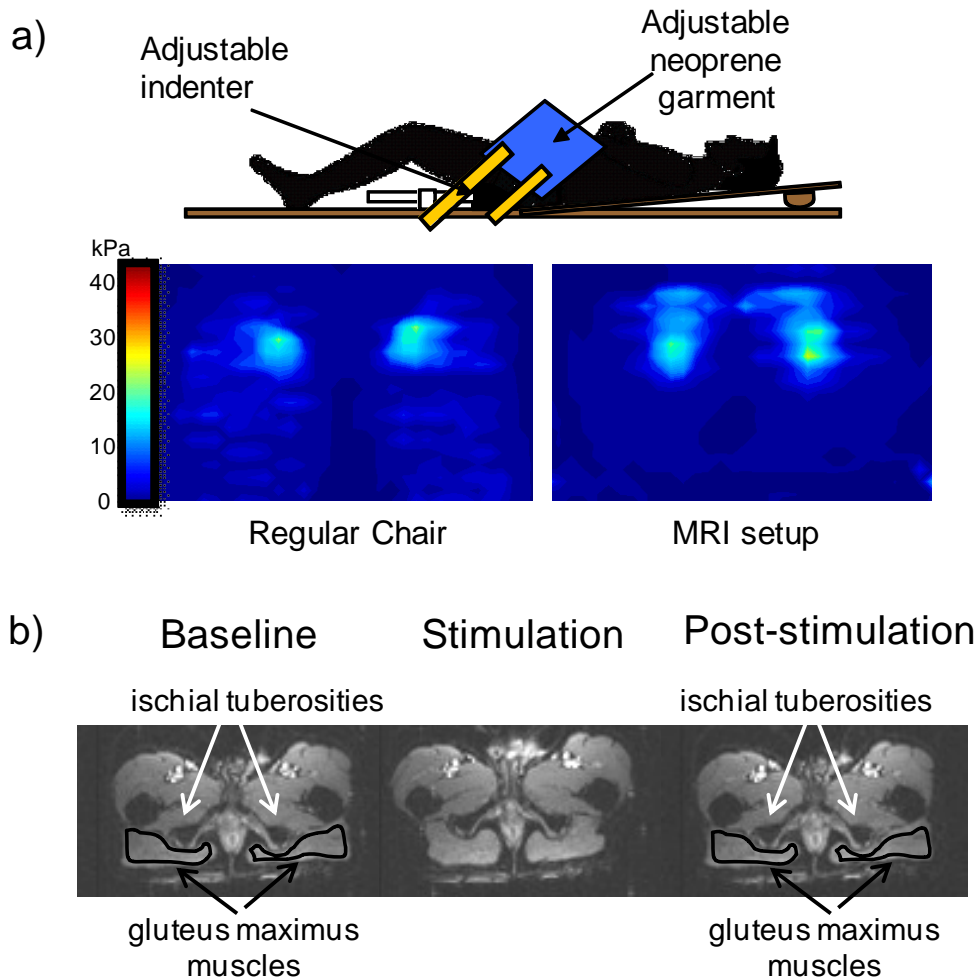


**Figure 1.** Reproduction of sitting pressure inside the MRI magnet. (a) *Top:* Setup utilized to load the ischial tuberosities inside the MRI magnet. *Bottom left:* Pressure map of ischial tuberosities of a volunteer sitting in a regular chair. *Bottom right:* Pressure map of ischial tuberosities of the same volunteer “sitting” in the MRI setup. *Color bar* denotes pressure magnitude. (b) MRI images of gluteus maximus muscles from one volunteer during baseline, stimulation, and post-stimulation periods.

The results from the three trials within each protocol from all volunteers were averaged and a 95% confidence interval was calculated for each time point of data acquisition. The signal intensity measurements from each protocol were binned in 30 sec time windows and averaged.

### *1.3.6 Volunteers' perception of discomfort due to sitting and IES*

During both experimental sessions, the volunteers were asked to answer a questionnaire that ranked their perception of discomfort due to prolonged sitting and the change in that discomfort as a result of the IES protocols, voluntary contractions or conventional relief. This scale was designed specifically for this study and was not validated against other similar scales. Discomfort was rated on a 10 point scale, ranging from 1 (no discomfort), to 10 (unbearable pain). The following 5 questions were asked during each trial: 1) Rate the level of discomfort in your buttocks due to sitting? 2) Rate the level of discomfort in your buttocks during muscle contraction? 3) Rate the level of discomfort in your buttocks at the end of muscle contraction? 4) If a reduction in discomfort level is maintained after the cessation of muscle contraction, notify us when the discomfort returns to the level reported in question 1. 5) Rate the level of skin discomfort caused by the application of electrical stimulation? Question 1 was asked at the beginning of each trial. Questions 2-4 were asked after the "ON phase" of each trial, and the reported measurement in question 4 was the time elapsed from the end of the contraction or conventional pressure relief to the time at which discomfort returned to pre-contraction/relief levels. Question 5 was asked immediately after each IES trial to assess if the electrical current necessary to elicit a muscle contraction causes skin discomfort.

All responses were tabulated using Microsoft Excel and the median score was calculated.

### *1.3.7 Statistical Analyses*

The main hypothesis of this study was that the use of IES would provide improved relief of superficial pressure, increase in tissue oxygenation, and a reduction in sitting discomfort compared to rest and the conventional interventions tested. Therefore, this study tried to reject three different null hypotheses: 1) No statistical difference would be found in superficial pressure relief between the different conditions tested (IES and non-IES). 2) No statistical difference would be found in tissue oxygenation changes between the conditions tested. 3) No statistical difference would be found in discomfort perception between the different conditions tested.

A one-way ANOVA ( $\alpha = 0.05$ ) and Tukey's HSD multiple comparison test were used to assess if the protocols tested produced significant changes in superficial pressure. A one-way ANOVA and Tukey's HSD multiple-comparison post-hoc test ( $\alpha = 0.05$ ) were used to establish statistical significance between signal intensity levels (an indicator of tissue oxygenation) before (baseline) and after IES-induced/voluntary contractions and conventional pressure relief. Friedman's test was utilized to assess statistical differences between perceived discomfort before, during, and after the administration of each test protocol (Questions 1 - 3). The non-parametric Kruskal-Wallis test was utilized to assess statistical significance between protocols for the perceived skin discomfort as a result of the application of IES (Question 5), as well as to compare the duration of sustained reduction in discomfort level after each protocol (Question 4). These

non-parametric tests were selected given the non-normality of the data observed after doing a normality test.

## **1.4. Results**

### *1.4.1 Pressure Reduction due to IES*

#### *1.4.1.1 Effectiveness of different IES protocols in reducing pressure at the ischial tuberosities*

In all volunteers, the highest points of superficial pressure were located under the ischial tuberosities (**figures 2, 3, rest period**). The average pressure in this region was  $15.16 \pm 3.25$  kPa (mean  $\pm$  standard deviation). All IES protocols resulted in a redistribution of pressure around the ischial tuberosities; specifically, IES significantly reduced pressure under the ischial tuberosities, and significantly increased pressure in regions adjacent to the ischial tuberosities.

A comparison of the *bilateral* and *alternating continuous* protocols in one volunteer is shown in **figure 2**. The bilateral continuous protocol (**figure 2A**) produced an upwards push during the contraction and redistributed pressure around the ischial tuberosities (**figure 2B**). The resulting movement produced a significant reduction in pressure under the ischial tuberosities of  $10.3 \pm 2.9$  % relative to baseline in 4 of 6 volunteers (e.g., **figure 2C**). The alternating continuous protocol also significantly reduced pressure under the ischial tuberosities in 4 of 6 volunteers (e.g., **figure 2G,H**); however, the reduction was

only by  $6.6 \pm 17.0\%$ . The alternating IES protocol generated a push-up effect in the contracting side of the buttocks, causing a slight side-to-side lean. In the contracting side superficial pressure was redistributed in a similar manner to the bilateral protocols, with a decrease in pressure under the ischial tuberosities, and an increase in the surrounding areas; however, changes in the contralateral side (non-contracting side) did not follow this pattern. Interestingly, changes in the contralateral side were dependant on the handedness of each volunteer. In right handed volunteers ( $n = 5$ ), contraction of the right gluteus generated a significant reduction of pressure throughout the left (non-contracting) gluteus. When the left gluteus was contracted, there were no significant changes on the right (non-contracting). The opposite of this effect occurred in the left handed volunteer ( $n = 1$ ). This suggests that the IES-induced contractions were slightly stronger in the dominant side, even though visually, both sides appeared to be contracting with the same strength.

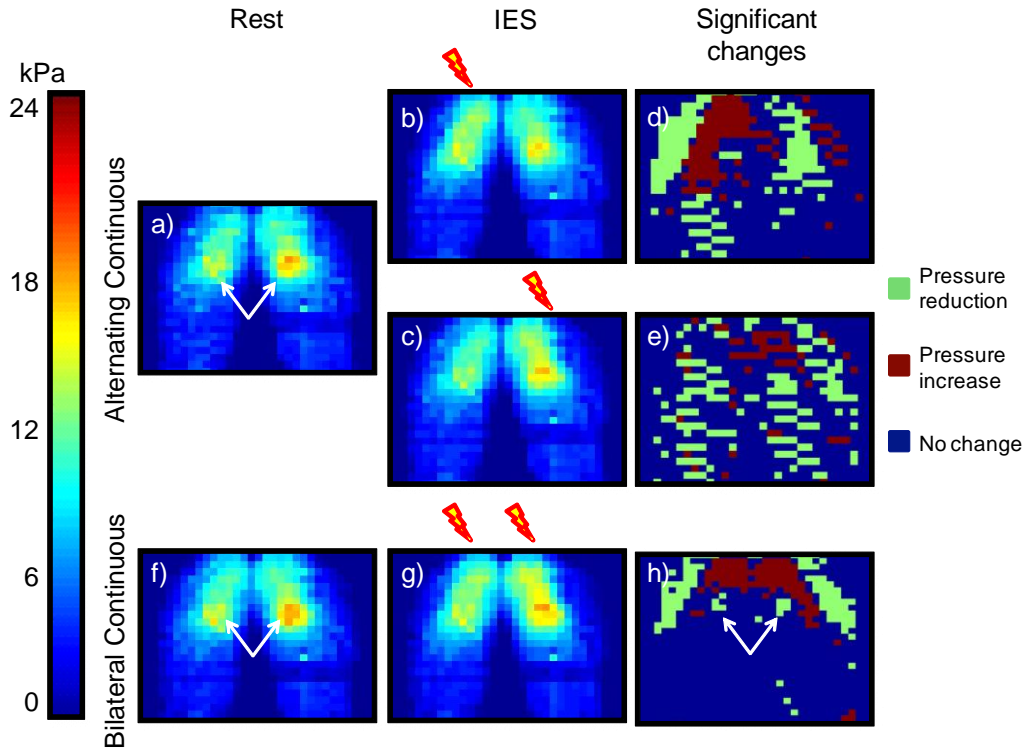


**Figure 2.** Pressure measurements during alternating continuous and bilateral continuous IES protocols in one volunteer. Baseline pressure map obtained by averaging the sensor values over a 5 s period prior to IES delivery (a). Average pressure maps during *alternating continuous* IES that produced a contraction in the *right* (b) and *left* (c) gluteus. Distribution of sensors that experienced a significant change in pressure (reduction or increase) during contraction of the *right* (d) and *left* (e) gluteus. Baseline pressure map obtained by averaging the sensor values over a 5 s period prior to IES delivery (f). Average pressure map during *bilateral continuous* IES producing contraction of both *left and right* gluteus simultaneously (g). Distribution of sensors that measured a significant change in pressure during contraction (h).

An example of the pressure redistribution produced by the *bilateral continuous* and *bursting* IES protocols in one volunteer is shown in **figure 3A-F**. Similar to the bilateral continuous protocol, the bilateral bursting protocol generated significant reductions in pressure under the ischial tuberosities in 5 of 6 volunteers (e.g., **figure 3F**) by  $9.9 \pm 5.3\%$  relative to baseline. The *alternating bursting* protocol was the least effective of the four IES protocols tested, generating a significant reduction in pressure of  $5.6 \pm 2.6\%$  from baseline at the

ischial tuberosities in 3 of 6 volunteers.

Two of 6 volunteers were unable to generate consistent *bilateral voluntary* contractions while sitting; therefore, only data collected from the remaining 4 were analyzed. The pattern of pressure redistribution evoked by voluntary contractions was similar to the pattern generated by the two *bilateral* IES protocols (**figure 3C, F, I**). Of the 4 volunteers, voluntary contractions generated a significant reduction in pressure under the ischial tuberosities of  $7.0 \pm 4.6\%$  in three.

A one-way ANOVA revealed no significant differences in pressure reduction between the IES protocols. Furthermore, the reductions produced by IES were similar to those produced by voluntary contractions.

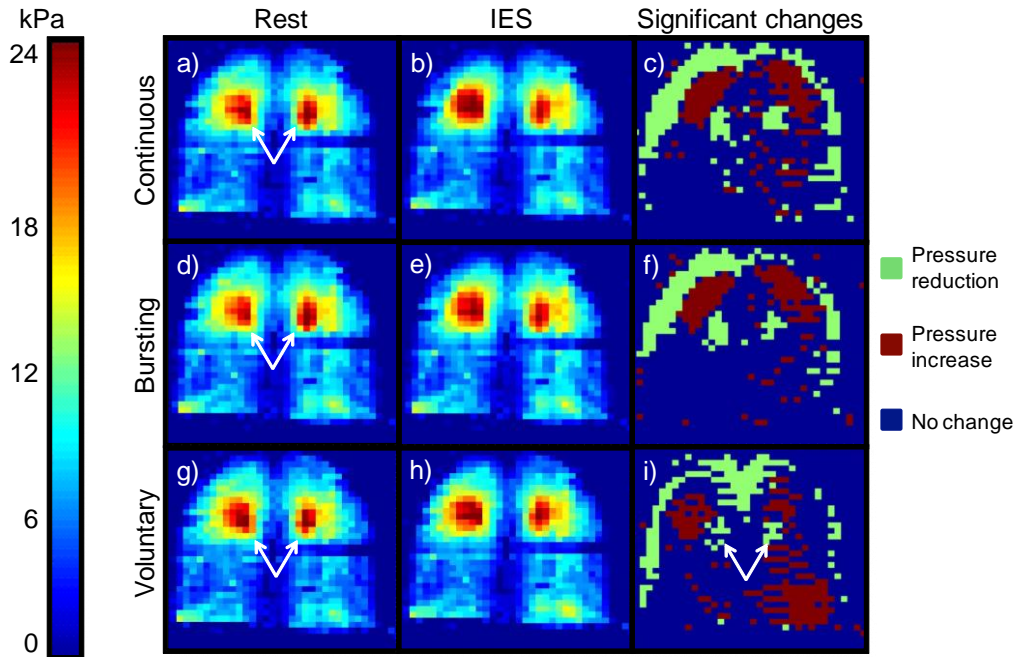


**Figure 3.** Pressure measurements during bilateral continuous IES, bilateral bursting IES and voluntary contractions in one volunteer. *Top row* (a–c): baseline pressure map obtained by averaging the sensor values over a 5 s period prior to IES delivery (a). Average pressure map during contractions produced by *bilateral continuous* IES (b). *Color* indicates magnitude of pressure. Highest levels of pressure were located around the ischial tuberosities (*arrows*). Distribution of sensors experiencing a significant change in pressure (reduction or increase) due to IES (c). *Middle row* (d–f): baseline pressure map obtained by averaging the sensor values over a 5 s period prior to IES delivery (d). Average pressure map during contractions produced by *bilateral bursting* IES (e). Distribution of sensors experiencing a significant change in pressure (reduction or increase) due to IES (f). *Bottom row* (g–i): baseline pressure map obtained by averaging the sensor values over a 5 s period prior to IES delivery (g). Average pressure map during voluntary contractions of the gluteal muscles (h). Distribution of sensors experiencing a significant change in pressure (reduction or increase) due to IES (i).

#### 1.4.1.2 Effectiveness of IES in reducing pressure under increased loading conditions

In volunteers subjected to increased loading equivalent to 30% of BW, the pressure under the ischial tuberosities increased by a similar percentage (average pressure increased from  $12.53 \pm 2.9$  kPa to  $17.27 \pm 4.16$  kPa). An example of the effectiveness of the two *bilateral* IES protocols in reducing pressure under increased loading in one volunteer is shown in **figure 4**.

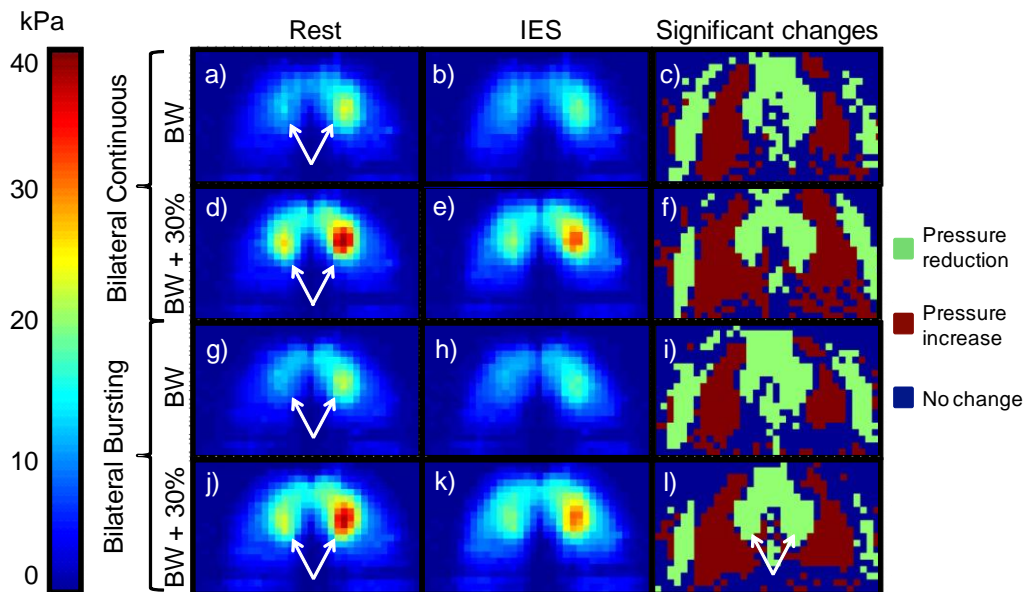


**Figure 4.** Pressure measurements during bilateral continuous and bilateral bursting IES protocols under normal and increased loading conditions. (a–c) Baseline pressure map with BW loading obtained by averaging the sensor values over a 5 s period prior to IES delivery (a). Average pressure map during contractions produced by *bilateral continuous* IES (b). Color indicates magnitude of pressure. Highest levels of pressure were located around ischial tuberosities (arrows). Distribution of sensors experiencing a significant change in pressure (reduction or increase) due to IES (c). (d–f) Baseline pressure map with BW + 30% loading obtained by averaging the sensor values over a 5 s period prior to IES delivery (d). Average pressure map during contractions produced by *bilateral continuous* IES (e). Distribution of sensors experiencing a significant change in pressure due to IES (f). (g–i) Baseline pressure map with BW loading obtained by averaging the sensor values over a 5 s period prior to IES delivery (g). Average pressure map during contractions produced by *bilateral bursting* IES (h). Distribution of sensors experiencing a significant change in pressure due to IES (i). (j–l) Baseline pressure map with BW + 30% loading obtained by averaging the sensor values over a 5 s period prior to IES delivery (j). Average pressure map during contractions produced by *bilateral bursting* IES (k). Distribution of sensors experiencing a significant change in pressure due to IES (l).

With increased loading, the continuous protocol generated a significant reduction in pressure under the ischial tuberosities in 3 of 6 volunteers by  $8.9 \pm 6.2\%$  compared to baseline. The bursting protocol significantly reduced pressure in 5 of 6 volunteers by  $8.1 \pm 4\%$ . A two-way ANOVA revealed no significant difference in the reductions in pressure produced by the IES protocol ( $p = 0.79$ ),

loading level ( $p = 0.98$ ), nor the interaction between loading level and protocol used ( $p = 0.39$ ).

Chair push-ups produced a 100% pressure reduction throughout the buttocks regardless of the loading level. This was because all volunteers were able to lift their buttocks fully off the chair.

In summary, all IES protocols were capable of reducing pressure under the ischial tuberosities; however, the *bilateral* protocols produced a larger reduction in pressure than the *alternating* protocols. Furthermore, the reduction in pressure achieved by the bilateral protocols was similar to that achieved by voluntary contractions. The effectiveness of the bilateral protocols in redistributing pressure was maintained even under conditions of increased loading on the ischial tuberosities.

#### *1.4.2 Increases in Tissue Oxygenation due to IES*

Based on the results from the superficial pressure measurements and feedback from the volunteers, only the bilateral IES protocols were tested inside the MRI magnet to assess changes in tissue oxygenation. Voluntary contractions and chair push-ups were also used to compare with the results obtained from the IES protocols.

#### *1.4.2.1 Effectiveness of IES protocols in increasing oxygenation in the gluteus maximus muscles*

An example of the average changes in tissue oxygenation due to the two bilateral IES protocols and voluntary contraction in one volunteer is shown in **figure 5A**. The results from the 6 volunteers in this group followed a similar pattern. In all trials, there was an immediate increase in signal intensity in the gluteus maximus muscles following the IES-induced or voluntary contraction. The increase in signal intensity reflected the increase in tissue oxygenation throughout the gluteus muscles. After the initial peak, the signal intensity decayed for ~2.5 minutes and plateaued at an elevated level relative to baseline for the remainder of the scan time (7 min).

The average signal intensity  $\pm$  95% confidence interval of 30 sec time window bins from all protocols is shown in **figure 5B (top)**. All time windows following the IES-induced or voluntary muscle contractions were significantly different from baseline. To compare the changes in signal intensity between protocols, grouped data from each protocol were fitted with an exponential decay curve and compared using a one-way ANOVA and Tukey's HSD post-hoc test (**figure 5B, bottom**). The post-IES and voluntary contraction periods from all protocols were significantly different from each other. The bilateral continuous IES protocol produced the highest changes in signal intensity, followed by the bilateral bursting protocol and voluntary contractions, respectively.

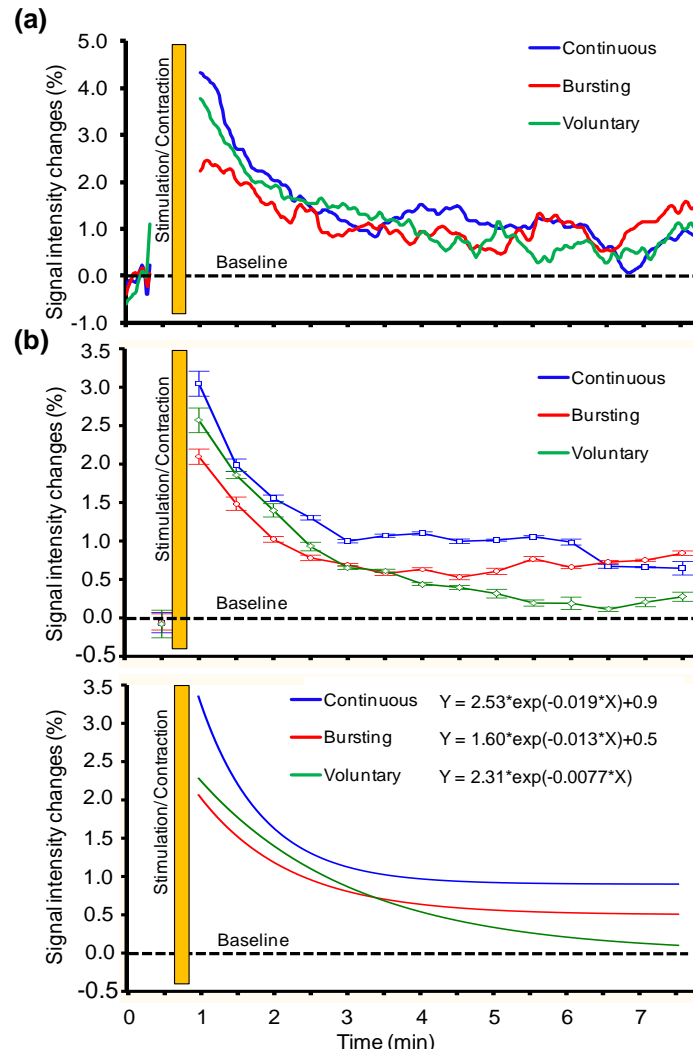


**Figure 5.** Changes in tissue oxygenation induced by bilateral continuous IES, bilateral bursting IES, and voluntary contractions. (a) Average change in signal intensity (%) from baseline. No data were quantified during the stimulation/contraction period. (b) *Top:* comparison of time points after stimulation/contraction to baseline for *bilateral continuous IES*, *bilateral bursting IES*, and *voluntary contraction* protocols. Time points were grouped in 30 s time windows for comparison. (b) *Bottom:* exponential decay curves fitted for data from time points after contraction for *continuous*, *bursting*, and *voluntary* protocols.

#### 1.4.2.2 Effectiveness of IES in increasing tissue oxygenation under increased loading conditions

A summary of the effects of IES on tissue oxygenation under conditions of increased loading around the ischial tuberosities is shown for one volunteer in

**figure 6A.** The average changes in tissue oxygenation due to each IES protocol under BW and BW + 30% loading are shown. For all 6 volunteers in this group, there was an increase in signal intensity in the gluteus maximus muscles as a result of both IES protocols, even with the additional load. The additional load (BW + 30%) caused an overall drop in the signal intensity of ~23% and ~30% for the bilateral continuous and bursting protocols, respectively; however, the same pattern of change in signal intensity was maintained. The signal intensity levels remained elevated throughout the imaging duration after the bilateral IES protocols.

The average signal intensity  $\pm$  95% confidence interval for 30 sec time windows associated with each IES protocol is shown in **figure 6B (top)**, and fitted exponential decay curves are shown in **figure 6B (bottom)**. The additional loading (BW + 30%) caused a significant decrease in the signal intensity induced by both the continuous and bursting IES protocols; however, the signal intensity patterns produced by the two IES protocols were not significantly different from each other under each loading condition ( $p = 0.4$ ).

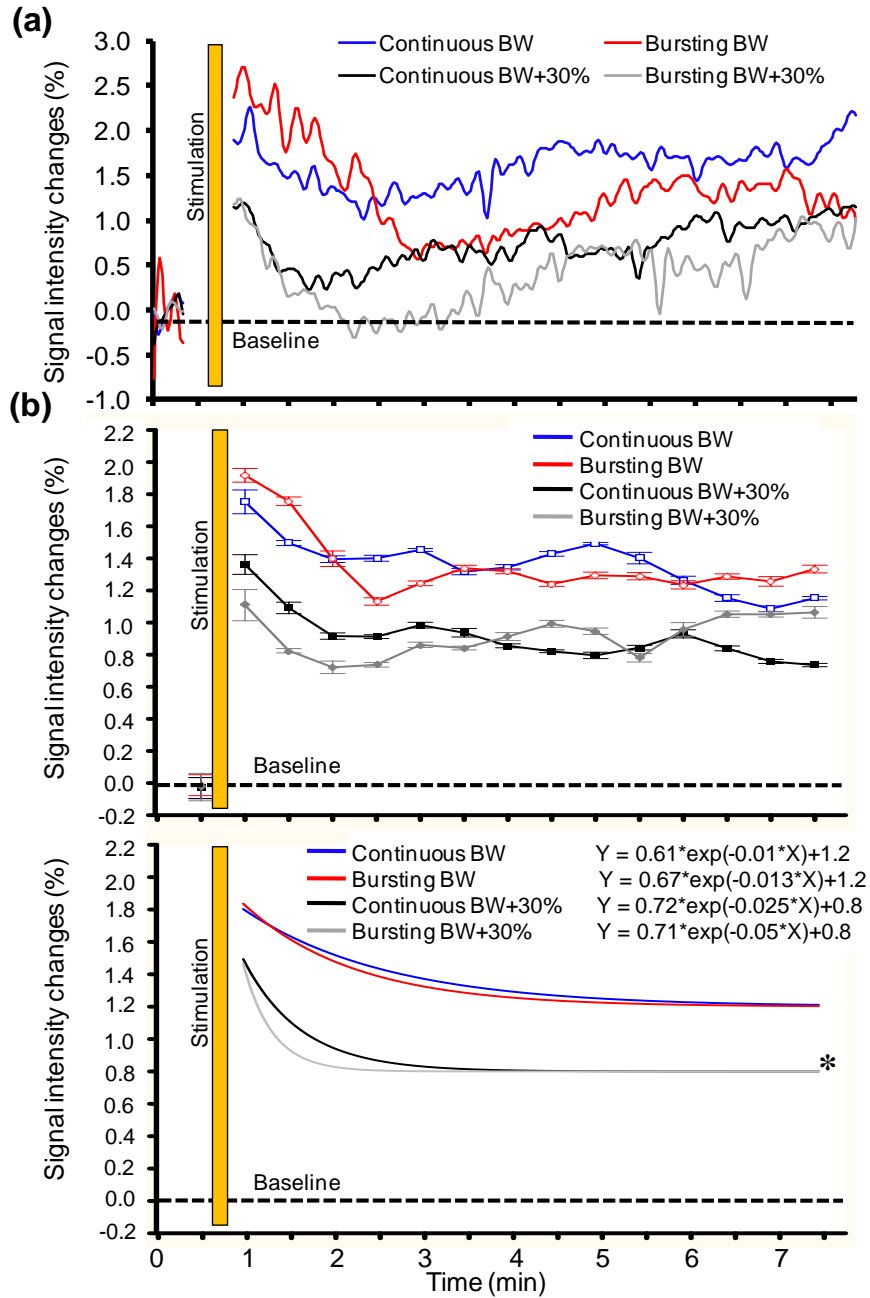


**Figure 6.** Changes in tissue oxygenation induced by bilateral continuous and bilateral bursting IES under normal and increased loading conditions. (a) Average change in signal intensity (%) from baseline. No data were quantified during the stimulation/contraction period. (b) *Top*: comparison of time points after stimulation against baseline under both loading conditions (BW and BW + 30%). Time points were grouped in 30 s time windows for comparison. (b) *Bottom*: exponential decay curves fitted for data from time points after contraction for *continuous* IES with BW, *continuous* IES with BW + 30%, *bursting* IES with BW, and *bursting* IES with BW + 30% protocols. \* Denotes significant difference.

The effect of a chair push-up on tissue oxygenation was compared to the pattern of tissue oxygenation produced by the bilateral continuous IES protocol. The average changes in signal intensity due to both pressure relief approaches are shown for one volunteer in **figure 7A**. Both protocols generated an immediate increase in signal intensity following the IES-elicited contraction or chair push-up. The increase in signal intensity was maintained for the duration of the scan time.

After both the IES and chair push-up maneuvers, all time points had signal intensities that were significantly higher than baseline (**figure 7B, top**). A comparison of the exponential decay curves (**Figure 7B, bottom**) revealed that the signal intensity generated by the bilateral continuous IES protocol was significantly higher than that produced by the chair push-up.

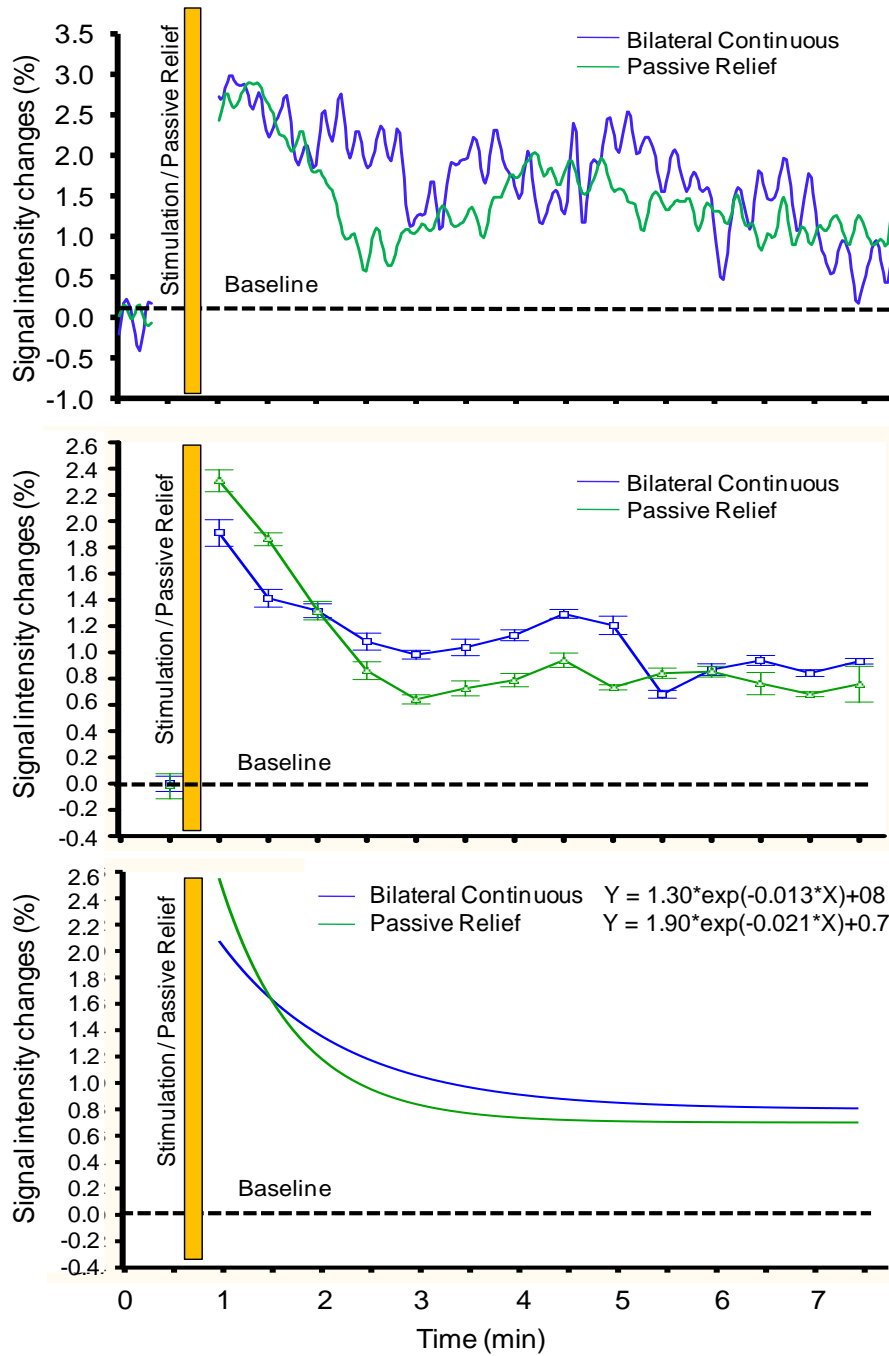


**Figure 7.** Changes in tissue oxygenation induced by bilateral continuous IES and chair push-ups under normal loading conditions. (a) Average change in signal intensity (%) from baseline. (b) *Top*: comparison of time points after stimulation/conventional relief and baseline for *bilateral continuous* IES and *chair push-ups*. Time points were grouped in 30 s time windows for comparison. (b) *Bottom*: exponential decay curves fitted for data from time points after contraction for *bilateral continuous* IES and for *chair push-up* protocol.

In summary, bilateral IES produced prolonged increases in tissue oxygenation throughout the gluteus maximus muscles under both natural and increased loading conditions. Interestingly, IES resulted in larger increases in tissue oxygenation than voluntary contractions. Moreover, for both natural and increased loading conditions, the bilateral continuous IES protocol was more effective in producing elevated and sustained increases in tissue oxygenation than the conventional chair push-up maneuver for pressure relief.

#### *1.4.2.3 Perception of Discomfort due to Sitting Pressure and IES*

Information was obtained regarding the volunteers' perceived discomfort due to prolonged sitting (~2 hrs), as well as perceived changes in discomfort due to the various IES protocols, voluntary contraction and chair push-up. The level of discomfort due to sitting increased in all volunteers as the experimental session progressed. **Figure 8A** shows the median discomfort level reported before each trial by the volunteers who participated in the first set of experiments which focused on testing different IES protocols without additional loading. **Figure 8B** summarizes the average median scores of perceived discomfort before, during and after IES-induced or voluntary contractions from these volunteers. The levels of perceived discomfort during and at the end of all 4 IES protocols were significantly lower than the discomfort perceived before the application of IES. Moreover, all IES protocols produced a similar reduction in perceived discomfort during and at the end of the "ON" phase of IES. In contrast, voluntary contractions did not produce significant changes in discomfort level during or at

the end of the contraction relative to pre-contraction levels ( $p = 0.08$ ).

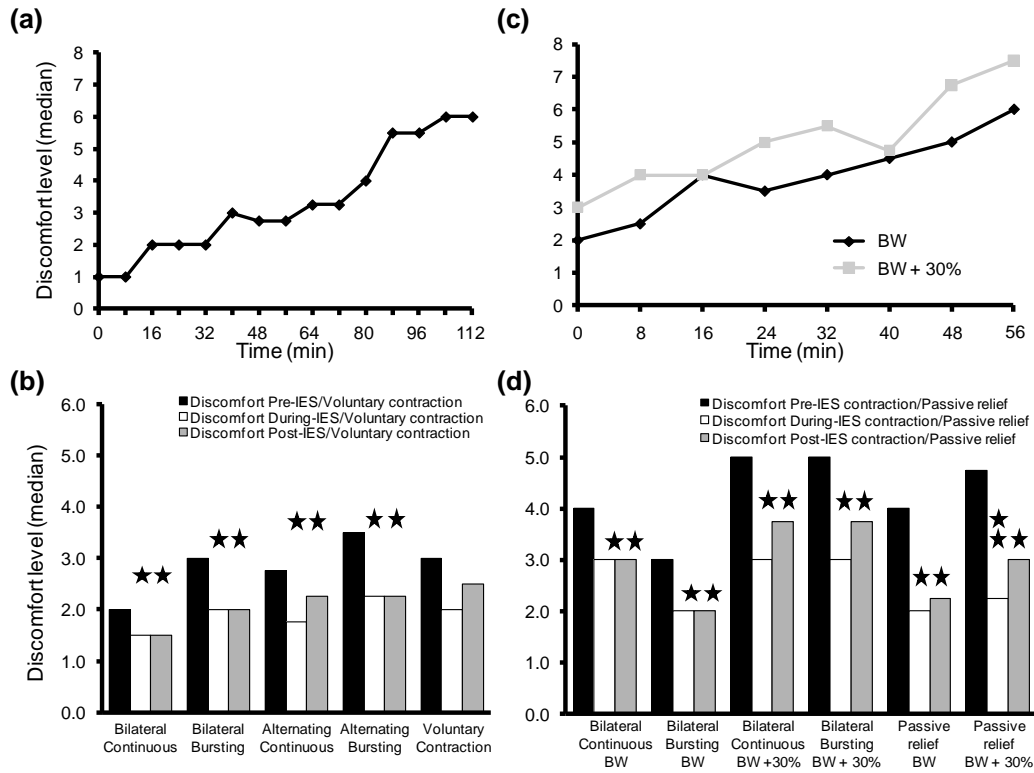


**Figure 8.** Perception of discomfort due to prolonged sitting and pressure relief protocols. (a) Median level of discomfort for all volunteers in group 1 as time progressed during the experimental session. (b) Comparison of discomfort levels before, during, and after the use of IES for each protocol in group 1. *Star* denotes a significant difference from discomfort level perceived before the use of IES. (c) Median level of discomfort for all volunteers in group 2 as time progressed during the experimental session. *Black line* corresponds to discomfort level as result of natural BW. *Gray line* corresponds to discomfort level as a result of additional loading (BW + 30%). (d) Comparison of discomfort levels before, during, and after the use of IES for each protocol in group 1. *Star* denotes a significant difference from discomfort level perceived before the use of IES. *Star* denotes a significant difference from discomfort level perceived both, before and during the use of IES.

Electrical stimulation during the “ON” phase of all IES protocols did not produce an increase in skin discomfort ( $p = 0.73$ ). Furthermore, the duration of reduction in perceived discomfort following the IES-induced contractions was similar for all IES protocols and voluntary contractions ( $p = 0.94$ ). Nonetheless, when asked about their general preference regarding the perceived effectiveness

of the IES protocols in reducing discomfort, all volunteers chose the bilateral protocols (4 continuous, 2 bursting) over the alternating protocols. All volunteers also preferred IES over voluntary contractions for reducing the discomfort produced by prolonged sitting.

As expected, increased loading on the ischial tuberosities in the second set of 6 volunteers increased the level of perceived discomfort due to prolonged sitting (**figure 8C**). For most time points during the experimental session, the perceived discomfort with additional weight ( $BW \pm 30\%$ ) was 1.5 to 2.5 levels higher than that with natural BW. The average median responses of discomfort levels obtained throughout the experimental session in these volunteers are summarized in **figure 8D**. Under both loading conditions, a significant reduction in perceived discomfort was reported during and after the bilateral IES protocols (**figure 9D**). Similarly, chair push-ups induced a significant reduction in perceived discomfort under both loading conditions. Similar to the results reported by the volunteers participating in the first set of experiments, electrical stimulation during the “ON” phase of IES did not increase the level of perceived skin discomfort ( $p = 0.88$ ). Furthermore, there were no significant differences ( $p = 0.68$ ) in the duration of reduction in perceived discomfort produced by the IES or chair push-up protocols.

Five of the six volunteers subjected to increased loading at the ischial tuberosities preferred the bilateral continuous IES protocol over the bilateral

bursting protocol, particularly in the presence of the extra load. While the chair push-up was perceived to reduce discomfort in a similar amount to the IES protocols, pushing up on the chair and holding that position for 10 sec was considered straining for most volunteers, especially with the additional load.

In summary, all IES protocols were effective in reducing perceived discomfort due to prolonged sitting. Volunteers preferred the bilateral protocols over the alternating protocols. Interestingly, IES was found to be more effective in reducing perceived discomfort than voluntary contractions. In the presence of increased loading, IES continued to be effective in reducing the level of perceived discomfort. While the reduction in perceived discomfort and its duration were similar to those obtained with the chair push-up pressure relief maneuver, all volunteers preferred IES for relief from discomfort due to prolonged sitting.

## **1.5 Discussion**

### *1.5.1 Overview*

The goal of this study was to identify the effects of different intermittent electrical stimulation protocols and identify those best suited for preventing the formation of deep pressure ulcers. The effects of IES were compared to voluntary contractions and conventional pressure relief maneuvers that resembled the repositioning performed by able-bodied individuals and pressure relieving exercises performed by wheelchair users, respectively.

### *1.5.2 IES decreases pressure around bony prominences*

Pressure measured at the seating interface is dependent on several factors such as body weight, body build, geometry of the ischial tuberosities, and the type of surface used to sit. For this study, the average superficial pressure under the ischial tuberosities ranged from 6.8 to 23.7 kPa, which corresponded to a range of ~70 – 80% of each person's body weight (given an ischial tuberosity surface area of ~3 cm<sup>2</sup>). Although the understanding of pressure ulcer etiology, in particular that of DTI has improved over the years, the exact mechanisms that cause DTI are still not fully understood.

An aspect of pressure ulcer etiology that has received particular attention lately is the extent of muscle damage caused directly by the mechanical deformation of the tissue. There is growing evidence that, especially in the earliest stages of DTI development (first 2 hrs), mechanical deformation may be the primary cause of tissue injury [44]. To better assess individuals at risk of developing DTI it is necessary to identify the pressure at the bone-muscle interface, and its relationship to the externally measured pressure at the seating interface. Obtaining a direct measurement of internal pressure (bone-muscle interface) is not possible without invasive procedures; however, estimates have been made through the use of finite element modeling [21, 45-46]. The overall consensus of these computer models is that internal pressures at the bone-muscle interface are likely to be higher than those measured at the seating interface. This suggests that superficial pressure measurements should not be the only

consideration when assessing individuals at risk of developing DTI [30, 47]. Nonetheless, measuring superficial pressure is relatively easy and can be routinely performed in a clinical setting. In addition, given that internal pressure is still dependent to a degree on superficial pressure, these measurements can provide valuable information regarding the effectiveness of interventions aimed at preventing the onset of DTI.

The novelty and significance of the current work lies in the pattern of stimulation used to elicit contractions in the gluteus muscles of immobilized individuals. Able-bodied individuals typically reposition themselves every 6 – 9 minutes as a result of discomfort from prolonged sitting [48-49]. Trying to mimic this repositioning pattern, IES stimulates the gluteus muscles for a short duration of time (5 – 15 sec) every 5 – 10 minutes. This intermittent use of electrical stimulation reduces the chance of fatiguing the muscles in users with SCI, whom as a result of the spinal injury often have muscles which are severely atrophied and highly fatigable, while still providing all the beneficial effects of each contraction.

The use of electrical stimulation as a prophylactic intervention for pressure ulcers was originally proposed by Levine et al in studies in both able-bodied subjects as well as subjects with spinal cord injury [50-52]. In those studies each electrical stimulation-induced contraction significantly reduced superficial pressure under the ischial tuberosities, while at the same time increasing it in the

surrounding areas. More recently, van Londen et al. [53] showed very similar results in a group of volunteers with SCI.

The main difference between IES and these previous electrical stimulation paradigms is the pattern of stimulation. For this study, IES was applied every 7 minutes. When IES was applied simultaneously to both the left and right gluteus muscles, our results were in accord with those reported by Levine et al. [51], and van Londen et al. [53]. In the same manner, when IES was applied alternatively to one side first and then to the other, our results agree with those reported by van Londen et al. [53]. Unlike findings from these studies, muscle fatigue did not develop with IES as measured by the force generated during each muscle contraction, suggesting that it can be applied for long durations of time (e.g., throughout the hours of sitting). Moreover, we have extended the above studies by testing how superficial pressure is redistributed as a result of two different patterns of muscle contractions. In these additional protocols, stimulation was applied to induce three short contractions for the duration of the “ON” phase instead of a single strong contraction. This bursting protocol was applied both simultaneously and in an alternating fashion between the left and right gluteus muscles.

In all IES protocols tested, we observed a significant reduction of pressure under the ischial tuberosities and an increase in pressure in the surrounding areas. The redistribution of pressure was also comparable to, or better than that achieved

by voluntary contractions. The effectiveness of IES in redistributing superficial pressure was maintained even under the increased superficial pressure generated by the additional load placed on the volunteers. This indicates that IES can effectively redistribute at least up to 17.27 kPa of pressure. While it is possible that IES could become ineffective in redistributing superficial pressure with loading levels higher than those tested in this study, the tests were performed with the volunteers seated on a lightly padded office chair. Given that people using wheelchairs typically sit on specialized cushions which greatly reduce superficial pressure, such high levels of superficial pressure are unlikely to arise in the majority of wheelchair users.

The chair push-ups, similar to those performed by wheelchair users, completely relieved superficial pressure as expected; however, although in good health and average fitness, all volunteers struggled to maintain the push-up position for the required 10 seconds. This was exacerbated in instances where push-up trials occurred back to back, even with the 7 min of rest in between. This highlights one of the difficulties people with SCI face in performing some of the recommended repositioning maneuvers to alleviate pressure, and may partly explain the consistent pressure ulcer incidence rates reported among this population over the years [54-56].

In a similar study conducted in our laboratory, Gyawali et al.[37] tested the effects of the bursting and continuous IES protocols in volunteers with SCI

who had varying degrees of muscle atrophy, and were seated on a specialized wheelchair cushion. The effectiveness of IES in redistributing pressure in those volunteers was similar to the one reported in this study. This suggests that the effectiveness of IES-induced contractions to redistribute superficial pressure is not dependent upon muscle mass, as these results were shown in volunteers with atrophied muscles.

### *1.5.3 IES increases tissue oxygenation in compressed muscles*

When muscle becomes compressed, inflow and outflow of blood in the compressed tissue is compromised due to the occlusion of capillaries and major blood vessels. This ischemia prevents the exchange of oxygen, nutrients, and metabolic waste required to maintain proper cellular health, leading to cellular damage. Paradoxically, restoration of blood flow after prolonged periods of ischemia can lead to further injury as a result of reperfusion injury. The role of ischemia/reperfusion injury in pressure ulcer development has been the focus of much of the literature addressing pressure ulcer etiology [22, 57-58].

Although it was believed that damage initiated both in the deep muscle and skin simultaneously [22-24], it is now accepted that muscle is more prone to damage due to ischemia/reperfusion injury than skin [18, 29]. The reason for this increased muscle susceptibility is that muscle has a higher metabolic demand, thus is more vascularized than skin. To assess the effectiveness of IES in preventing DTI formation, it was also necessary to obtain a measurement of deep

tissue oxygenation and measure the changes generated by each IES-elicited contraction.

Our results show that each IES-elicited contraction causes tissue oxygenation levels to increase significantly, and *to remain elevated* for several minutes. These results are important because it has been suggested that the compressed muscles need to be fully unloaded in order to properly restore blood flow and prevent pressure ulcer development [59-60]. Our results demonstrate that the oxygenation levels achieved by IES-induced contractions are comparable to those generated by fully unloading the muscles, despite the fact that the target muscles remain compressed to some degree. Gyawali et al. reported similar changes in tissue oxygenation levels as a result of IES-elicited contractions when IES was tested in volunteers with SCI [37].

The rapid increase in tissue oxygenation immediately after the IES-induced contractions is likely a result of reactive hyperemia or to the pumping effect of muscular contractions. The sustained increase in tissue oxygenation which lasted for the duration of the acquisition time, however, is not completely understood. Changes in blood flow due to reactive hyperemia only last for seconds. Jordan et al. [42] suggested that the prolonged duration of elevated oxygen levels is due to a decrease in oxygen demand by the muscle, which is regulated by nitric oxide. As muscles exercise, nitric oxide is produced, which can inhibit mitochondrial respiration, reducing the consumption of oxygen by the

muscle. With a lower demand for oxygen, the surplus of oxygen that comes into the tissue immediately after the muscle contraction lasts longer, thus giving a higher  $T_2^*$  signal intensity. Because of this, the long-term effect of active contractions should be a lowered oxygen demand, making the muscle more resistant to ischemic injury. It has also been shown that in people with SCI, the long-term use of electrical stimulation can improve tissue health by reducing atrophy and improving partial pressure levels of transcutaneous oxygen[61-62]. This suggests that IES could be an effective alternative where repositioning is not possible, especially in individuals who are incapable of performing the recommended exercises to relieve pressure passively.

#### *1.5.4 IES reduces perceived discomfort due to sitting*

To date, the effect of pressure ulcer prevention techniques on sitting discomfort has been overlooked, likely due to the fact that pressure ulcer research usually focuses on individuals with diminished sensation. To the best of our knowledge, this study is the first to assess in able-bodied individuals the changes in sitting discomfort that are generated by an intervention aimed at preventing the formation of DTI. This is significant because, in able-bodied individuals, the development of discomfort in the compressed tissue (e.g., gluteus muscles) is the signal that encourages the person to subconsciously change position after prolonged sitting. Various factors which can contribute to the generation of discomfort in the compressed muscle include the buildup of metabolic waste, and the “pins and needles” or numbness sensation that accompanies transient ischemia

caused by alterations in the activity of mechanosensitive neurons [63]. After repositioning, it is likely that the influx of fresh oxygenated blood and the removal of metabolic waste from the previously compressed region help to alleviate the discomfort, resetting the counter, figuratively speaking, before the next repositioning event. It is this mechanism that allows able-bodied individuals to remain seated for several hours a day whether at home, work, or while traveling without developing pressure ulcers.

All of the IES-protocols tested generated a reduction in the level of sitting discomfort perceived by the study participants. This reduction took place even in trials where a higher initial discomfort was reported as the result of placing an additional load on the volunteers. An unexpected finding was that the reduction in discomfort generated by the different IES-protocols, and the duration of this reduction, were perceived to be as good as or even better than those generated by voluntary contractions or complete unloading through chair push-ups. This effect became more evident in the latter parts of the experimental session, when some volunteers were impatiently requesting to know when the next IES bout would start in order to alleviate sitting discomfort.

The lasting effect of the elevated oxygenation levels in the muscle can explain the lasting effects in the relief of discomfort after the contraction ends. With an increased pool of oxygen available for the muscle, the production of metabolic waste that results from muscular anaerobic respiration should be

reduced, in turn slowing down the buildup of discomfort. Additionally, the reduction in pressure under the ischial tuberosities during each IES-elicited contraction is likely to change the mechanical stress levels within the muscle.

The reduction in sitting discomfort is important because it suggests that the 10 second IES-induced contraction may be enough to restore the muscle's capability to withstand another period of sustained loading.

#### *1.5.5 Conclusion*

This study demonstrated that IES is effective in reducing superficial pressure at the ischial tuberosities while sitting, increasing oxygenation levels in the compressed gluteus maximus muscles, and providing relief from discomfort due to prolonged sitting. The benefits of the bilateral IES protocols were similar to, and at times superseded those produced by voluntary contractions and conventional pressure relief maneuvers. The long-term effects of periodical active contractions produced by IES could include improved muscle conditioning and resistance to breakdown due to prolonged compression. The use of IES in combination with existing specialized surfaces provides an exciting new avenue for effectively reducing the incidence of DTI and pressure ulcers in people with compromised mobility and sensation.

## 1.6 REFERENCES

- [1] R. M. Woolsey and J. D. McGarry, "The cause, prevention, and treatment of pressure sores," *Neurologic Clinics.*, vol. 9, pp. 797-808, 1991.
- [2] J. M. Zanca, D. M. Brienza, D. Berlowitz, R. G. Bennett, C. H. Lyder, and N. P. U. A. Panel., "Pressure ulcer research funding in America: creation and analysis of an on-line database," *Advances in Skin & Wound Care*, vol. 16, pp. 190-7, 2003.
- [3] H. Sanada, G. Nakagami, Y. Mizokami, Y. Minami, A. Yamamoto, M. Oe, T. Kaitani, and S. Iizaka, "Evaluating the effect of the new incentive system for high-risk pressure ulcer patients on wound healing and cost-effectiveness: A cohort study.," *Intenrational Journal of Nursing Studies*, vol. 4, pp. 279 - 286, 2010.
- [4] T. A. Krouskop, P. C. Noble, S. L. Garber, and W. A. Spencer, "The effectiveness of preventive management in reducing the occurrence of pressure sores," *Journal of Rehabilitation Research & Development*, vol. 20, pp. 74-83, 1983.
- [5] J. Schiffman, M. S. Golinko, A. Yan, A. Flattau, M. Tomic-Canic, and H. Brem, "Operative debridement of pressure ulcers.," *World Journal of Surgery*, vol. 33, pp. 1396 - 1402, 2009.
- [6] P. W. Smith, J. M. Black, and S. B. Black, "Infected pressure ulcers in the long-term-care facility.," *Infection Control and Hospital Epidemiology*, vol. 20, pp. 358 - 361, 1999.
- [7] H. Rischbieth, M. Jelbart, and R. Marshall, "Neuromuscular electrical stimulation keeps a tetraplegic subject in his chair: a case study," *Spinal Cord.*, vol. 36, pp. 443-5, 1998.
- [8] J. C. Grip and C. T. Merbitz, "Wheelchair-based mobile measurement of behavior for pressure sore prevention," *Computer Methods & Programs in Biomedicine*, vol. 22, pp. 137-44, 1986.
- [9] G. Bennett, C. Dealey, and J. Posnett, "The cost of pressure ulcers in the UK," *Age & Ageing*, vol. 33, pp. 230-5, 2004.
- [10] J. L. Severens, J. M. Habraken, S. Duivenvoorden, and C. M. Frederiks, "The cost of illness of pressure ulcers in The Netherlands.," *Advances in Skin and Wound Care*, vol. 15, pp. 72 - 77, 2002.
- [11] R. Salcido, S. B. Fisher, J. C. Donofrio, M. Bieschke, C. Knapp, R. Liang, E. K. LeGrand, and J. M. Carney, "An animal model and computer-controlled surface pressure delivery system for the production of pressure ulcers," *Journal of Rehabilitation Research & Development*, vol. 32, pp. 149-61, 1995.
- [12] M. A. Ankrom, R. G. Bennett, S. Sprigle, D. Langemo, J. M. Black, D. R. Berlowitz, C. H. Lyder, and N. P. U. A. Panel., "Pressure-related deep tissue injury under intact skin and the current pressure ulcer staging systems.," *Advances in Skin and Wound Care*, vol. 18, pp. 35 - 42, 2005.
- [13] J. M. Black and N. P. U. A. Panel., "Moving toward consensus on deep tissue injury and pressure ulcer staging.," *Advances in Skin and Wound Care*, vol. 18, pp. 415 - 416, 418, 420 - 421, 2005.
- [14] H. M. Finestone, S. P. Levine, G. A. Carlson, K. A. Chizinsky, and R. L. Kett, "Erythema and skin temperature following continuous sitting in spinal cord injured individuals," *Journal of Rehabilitation Research & Development*, vol. 28, pp. 27-32, 1991.
- [15] R. H. Guthrie and D. Goulian, "Decubitus ulcers: Prevention and Treatment," *Geriatrics*, vol. 28, pp. 67-71, 1973.
- [16] A. E. Swarts, T. A. Krouskop, and D. R. Smith, "Tissue pressure management in the vocational setting," *Archives of Physical Medicine & Rehabilitation*, vol. 69, pp. 97-100, 1988.
- [17] A. Gefen, "Risk factors for a pressure-related deep tissue injury: a theoretical model.," *Medical and Biological Engineering and Computing*, vol. 45, pp. 563 - 573, 2007.
- [18] C. V. Bouten, C. W. Oomens, F. P. Baaijens, and D. L. Bader, "The etiology of pressure ulcers: skin deep or muscle bound?," *Archives of Physical Medicine and Rehabilitation*, vol. 84, pp. 616-619, 2003.
- [19] R. G. Breuls, C. V. Bouten, C. W. Oomens, D. L. Bader, and F. P. Baaijens, "Compression induced cell damage in engineered muscle tissue: an in vitro model to

- study pressure ulcer aetiology.," *Annals of Biomedical Engineering*, vol. 31, pp. 1357 - 1364, 2003.
- [20] T. Nagel, S. Loerakker, and C. W. Oomens, "A theoretical model to study the effects of cellular stiffening on the damage evolution in deep tissue injury.," *Computer Methods in Biomechanics and Biomedical Engineering*, vol. 12, pp. 585 - 597, 2009.
- [21] E. Linder-Ganz, N. Shabshin, Y. Itzchak, and A. Gefen, "Assessment of mechanical conditions in sub-dermal tissues during sitting: A combined experimental-MRI and finite element approach.," *Journal of Biomechanics*, vol. 40, pp. 1443 - 1454, 2007.
- [22] M. Kosiak, "Etiology and pathology of ischemic ulcers," *Archives of Physical Medicine & Rehabilitation*, vol. 40, pp. 62-9, 1959.
- [23] M. Kosiak, "Etiology of decubitus ulcers," *Archives of Physical Medicine & Rehabilitation*, vol. 42, pp. 19-29, 1961.
- [24] M. Kosiak, W. G. Kubicek, M. Olson, J. N. Danz, and F. J. Kottke, "Evaluation of pressure as factor in production of ischial ulcers," *Archives of Physical Medicine & Rehabilitation*, vol. 39, pp. 623-629, 1958.
- [25] T. A. Krouskop, "A synthesis of the factors that contribute to pressure sore formation.," *Medical Hypotheses*, vol. 11, pp. 255 - 267, 1983.
- [26] P. A. Grace, "Ischaemia-reperfusion injury," *British Journal of Surgery*, vol. 81, pp. 637-47, 1994.
- [27] D. C. Gute, T. Ishida, K. Yarimizu, and R. J. Korthuis, "Inflammatory responses to ischemia and reperfusion in skeletal muscle," *Molecular & Cellular Biochemistry*, vol. 179, pp. 169-87, 1998.
- [28] S. Tsuji, S. Ichioka, N. Sekiya, and T. Nakatsuka, "Analysis of ischemia-reperfusion injury in a microcirculatory model of pressure ulcers," *Wound Repair and Regeneration*, vol. 13, pp. 209-215, 2005.
- [29] R. Labbe, T. Lindsay, and P. M. Walker, "The extent and distribution of skeletal muscle necrosis after graded periods of complete ischemia.," *Journal of Vascular Surgery*, vol. 6, pp. 152 - 157, 1987.
- [30] E. Linder-Ganz and A. Gefen, "Stress analyses coupled with damage laws to determine biomechanical risk factors for deep tissue injury during sitting.," *Journal of Biomechanical Engineering*, vol. 131, pp. 011003, 2009.
- [31] M. H. Liu, D. R. Grimm, V. Teodorescu, S. J. Kronowitz, and W. A. Bauman, "Transcutaneous oxygen tension in subjects with tetraplegia with and without pressure ulcers: a preliminary report," *Journal of Rehabilitation Research & Development*, vol. 36, pp. 202-6, 1999.
- [32] E. McInnes, S. E. Bell-Syer, J. C. Dumville, R. Legood, and N. A. Cullum, "Support surfaces for pressure ulcer prevention.," *Cochrane Database of Systematic Reviews*, pp. CD001735, 2008.
- [33] T. A. Conine, A. K. Choi, and R. Lim, "The user-friendliness of protective support surfaces in prevention of pressure sores," *Rehabilitation Nursing*, vol. 14, pp. 261-3, 1989.
- [34] G. W. White, R. M. Mathews, and S. B. Fawcett, "Reducing risk of pressure sores: effects of watch prompts and alarm avoidance on wheelchair push-ups," *Journal of Applied Behavior Analysis*, vol. 22, pp. 287-95, 1989.
- [35] C. T. Merbitz, R. B. King, J. Bleiberg, and J. C. Grip, "Wheelchair push-ups: measuring pressure relief frequency," *Archives of Physical Medicine & Rehabilitation*, vol. 66, pp. 433-8, 1985.
- [36] L. R. Solis, D. P. Hallihan, R. R. Uwiera, R. B. Thompson, E. D. Pehowich, and V. K. Mushahwar, "Prevention of pressure-induced deep tissue injury using intermittent electrical stimulation.," *Journal of Applied Physiology*, vol. 102, pp. 1992-2001, 2007.
- [37] S. Gyawali, L. R. Solis, S. L. Chong, C. A. Curtis, P. Seres, I. Kornelsen, R. B. Thompson, and V. K. Mushahwar, "Intermittent electrical stimulation redistributes pressure and promotes tissue oxygenation in loaded muscles of individuals with spinal cord injury," *Journal of Applied Physiology*, vol. 110, pp. 246 - 255, 2011.
- [38] B. M. Damon, M. C. Wadlington, J. L. Hornberger, and D. A. Lansdown, "Absolute and relative contributions of BOLD effects to the muscle functional MRI signal intensity time

- course: effect of exercise intensity.," *Magnetic Resonance in Imaging*, vol. 58, pp. 335 - 345, 2007.
- [39] B. M. Damon, J. L. Hornberger, M. C. Wadington, D. A. Lansdown, and J. A. Kent-Braun, "Dual gradient-echo MRI of post-contraction changes in skeletal muscle blood volume and oxygenation.," *Magnetic Resonance in Medicine*, vol. 57, pp. 670 - 679, 2007.
- [40] H. P. Ledermann, H. G. Heidecker, A. C. Schulte, C. Thalhammer, M. Aschwanden, K. A. Jaeger, K. Scheffler, and D. Bilecen, "Calf muscles imaged at BOLD MR: correlation with TcPO<sub>2</sub> and flowmetry measurements during ischemia and reactive hyperemia--initial experience.," *Radiology*, vol. 241, pp. 477 - 484, 2006.
- [41] R. A. Meyer, T. F. Towse, R. W. Reid, R. C. Jayaraman, R. W. Wiseman, and K. K. McCully, "BOLD MRI mapping of transient hyperemia in skeletal muscle after single contractions.," *NMR in Biomedicine*, vol. 17, pp. 392 - 398, 2004.
- [42] B. F. Jordan, J. Z. Kimpalou, N. Beghein, C. Dessy, O. Feron, and B. Gallez, "Contribution of oxygenation to BOLD contrast in exercising muscle," *Magnetic Resonance in Medicine*, vol. 52, pp. 391-6, 2004.
- [43] T. F. Towse, J. M. Slade, and R. A. Meyer, "Effect of physical activity on MRI-measured blood oxygen level-dependent transients in skeletal muscle after brief contractions.," *Journal of Applied Physiology*, vol. 99, pp. 715 - 722, 2005.
- [44] A. Stekelenburg, D. Gawlitta, D. L. Bader, and C. W. Oomens, "Deep tissue injury: how deep is our understanding?," *Archives of Physical Medicine and Rehabilitation*, vol. 89, pp. 1410 - 1413, 2008.
- [45] C. W. Oomens, O. F. Bressers, E. M. Bosboom, C. V. Bouten, and D. L. Blader, "Can loaded interface characteristics influence strain distributions in muscle adjacent to bony prominences?," *Computer Methods in Biomechanics & Biomedical Engineering*, vol. 6, pp. 171-80, 2003.
- [46] M. M. Verver, J. van Hoof, C. W. Oomens, J. S. Wismans, and F. P. Baaijens, "A finite element model of the human buttocks for prediction of seat pressure distributions," *Computer Methods in Biomechanics & Biomedical Engineering*, vol. 7, pp. 193-203, 2004.
- [47] A. Gefen and J. Levine, "The false premise in measuring body-support interface pressures for preventing serious pressure ulcers.," *Journal of Medical Engineering & Technology*, vol. 31, pp. 375 - 380, 2007.
- [48] E. Linder-Ganz, M. Scheinowitz, Z. Yizhar, S. S. Margulies, and A. Gefen, "How do normals move during prolonged wheelchair-sitting?," *Technology and Healthcare*, vol. 15, pp. 195 - 202, 2007.
- [49] J. Reenalda, P. Van Geffen, M. Nederhand, M. Jannink, M. IJzerman, and H. Rietman, "Analysis of healthy sitting behavior: interface pressure distribution and subcutaneous tissue oxygenation.," *Journal of Rehabilitation Research and Development*, vol. 46, pp. 577 - 586, 2009.
- [50] S. P. Levine, R. L. Kett, M. D. Gross, B. A. Wilson, P. S. Cederna, and J. E. Juni, "Blood flow in the gluteus maximus of seated individuals during electrical muscle stimulation," *Archives of Physical Medicine & Rehabilitation*, vol. 71, pp. 682-6, 1990.
- [51] S. P. Levine, R. L. Kett, P. S. Cederna, L. D. Bowers, and S. V. Brooks, "Electrical muscle stimulation for pressure variation at the seating interface," *Journal of Rehabilitation Research & Development*, vol. 26, pp. 1-8, 1989.
- [52] S. P. Levine, R. L. Kett, P. S. Cederna, and S. V. Brooks, "Electric muscle stimulation for pressure sore prevention: tissue shape variation," *Archives of Physical Medicine & Rehabilitation*, vol. 71, pp. 210-5, 1990.
- [53] A. van Londen, M. Herwegh, C. H. van der Zee, A. Daffertshofer, C. A. Smit, A. Niezen, and T. W. Janssen, "The effect of surface electric stimulation of the gluteal muscles on the interface pressure in seated people with spinal cord injury.," *Archives of Physical Medicine and Rehabilitation*, vol. 89, pp. 1724 - 1732, 2008.
- [54] J. Cuddigan, D. Berlowitz, and E. A. Ayello, "PRESSURE ULCERS IN AMERICA: Prevalence, Incidence, and Implications for the future: An executive summary of the

- National Pressure Ulcer Advisory Panel Monograph," *Advances in Skin & Wound Care.*, vol. 14, pp. 208-215, 2001.
- [55] D. K. Langemo, J. Anderson, and C. Volden, "Uncovering pressure ulcer incidence," *Nursing Management.*, vol. 34, pp. 54-7, 2003.
- [56] E. S. Marks and C. L. Cogbill, "Surgical therapy of decubitus ulcers in the paraplegic patient.," *Annals of Surgery*, vol. 132, pp. 994 - 1002, 1950.
- [57] S. M. Peirce, T. C. Skalak, and G. T. Rodeheaver, "Ischemia-reperfusion injury in chronic pressure ulcer formation: a skin model in the rat," *Wound Repair and Regeneration*, vol. 8, pp. 68-76, 2000.
- [58] A. Stekelenburg, G. J. Strijkers, H. Parusel, D. L. Bader, K. Nicolay, and C. W. Oomens, "Role of ischemia and deformation in the onset of compression-induced deep tissue injury: MRI-based studies in a rat model.," *Journal of Applied Physiology*, vol. 102, pp. 2002-2011, 2007.
- [59] A. C. Ferguson, J. F. Keating, M. A. Delargy, and B. J. Andrews, "Reduction of seating pressure using FES in patients with spinal cord injury. A preliminary report," *Paraplegia*, vol. 30, pp. 474-8, 1992.
- [60] H. M. Kaplan, G. E. Loeb, L. L. Baker, and R. Davoodi, "BION™ Active Seating for Pressure Ulcer Prevention: Surface Stimulation & Finite Element Modeling for Planning Treatments," presented at 11<sup>th</sup> Annual Conference of the International FES Society, Zao, Japan, 2006.
- [61] K. M. Bogie and R. J. Triolo, "Effects of regular use of neuromuscular electrical stimulation on tissue health," *Journal of Rehabilitation Research & Development*, vol. 40, pp. 469-75, 2003.
- [62] L. Giangregorio and N. McCartney, "Bone loss and muscle atrophy in spinal cord injury: epidemiology, fracture prediction, and rehabilitation strategies.," *The Journal of Spinal Cord Medicine*, vol. 29, pp. 489 - 500, 2006.
- [63] R. C. Lennertz, M. Tsunozaki, D. M. Bautista, and C. L. Stucky, "Physiological Basis of Tingling Paresthesia Evoked by Hydroxy- $\alpha$ -Sanshool.," *Journal of Neuroscience*, vol. 30, pp. 4353 - 4361, 2010.

## CHAPTER 2

# Distribution of Internal Pressure around Bony Prominences: Implications to Deep Tissue Injury and Effectiveness of Intermittent Electrical Stimulation

### 2.2 INTRODUCTION

Pressure ulcers refer to the breakdown of soft tissue around bony prominences in people with reduced mobility or sensation due to prolonged sitting or lying down. These ulcers are particularly prevalent among the elderly, people with mobility impairments due to spinal cord injury, head trauma or multiple sclerosis, those with musculoskeletal diseases, people in coma or those undergoing long surgical procedures. The incidence of pressure ulcers in clinical centers varies, but is as high as 40% in acute care facilities and 39.4% in nursing homes [1-5]. The prevalence of pressure ulcers in people with spinal cord injury is 25-33% [6-21]. Moreover, 80% of people with spinal cord injury develop at least one pressure ulcer following their injury [6]. These ulcers interfere with rehabilitation efforts, disrupt work, and reduce independence.

Pressure ulcers develop at the surface of the skin and progress inwards, or at deep bone-muscle interfaces and progress outwards. Outside-in ulcers develop due to skin abrasion, poor nutrition or hygiene, and excessive skin moisture or dryness [22]. These ulcers are detected via skin inspection and can be prevented early on in their stage of development. Inside-out ulcers, known as deep tissue

injury (DTI), develop due to prolonged loading and deformation of soft tissue trapped between a bony prominence and an external surface [2, 22-28]. Because of their deep origin, these ulcers develop unbeknownst to the individuals or their caregivers. Once skin signs are detected, extensive damage of the underlying tissue would have already occurred.

Pressure in the deep tissue around bony prominences is the primary factor for the development of DTI. Muscle is more susceptible to breakdown due to loading than skin [26-27, 29-31]; nonetheless, there are currently no empirical measures of pressure or strain in tissue located deep around bony prominences. Instead, surface pressure measurements are obtained using pressure mattresses placed between the seated individual and the support surface. The resulting measurements describe the distribution of interfacial pressure around the bony prominences [32-33], but do not provide quantitative assessments of pressure or strain in the deep tissue [28, 34-35].

Computer models of the buttocks in seated individuals indicate that the levels of internal pressure are substantially higher than those measured at the surface [30, 36-38]. Initial validations of these models have been conducted in the thighs of rodents [39]; however, empirical measurements of internal pressure from humans or animal models with pelvic anatomy that closely resembles that of humans are not available. Initial measurements of hydrostatic pressure in the deep tissue of pigs were provided by the seminal work of Le et al [40].

The goals of the present study were twofold. *First*, obtain direct measurements of pressure around the ischial tuberosities of adult pigs subjected to different levels of external loading, and assess the effect of muscle atrophy secondary to spinal cord injury on the levels of internal pressure. *Second*, determine the effect of intermittent electrical stimulation (IES), a novel rehabilitation intervention currently under investigation for the prevention of DTI [32-33, 41-42], on the distribution of internal pressure around bony prominences in healthy and atrophied muscles.

## **2.3 METHODS**

### *2.3.1 Overview*

Acute experiments were conducted in 6 adult, female pigs (Yucatan minipig strain, 45 – 75 kg). All experimental protocols were approved by the University of Alberta Animal Care and Use Committee. At the time of the experiment, 5 animals had intact spinal cords and healthy muscles around the ischial tuberosities. One animal received a hemi-lesion of the spinal cord 4 weeks prior to the experiment, which caused paralysis and muscle atrophy in the ipsilateral hindleg. With the animals in a prone position, controlled levels of pressure were applied to the buttocks region to load the muscles around the ischial tuberosities. Magnetic resonance images (MRIs) of the buttocks and hip regions were obtained to document the anatomical features of the soft tissue under unloaded and loaded conditions, and during muscle contractions induced by IES. Constant levels of external loading were applied using a servo-controlled motor.

Corresponding levels of internal pressure around the ischial tuberosity of the left hindleg were recorded using a catheter with an indwelling pressure transducer near the tip. Upon completion of the mapping of internal pressure, the animals were euthanized with an overdose injection of Euthanyl (i.v., 30mg/kg).

### *2.3.2 Spinal Cord Hemi-transection and Palliative Care*

A hemi-lesion of the spinal cord was induced in one animal at the second lumbar level (L2). This led to the loss of voluntary control of the ipsilateral hind leg, but retained bowel and bladder function. The transection procedure was performed under complete aseptic conditions. The pig was premedicated with a mixture of Ketamine, Glycopyrrolate and Xylazine (22mg/kg, 0.01mg/kg, and 2.2mg/kg, respectively) administered intramuscularly. The trachea was then intubated and isoflurane inhalation anesthesia was administered (2-3% in oxygen). The opioid analgesic, buprenorphine, was administered (0.005mg/kg) and the surgical area was washed with antiseptic soap and rubbed with betadine. A small laminectomy exposing the L2 lumbar segment was performed and a transverse cut was placed in the dura mater using fine ophthalmic scissors. Lidocane (2%) was then injected in the left side of the spinal cord, and the cord was progressively transected dorso-ventrally. The completeness of the hemi-lesion was verified visually and small pieces of Surgicel (Ethicon, Inc. Somerville, NJ, USA) were inserted in the lesion site to reduce the incidence and extent of bleeding. The back wound was sutured shut in layers and the incision site was cleaned with sterile saline and alcohol. Another intravenous injection of

buprenorphine was administered and isoflurane anesthesia was terminated.

The pig recovered in its cage which had been fitted with Tempur-Pedic mattresses in order to reduce the incidence of pressure ulcers in the paralyzed hind leg. Saline (0.9% NaCl) was administered (i.v., 3L per day, for 3 days) to ensure proper hydration, and buprenorphine (i.v., 0.005mg/kg) every eight hours for the first three days post-surgery. Antibiotics (Cephalexin 20mg/kg, orally) were also administered twice per day throughout the post-surgery duration and until the day of the terminal experiment.

### *2.3.3 Animal Preparation and Magnetic Resonance Imaging*

On the day of the terminal experiment, all animals were premedicated with Ketamine, Glycopyrrolate and Xylazine (22mg/kg, 0.01mg/kg, and 2.2mg/kg, respectively) administered intramuscularly. Anesthesia was initially induced using isoflurane anaesthesia (2 - 3% in oxygen) and maintained with sodium pentobarbital (i.v., 10 mg/kg). The pigs were then transported to the Peter S. Allen MR Research Centre at the University of Alberta, and placed inside a 1.5T, one meter-bore magnet (Siemens Sonata Scanner, Siemens Medical Solution, Malvern, Pennsylvania, USA). They were placed in a prone position in an MR-compatible custom-built carrier with the hind legs flexed and tucked under the body such that both the femur and the feet were positioned parallel to the horizontal plane (Figure 1A). Morphological magnetic resonance images (MRIs) of the buttocks region were obtained using a 3D gradient echo imaging sequence

with the following parameters: echo time = 2.33 ms, relaxation time = 4.92 ms, flip angle = 12°, slice thickness = 2.5 mm, number of slices = 104, slice separation = 0 mm, in-plane matrix size = 320 x 320 pixels, field of view = 400 mm x 400 mm, in-plane resolution = 1.25 x 1.25 mm.

Images were obtained when the tissue of the buttocks was unloaded, and when loaded through an indenter to levels corresponding to 25, 50 or 75% of body weight (BW). These levels of loading represented the range of interfacial pressure measured around the buttocks in people sitting on various support surfaces (unpublished data). Images were also obtained during muscle contractions induced by IES in one hind leg. Electrical stimulation was delivered through a pair of 5 cm x 10 cm MR-compatible surface electrodes (Pure Care, Sherwood Park, Alberta, Canada). The cathode was placed over the motor point of the semimembranosus muscle, which in the pig is the muscle that directly overlies the ischial tuberosity. The return electrode was placed rostrally and medially along the pelvis. Trains of biphasic, charge-balanced stimulation pulses, 200  $\mu$ s wide, were delivered at a frequency of 50 Hz using a BioStim NMS+ stimulator (Biomedical Life Systems, California, USA). The amplitude of the pulses was set to the level that produced maximal contractions. The strength of the contractions was assessed visually.

#### 2.3.4 *External Loading and Internal Pressure Mapping*

Loading of the tissue around the ischial tuberosities was achieved using an indenter (10 cm x 30 cm) attached to a feedback-controlled servomotor (Danaher AKM23D, Danaher Motion, Washington DC, USA) (Figure 1A). A force transducer (Interface SMT2-225, Interface Inc., Scottsdale, Arizona, USA) was placed serially between the indenter and shaft of the servomotor and provided the signal for feedback control. The servomotor was supported by a horizontal panel attached to the vertical rod of a drill press that allowed for accurate positioning of the indenter in three planes. To eliminate forward translation during loading, the pelvis was secured through straps to the animal carrier, and the carrier was secured via additional straps to the vertical rod. The base of the rod was heavily loaded and securely anchored to the floor.

A controller was used to maintain a constant loading level to within  $\pm 900$  g of the target load. Readings from the force transducer were sampled every 2 ms by the controller. Following a control signal, the servomotor pushed the indenter at a continuous speed of 0.5 cm/s until the target loading level was reached. At this point, the servomotor was automatically set to a hold position, keeping the indenter in place. If the load dropped below or increased above the target load by 900 g, the servomotor automatically adjusted the position until the target load was reached again. The controller code was developed in the DMC Smart Terminal (Galil Motion Control, Rocklin, California, USA) software environment.

For each target loading level, the distribution of interfacial pressure on the buttocks was measured using a pressure sensing mattress (PX200:36:36, XSensor Technology Corporation, Calgary, Alberta, Canada) placed between the indenter and the surface of the skin (Figure 1A). The mattress had an array of 36 x 36 sensors, each covering an area of 1 cm<sup>2</sup> (1 cm x 1 cm). After removal of the mattress, measurements of internal pressure in the left hind leg proceeded by advancing a pressure sensing catheter (FTS-3011B-0024, Scisense, Ontario, Canada) within a 13.3 cm-long 14 gauge needle (BD Angiocath, BD, Franklin Lakes, NJ, USA) through a grid of holes in the indenter. The solid state pressure sensor was positioned inside the catheter 3 mm from the tip, and pressure measurements were obtained along a 1 cm x 1cm grid of holes in the indenter (Figure 1B, C). The 9 x 13 grid was positioned such that, as much as possible, the second or third row from the top and the second column from the right corresponded to the center of the ischial tuberosity of the left hind leg. One to three rows were available for mapping the internal pressure above (dorsal) or below (ventral) the ischial tuberosity. One column to the right (medial) of the ischial tuberosity and up to twelve columns to the left (lateral) were also available for mapping.

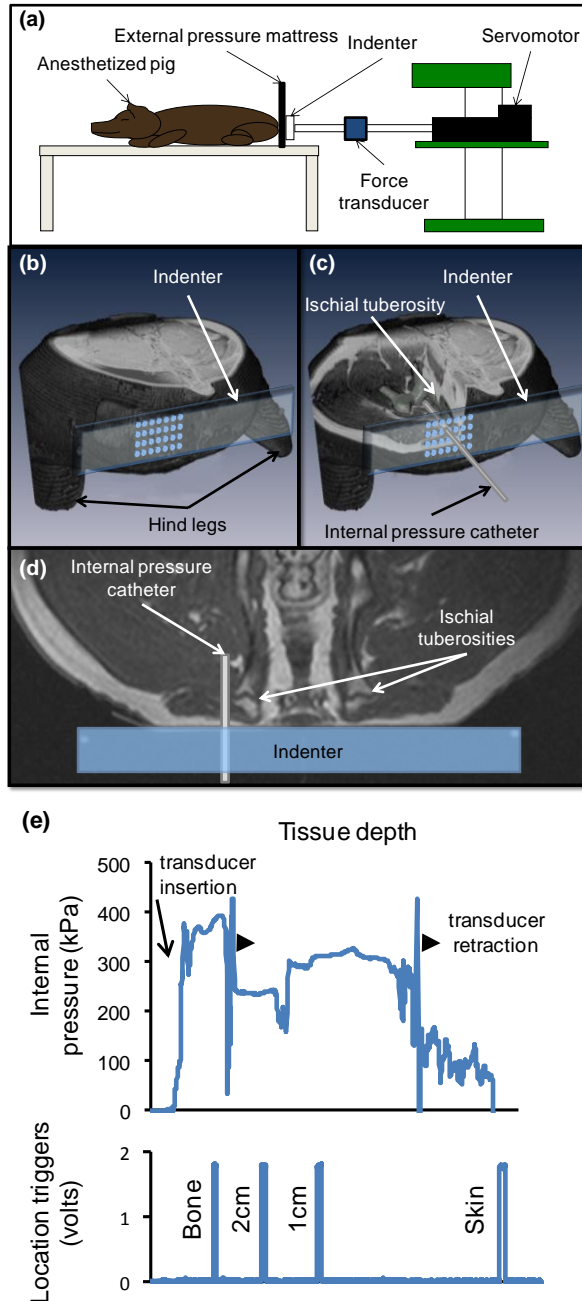


**Figure 1.** Experimental setup. (a) A computer controlled servo motor was used to push an indenter against the buttocks of an anesthetized pig. Loading levels equivalent to 25%, 50%, and 75% BW of each pig were applied to the buttocks. (b, c) A pressure catheter was introduced through small openings (1 mm diameter) in the indenter and into the pig's buttocks. (d) With the buttocks loaded, a map of internal pressure was formed by acquiring measurements at different dorso-ventral, medio-lateral and antero-posterior locations relative to the ischial tuberosity. (e) Top: An example of a raw trace of internal pressure recorded as the pressure transducer was retracted toward the skin from a location next to the bone. Bottom: Trigger signals recorded in conjunction with the raw pressure traces. Each trigger indicates the location, relative to the bone, from which internal pressure measurements were acquired. Arrow indicates the instance of transducer insertion toward the bone; arrow heads indicate two instances of transducer retraction in 1 cm steps through the tissue.

Measurements of internal pressure were obtained every 2 centimeters horizontally and vertically in the plane parallel to the ischial tuberosity. This allowed for adequate mapping of internal pressure under multiple loading levels and IES without causing tissue damage due to repeated catheter insertions in a given location. Thus, measurements under different conditions were obtained from locations that were at most 1 cm apart from each other. Collectively, the measurements provided full characterization of pressure within the soft tissue around the ischial tuberosity.

Once a stable level of external loading was achieved by the servomotor, measurements of internal pressure were taken. For each location on the grid, the 14G needle was advanced to a depth of 9 cm or until the bone was reached (Figure 1D). The pressure sensing catheter was inserted through the length of the needle and the needle was withdrawn, leaving the catheter in place within the soft tissue. The pressure sensing catheter was then retracted in 1 cm steps and measurements were continuously sampled at each location until steady state was achieved (Figure 1E). The process of acquiring internal pressure measurements through a grid location required a maximum of 15 - 20 seconds. The same mapping process was repeated for all three loading conditions.

### *2.3.5 Internal Pressure Mapping during Intermittent Electrical Stimulation*

The changes in the distribution of internal pressure due to IES were quantified for each level of external loading in order to assess the effectiveness of

this approach in alleviating pressure in deep tissue around the ischial tuberosities. Upon applying the target external load (25, 50, or 75% BW), the pressure sensing catheter was inserted through one of the grid locations and the guide needle was removed. Electrical stimulation was then initiated to induce a maximal muscle contraction. During the contraction (which lasted 10 – 12 seconds), pressure measurements were recorded by retracting the catheter in the same manner described above. The muscle contraction was sustained throughout the period of catheter retraction. A 10 minute resting period was imposed between trials with IES to ensure that muscle fatigue does not develop.

#### *2.3.6 Data Acquisition*

Interfacial pressure measurements were obtained at a rate of 10 frames/second using XSensor proprietary software (X3 Pro V5, XSensor Technology Corporation, Calgary, Alberta, Canada). The recordings from each sensor were exported to Matlab (Mathworks, Massachusetts, USA) for analysis using custom-written routines.

Internal pressure measurements were amplified 1000 times and low-pass filtered with a cut-off frequency of 500Hz. The values were sampled at a rate of 1000 samples/second using the CED Power 1401 analog-to-digital conversion interface and Spike2 software (Cambridge Electronic Design, Cambridge, England). The signal from a trigger switch indicating when a pressure measurement was acquired was also recorded at the same sampling rate. The

recorded values were then exported to Matlab for analysis using custom-written routines.

### 2.3.7 *Data Analysis and Statistics*

#### a) Interfacial pressure

A 2D distribution of interfacial pressure was constructed for each level of external loading based on measurements obtained from the 36 x 36 array of individual sensors in the pressure sensing mattress. The center of the ischial tuberosity in the left hind leg was identified by the sensor with the highest interfacial pressure. This sensor was always surrounded by sensors with lower pressure values. Measurements from the sensor at the center of the ischial tuberosity and those surrounding it were given coordinates to match the coordinate system used for the internal pressure measurements.

#### b) Internal pressure

Measurements of internal pressure were analyzed individually for each grid location in all animals. For each location, the average internal pressure (~1sec of data) at a given depth was calculated and stored in a 3D matrix according to the spatial location of that measurement. The combined measurements from all locations provided 3D coverage around the ischial tuberosity. Values were interpolated using a 3D cubic-spline function to fill in missing measurements.

c) Comparison of internal and interfacial pressure

To allow for comparisons between the levels of internal and interfacial pressure across animals, the ratio of internal to maximal interfacial pressure was calculated. For a given level of external loading, the maximal interfacial pressure, located at the center of the ischial tuberosity, was identified. All pressure measurements, both internal and interfacial were then divided by this value, and a 3D map of the ratio of internal to maximal interfacial pressure was constructed for each animal. The same process was performed for all levels of external loading with and without the use of IES.

To compare the redistribution in internal pressure as a result of IES, a pressure displacement vector was calculated. The coordinates of the point with highest internal pressure without IES were used as the starting point of the vector, and the coordinates of the point with highest internal pressure during IES were used as the end point.

d) Statistics

This study had three null hypotheses. 1) There would be no statistical difference in internal pressure levels between the different external loading levels. 2) There would be no statistical difference between internal pressure levels and superficial pressure levels at each respective external loading level. 3) There would be no statistical difference in internal pressure levels between the use and non-use of IES for each respective loading level.

A one-way ANOVA was used to compare the maximal interfacial pressure and the area of elevated interfacial pressure around the ischial tuberosities across the three levels of external loading. The region of the ischial tuberosity was determined by the sensor with the highest interfacial pressure. The area of elevated interfacial pressure was determined by the sensor with the highest interfacial pressure and surrounding sensors with pressures higher than one standard deviation over the mean interfacial pressure of the entire buttock contact area. A two-way ANOVA was used to compare the ratios of peak internal pressure relative to maximal interfacial pressure across the three levels of loading, as well as the changes in these ratios due to the use of IES. Statistical significance was established at  $p < 0.05$ .

## **2.4 RESULTS**

### *2.4.1 Appropriateness of the Yucatan Minipig as an Animal Model*

The adult Yucatan minipigs were the most suitable animal model for these experiments due to the close resemblance of their size, anatomy of the buttocks, and skin, fat and muscle characteristics to that of adult humans. Examples of MR images of the buttocks region of animals and humans are shown in Figures 2A and B. The images from pigs (left) were obtained during the application of external loading equivalent to 50% BW. The images from human volunteers (right) were obtained while they were seated in an MR-compatible apparatus that loaded the tissue around the ischial tuberosities to the same levels experienced

while sitting [32-33]. The loading levels were calculated from interfacial pressure measurements and were  $60.90 \pm 17.95\%$  BW (mean  $\pm$  standard deviation) for volunteers with intact spinal cords ( $n = 12$ ) [33], and  $69.87 \pm 13.47\%$  BW for volunteers with chronic spinal cord injury ( $n = 8$ ) [32]. While the volume of the ischial tuberosities in the pigs was approximately half of that in humans, both pigs and humans had similar thicknesses of skin, fat and proportional muscle tissue around the bony prominences. On average, muscle volume in the buttocks region of the pigs was half of that in humans (Figure 2C). Four weeks following spinal cord injury, substantial disuse atrophy was seen in the muscles of the paralyzed legs exemplified by the reduction in muscle volume. Muscle volume was  $249.83 \pm 48.89 \text{ cm}^3$  in intact pigs ( $n = 5$ ) and  $127.26 \pm 41.61 \text{ cm}^3$  in pigs with spinal cord injury ( $n = 3$ ) [43]. The reduction in muscle volume by 50.94% after spinal cord injury in the pigs was similar to the reduction in muscle volume seen in humans 11 years post spinal cord injury (51.37%; from  $535.68 \text{ cm}^3$  to  $275.20 \text{ cm}^3$ , Figure 2C).

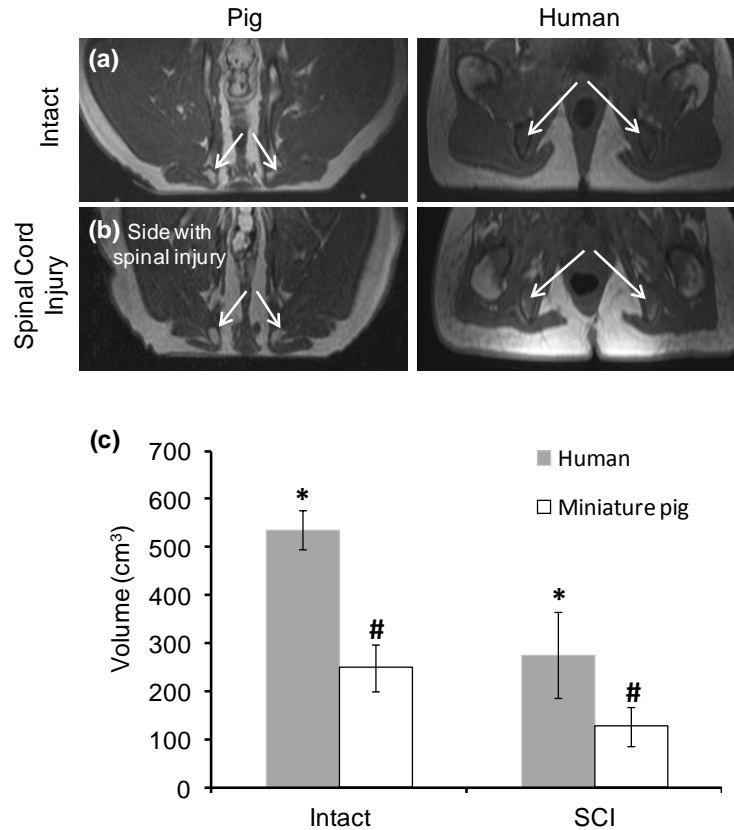


**Figure 2.** Anatomy of the buttocks in pigs and humans with intact and injured spinal cords. (a) Coronal MRI of a pig (left column) and a human (right column) with intact spinal cord, and muscles loaded to 50 and 60% of BW, respectively. Arrows indicate ischial tuberosities. (b) Coronal MRI of a pig and a human with spinal cord injury and muscles loaded to 50 and 60% of BW, respectively. The spinal hemisection affected the hind leg ipsilateral to the lesion (left side of MRI) in the pig; however, the contralateral hind leg also experienced muscle atrophy due to the reduction in the overall level of movement following injury. (c) Muscle volume around the buttocks in humans and pigs with and without spinal cord injury. Quantifications from the paralyzed side in three pigs were used (one pig used in this study and two used in a separate study).

#### 2.4.2 Distribution of Interfacial Pressure

An example of the distribution of interfacial pressure in the buttocks of pigs is shown in Figure 3 A (Top and Middle panels) for the 50% BW loading level. This closely resembled the distribution of interfacial pressure seen in seated human volunteers. The highest regions of pressure were focused around the ischial tuberosities in both spinally intact (Top Panel) and spinally injured (Middle Panel) animals. The *maximal* interfacial pressure at the 50% BW loading

level was  $54.94 \pm 11.73$  kPa (mean  $\pm$  standard deviation) and 65.64 kPa in intact animals and animal with spinal cord injury, respectively. Figure 3 B summarizes the maximal interfacial pressure measured at each loading level for both intact (n=5) and spinally injured (n=1) pigs.

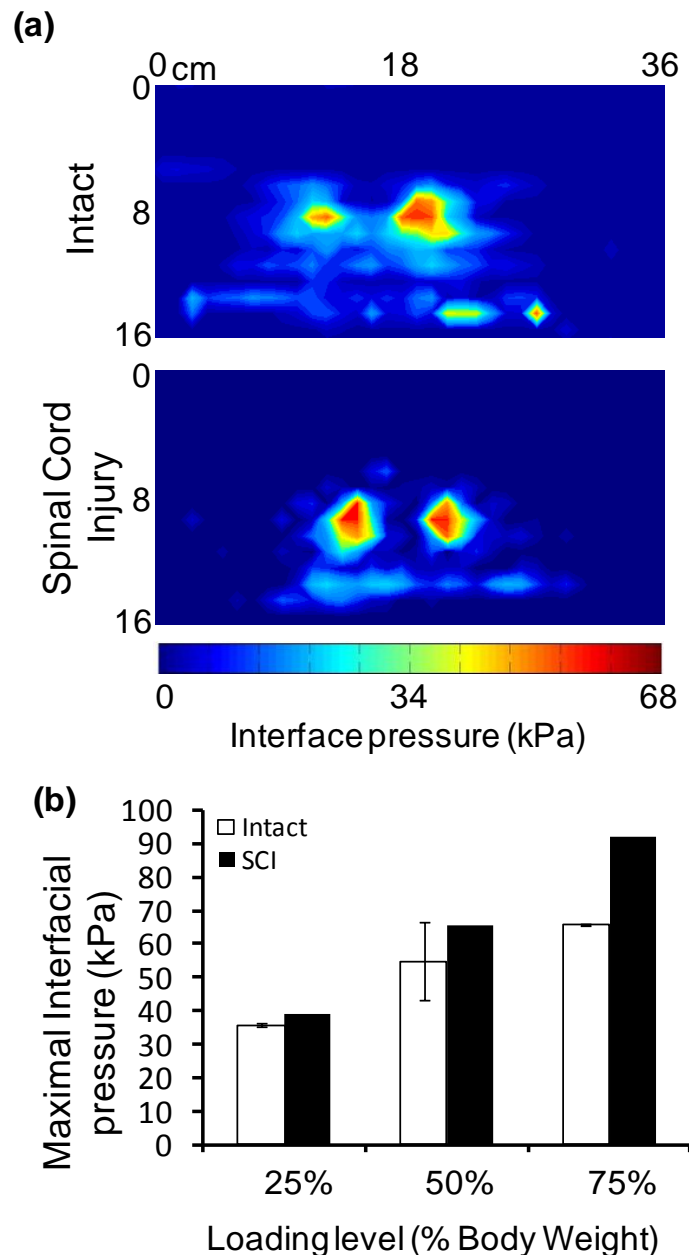


**Figure 3.** Interfacial pressure distribution in pigs with intact and injured spinal cords. (a) Top: Interfacial pressure distribution of an intact pig loaded to 50% BW. Bottom: Interfacial pressure distribution of a pig with spinal cord injury loaded to 50% BW. (b) Summary of maximal interfacial pressure in spinally intact pigs (mean  $\pm$  standard deviation) and the pig with spinal cord injury for the 25%, 50%, and 75% BW loading.

50% BW loading level was  $28.10 \pm 3.15$  kPa (over an area of  $39.52 \pm 5.59$  cm<sup>2</sup>) and 34.13 kPa (over an area of 24.19cm<sup>2</sup>) for the intact and spinally injured pigs, respectively. In addition to the increase in the absolute values of interfacial pressure after spinal cord injury, the area experiencing high pressures decreased. Because of the smaller volume of ischial tuberosities and surrounding muscle, the average values of interfacial pressure in the spinally intact and injured pigs were nearly twice those measured in able-bodied ( $15.16 \pm 3.25$  kPa) and spinal cord injured ( $13.85 \pm 3.81$  kPa) volunteers seated on a lightly padded chair and a gel wheelchair cushion, respectively [32-33].

#### *2.4.3 Distribution of Internal Pressure in Spinally Intact Pigs*

Recordings of pressure in the medio-lateral, dorso-ventral and antero-posterior planes around the left ischial tuberosity are shown in Figure 4 for one spinally intact pig with 50% BW loading. Figure 4A shows the recordings from the dorso-ventral plane centered on the ischial tuberosity (corresponding, in this case, to the top row of measurements in the grid of Figure 2B, C). Pressure levels were highest at the center of the ischial tuberosity and exceeded 100 kPa (106.86 kPa). The highest levels of internal pressure were focused immediately around the bone and dropped substantially 2 cm posteriorly from the ischial tuberosity, at the level of the skin. Peak levels of internal pressure dropped to 86.15 kPa 1 cm laterally from the ischial tuberosity and to 63.32 kPa 2 cm laterally. For locations 2 cm lateral from the ischial tuberosity (green line), relatively low levels of internal pressure were recorded at the level of the skin and anterior locations

(depths) of 3.5 cm and higher.

Internal pressure levels had a similar profile 1 cm ventrally from the plane centered on the ischial tuberosity (Figure 4B; corresponding to recordings from the second row in the grid of Figure 2B, C); however, the peak amplitudes were lower and the antero-posterior distribution was wider. The highest pressure values were 70.15, 60.01, and 42.93 kPa 0, 1 and 2 cm lateral from the ischial tuberosity, respectively. Pressure was lowest at the level of the skin and at anterior locations of 5 cm and higher. Ventral locations 2 and 3 cm away from the ischial tuberosity (Figure 4C and D; corresponding to recordings from the third and fourth rows in the grid in Figure 2B, C) experienced substantially lower levels of internal pressure. At these locations, maximal internal pressure was 60% and 83% lower than that measured directly around the ischial tuberosity (Figure 4A), respectively.

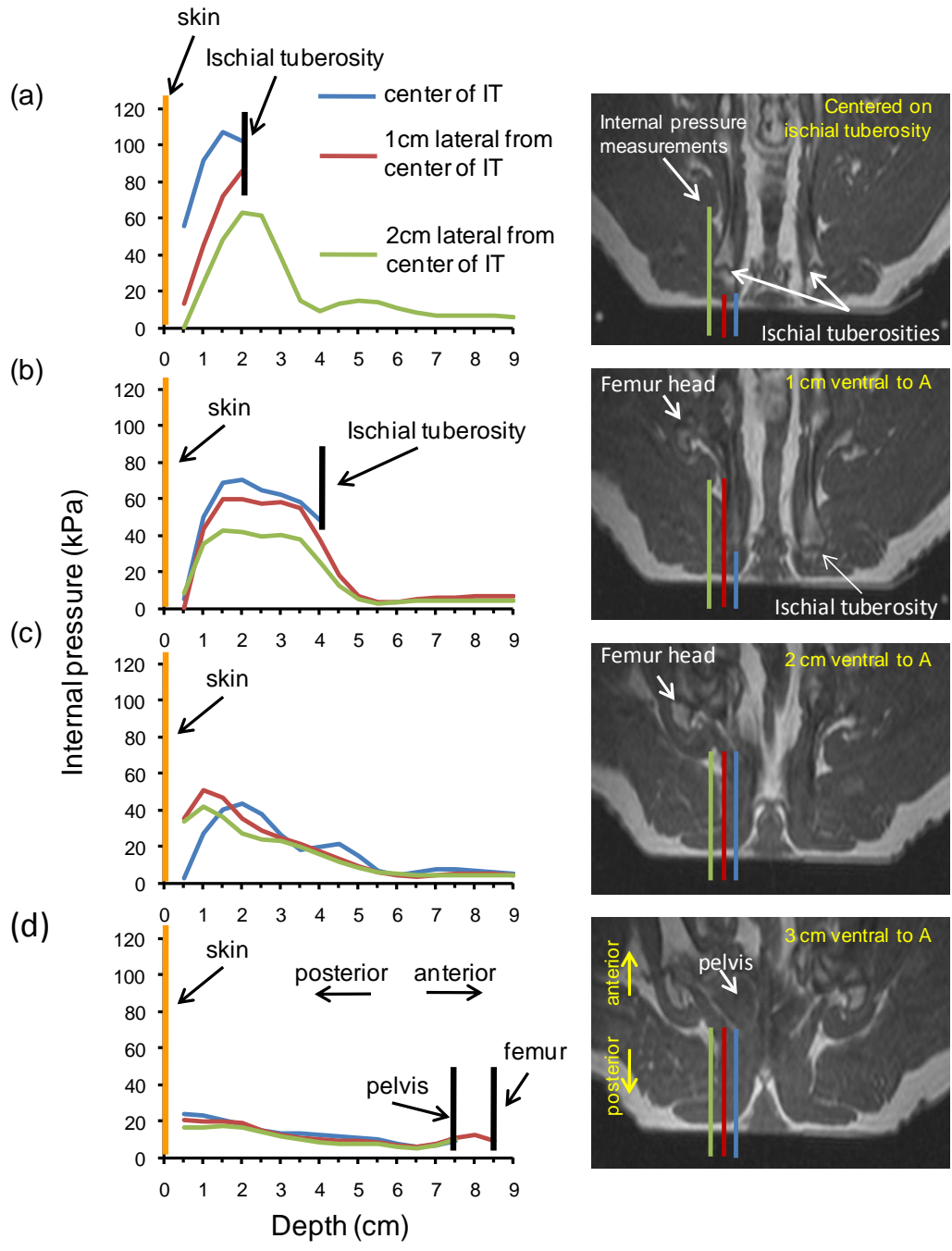


**Figure 4.** Internal pressure measurements obtained from a spinally intact pig. Example of internal pressure measurements obtained from one pig at different dorso-ventral, medio-lateral and antero-posterior (depths) locations with respect to the ischial tuberosity in one hind leg during 50% BW loading of the buttocks. (a) Medio-lateral and antero-posterior (depth) measurements along a dorso-ventral (horizontal) plane centered on the ischial tuberosities. Medio-lateral and antero-posterior measurements along (b) a dorso-ventral plane located 1 cm ventrally relative to “a”, (c) a dorso-ventral plane located 2 cm ventrally relative to “a”, (d) a dorso-ventral plane located 3 cm ventrally relative to “a”. The location of the antero-posterior measurements for each lateral location is shown in the corresponding MRI on the right.

Maps of *interfacial* pressure for the 25%, 50% and 75% BW loading levels in one spinally intact animal are shown in Figure 5A. Maximal interfacial pressure was 36.40, 62.26, and 65.74 kPa for the 25%, 50% and 75% BW loading levels, respectively. The corresponding distributions of internal pressure in the dorso-ventral plane centered on the ischial tuberosity (top row in the grid, Figure 2B, C) as well as ventral planes 1, 2 and 3 cm away (second to fourth rows in grid, Figure 2B, C) are shown in Figures 5B, C, D and E, respectively. As expected, the levels of *internal* pressure increased with increasing levels of external loading. Importantly, *the magnitude of peak internal pressure exceeded that of maximal interfacial peak pressure for all levels of external loading*. This was particularly evident in the dorso-ventral plane centered on the ischial tuberosity (Figure 5B), where peak internal pressures were 72.23, 106.90, and 105.60 kPa for the 25%, 50% and 75% BW loading, respectively. For all levels of external loading in this animal, peak internal pressure *continued to exceed that of maximal interfacial pressure 1 cm ventrally* from the central plane (Figure 5C), where peak internal pressures were 50.4, 70.16, and 96.66 kPa for the 25%, 50% and 75% BW loading, respectively. This also continued to be the case 2 cm ventrally for the 75% BW loading level (Figure 5D), where peak internal pressure was 71.62 kPa.

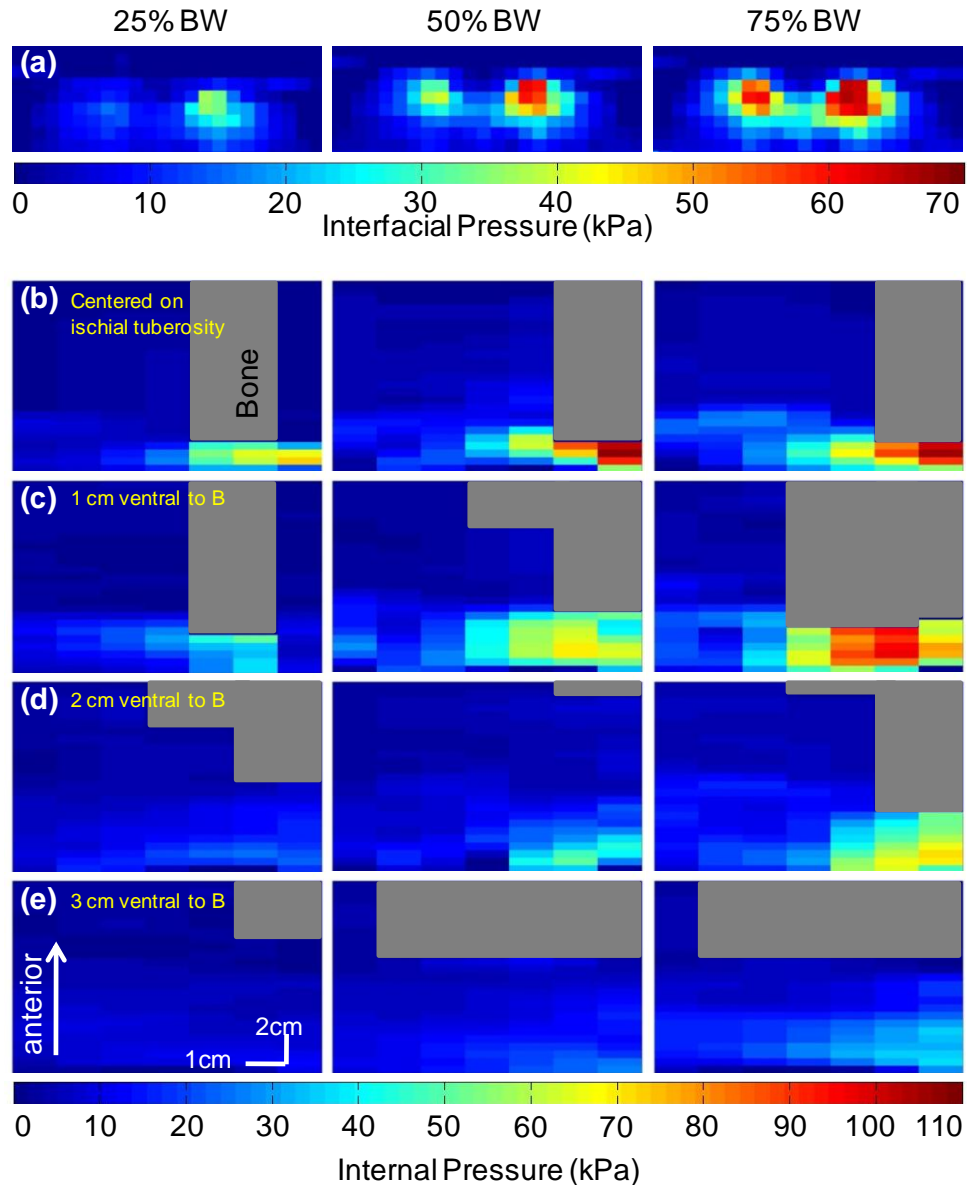


**Figure 5.** Distribution of interfacial and internal pressure in a spinally intact pig. (a) Map of interfacial pressure for the 25%, 50%, and 75% BW loading levels. Medio-lateral and antero-posterior map of internal pressure (b) in the dorso-ventral plane centered on the ischial tuberosities, (c) in the dorso-ventral plane located 1 cm ventral to “b”, (d) in the dorso-ventral plane located 2 cm ventral to “b”, (e) in the dorso-ventral plane located 3 cm ventral to “b”.

To further understand the relationship between internal and interfacial pressure and allow for comparison of measurements between animals, internal pressure recordings in a given animal were divided by the value of the maximal interfacial pressure measured in that animal. The normalized results, grouped

across all intact animals, are shown in Figure 6. Interestingly, *the highest values of internal pressure were approximately two times larger than the maximal values of interfacial pressure.* Furthermore, the highest levels of internal pressure were not located directly next to the bone, *but about 0.5 – 1.0 cm posterior to the bone.* Across animals, the ratio of peak internal pressure to maximal interfacial pressure for the 25%, 50% and 75% BW loading was similar ( $2.11 \pm 0.18$ ,  $1.80 \pm 0.16$ , and  $2.12 \pm 0.20$ , respectively (mean  $\pm$  standard error)). The average ratio of peak internal pressure to maximal interfacial pressure across all loading levels was  $2.01 \pm 0.08$ . With the exception of the 25% external loading condition (Figure 6B), the average ratio of peak internal to maximal interfacial pressure dropped to approximately 1 ( $1.1 \pm 0.17$ ) 1 cm ventral to the plane centered on the ischial tuberosities. This ratio was less than 1 ( $0.84 \pm 0.12$ ) 2 cm ventrally (Figure 6C), and less than 0.5 ( $0.34 \pm 0.04$ ) 3 cm ventrally (Figure 6D).

#### 2.4.4 *Distribution of Internal Pressure following Chronic Spinal Cord Injury*

The thickness of the soft tissue between the bone and skin was substantially reduced one month after spinal cord injury (2.98 cm relative to  $3.5 \pm 0.8$  cm (mean  $\pm$  standard deviation) in intact animals). Therefore, fewer measurements of internal pressure could be obtained around the ischial tuberosity of the paralyzed hind leg. Figure 7 shows the distribution of interfacial (A) and internal pressure (B-D) in the animal with spinal cord injury with external loading levels of 50% and 75% BW. Peak *interfacial* pressures were 65.64 and 92.17 kPa for the 50% and 75% loading levels, respectively (Figure 7A). Similar to the

intact animals, peak *internal* pressure was highest around the ischial tuberosity (Figure 7C, dorso-ventral plane centered on the ischial tuberosities) and was 97.31 and 111.77 kPa for the 50% and 75% BW loading, respectively. For the 50% loading level, peak internal pressure dropped to 73.59 kPa one cm dorsal to the ischial tuberosity (Figure 7B, left) and to 52.66 kPa one cm ventral to the tuberosity (Figure 7D, left). The 75% BW loading condition tilted the pelvis and caused high levels of internal pressure in the planes centered on the ischial tuberosity and one cm dorsally (111.77 kPa and 126.11 kPa, respectively. Figure 7B, C right). Internal pressure dropped to 75.16 kPa 1 cm ventrally (Figure 7D, right). For all dorso-ventral planes sampled except one (Figure 7D, left), peak internal pressure was higher than the maximal interfacial pressure.

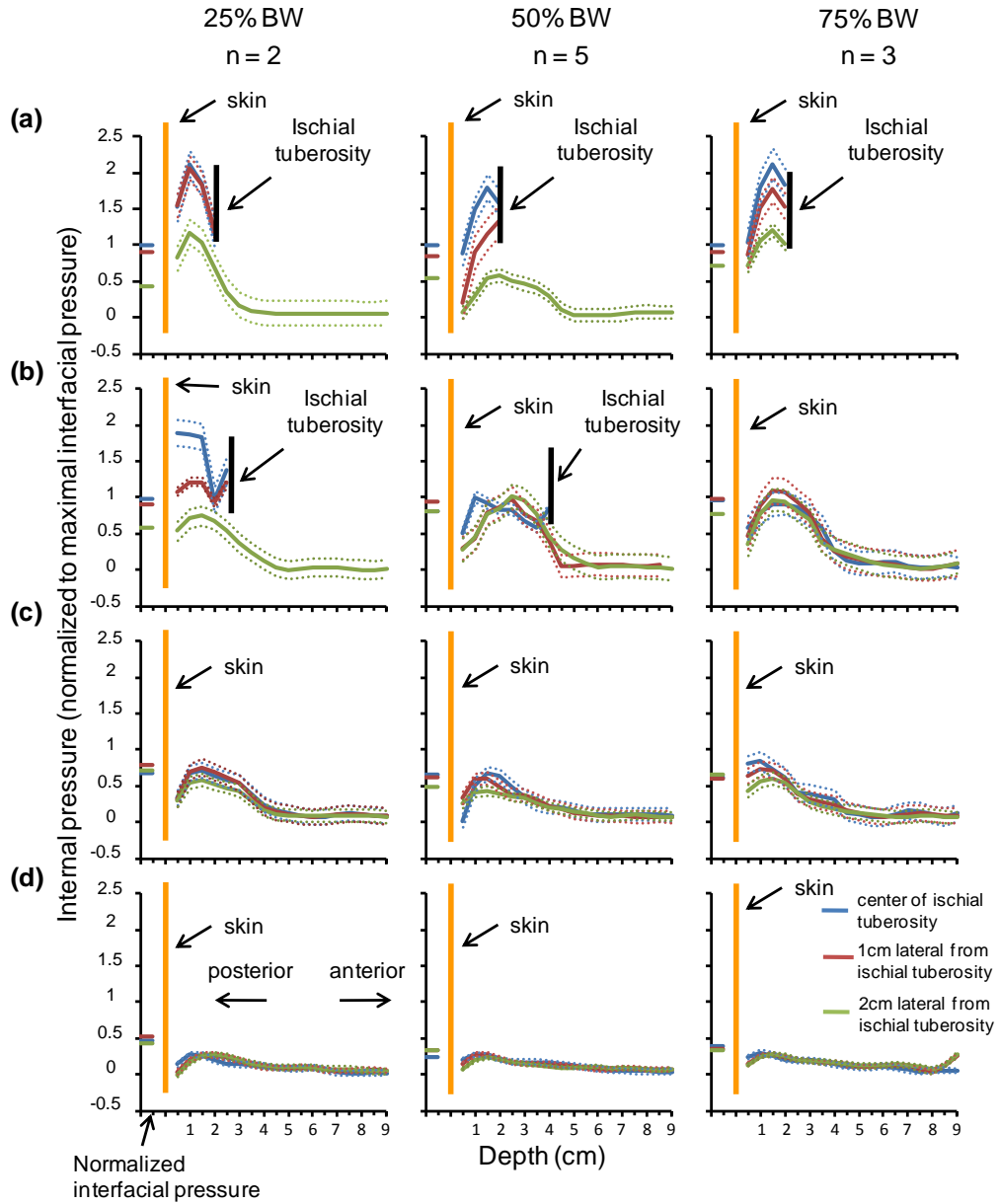


**Figure 6.** Relationship between internal pressure and maximal interfacial pressure in spinally intact pigs. Ratio of internal to maximal interfacial pressure for all dorso-ventral, medio-lateral and antero-posterior locations sampled in all intact animals, and for all external loading levels. (a) Mean and standard error of internal pressure (relative to maximal interfacial pressure) for mediolateral and antero-posterior locations in the dorso-ventral plane centered on the ischial tuberosities. Internal pressure in the dorsoventral plane located (b) 1 cm ventral to “a”, (c) 2 cm ventral to “a”, (d) 3 cm ventral to “a”. Solid lines indicate the mean proportional value of internal pressure with respect to maximal interfacial pressure, dotted lines indicate standard errors. The values to the left of the skin indicate the normalized interfacial pressure at the corresponding dorso-ventral, medio-lateral locations.

Recordings of internal pressure normalized to maximal interfacial pressure for the same pig are shown in Figure 8. Due to the larger values of maximal interfacial pressure, the ratio of peak internal to maximal interfacial pressure was smaller than that in intact animals (1.48 and 1.37 for the 50% and 75% BW loading levels, respectively). Nonetheless, Figure 8 demonstrates that peak internal pressure was more highly focused around the ischial tuberosity than in intact animals. Moreover, peak levels of internal pressure were located immediately posterior to the bone for both the 50% and 75% BW loading conditions (Figure 8B, dorso-ventral plane centered on the ischial tuberosities). For the 50% BW loading, the ratio of peak internal to maximal interfacial pressure in the dorso-ventral plane centered on the ischial tuberosity dropped to 1.22 1 cm posterior to the bone, and to 0.90 2 cm posteriorly (Figure 8B, left). The ratios also dropped to 0.49 1 cm dorsally and 0.35 1 cm ventrally (Figure 8A, C, left). In all dorso-ventral planes, the ratio of internal to maximal interfacial pressure approached zero within a 2-3 cm antero-posterior span.

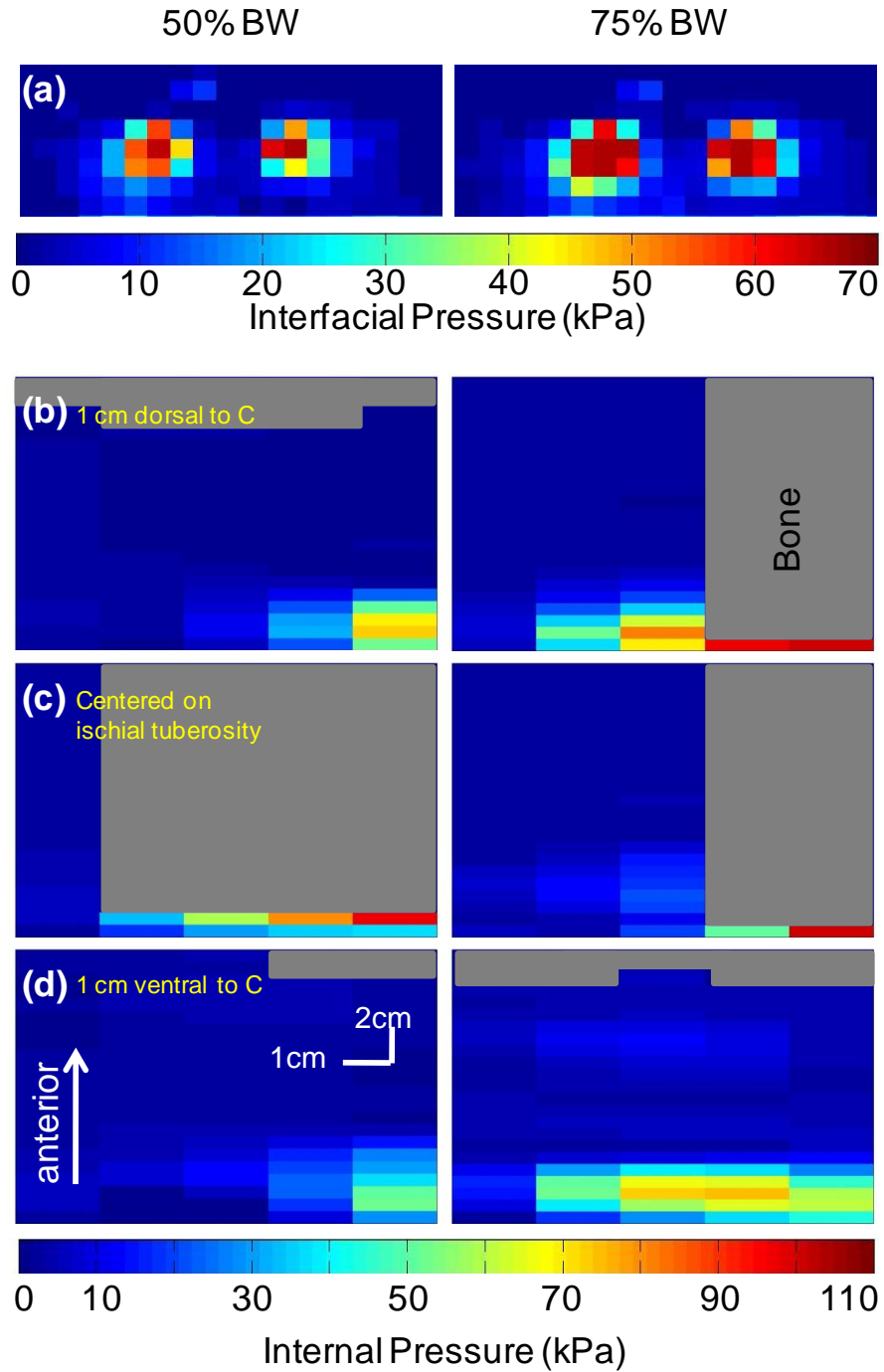


**Figure 7.** Distribution of interfacial and internal pressure in a pig with spinal cord injury. (a) Map of interfacial pressure for the 50 and 75% BW loading levels. Medio-lateral and anteroposterior map of internal pressure (b) in the dorso-ventral plane located 1 cm dorsal to the ischial tuberosities, (c) in the dorso-ventral plane centered on the ischial tuberosities, (d) in the dorso-ventral plane located 1 cm ventral to the ischial tuberosities.

With 75% BW loading (Figure 8, right), the region of peak internal pressure extended dorsally and laterally, with near peak levels still evident 1 cm dorsally and 1 cm dorso-laterally from the ischial tuberosity (Figure 8A, right). One centimeter ventrally and laterally (Figure 8C, right) peak internal pressure levels were still around 1.05 times the maximal interfacial pressure. Nonetheless, a substantial drop in the ratio of internal to maximal interfacial pressure was seen 2 mm lateral to the bone in the plane centered on the ischial tuberosity (Figure 8B, right).

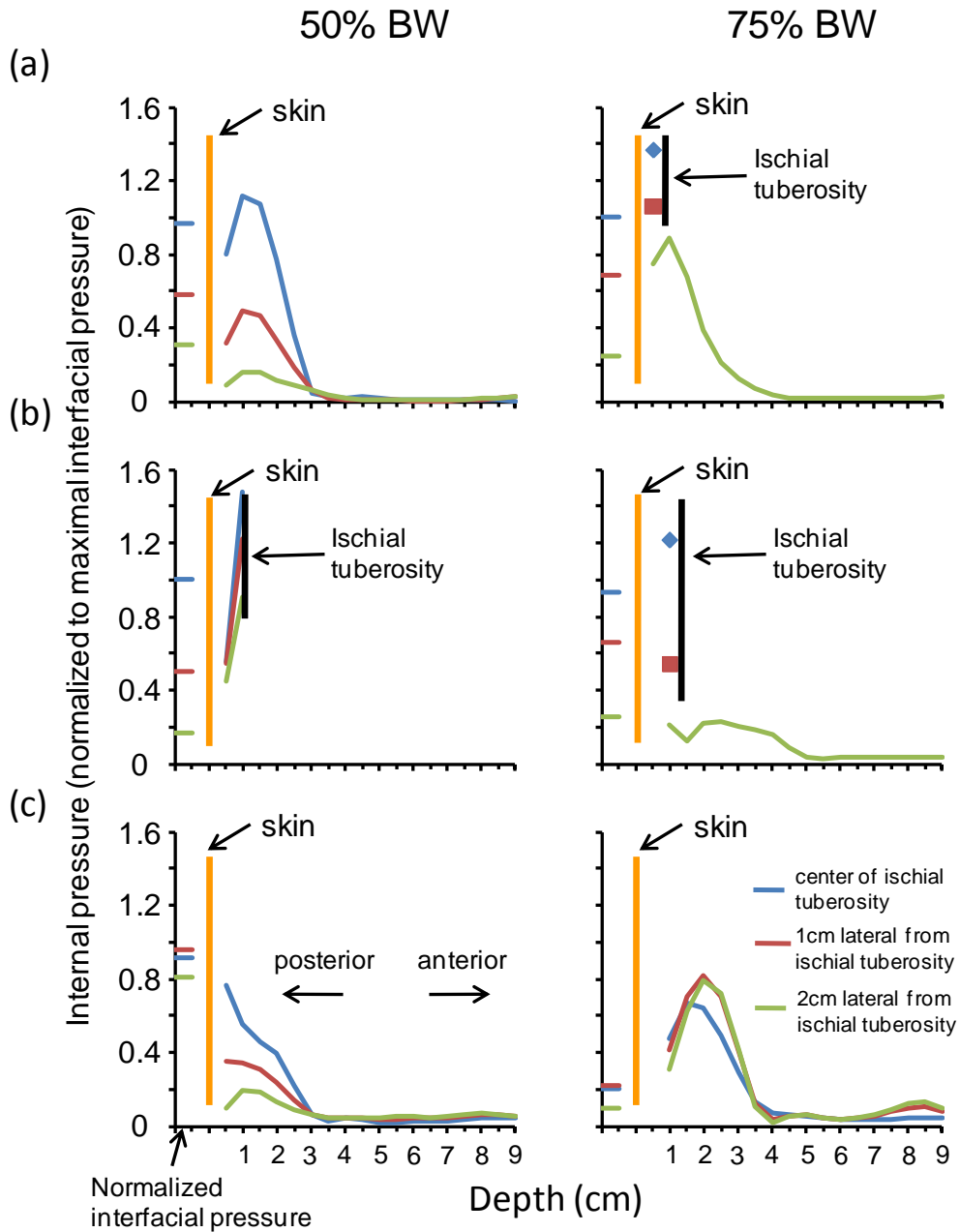


**Figure 8.** Relationship between internal pressure and maximal interfacial pressure in a pig with spinal cord injury. Ratio of internal to maximal interfacial pressure for all dorso-ventral, medio-lateral and antero-posterior locations sampled in the pig with chronic spinal cord injury, for the 50 and 75% BW loading levels. Internal pressure (relative to maximal interfacial pressure) for medio-lateral and antero-posterior locations (a) in the dorso-ventral plane located 1 cm dorsal to the ischial tuberosities, (b) in the dorso-ventral plane centered on the ischial tuberosities, (c) in the dorso-ventral plane located 1 cm ventral to the ischial tuberosities.

#### *2.4.5 Effects of IES on the Distribution of Internal Pressure*

In previous studies, we demonstrated that IES was effective in redistributing interfacial pressure in the buttocks of seated individuals, significantly reducing its magnitude around the ischial tuberosities [32-33]. In the present study, we assessed the effectiveness of IES in redistributing pressure in deep tissue around the ischial tuberosity.

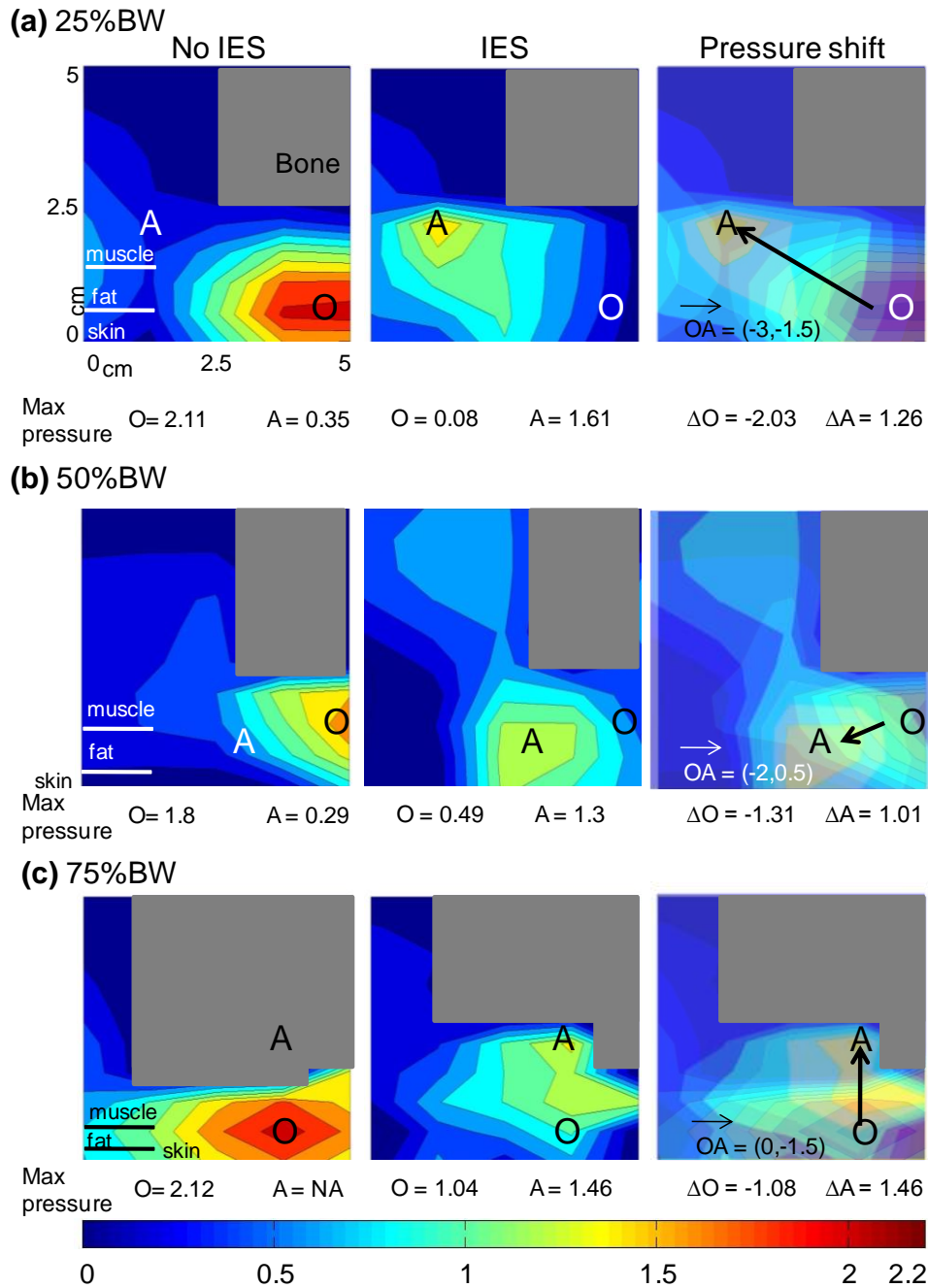


**Figure 9.** Redistribuition of internal pressure due to IES in spinally intact pigs. Maps indicate the distribution of internal pressure (relative to maximal interfacial pressure) in the dorso-ventral plane centered on the ischial tuberosities from all spinally intact animals, and for all levels of external loading. Left: Internal pressure before the use of IES. Center: Internal pressure during muscle contraction due to IES. Right: Shift in location of peak internal pressure due to the IES-induced muscle contractions. “O” indicates the location of peak internal pressure (relative to maximal interfacial pressure) before the use of IES. “A” indicates the location of peak internal pressure during the IES-induced muscle contractions. (a) 25% BW loading. (b) 50% BW loading. (c) 75% BW loading.

Composite reconstructions of internal pressure maps (normalized to maximal interfacial pressure) in the dorso-ventral plane centered on the ischial tuberosities from all spinally intact animals without IES are shown in Figure 9 (left column) for 25%, 50% and 75% BW loading. As the external loading increased, the compression of tissue between the bone and the indenter increased and the thickness of the soft tissue layer decreased. The highest levels of internal pressure were located posteriorly to the bone, and the focal point of peak internal pressure moved anteriorly towards the bone as the level of external loading increased. The point of peak internal pressure was approximately 1.75 cm posterior to the bone with 25% BW loading (Figure 9A, left), and 0.8 cm and 0.7 cm posterior to the bone for the 50% and 75% BW loading, respectively (Figure 9B, C). As the level of external loading increased, *the location of peak internal pressure corresponded to the zone between the muscle and fat.*

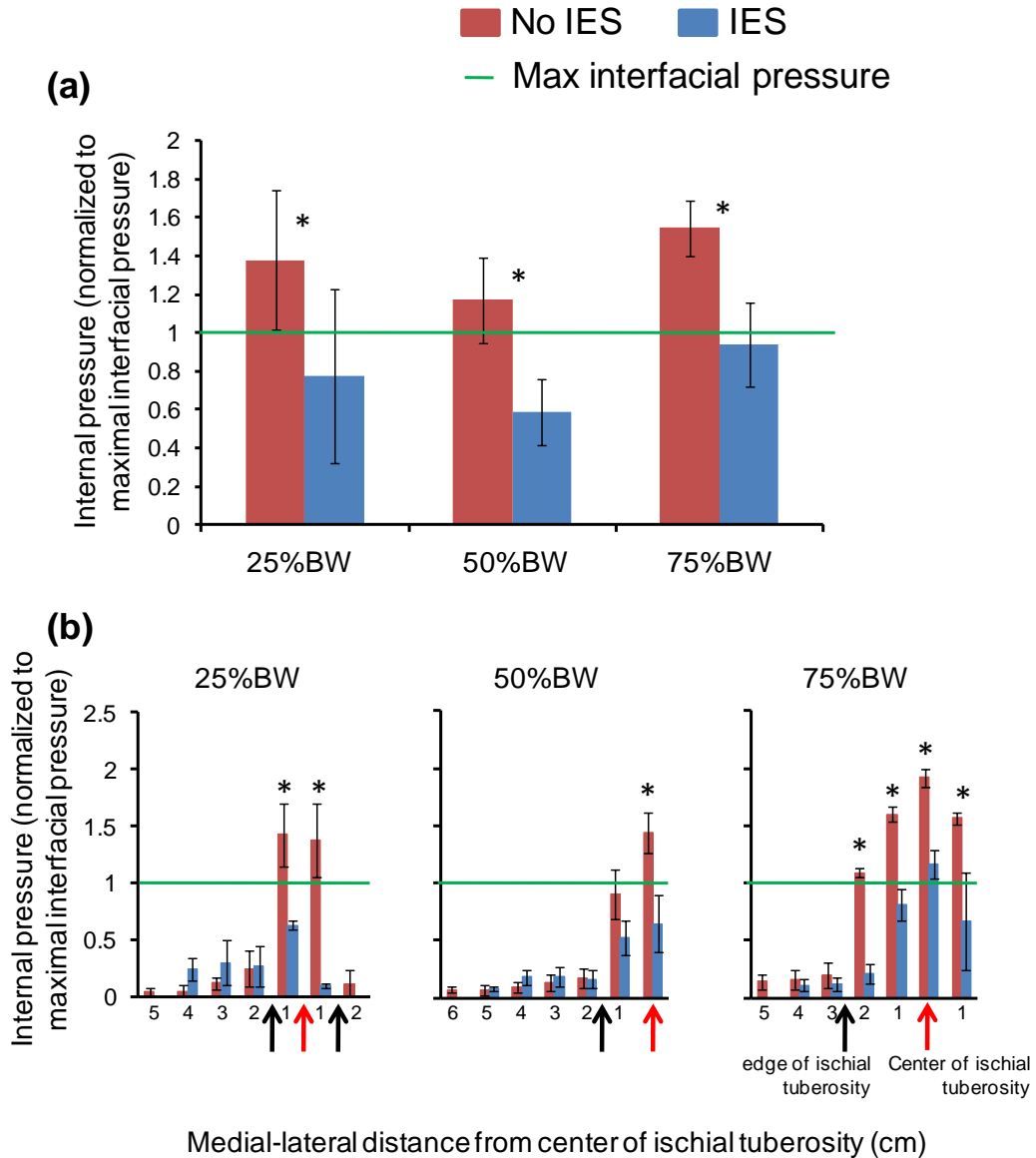


**Figure 10.** Statistical changes in internal pressure during IES-induced muscle contractions in intact pigs. (a) Mean internal pressure 6 standard error in the dorso-ventral plane centered on the ischial tuberosities for all levels of external loading. (b) Medio-lateral distribution of internal pressure (mean 6 standard error) relative to the ischial tuberosity in the dorso-ventral plane centered on the ischial tuberosities, for all levels of external loading, with and without IES. \*Significant reduction in internal pressure during IES.

The application of IES produced a muscle contraction that increased the thickness of the tissue directly between the ischial tuberosity and indenter (Figure 9, center column) in all animals. Measurements from MR images showed that

tissue thickness increased by an average of 25% with IES for the 25% BW loading, and by 32% and 31% for the 50% and 75% BW loading levels, respectively. Moreover, under all loading conditions, IES shifted the focal point of peak internal pressure. For the 25% and 50% BW loading conditions, the focal point shifted 3 cm laterally and 1 cm dorsally and ventrally (Figure 9A, B, right column), while for the 75% BW loading, the focal point shifted by 1 cm anteriorly and ventrally (Figure 9C, right column).

The ratio of internal to maximal interfacial pressure in the region surrounding the ischial tuberosity significantly decreased during IES ( $p < 0.001$ ) in intact animals for all loading levels. Internal pressure was reduced by 44%, 50% and 39% for the 25%, 50% and 75% BW external loading conditions, respectively (Figure 10A). The medio-lateral distribution of reductions in the average ratio of internal to maximal interfacial pressure during IES in the dorso-ventral plane centered on the ischial tuberosity is shown in Figure 10B. The maximal reductions in internal pressure were seen immediately around the ischial tuberosity. These reductions were significant ( $p < 0.001$ ) for areas within  $\pm 1$  cm from the ischial tuberosity for the 25% and 50% BW loading levels, and within  $\pm 2$ cm for the 75% BW loading level.

The effect of IES on redistributing internal pressure was measured in one animal with chronic spinal cord injury. During IES, the thickness of tissue between the surface and ischial tuberosity increased by 38%, 43%, and 35%, for

the 25%, 50%, and 75% BW loading, respectively. The distribution of internal pressure (relative to maximal interfacial pressure) for the 50% BW loading is shown in Figure 11A. Prior to IES, the focal point of peak internal pressure was located 0.51 cm posterior to the bone under this level of loading. During IES, the peak internal pressure dropped to 0.36 of the maximal interfacial pressure, and the focal pressure point shifted 2 cm laterally and 2 cm anteriorly. Due to the scarcity of measurements obtained during the 25% BW loading, only the results from the 50% and 75% BW loading were further quantified (Figure 11B). Intermittent electrical stimulation was effective in substantially redistributing internal pressure for areas within  $\pm 1$  cm from the ischial tuberosity under the 50% BW (Figure 11B, left). It also redistributed internal pressure in areas within  $\pm 1$  cm from the ischial tuberosity under the 75% BW loading (Figure 11B, right), albeit not substantially.

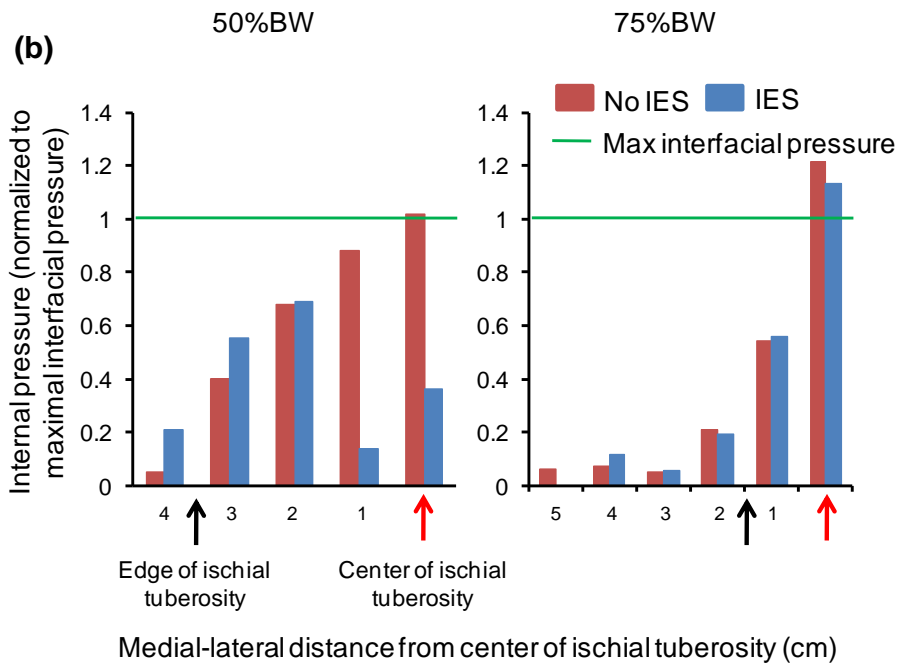
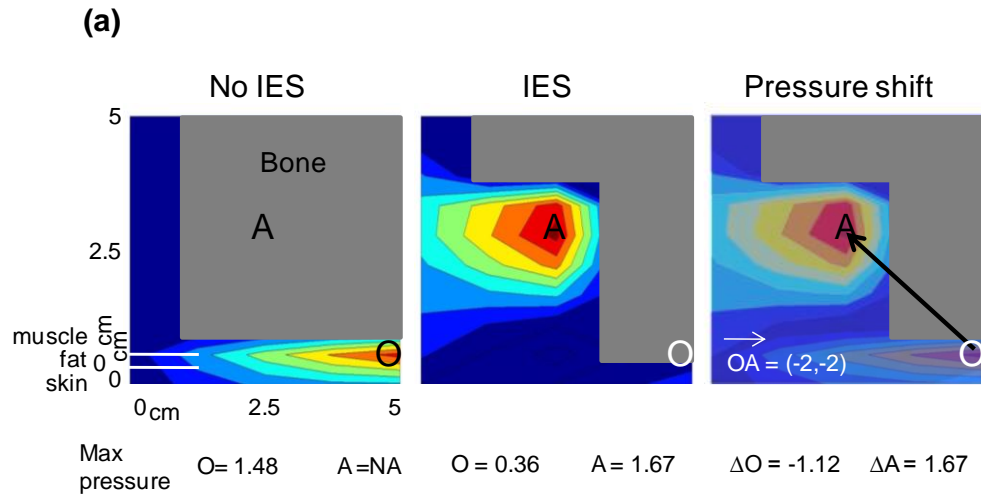


**Figure 11.** Redistribution of internal pressure due to IES in a pig with spinal cord injury. (a) Maps indicate the distribution of internal pressure (relative to maximal interfacial pressure) in the dorso-ventral plane centered on the ischial tuberosities for the 50% BW loading level. Left: Internal pressure before the use of IES. Center: Internal pressure during muscle contraction due to IES. Right: Shift in location of internal pressure due to the IES-induced muscle contractions. “O” indicates the location of peak internal pressure (relative to maximal interfacial pressure) before the use of IES. “A” indicates the location and of peak internal pressure during the IES-induced muscle contractions. During muscle contraction, the hip rotated downwards, thus allowing for the recording of internal pressure from regions of soft tissue that were occluded by the bone prior to the contraction. (b) Medio-lateral distribution of internal pressure relative to the ischial tuberosity in the dorso-ventral plane centered on the ischial tuberosities, for the 50 and 75% BW loading, with and without IES.

## **2.5 DISCUSSION**

### *2.5.1 Overview*

The overall goal of this study was to investigate the relationship between internal and interfacial pressure around the ischial tuberosities during various levels of external loading, and to determine the effectiveness of IES in redistributing pressure in tissue deep around the bony prominences. An adult pig model was used because of the similarity of size, tissue morphology and tissue properties around the ischial tuberosities to those of humans. We demonstrated for the first time, that the absolute peak levels of internal pressure were 1.5 to 2.1 times as large as the maximal levels of interfacial pressure in the spinal cord injured and spinally intact animals, respectively. The peak values of internal pressure were focused posterior to the ischial tuberosity, at the interface between muscle and fat. We also demonstrated, that IES effectively reduces the levels of internal pressure around the ischial tuberosities.

### *2.5.2 Internal Pressure is Highly Concentrated around the Bone*

To the best of our knowledge, this study provides the first direct quantification of internal pressure in the tissue deep around the ischial tuberosities for a large range of external loading. While the outcomes generally agree with the predictions of computer simulations [30, 36-38], they provide a number of critical findings that could enhance existing computer models. The findings also shed new light on the importance of considering internal pressure in the prescription of seating surfaces for people with reduced mobility.

*First*, the absolute values of internal pressure obtained in this study were smaller than those predicted from computer models. For example, Gefen et al [44] suggested that compressive stress around the sacrum is two orders of magnitude higher than the wheelchair-skin interfacial pressure. Moreover, Bouten et al [30] proposed that the Von Mises stress around the ischial tuberosity is 2.0 MPa for an 80kg seated individual. This suggests that the assumptions of interfacial loads may have been too high in the computer simulations, the viscoelastic moduli of the various tissues were too low, or conditions of tissue anisotropy were not accounted for. These factors could collectively lead to assumptions of increased stress or deformation in the deep tissues. Because a range of external loading levels that produced interfacial pressures similar to those seen in human volunteers sitting on various support surfaces were used in this study, the results suggest that the threshold for damage due to external loading is smaller than that predicted from computer simulations. While the level of internal pressure leading to tissue breakdown is unknown, findings from rat studies conducted in our lab demonstrated that loading one leg to 20-28% of body weight for 2 hours produces detectable muscle damage [42].

*Second*, a constant relationship between peak internal pressure and maximal interfacial pressure was revealed for all levels of external loading (i.e., type of seating surface). In intact animals, peak internal pressure was twice as high as the maximal interfacial pressure. In the animal with spinal cord injury, this constant was slightly lower than 1.5 (1.48 and 1.37 for 50% and 75% BW,

respectively) due to the increase in maximal interfacial pressure for the same levels of external loading. Interestingly, the absolute levels of peak internal pressure remained the same following spinal cord injury. This could suggest that a similar threshold of DTI should be expected in people with spinal cord injury relative to spinally-intact individuals. Nonetheless, the substantial muscle atrophy and the changes in tissue properties (e.g., reductions in muscle stiffness [45-47]) make the spinal cord injured population highly at risk of developing pressure ulcers.

*Third*, the maximal levels of internal pressure were highly focused around the bone for all levels of external loading. A 2 cm shift dorso-ventrally or medio-laterally led to more than 50% reduction in peak internal pressure in intact pigs and 25% reduction in the animal with spinal cord injury. This substantial anisotropy in internal pressure distribution suggests that uniform support cushions may not provide the best relief of pressure in wheelchair users with spinal cord injury. Cushions with non-uniform properties leading to differential spatial alleviation of internal pressure in the buttocks would likely be more responsive to the internal loading profiles around the ischial tuberosities.

*Fourth*, surprisingly, the location of peak internal pressure was not directly next to the bone in intact animals, but about 1 cm away (Figures 5, 9). This corresponded to the interface between muscle and fat, particularly in the case of the 50% and 75% body weight loading (Figure 9B and C, left column).

Furthermore, as the level of external loading increased, the muscle thickness decreased substantially relative to that of the fat. Previous computer models suggested that a region of high internal pressure exists within the fat posterior to the ischial tuberosity in seated individuals [30, 36], similar to that corresponding to the peak internal pressure under the 25% body weight loading condition (Figure 9A, left column). As external loading increased the location of peak internal pressure moved anteriorly towards the interface between muscle and fat. The difference in material properties between muscle and fat [48-50] could explain the concentration of internal pressure at this interfacial region. Recent computer simulations analyzing the changes in strain in the same animal model used in this study also demonstrated that maximal shear strain is localized within the region of the interface between muscle and fat [51].

In the animal with spinal cord injury, the peak internal pressure was directly next to the bone (Figure 7, Figure 11A left). This is primarily a result of the disuse atrophy of the muscles following chronic injury, and could also correspond to the interfacial region between the muscle and fat. Nonetheless, under the loading conditions tested in this study, deep tissue damage still originates within the muscle [41-42]. Moreover, a preliminary study in our lab investigating the origin and progression of deep tissue damage due to prolonged loading (3 hours) in an adult pig demonstrated that damage originated in the muscle and subsequently spread to the fat over a 4 day period (unpublished data). This affirms the presence of a differential threshold for damage in muscle and fat

tissue as suggested by others [26-27, 29-31]; however, these thresholds remain unclear.

### *2.5.3 Intermittent Electrical Stimulation Effectively Redistributes Internal Pressure*

The leading factor for the formation of DTI is the entrapment of tissue between a bony prominence and an external surface for extended periods of time [2, 22-28]. This leads to substantial increases in pressure around bony prominences (as demonstrated in this study) and deformation of the tissue in these regions (as described in a companion paper [47]). These in turn lead to capillary occlusion and mechanical breakdown of the tissue [52-64]. These factors are further extenuated in people with spinal cord injury who have atrophied muscles, and reduced tissue stiffness [45-47]. Reductions in tissue stiffness lead to increased deformation for a given level of pressure, thus resulting in further damage. A means for frequently redistributing internal pressure, restoring tissue oxygenation and alleviating tissue deformation is needed for the prevention of DTI.

Intermittent electrical stimulation, whereby a loaded muscle is electrically activated to produce a brief contraction every few minutes, is a novel intervention developed for the prevention of DTI [32-33, 41-42]. We demonstrated that this intervention produces significant reductions in interfacial pressure and sustained increases in tissue oxygenation in the loaded gluteal muscles of seated volunteers

with intact [33] or chronically injured [32] spinal cord. We also demonstrated in a rat model that IES significantly reduces the extent of tissue damage following 2 hours of external loading to levels similar to the ones used in this study [41-42]. Moreover, this approach was more effective in reducing deep tissue damage than presently prescribed interventions [42]. Nonetheless, the effect of IES on internal pressure remained unknown.

In this study, we demonstrated for the first time, that IES *redistributes internal pressure*, significantly reducing its level in the deep tissue surrounding the ischial tuberosities. This was the case in spinally-intact animals for all levels of external loading (up to 75% of body weight). It was also the case in animals with a chronic spinal cord injury for levels of external loading up to 50% of body weight. This result is very exciting given the substantial muscle atrophy in these animals.

Muscle contractions induced by IES redistribute internal pressure by periodically increasing muscle stiffness and reconfiguring muscle shape. The periodical increases in muscle stiffness ‘reset’ the viscoelastic properties of the loaded muscle and restore them to preloaded conditions, thus alleviating the time-dependent, non-reversible changes (e.g., creep) that occur due to prolonged deformation. Recent modeling work suggested that increases in tissue stiffness has little effect on the levels of internal stress [51]; however, coupled with the changes in muscle shape, this study demonstrates that a substantial distribution of

internal pressure from areas at risk of breakdown to regions of lower initial pressure occurs.

Very importantly, the dynamical distributions of internal pressure and “resetting” of tissue properties through IES take place *without* the need for muscle unloading (i.e., removal of the external pressure). This provides an attractive pressure relieving strategy for wheelchair users who are unable to conduct postural adjustments independently such as wheelchair push-ups or side-to-side leans. Together with the advantageous changes in tissue oxygenation produced by IES [32-33], we believe that this intervention may be effective in preventing the formation of DTI. Nonetheless, the long-term effectiveness of IES needs to be established. Moreover, the effects of IES on the vascular and viscoelastic properties of fat and skin need to be investigated.

#### 2.5.4 *Study Limitations*

In this study, internal pressure was measured through a one-dimensional sensor; thus, the contribution of compressive, tensile and shear stresses could not be independently deciphered. Nonetheless, in a companion study [47] as well as in recent computer simulations [51], normal and shear strains were investigated in adult pigs. These results will be consolidated in future studies to investigate the relative contribution of various stresses and strains to the breakdown of muscle, fat and skin.

Due to experimental considerations, the resolution of the internal pressure maps was limited to 1 cm. Furthermore, the utilized internal pressure measurement method precluded measurements around curved portions of the bone. Therefore, we could not assess the levels of internal pressure around the lateral-anterior edge of the ischial tuberosity, a region suggested by computer simulations to have high internal pressures [30, 36]. Nonetheless, the information gained from the empirical mapping could in the future be included in computer models, and more accurate predictions of the distributions of internal pressure around the bony prominences could be achieved.

#### 2.5.5 *Conclusion*

This study established, for the first time, the distribution of internal pressure relative to interfacial pressure in the tissue surrounding the ischial tuberosities of intact and spinally-injured animals for a wide range of levels of external loading. Regions of peak internal pressure were highly localized around the bony prominences and exceeded the maximal levels of interfacial levels by a factor of 2.0 in intact animals and 1.5 in animals with muscle atrophy due to a chronic spinal cord injury. Intermittent electrical stimulation was highly effective in redistributing internal pressure by reconfiguring muscle shape and increasing muscle stiffness. These findings contribute valuable information to computer models focusing on understanding the mechanisms of DTI. They also provide important considerations for the design and prescription of wheelchair cushions. The work also highlights the potential role of IES as a novel strategy for the

prevention of DTI.

### 2.5.6 Acknowledgements

Mr. Robert Lederer designed and built the MR-compatible pig carrier. Mr. Glen Isaacson designed and built the body-support sling for partial suspension of the pigs with hemi-lesion of the spinal cord. This work was funded by the Alberta Heritage Foundation for Medical Research (AHFMR), the Canadian Institutes of Health Research (CIHR), and the Spinal Cord Injury Treatment Centre Society (SCITCS). VKM is an AHFMR Senior Scholar.

## 2.6 REFERENCES

- [1] J. M. Zanca, D. M. Brienza, D. Berlowitz, R. G. Bennett, C. H. Lyder, and N. P. U. A. Panel., "Pressure ulcer research funding in America: creation and analysis of an on-line database," *Advances in Skin & Wound Care*, vol. 16, pp. 190-7, 2003.
- [2] R. M. Woolsey and J. D. McGarry, "The cause, prevention, and treatment of pressure sores," *Neurologic Clinics.*, vol. 9, pp. 797-808, 1991.
- [3] B. P. Keller, J. Wille, B. van Ramshorst, and C. van der Werken, "Pressure ulcers in intensive care patients: a review of risks and prevention," *Intensive Care Med*, vol. 28, pp. 1379-88, 2002.
- [4] C. I. Webster, "A pressure care survey in the operating theatres," *Aust Clin Rev*, vol. 13, pp. 29-37, 1993.
- [5] J. Cox, "Predictors of pressure ulcers in adult critical care patients," *Am J Crit Care*, vol. 20, pp. 364-75, 2011.
- [6] C. A. Salzberg, D. W. Byrne, C. G. Cayten, P. van Niewerburgh, J. G. Murphy, and M. Viehbeck, "A new pressure ulcer risk assessment scale for individuals with spinal cord injury," *American Journal of Physical Medicine & Rehabilitation*, vol. 75, pp. 96-104, 1996.
- [7] S. L. Garber and L. R. Dyerly, "Wheelchair cushions for persons with spinal cord injury: an update," *American Journal of Occupational Therapy*, vol. 45, pp. 550-4, 1991.
- [8] R. J. Seymour and W. E. Lacefield, "Wheelchair cushion effect on pressure and skin temperature," *Archives of Physical Medicine & Rehabilitation*, vol. 66, pp. 103-8, 1985.
- [9] D. S. Drummond, R. G. Narechania, A. N. Rosenthal, A. L. Breed, T. A. Lange, and D. K. Drummond, "A study of pressure distributions measured during balanced and unbalanced sitting," *Journal of Bone and Joint Surgery*, vol. 64, pp. 1034-1039, 1982.
- [10] T. A. Conine, A. K. Choi, and R. Lim, "The user-friendliness of protective support surfaces in prevention of pressure sores," *Rehabilitation Nursing*, vol. 14, pp. 261-3, 1989.
- [11] S. L. Garber and T. A. Krouskop, "Body build and its relationship to pressure distribution in the seated wheelchair patient," *Archives of Physical Medicine & Rehabilitation*, vol. 63, pp. 17-20, 1982.

- [12] T. A. Krouskop, R. Williams, P. Noble, and J. Brown, "Inflation pressure effect on performance of air-filled wheelchair cushions," *Archives of Physical Medicine & Rehabilitation*, vol. 67, pp. 126-8, 1986.
- [13] I. R. Odderson, K. M. Jaffe, C. A. Sleicher, R. Price, and R. J. Kropp, "Gel wheelchair cushions: a potential cold weather hazard," *Archives of Physical Medicine & Rehabilitation*, vol. 72, pp. 1017-20, 1991.
- [14] J. S. Krause and L. Broderick, "Patterns of recurrent pressure ulcers after spinal cord injury: identification of risk and protective factors 5 or more years after onset," *Archives of Physical Medicine & Rehabilitation*, vol. 85, pp. 1257-64, 2004.
- [15] D. R. Thomas, "Are all pressure ulcers avoidable?," *Journal of the American Medical Directors Association*, vol. 4, pp. S43-S48, 2003.
- [16] P. Werner and I. Perlash, "Warning mat to signal air seat cushion failure," *Archives of Physical Medicine and Rehabilitation*, vol. 63, pp. 188-190, 1982.
- [17] C. Bansal, R. Scott, D. Stewart, and C. J. Cockerell, "Decubitus ulcers: a review of the literature," *Int J Dermatol*, vol. 44, pp. 805-10, 2005.
- [18] L. Noreau, P. Proulx, L. Gagnon, M. Drolet, and M. T. Laramée, "Secondary impairments after spinal cord injury: a population-based study," *Am J Phys Med Rehabil*, vol. 79, pp. 526-35, 2000.
- [19] P. Raghavan, W. A. Raza, Y. S. Ahmed, and M. A. Chamberlain, "Prevalence of pressure sores in a community sample of spinal injury patients," *Clin Rehabil*, vol. 17, pp. 879-84, 2003.
- [20] R. Klotz, P. A. Joseph, J. F. Ravaud, L. Wiart, and M. Barat, "The Tetrafigap Survey on the long-term outcome of tetraplegic spinal cord injured persons: Part III. Medical complications and associated factors," *Spinal Cord*, vol. 40, pp. 457-67, 2002.
- [21] W. O. McKinley, A. B. Jackson, D. D. Cardenas, and M. J. DeVivo, "Long-term medical complications after traumatic spinal cord injury: a regional model systems analysis," *Arch Phys Med Rehabil*, vol. 80, pp. 1402-10, 1999.
- [22] R. Salcido, S. B. Fisher, J. C. Donofrio, M. Bieschke, C. Knapp, R. Liang, E. K. LeGrand, and J. M. Carney, "An animal model and computer-controlled surface pressure delivery system for the production of pressure ulcers," *Journal of Rehabilitation Research & Development*, vol. 32, pp. 149-61, 1995.
- [23] R. H. Guthrie and D. Goulian, "Decubitus ulcers: Prevention and Treatment," *Geriatrics*, vol. 28, pp. 67-71, 1973.
- [24] A. E. Swarts, T. A. Krouskop, and D. R. Smith, "Tissue pressure management in the vocational setting," *Archives of Physical Medicine & Rehabilitation*, vol. 69, pp. 97-100, 1988.
- [25] D. Fennegan, "Positive living or negative existence?," *Nursing Times*, vol. 15, pp. 51-54, 1983.
- [26] G. T. Nola and L. M. Vistnes, "Differential response of skin and muscle in the experimental production of pressure sores," *Plast Reconstr Surg*, vol. 66, pp. 728-33, 1980.
- [27] R. K. Daniel, D. Wheatley, and D. Priest, "Pressure sores and paraplegia: an experimental model," *Annals of Plastic Surgery*, vol. 15, pp. 41-9, 1985.
- [28] C. W. Oomens, S. Loerakker, and D. L. Bader, "The importance of internal strain as opposed to interface pressure in the prevention of pressure related deep tissue injury," *J Tissue Viability*, vol. 19, pp. 35-42, 2010.
- [29] R. Labbe, T. Lindsay, and P. M. Walker, "The extent and distribution of skeletal muscle necrosis after graded periods of complete ischemia," *Journal of Vascular Surgery*, vol. 6, pp. 152-7, 1987.
- [30] C. V. Bouten, C. W. Oomens, F. P. Baaijens, and D. L. Bader, "The etiology of pressure ulcers: skin deep or muscle bound?," *Archives of Physical Medicine and Rehabilitation*, vol. 84, pp. 616-619, 2003.
- [31] R. K. Daniel, D. L. Priest, and D. C. Wheatley, "Etiologic factors in pressure sores: an experimental model," *Archives of Physical Medicine & Rehabilitation*, vol. 62, pp. 492-8, 1981.

- [32] S. Gyawali, L. Solis, S. L. Chong, C. Curtis, P. Seres, I. Kornelsen, R. Thompson, and V. K. Mushahwar, "Intermittent electrical stimulation redistributes pressure and promotes tissue oxygenation in loaded muscles of individuals with spinal cord injury," *J Appl Physiol*, vol. 110, pp. 246-55, 2011.
- [33] L. R. Solis, S. Gyawali, P. Seres, C. A. Curtis, S. L. Chong, R. B. Thompson, and V. K. Mushahwar, "Effects of intermittent electrical stimulation on superficial pressure, tissue oxygenation, and discomfort levels for the prevention of deep tissue injury," *Ann Biomed Eng*, vol. 39, pp. 649-63, 2011.
- [34] J. Reenalda, M. Jannink, M. Nederhand, and I. J. M., "Clinical use of interface pressure to predict pressure ulcer development: a systematic review," *Assist Technol*, vol. 21, pp. 76-85, 2009.
- [35] S. I. Reger, V. K. Ranganathan, and V. Sahgal, "Support surface interface pressure, microenvironment, and the prevalence of pressure ulcers: an analysis of the literature," *Ostomy Wound Manage*, vol. 53, pp. 50-8, 2007.
- [36] C. W. Oomens, O. F. Bressers, E. M. Bosboom, C. V. Bouten, and D. L. Blader, "Can loaded interface characteristics influence strain distributions in muscle adjacent to bony prominences?," *Computer Methods in Biomechanics & Biomedical Engineering*, vol. 6, pp. 171-80, 2003.
- [37] L. Agam and A. Gefen, "Toward real-time detection of deep tissue injury risk in wheelchair users using Hertz contact theory," *J Rehabil Res Dev*, vol. 45, pp. 537-50, 8 p following 550, 2008.
- [38] E. Linder-Ganz, M. Scheinowitz, Z. Yizhar, S. S. Margulies, and A. Gefen, "How do normals move during prolonged wheelchair-sitting?," *Technol Health Care*, vol. 15, pp. 195-202, 2007.
- [39] K. K. Ceelen, A. Stekelenburg, J. L. Mulders, G. J. Strijkers, F. P. Baaijens, K. Nicolay, and C. W. Oomens, "Validation of a numerical model of skeletal muscle compression with MR tagging: a contribution to pressure ulcer research," *J Biomech Eng*, vol. 130, pp. 061015, 2008.
- [40] K. M. Le, B. L. Madsen, P. W. Barth, G. A. Ksander, J. B. Angell, and L. M. Vistnes, "An in-depth look at pressure sores using monolithic silicon pressure sensors," *Plast Reconstr Surg*, vol. 74, pp. 745-56, 1984.
- [41] L. R. Solis, D. P. Hallihan, R. R. Uwiera, R. B. Thompson, E. D. Pehowich, and V. K. Mushahwar, "Prevention of pressure-induced deep tissue injury using intermittent electrical stimulation," *J Appl Physiol*, vol. 102, pp. 1992-2001, 2007.
- [42] C. A. Curtis, S. L. Chong, I. Kornelsen, R. R. Uwiera, P. Seres, and V. K. Mushahwar, "The effects of intermittent electrical stimulation on the prevention of deep tissue injury: varying loads and stimulation paradigms," *Artif Organs*, vol. 35, pp. 226-36, 2011.
- [43] L. Solis, P. Seres, R. B. Thompson, and V. K. Mushahwar, "Long-term effectiveness of Intermittent Electrical Stimulation in the Prevention of Deep Tissue Injury: Preliminary Study," submitted.
- [44] A. Gefen, N. Gefen, E. Linder-Ganz, and S. S. Margulies, "In vivo muscle stiffening under bone compression promotes deep pressure sores," *Journal of Biomechanical Engineering*, vol. 127, pp. 512-524, 2005.
- [45] E. Linder-Ganz, N. Shabshin, Y. Itzchak, Z. Yizhar, I. Siev-Ner, and A. Gefen, "Strains and stresses in sub-dermal tissues of the buttocks are greater in paraplegics than in healthy during sitting," *J Biomech*, vol. 41, pp. 567-80, 2008.
- [46] M. Makhsous, G. Venkatasubramanian, A. Chawla, Y. Pathak, M. Priebe, W. Z. Rymer, and F. Lin, "Investigation of soft-tissue stiffness alteration in denervated human tissue using an ultrasound indentation system," *J Spinal Cord Med*, vol. 31, pp. 88-96, 2008.
- [47] L. R. Solis, A. Liggins, P. Seres, R. R. E. Uwiera, N. Poppe, E. Pehowich, R. B. Thompson, and V. K. Mushahwar, "Distribution of Internal Strain around Bony Prominences," submitted.
- [48] S. A. Kruse, J. A. Smith, A. J. Lawrence, M. A. Dresner, A. Manduca, J. F. Greenleaf, and R. L. Ehman, "Tissue characterization using magnetic resonance elastography: preliminary results," *Phys Med Biol*, vol. 45, pp. 1579-90, 2000.

- [49] J. R. Basford, T. R. Jenkyn, K. N. An, R. L. Ehman, G. Heers, and K. R. Kaufman, "Evaluation of healthy and diseased muscle with magnetic resonance elastography," *Arch Phys Med Rehabil*, vol. 83, pp. 1530-6, 2002.
- [50] M. Geerligs, G. W. Peters, P. A. Ackermans, C. W. Oomens, and F. P. Baaijens, "Linear viscoelastic behavior of subcutaneous adipose tissue," *Biorheology*, vol. 45, pp. 677-88, 2008.
- [51] S. Loerakker, L. R. Solis, D. L. Bader, F. P. T. Baaijens, V. K. Mushahwar, and C. W. J. Oomens, "How does muscle stiffness affect the internal deformations within the soft tissue layers of the buttocks under constant loading?," submitted.
- [52] L. Solis, S. Gyawali, and V. K. Mushahwar, "Mechanisms and Prevention of Deep Tissue Injury," in *The Pathomechanics of Tissue Injury and Disease, and the Mechanophysiology of Healing*, A. Gefen, Ed.: Research Signpost Co., 2009, pp. 283-312.
- [53] C. H. Lyder, "Pressure ulcer prevention and management," *Journal of the American Medical Association*, vol. 289, pp. 223-6, 2003.
- [54] V. F. Sagach, A. M. Kindybalyuk, and T. N. Kovalenko, "Functional hyperemia of skeletal muscle: role of endothelium," *Journal of Cardiovascular Pharmacology*, vol. 20, pp. S170-5, 1992.
- [55] H. M. Finestone, S. P. Levine, G. A. Carlson, K. A. Chizinsky, and R. L. Kett, "Erythema and skin temperature following continuous sitting in spinal cord injured individuals," *Journal of Rehabilitation Research & Development*, vol. 28, pp. 27-32, 1991.
- [56] P. Gilsdorf, R. Patterson, and S. Fisher, "Thirty-minute continuous sitting force measurements with different support surfaces in the spinal cord injured and able-bodied," *Journal of Rehabilitation Research & Development*, vol. 28, pp. 33-8, 1991.
- [57] P. A. Grace, "Ischaemia-reperfusion injury," *British Journal of Surgery*, vol. 81, pp. 637-47, 1994.
- [58] R. Tupling, H. Green, G. Senisterra, J. Lepock, and N. McKee, "Ischemia-induced structural change in SR Ca<sup>2+</sup>-ATPase is associated with reduced enzyme activity in rat muscle," *American Journal of Physiology Regulatory Integrative & Comparative Physiology*, vol. 281, pp. R1681-88, 2001.
- [59] R. Tupling, H. Green, G. Senisterra, J. Lepock, and N. McKee, "Effects of ischemia on sarcoplasmic reticulum Ca(2+) uptake and Ca(2+) release in rat skeletal muscle," *American Journal of Physiology Endocrinology & Metabolism*, vol. 281, pp. E224-232, 2001.
- [60] S. Loerakker, E. Manders, G. J. Strijkers, K. Nicolay, F. P. Baaijens, D. L. Bader, and C. W. Oomens, "The effects of deformation, ischemia, and reperfusion on the development of muscle damage during prolonged loading," *J Appl Physiol*, 2011.
- [61] A. Stekelenburg, G. J. Strijkers, H. Parusel, D. L. Bader, K. Nicolay, and C. W. Oomens, "Role of ischemia and deformation in the onset of compression-induced deep tissue injury: MRI-based studies in a rat model," *J Appl Physiol*, vol. 102, pp. 2002-11, 2007.
- [62] A. Stekelenburg, D. Gawlitta, D. L. Bader, and C. W. Oomens, "Deep tissue injury: how deep is our understanding?," *Arch Phys Med Rehabil*, vol. 89, pp. 1410-3, 2008.
- [63] J. M. Giles, A. E. Black, and J. E. Bischoff, "Anomalous rate dependence of the preconditioned response of soft tissue during load controlled deformation," *J Biomech*, vol. 40, pp. 777-85, 2007.
- [64] S. Aritan, S. O. Oyadiji, and R. M. Bartlett, "A mechanical model representation of the in vivo creep behaviour of muscular bulk tissue," *J Biomech*, vol. 41, pp. 2760-5, 2008.

## CHAPTER 3

### Distribution of Internal Strains around Bony Prominences in Pigs

#### 3.2 INTRODUCTION

Pressure ulcers are a type of soft tissue injury commonly found in individuals with reduced mobility and sensation as a result of age, disease, or injury. Populations typically affected by pressure ulcers include the elderly[1-3], patients in intensive and acute care units[4-5], residents of long-term care institutions[6], patients undergoing lengthy surgeries[7], as well as people with neurological injuries or diseases, such as those with spinal cord injury (SCI)[8-14]. People with SCI are particularly susceptible to pressure ulcers with up to 80% developing at least one pressure ulcer during their lifetime[12]. Locations around the pelvic area (trochanters, ischial tuberosities, sacrum) are most susceptible to pressure ulcer development, with approximately 67% of all pressure ulcers developing around this area[13].

Pressure ulcers can greatly affect the quality of life of those affected[15]. Treatment of these ulcers can be a lengthy and costly process[16-17], in many cases requiring surgery to repair the extensive tissue damage. Furthermore, with pressure ulcer recurrence rates as high as 91%[18], those who have acquired pressure ulcers are likely to develop them again. This highlights the importance of preventing pressure ulcers from developing in the first place.

Pressure ulcers can be classified into two categories, those that initiate at the level of the skin[19], and those that initiate at deep bone-muscle interfaces[19-23]. Pressure ulcers of superficial origin are caused primarily by factors like friction between the skin and an external surface (i.e., bed), poor tissue hygiene, excessive or insufficient skin moisture, and elevated skin temperature[1, 24]. With proper nursing care and diligent skin inspections, these ulcers can be detected early in their course of development and prevented from progressing to deeper tissue layers. Pressure ulcers of deep origin, known as deep tissue injury (DTI), are caused primarily by prolonged loading of soft tissue between a bony prominence and a surface[25-28] (e.g., chair, bed) in the absence of volitional motion for pressure re-distribution. Due to their deep origin, this type of pressure ulcers can cause extensive tissue damage before signs of the injury are exhibited at the skin level. Deep tissue injury was recognized as a new category of pressure ulcers by the National Pressure Ulcer Advisory Panel in the United States[29] in 2007. Nonetheless, evidence for this class of pressure ulcers in animal models dates back to the early 1980s [19, 23, 30-31] .

During prolonged tissue loading two different mechanisms of tissue damage have been identified. One mechanism is vascular, in which tissue compression occludes blood vessels in the affected region causing ischemia, which if sustained for a long time (>2hrs) leads to tissue death due to the lack of oxygen and nutrients in the tissue, as well as the accumulation of metabolic waste like lactic acid [15, 32-35]. After prolonged periods of ischemia, reperfusion of the affected

tissue further exacerbates tissue breakdown as a result of both the activation of free radicals accumulated during ischemia, and the inflammatory response occurring upon restoration of blood flow[36-39]. The second mechanism of tissue injury is the direct effect of mechanical forces acting on the tissue. Data from animal models, engineered tissue, as well as finite element modeling suggest that excessive strain and stress magnitudes in the tissue can directly lead to cell death[19, 40-41]. A strain-time model proposed by Gefen et al suggests that muscle cells can endure strains of up to 60% for 1 hour, or 40% for 285 minutes before damage takes place[42]. It is suggested that the highest magnitudes of internal strain and stress occur in the deep tissue closest to the bone, and that these levels are much higher than those measured at the skin level[31]. Magnetic Resonance Imaging (MRI) has been used to assess the deformation of the tissue occurring during sitting in order to estimate the strain levels in the gluteal muscles in human volunteers and build finite element models of the buttocks[43-45]. In addition, measurements of strain due to external loading have also been obtained from rat studies with the use of MRI tagging[46].

The main goal of this study was to determine the levels of strain in different regions of the muscle surrounding the ischial tuberosities in adult, healthy pigs as a result of varying levels of external loading. In addition, we assessed the effect of muscle atrophy secondary to chronic SCI on the distribution of strain magnitudes in the soft tissue around the ischial tuberosity in one animal. Moreover, we determined the effect of DTI on the distribution of strain magnitudes in another

animal with SCI and DTI. Finally, we investigated the effect of intermittent electrical stimulation (IES)[47-49], an intervention for preventing the formation of DTI, on the levels of soft tissue compression around the ischial tuberosity.

### **3.3 METHODS**

#### *3.3.1 Overview*

All animal experiments were approved by the University of Alberta Animal Use and Care Committee (IACUC number A5070-01). The experiments were performed in adult, anaesthetised pigs (Yucatan miniature pig strain) with intact spinal cords, as well as pigs with an incomplete SCI. In all animals, a range of external loading levels was utilized to entrap the semimembranosus muscles, which in the pig overly the ischial tuberosities, between an indenter and the bony prominences. Levels of muscle strain were assessed using data from MRI tagging images of the loaded muscles in one hind-limb.

#### *3.3.2 Test subjects*

A total of seven adult pigs were used, weighing  $68 \pm 8$  kg (mean  $\pm$  SD). Five of the animals had intact spinal cords and healthy muscles on the day of the terminal experiment. The number of intact pigs utilized was the minimal number required to obtain a statistical power greater than 0.8 (actual power was 0.83). The other two animals underwent a surgical hemisection of the spinal cord at the level of the 2<sup>nd</sup> lumbar vertebra one month prior to the experiment. The lesion caused paralysis of the ipsilateral hind-limb but retained voluntary bladder and bowel

function. Detailed descriptions of the surgical procedure and palliative care are provided in Solis et al[50]. During the 4 weeks between surgery and the terminal experiment, noticeable atrophy occurred in the paralyzed hind-limb. A quantification of muscle atrophy due to the spinal hemisection was obtained from MR images, in which the volume of muscles around the ischial tuberosity in the affected hind-limb in the pigs with SCI was compared to the muscle volume in the intact pigs on the day of the terminal experiment. For muscle atrophy quantification purposes only, an additional pig which was part of a separate study but had undergone the same surgical and recovery procedures as the pigs used in this study, was included (for a total N = 3).

### *3.3.3 Development of DTI in one pig with spinal cord injury*

One of the two pigs with incomplete SCI developed, unbeknownst to the researchers, a DTI in the semimembranosus, semitendinosus, and parts of the biceps femoris muscles of the paralyzed limb prior to the terminal experiment. After surgery, both pigs with SCI received as much attention as possible to prevent the formation of pressure ulcers. The flooring of their kennels was padded with memory foam to reduce the level of pressure when the pigs sat or lay down. Every day the pigs were suspended in a sling for up to 4 hours help maintain them in a standing position. When not in the sling, the pigs were assisted every two hours to move around their cage. In spite of this care, one of the pigs developed a DTI. The DTI exhibited no visible skin signs during the time elapsed between the hemisection surgery and the terminal experiment. Instead, the DTI was detected

in the MR images on the day of the terminal experiment. For analyses purposes, the two pigs with SCI, with and without DTI, were treated as individual case studies, and therefore were not included in any statistical quantifications of strain magnitudes.

#### 3.3.4 *Experimental setup*

The experiments were performed at the Peter S. Allen MR Research Centre at the University of Alberta. On the day of the experiment the animals were sedated using a combination of the drugs Ketamine (22mg/kg), Glycopyrrolate (0.01mg/kg), Xylazine (2.2mg/kg), and Buprenorphine (0.005mg/kg) administered intra-muscularly. A tracheal tube was then inserted to ensure proper ventilation throughout the experimental procedures, and an intravenous catheter was placed in each ear to allow for the administration of fluids (NaCl 0.9%) and drugs as needed. Anaesthesia was maintained through continuous administration of sodium pentobarbital (10mg/kg/hr; intravenous) for the duration of the experiment. Vital signs (respiration and heart rate) and the level of anaesthesia were monitored at all times by a veterinarian. The pigs were placed inside an MRI compatible containment unit (**Figure 1a**) which served two functions: 1) Sanitary containment of body fluids and particles while the pigs were inside the MRI magnet, and 2) provide a platform to hold the pig in place inside the MRI magnet during the external loading of the semimembranosus muscles.

### 3.3.5 *Application of external loading*

A custom-designed system was built to load the semimembranosus muscles of the animals (**Figure 1c**). The system consisted of: 1) A computer controlled servo motor (Danaher AKM23D, Danaher Motion, Washington, DC, USA) mounted horizontally on a drill press shaft located in a room adjacent to the MRI magnet room. 2) An MRI compatible indenter mounted on the pig's containment unit inside the MRI magnet (**Figure 1b**). 3) An MRI compatible 10 ft long-rod connecting the indenter (mounted on the pig's containment unit), and the servo motor located in the room adjacent to the MRI magnet room (**Figure 1c**). The rod had a force transducer (Interface SMT2-225, Interface, Arizona, USA) mounted in-line with the servo motor to record the level of external loading applied (**Figure 1b**). The levels of external loading were proportional to each animal's body weight (25%, 50%, and 75% of body weight). These loading levels are comparable to the range of loads measured for various seating surfaces in human volunteers with or without SCI in laboratory tests from this group (unpublished results). These levels are also within the range reported in literature for average percentage of body weight supported by the buttocks and upper thighs in seated individuals with or without SCI[51-53]. To prevent the pigs from sliding forward during the application of external loading, they were strapped in place inside the containment unit, and the containment unit was also attached to the servo motor through industrial quality straps. The control of the servo motor as well as the trigger to initiate each MRI acquisition was implemented using a Galil DMC-2123 (Galil Motion Control, California, USA) controller. The code for the

controller was written using the DMC Smart Terminal environment provided by the manufacturer. A built in displacement sensor was used for feedback control of the servo motor.

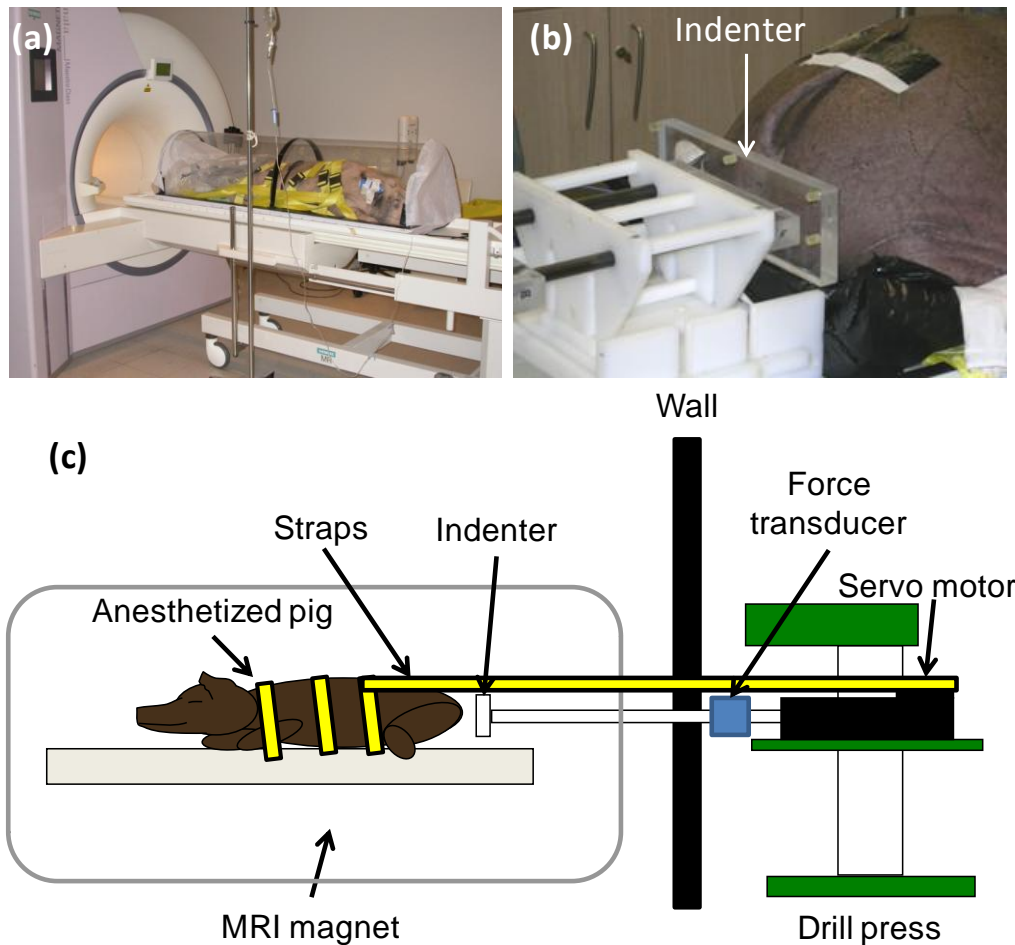


**Figure 1.** MRI compatible setup utilized to load pig muscles inside an MRI magnet. (a) MRI compatible containment unit. (b) MRI compatible indenter. (c) Diagram of loading setup.

### 3.3.6 MRI tagging sequence

All MRI data were collected using a 1.5T magnet (Siemens Sonata, Malvern, USA) and two flexible MRI body coils, one placed underneath and the other over the region of the pelvis. An MRI tagging sequence (slice thickness =

8mm, echo time = 1.36ms, repetition time = 360ms, field of view = 380mm x 317mm, matrix size = 192 x 136pixels, in-plane resolution = 2mm x 2.3mm, echo spacing = 2.6ms, flip angle = 12°, bandwidth = 810Hz) was used to obtain an assessment of tissue deformation during each loading protocol.

Four MRI slices were acquired to obtain a full coverage of the gluteal region (Figure 2) in intact animals. One slice was aligned with the anatomical frontal plane (parallel to the MRI bed), passing through the center of the ischial tuberosity, one dorsal to the central slice, and two ventral to it. The slices were separated by a 2mm gap, thus adjacent slices were positioned with a 1cm center-to-center distance between them. In the two animals with incomplete SCI, 3 slices were adequate for providing full coverage (one central, one dorsal, one ventral). This was because the muscles were smaller around the ischial tuberosities due to atrophy following the injury.

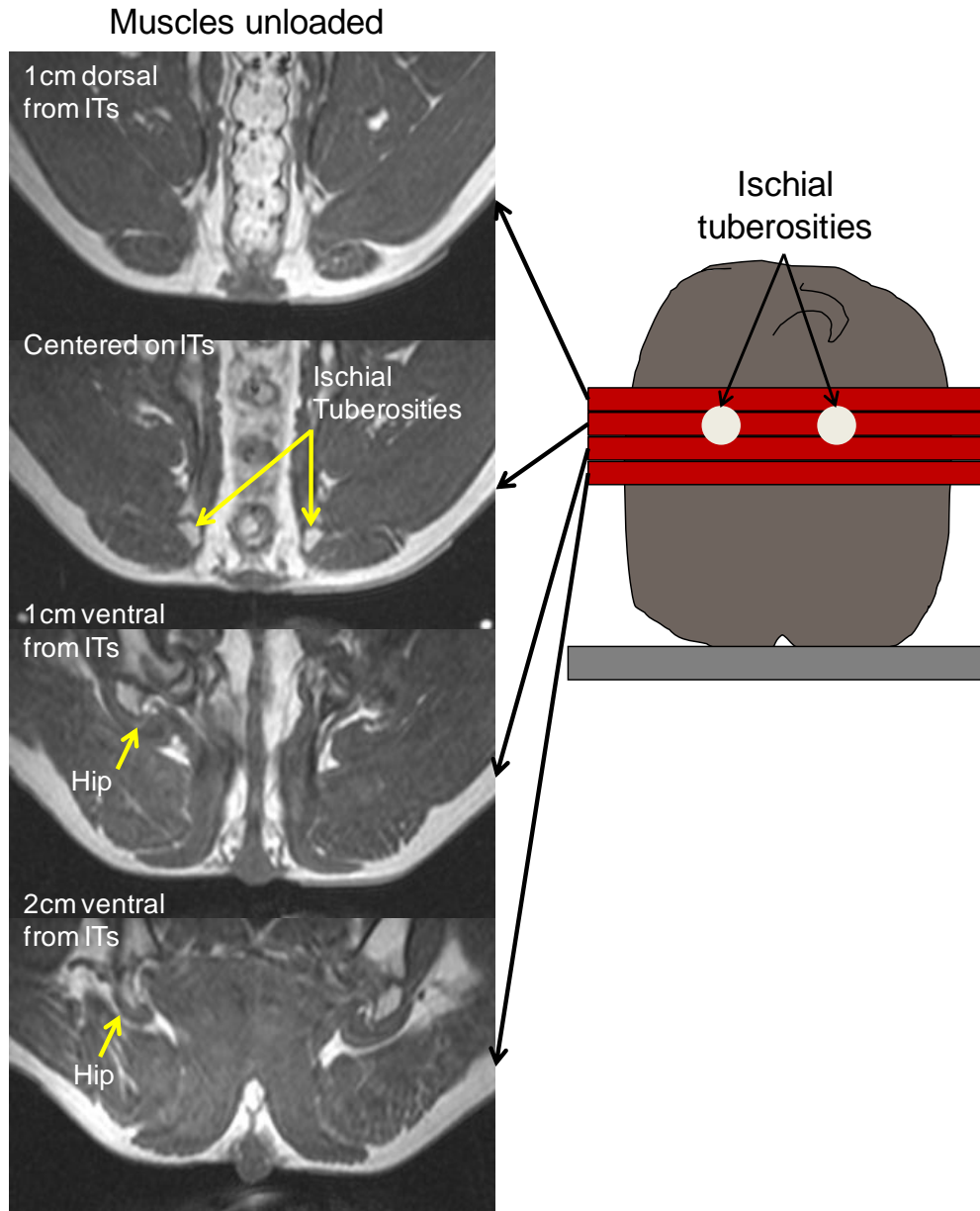


**Figure 2.** MR images acquired in 4 different slices. (1) 1 cm dorsal from the center of the ischial tuberosities. (2) Aligned with the center of the ischial tuberosities. (3) 1 cm ventral from the center of the ischial tuberosities. (4) 2 cm ventral from the ischial Tuberosities.

Loading of the muscles was applied in a stepped manner. For each target load, the displacement of the indenter required to reach the target load was divided into seven smaller steps (**Figure 3**). The number of steps was based on the desired total duration of each MRI acquisition ( $\leq 14$  sec). MR images were

acquired before (baseline image) and immediately after each loading step (deformed image). The acquisition of the baseline image, completion of the loading step, and acquisition of the deformed image all took place within 2 seconds. Given that muscle is a visco-elastic material, the slowest indentation speed possible (~1 cm/sec) was used for each loading step to minimize the viscous effects. This speed allowed for the completion of each loading step within the allotted time frame of the MRI acquisition (< 2 seconds).

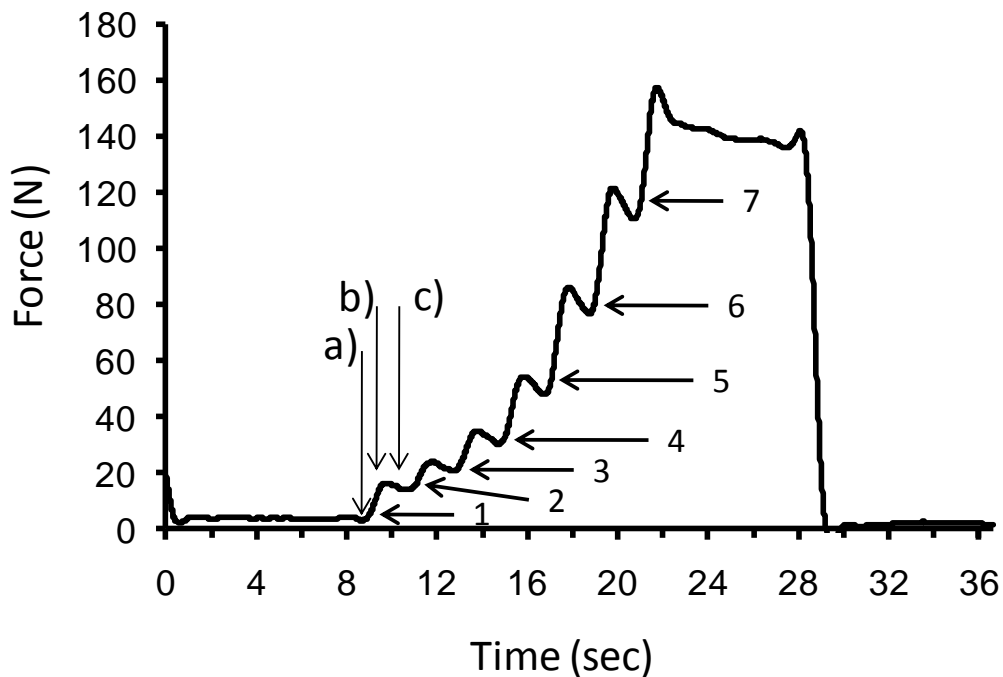


**Figure 3.** Target external loading level reached in 7 displacement increments (steps). MRI images acquired prior and immediately after each increment. (a) Acquisition of baseline image before loading step. (b) Start of loading step. (c) Acquisition of deformed image after loading step. Numbers (1–7): Loading steps taken to reach target load.

Loading in a stepped manner was a restriction of the MRI tagging technique, which can only work effectively if small deformations take place

(**Figure 4b**). If the deformation in the tissue becomes too large, as was the case to reach even the lowest loading level (25%BW) in a single step, the tag lines become indiscernible and strain vectors immeasurable (**Figure 4a**). Each external loading level was applied a total of four times in the intact animals, with each repetition corresponding to the acquisition of each slice. For the pigs with SCI, the loading levels were repeated three times, once for each acquired slice. For the 50% body weight level, in both spinally-intact and injured animals, the load was repeated once for each slice acquired, plus two additional times to replicate the MRI slice centered on the ischial tuberosities. The additional repetitions were to ensure the absence of variability due to repeated loading, and to assess researcher error during the manual analysis of the MR images. The order in which each loading level was applied and which slice was acquired was randomized in all animals.

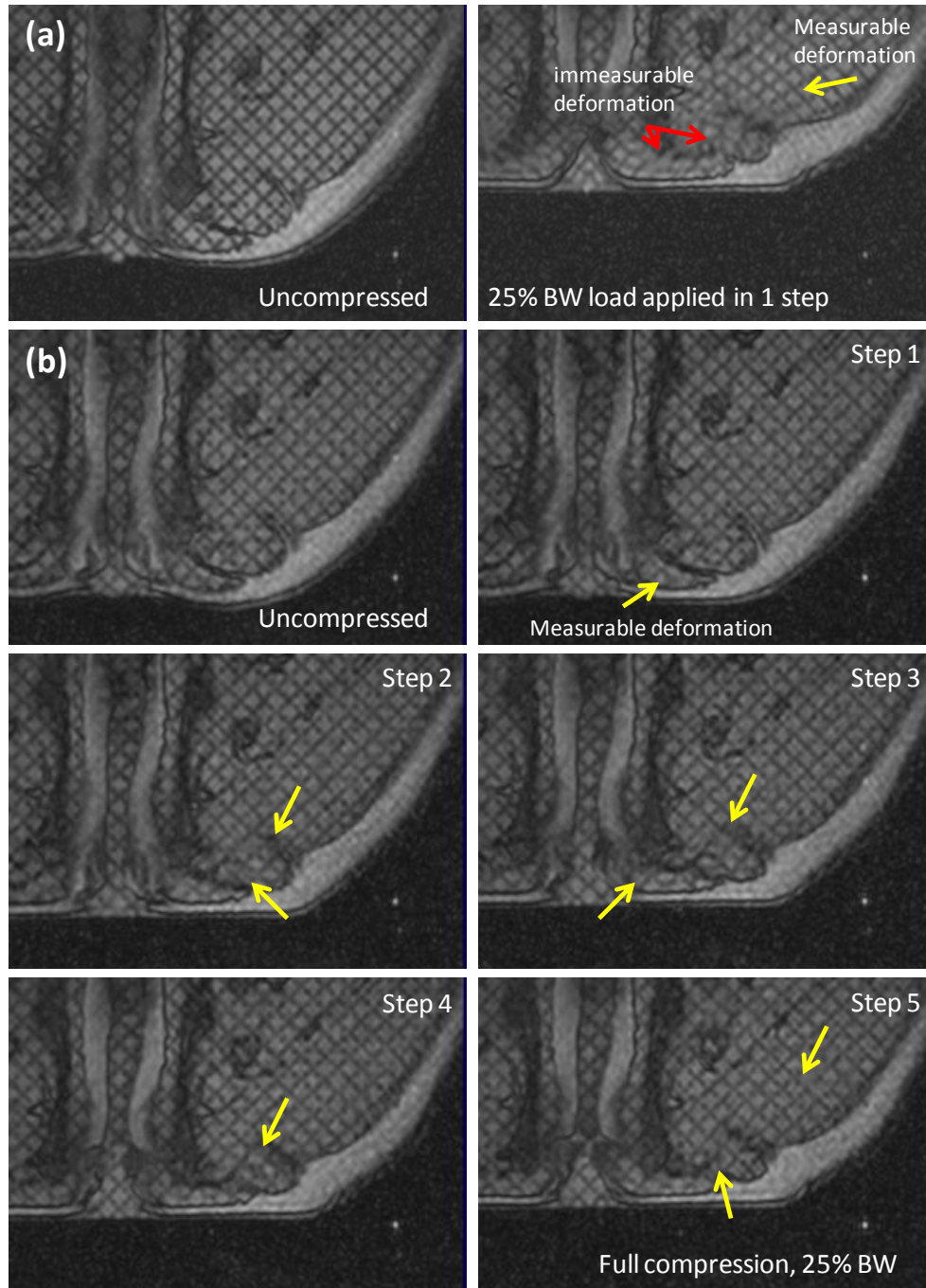


**Figure 4.** Large deformations in the tissue did not allow for loading to the desired level in a single step, as MRI tagging data became unquantifiable. (a) Tagging images of unloaded and loaded muscle to 25% BW load in a single loading step. (b) Tagging images of unloaded muscle and loaded muscle to 25% BW in multiple steps.

### 3.3.7 *Measurement of strain magnitudes*

All MR images were imported into Matlab (Mathworks, Cambridge, USA) and processed using custom-written scripts to track the changes in the tag lines as a result of each loading condition. Analyses of strain in the semimembranosus muscle in all animals were limited to one side. In the pigs with SCI this side corresponded to the paralyzed limb. For each external loading level, the sequence of loading steps required to reach the target load were analyzed in succession. The images comprising each step were classified as baseline image and deformed image, and the  $x$  and  $y$  coordinates of each intersection (node) in the tag lines in both images were obtained. The  $x$  and  $y$  coordinates from the baseline image were then displayed over those of the deformed image. If no deformation occurred in a particular region of the tissue after the loading step, the nodes corresponding to the baseline image matched exactly those of the deformed image (**Figure 5a**). If however, deformation occurred, the nodes from both images did not coincide and each node from the baseline image was moved manually to the location of the corresponding intersection in the deformed image (**Figure 5b**). The change in position was then calculated for each node and the process was repeated for all steps in the loading sequence. The final deformation vectors for the nodes were then calculated by vectorially summing the deformations in each individual step. The displacement of the nodes between each step of indentation was also used to calculate the maximal and minimal principal strains, as well as the maximal shear strain. The calculation of these strains was implemented according to the method proposed by Geers et al[54].

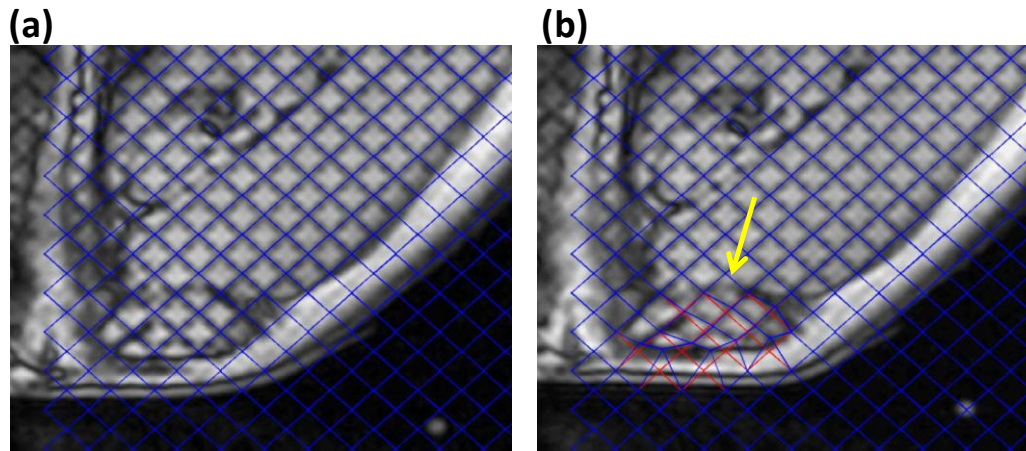


**Figure 5.** Quantification of strain by comparing the position of intersecting points in tag lines between baseline and deformed images. (a) Tagging image in which there was no deformation of tissue. (b) Tagging image in which deformation occurred (arrow). Original position of image tag lines represented by red lines. Nodes forming the deformed grid (blue lines) were manually repositioned to overlap with the deformed image tag lines. The change in the coordinates of each node moved between the original and deformed image was recorded and used in strain calculations.

### 3.3.8 Application of intermittent electrical stimulation

To test the effects of IES on tissue compression, MRI compatible electrodes (5cm x 10cm, Pure Care, Sherwood Park, Alberta, Canada) were used to elicit muscle contractions. The cathode electrode was placed over the motor point of the semimembranosus muscle in the left hind-limb in all pigs. The return electrode was placed rostrally between the iliac crest and the spinal column. Electrical stimulation was applied using a BioStim NMS+ stimulator (Biomedical Life Systems, California, USA), and stimulation was delivered in 50 Hz trains of biphasic, charge-balanced, 200  $\mu$ s wide pulses. Stimulation amplitude was set to the level required to generate maximal contractions, and stimulation was applied for 12 seconds. To document the changes in muscle thickness between the ischial tuberosities and indenter due to muscle contractions produced by IES, spin-echo

images (44 slices, echo time: 1.09ms, relaxation time: 2.45ms, slice thickness: 3.55mm, field of view: 333 x 400mm<sup>2</sup>, acquisition matrix: 320 x 384 pixels; in-plane resolution: 1.04 x 1.04mm<sup>2</sup>) were acquired before and during IES.

Loading of the semimembranosus muscles was accomplished through a very slow and continuous motion, moving the indenter at a speed of 0.2 cm/sec until the desired load was reached. Upon reaching the target loading level, the indenter automatically stopped, and 2 seconds later the stimulus bout was initiated and lasted for 12 seconds. MRI scanning was automatically initiated 1 sec after the initiation of stimulation. The total acquisition time for each scan was 11 seconds. Tissue thickness between the apex of the curvature of the ischial tuberosity and the edge of the skin with the semimembranosus muscles unloaded, loaded, and with and without IES was measured (e.g., **Figure 11**). The proportional change in tissue thickness for all levels of external loading relative to the unloaded muscle was then determined to assess the effectiveness of IES in counteracting tissue compression due to external loading.

### *3.3.9 Statistical Analysis*

The two null hypotheses that this study tried to reject were the following. 1) There would be no statistical difference in the muscle strain levels between the different external loading levels utilized, and 2) there would be no statistical difference in the muscle strain levels between the use and non-use of IES in the loaded muscles.

Changes in strain magnitudes due to the different levels of external loading in each imaging slice in intact animals were compared using two-way ANOVA (loading level and slice location used as the two main factors) and Fisher's Least Significant Difference (LSD) post-hoc analyses with  $\alpha = 0.05$ . The conservative, Bonferroni correction test, was used in conjunction with Fisher's LSD test to reduce false positives in the slice location factor due to multiple comparisons (6 comparisons: dorsal slice vs. central slice, dorsal slice vs. 1 cm ventral slice, dorsal slice vs. 2 cm ventral slice, central slice vs. 1 cm ventral slice, central slice vs. 2 cm ventral slice, and 1 cm ventral slice vs. 2 cm ventral slice). Under Bonferroni's test, an  $\alpha$  level of 0.008 was used for each individual comparison. A two-way ANOVA and Fisher's LSD post-hoc analyses were also used to assess if the changes in tissue thickness due to the different loading levels, and due to contractions produced by IES were statistically significant in the intact animals. Because single comparisons were used, a Bonferroni correction was not needed. A p value of 0.05 was selected to indicate significance for all tests. All statistical tests were done in SPSS.

### **3.4 Results**

#### *3.4.1 Tissue loading*

For all animals, a total of 7 steps of indentation were used to reach the target loading level. In a few trials some displacement of the hip occurred for loading steps 6 and/or 7. When this occurred, the displacement was noticeable by a shift in the position of the ischial tuberosities from image to image. In these

instances, the steps from the start of bone displacement and onwards were discarded and not included in further analyses. In all animals and all locations, the magnitude of the strains measured as a result of the 75% BW external loading level did not differ from those obtained from the 50% BW level ( $p = 0.675$ ). Strain measurements from the 75% BW loading level are therefore not shown and were not considered for further statistical comparisons of strain magnitudes.

#### *3.4.2 Distribution of strain in pigs with intact spinal cords*

The pattern of muscle deformation was the same in all animals with intact spinal cord for both the 25% and 50% BW loading levels. An example of the deformation vectors in one animal is shown in **Figure 6**. In the slice centered on the ischial tuberosities (**Figure 6**, 2<sup>nd</sup> row) the muscle tissue located directly between the apex of the ischial tuberosities and the edge of the skin moved towards the ischial tuberosity, indicating that it was compressed by the loading. Muscle tissue located laterally from the ischial tuberosity was displaced away from the bone, indicating that it had experienced tensile and shear deformations. The deformation vectors in the slice 1 cm dorsal to the ischial tuberosities (**Figure 6**, 1<sup>st</sup> row) were substantially smaller in amplitude due to the absence of bony prominences in that region. This, however, was not the case in the slices 1 cm and 2 cm ventral to the ischial tuberosities (**Figure 6**, 3<sup>rd</sup> and 4<sup>th</sup> rows). In these slices, the magnitude of the deformation vectors appeared to be larger than that in the central slice. Moreover, the direction of the vectors changed, at times becoming dominated by compression.

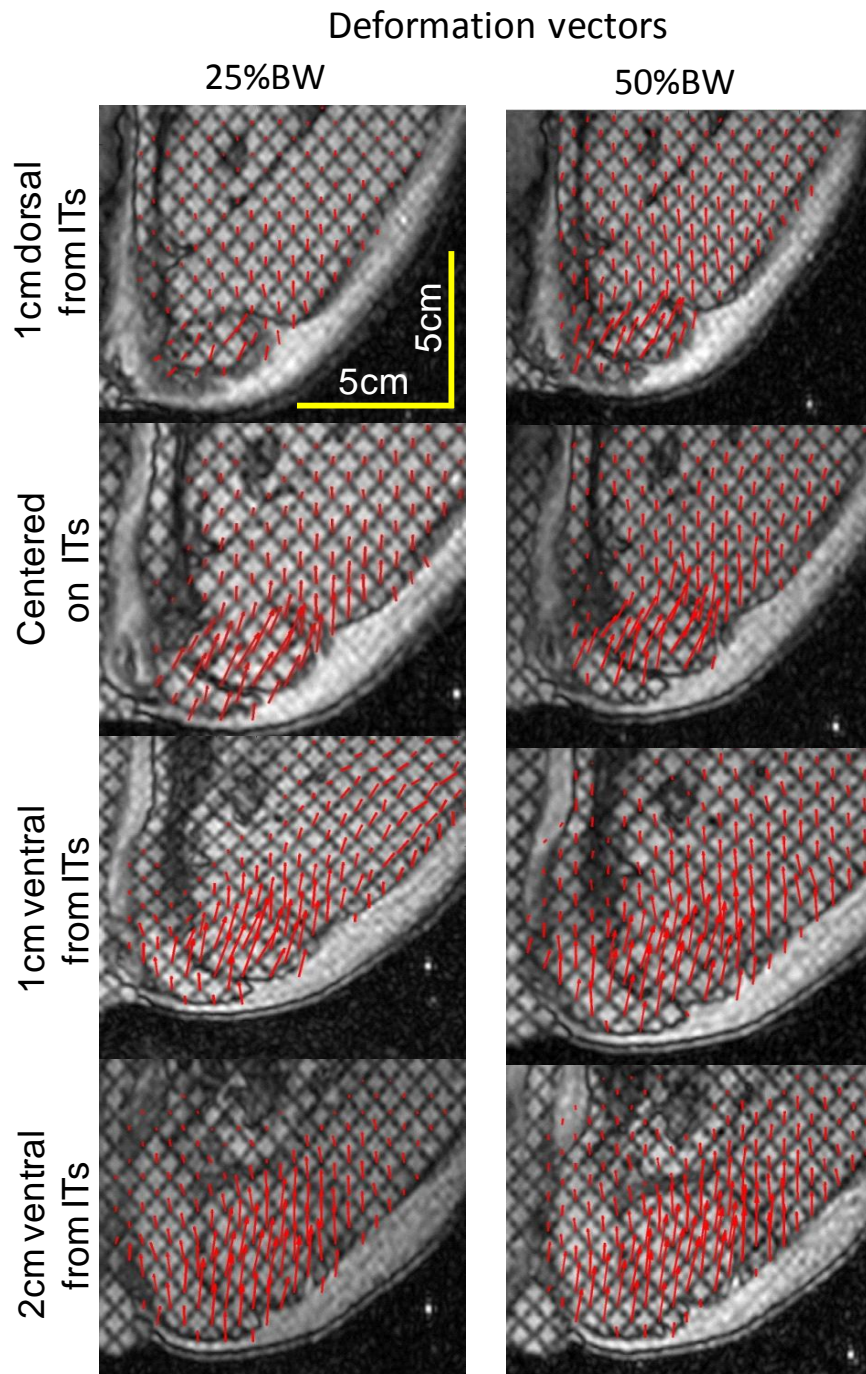


**Figure 6.** Deformation vectors in an intact pig. Shown are the deformation vectors in each imaged slice for the 25% BW (left) and 50% BW (right) external loading levels from one pig with intact spinal cord.

Maps of the distribution of the maximal principal, minimal principal and maximal shear strains from one intact pig for the 25% and 50% BW loading levels are shown in **Figures 7 and 8**, respectively. Pronounced minimal principal (compressive) strains were seen around the ischial tuberosity and hip bones in the slices centered on the ischial tuberosities and 1-2cm ventral, respectively (left column, rows 2-4). Under the 25% BW loading (**Figure 7**), minimal principal strain was the most prominent strain. Under 50% BW loading (**Figure 8**), maximal principal (tensile) and maximal shear strains became pronounced in locations lateral to the bony prominences (middle and right columns), especially in the plane 1 cm ventral to the ischial tuberosities. In general, peak strain magnitudes were seen within a 2 cm region ventral to the ischial tuberosities, and up to 5 cm laterally.

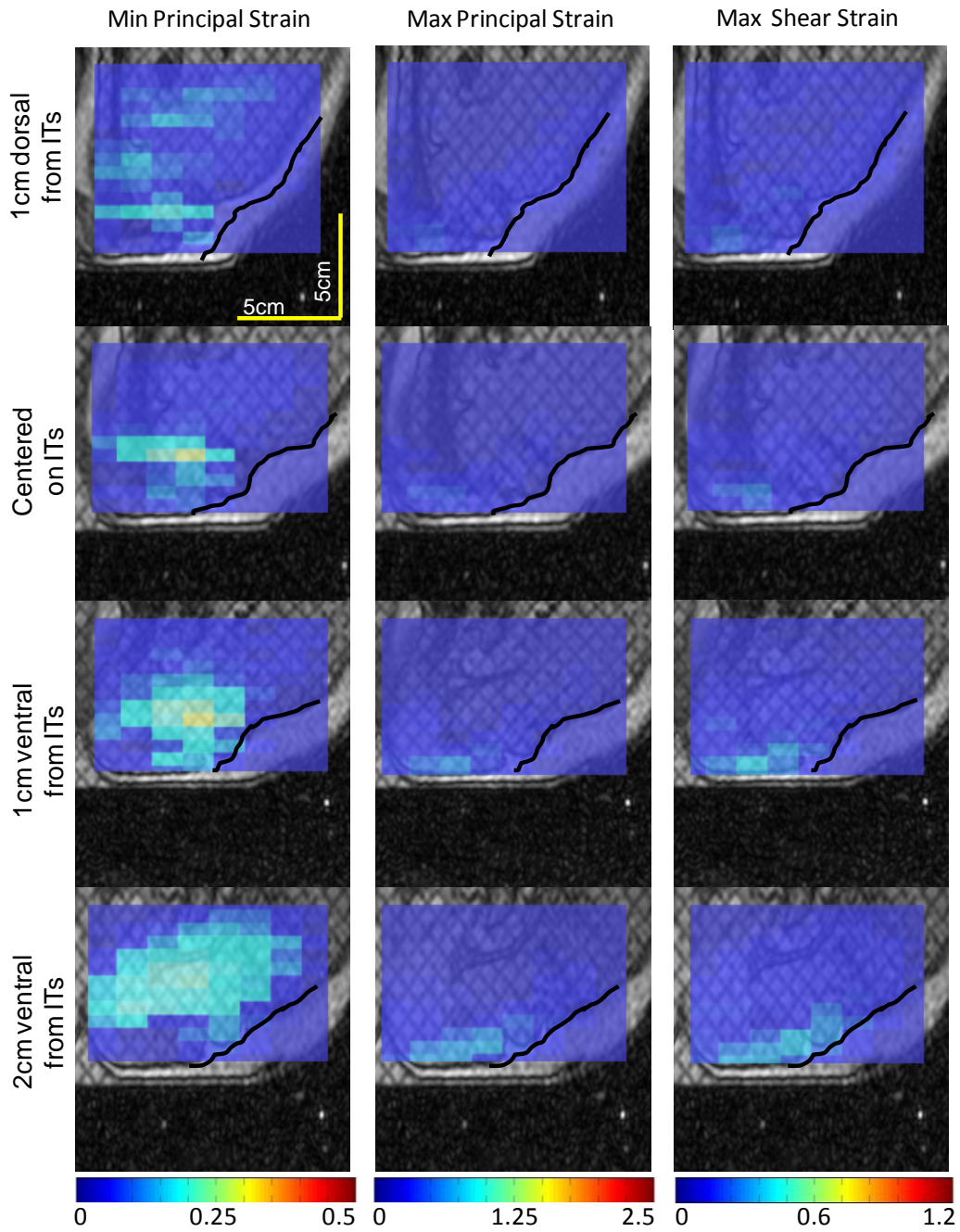


**Figure 7.** Distribution of principal and shear strains under 25% BW loading. Shown are the strain distributions in all imaging slices in an animal with an intact spinal cord.

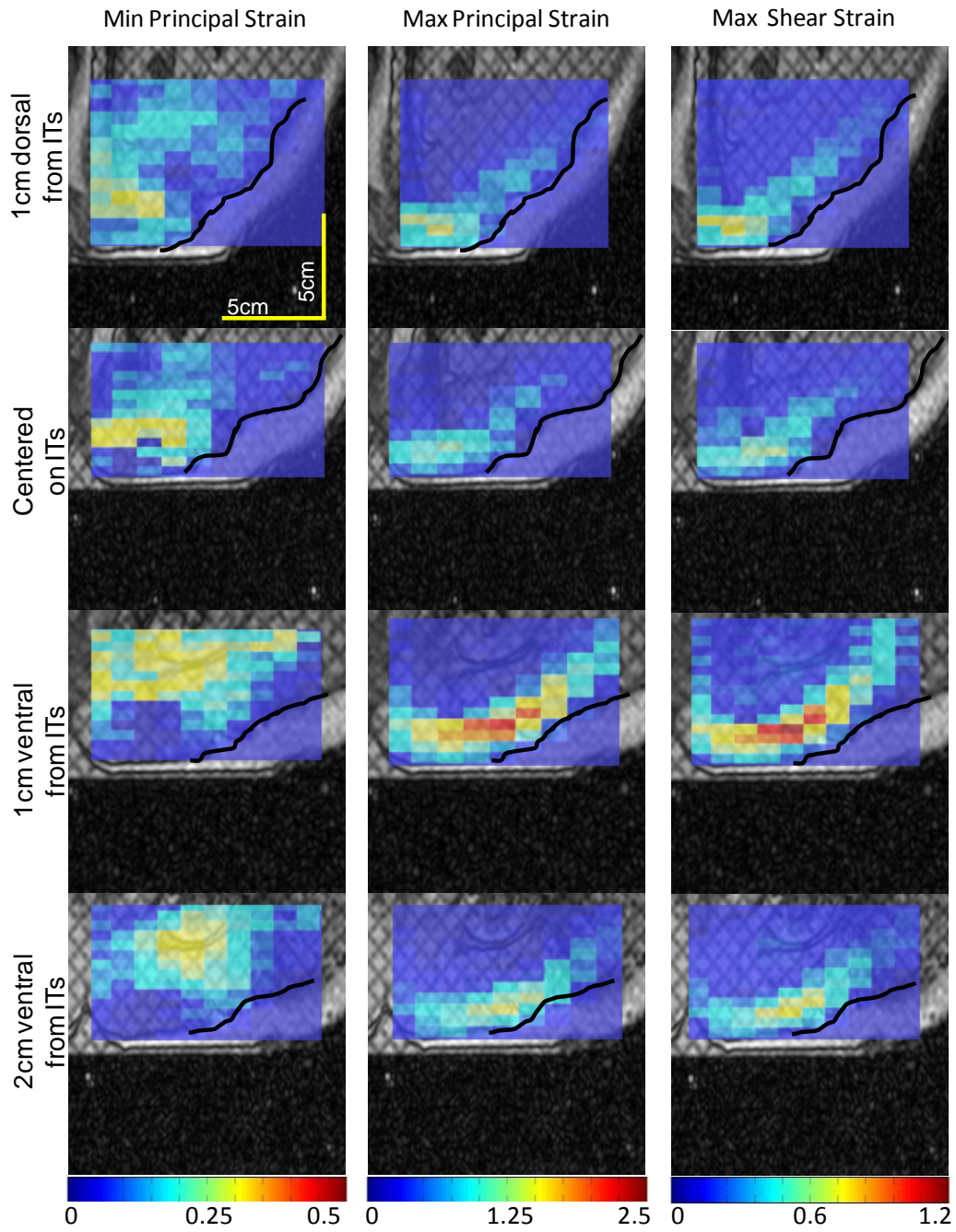


**Figure 8.** Distribution of principal and shear strains under 50% BW loading. Shown are the strain distributions in all imaging slices in an animal with an intact spinal cord.

The peak maximal and minimal principal strains and maximal shear strain were calculated for the 25% and 50% BW loading. These values are summarized for intact animals in Table 1. Under 25% BW loading, the average peak maximal principal strain magnitude was  $0.68 \pm 0.2$  (mean  $\pm$  SD), minimal principal strain magnitude was  $0.30 \pm 0.030$ , and maximal shear strain magnitude was  $0.40 \pm 0.11$  in the slice centred on the ischial tuberosities. Increasing external loading to 50% BW increased strain magnitude by 91.2%, 16.7%, and 68.8%, respectively, suggesting that most of the compression in the tissue occurred as a result of the initial 25% BW load. The slice 1 cm dorsal from the center of the ischial tuberosities experienced strain magnitudes of  $0.36 \pm 0.033$ ,  $0.085 \pm 0.035$ , and  $0.21 \pm 0.010$  for peak maximal principal strain, minimal principal strain, and maximal shear strain, respectively. Increasing the external load to 50% BW increased these strain magnitudes by 261%, 288%, and 214%, respectively. In the slice 1 cm ventral from the ischial tuberosities, increasing the loading from 25% to 50% BW increased the peak maximal principal, minimal principal and maximal shear strain magnitudes by 75.3%, 6.3% and 77.1%, respectively. In the slice 2 cm ventral to the ischial tuberosities, the increase in loading increased the peak strain magnitudes by 74.7%, 19.4% and 78.0%, respectively. The increase in loading from 25% to 50% BW resulted in significant increases in the peak values of all strain levels across all imaging planes.

The anatomical slice relative to the ischial tuberosities (1 cm dorsal, central, 1 cm ventral, or 2 cm ventral) also had an effect on the peak strain

magnitudes. Table 1 summarizes the percent differences in peak maximal principal, minimal principal and maximal shear strains between slices. Relative to the central slice, the 1 cm dorsal plane had the smallest overall strain under the 25% BW loading. However, with 50% BW loading, the strain magnitudes in the dorsal slice were similar to those experienced by the slice centered on the ischial tuberosities. The slice 1 cm ventral to the ischial tuberosities experienced an average increase of 20% and 37% in peak maximal principal and maximal shear strain magnitudes, respectively, relative to the central slice under both 25% and 50% BW loading, while the slice 2 cm ventral to the ischial tuberosities experienced an average of 25% and 46% increase, respectively. Interestingly, the peak minimal principal strain in the ventral slices remained roughly the same as that in the central slice. The slice 2 cm ventral to the ischial tuberosities experienced moderate increases in peak strain magnitudes relative to the slice 1 cm ventral, especially under the 50% BW loading.

Statistically, the peak minimal principal strain in the 1 cm dorsal location was significantly different from the 2 cm ventral location ( $p = 0.013$ , 2-way ANOVA, Fisher's LSD post-hoc analysis with Bonforreni correction) under the 25% BW loading level. The difference in the peak minimal principal strain between the 1 cm dorsal location and the central location approached significance ( $p = 0.072$ ). It also approached significance between the 1 cm dorsal and the 1 cm ventral locations ( $p = 0.092$ ). All peak strain magnitudes under the 25% BW loading level were significantly smaller than their corresponding magnitudes

under the 50% BW loading level for all imaging locations ( $p < 0.05$ ).

### *3.4.3 Degree of atrophy due to SCI*

The spinal hemisection surgery resulted in paralysis of one hind-limb. As a result, noticeable atrophy occurred in the affected leg. In the intact animals ( $n=5$ ), muscle volume in the hind limb was  $249.83 \pm 48.89 \text{ cm}^3$ , in comparison, in the pigs with SCI ( $n=3$ , one not used in this study) muscle volume in the paralyzed limb was  $127.26 \pm 41.61 \text{ cm}^3$ , indicating a reduction of 50.94% in muscle volume due to atrophy<sup>64</sup>. During the month that elapsed between surgery and the terminal experiment none of the pigs with SCI recuperated voluntary control of the ipsilateral hind-limb.

### *3.4.4 Distribution of strain magnitudes in pigs with SCI*

In the pig with SCI and no DTI (**Figure 9**, middle and right columns), the peak strain magnitudes under the 25% BW loading level were 0.74, 0.34, and 0.40, for the maximal principal, minimal principal and maximal shear strain, respectively, in the slice centered on the ischial tuberosity. Under the 50% BW loading level, the strain magnitude levels increased by 91.9%, 17.6%, and 87.5%, respectively. The changes in the magnitude of strains between the 25% and 50% BW load levels were comparable to those observed in the intact pigs; however, the absolute strain magnitudes were higher in the pig with SCI, and the area experiencing the strain was smaller (1 cm ventral to the ischial tuberosities and up to 5 cm laterally). Under 25% BW loading, the peak strain magnitudes were

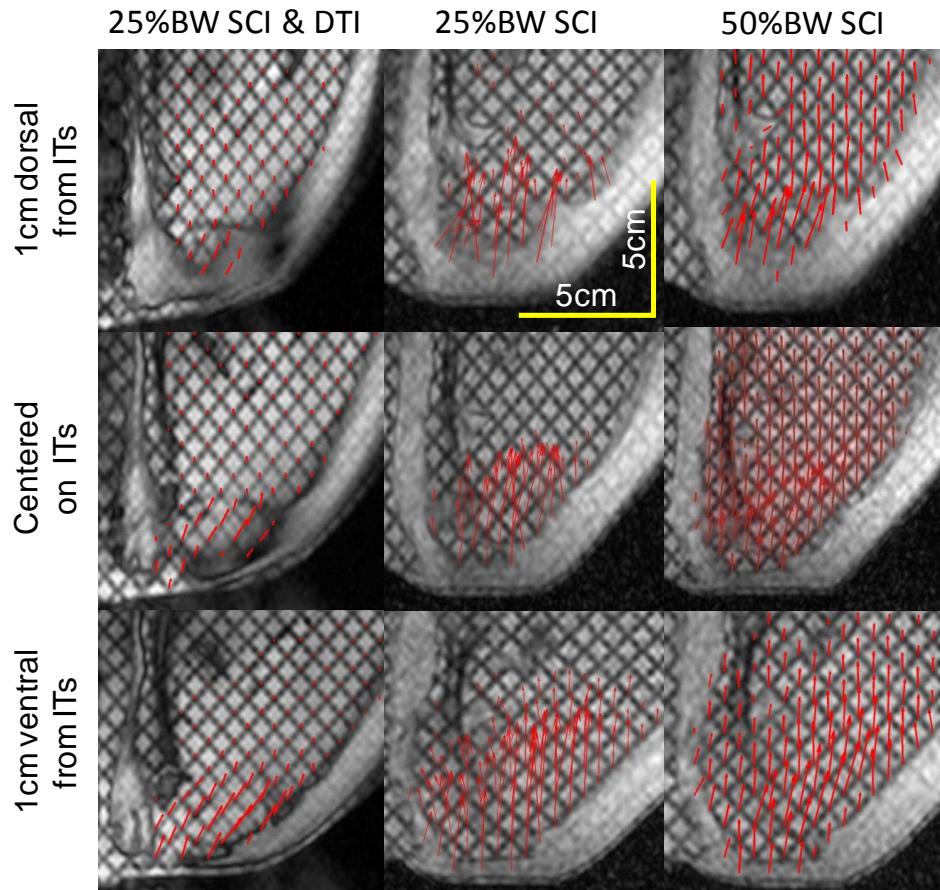
higher by 8.8%, 13.3%, and 0.75%, for the maximal principal, minimal principal and maximal shear strains, respectively, than that seen in the intact animals. Under the 50% BW loading, the peak strain magnitudes were higher by 9.2%, 14.3%, and 11.9%.

	25% BW loading				50% BW loading			
	1cm Dorsal vs Central	1cm Ventral vs Central	2cm Ventral vs Central	1cm Ventral vs 2cm Ventral	1cm Dorsal vs Central	1cm Ventral vs Central	2cm Ventral vs Central	1cm Ventral vs 2cm Ventral
<b>Maximal principal strain</b>	-47.1%	36.8%	45.6%	6.5%	0.0%	25.4%	33.1%	6.1%
<b>Minimal principal strain</b>	-73.3%	6.7%	3.3%	-3.1%	-2.9%	-2.9%	8.8%	12.1%
<b>Maximal shear strain</b>	-47.5%	20.0%	25.0%	4.2%	0.0%	28.8%	34.8%	4.7%

**Table 1:** Percent changes in peak strain levels as a function of imaged plane relative to the center of the ischial tuberosities in intact animals.

Unlike the intact animals, the peak strain magnitudes in the pig with SCI and no DTI in the slice 1 cm dorsal to the center of the ischial tuberosities were approximately the same as those measured at the center of the ischial tuberosities. Similar to the intact pigs, the highest magnitudes of strain were observed away from the centre of the ischial tuberosity, in the slice 1 cm ventral from the center of the bone.

**(a) Deformation vectors**



**(b) Morphology**

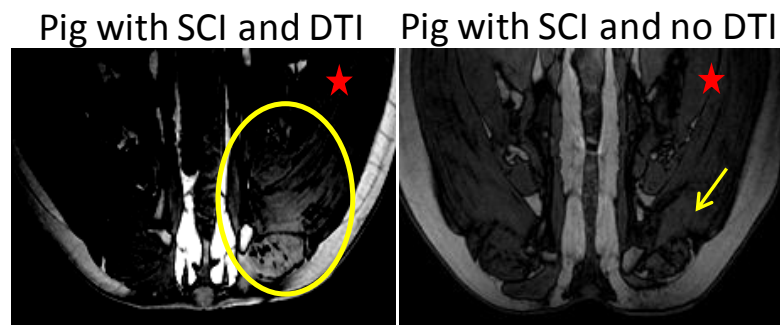


**Figure 9.** Deformation vectors in pigs with SCI. (a) Shown are the deformation vectors for an animal with SCI loaded under 25% BW (middle) and 50% BW (right) loading for all imaged slices around the ischial tuberosities. The deformation vectors under 25% BW loading in an animal with SCI and DTI are shown in the left column. (b) MR image centered on the ischial tuberosities showing regional morphology in an animal with SCI (right) and an animal with SCI and DTI (left). The red star marks the side affected by the SCI, and severe muscle atrophy can be observed (right, arrow). Image contrast was enhanced to better show the DTI in the animal with SCI and DTI (left). The region, marked with a yellow oval, has a brighter signal indicative of edema (water accumulation).

The presence of DTI in the second pig with SCI was confirmed using a T<sub>2</sub>-weighted MRI sequence[47], which is sensitive to the presence of freely moving water (edema) within the tissue (**Figure 9b**, left). Interestingly, in this animal (**Figure 9a**, left column), most strain magnitudes were smaller than even those observed in intact animals for both the 25% and 50% BW loading and the strain distribution pattern was altered. In the slice centered on the ischial tuberosity, the magnitudes of the peak maximal principal, minimal principal and maximal shear strain for the 25% BW loading were smaller by 33.8%, 13.3%, and 44.6%, respectively, than those measured in the intact pigs. Under the 50% BW loading level, the magnitudes of the peak maximal principal strain and maximal shear strain were also smaller by 43.1% and 41.8%, respectively, and only the minimal principal strain was higher by 2.9%. Therefore, in addition to the general reduction in magnitude, the pattern of strain distribution in the pig with SCI and DTI was different from that in intact pigs and the pig with SCI and no DTI. Relatively higher maximal principal and maximal shear strain magnitudes were observed than minimal principal strain. A summary of the peak maximal principal, minimal principal and maximal shear strains under the 25% and 50% BW loading for all animal groups and in all slices relative to the ischial tuberosities is provided in **Figure 10**.

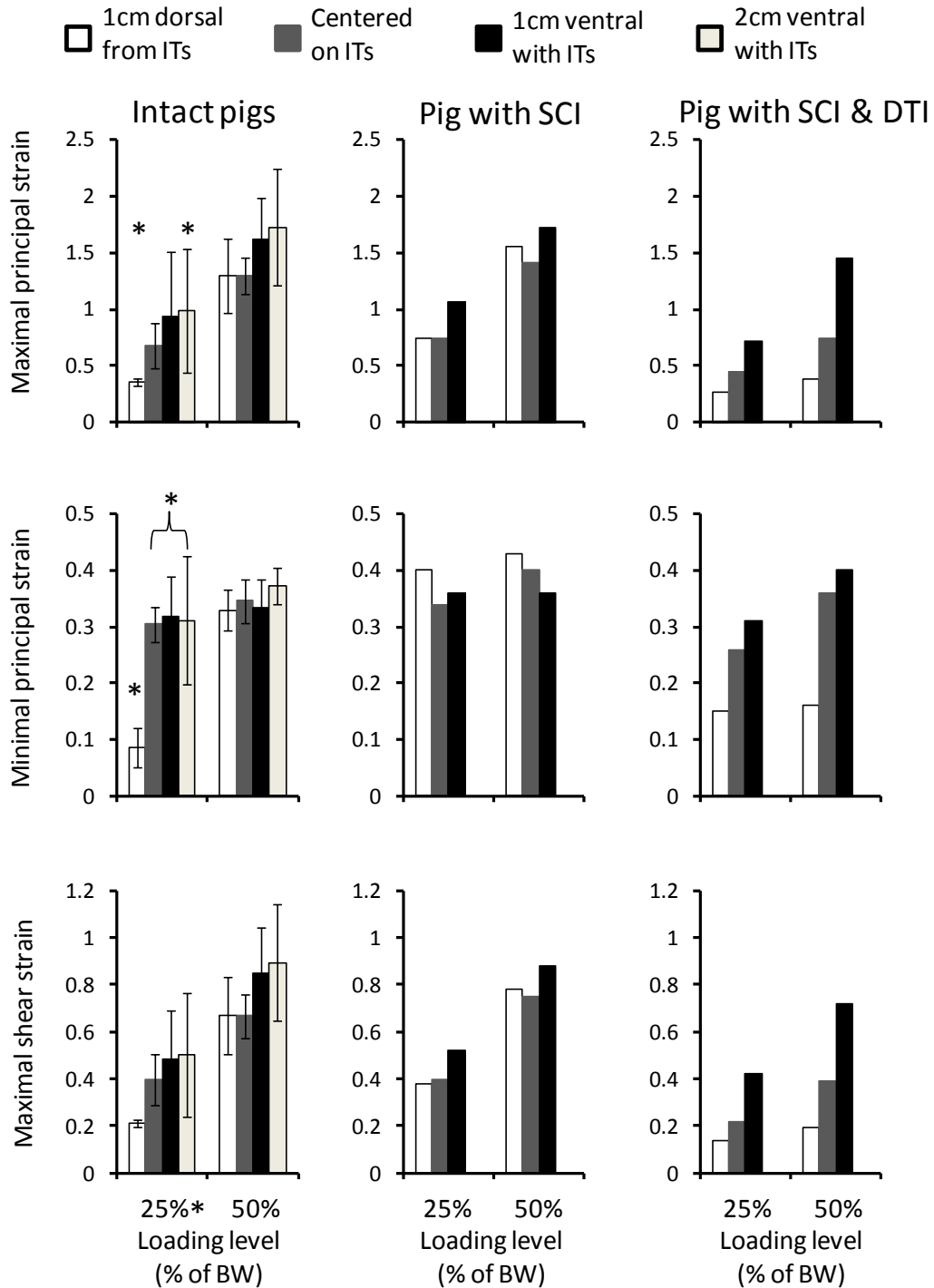


**Figure 10.** Summary of principal and shear strains. Shown are the peak maximal principal, minimal principal and maximal shear strains in intact pigs (mean 6 standard deviation), pig with SCI, and pig with SCI and DTI, for the 25% and 50% BW loading levels. Highest strain levels were generally located 2 cm ventral from the center of ischial tuberosities in intact animals, and 1 cm ventral in pigs with SCI. Averages in the group of intact pigs are based on measurements in 2 pigs for the 25% BW loading level and 5 pigs in the 50% BW loading level. For each imaging location (slice), all peak strain levels under 25% BW loading were significantly smaller than those under 50% BW loading. \*denotes an additional significant difference between the 1 cm dorsal and 2 cm ventral slices in peak minimal principle strain.

### 3.4.5 *Effects of IES*

An example of the thickness of tissue between the apex of the ischial tuberosity and the outer edge of the skin under loading and IES in one animal is shown in **Figure 11**. When unloaded, average muscle thickness between the center of the ischial tuberosity and the edge of the skin was  $34.93 \pm 8.27$  mm in the intact pigs. In comparison, average muscle thickness was 35.6mm and 26.5mm in the pigs with SCI. When externally loaded to 25%, and 50% of BW, average muscle thickness in the intact pigs was reduced by  $49\% \pm 11\%$  and  $42\% \pm 9\%$ , respectively. In the pigs with SCI, loaded muscle thickness were 54% and 44%, and 40% and 33% of the original measurements for the 25% and 50% of BW levels, respectively. Incidentally, when loaded to 75% BW there were no further reductions in tissue thickness relative to the that produced by 50% BW in any animal, with our without SCI. In all pigs and for all load levels, the use of IES increased the muscle thickness between the ischial tuberosity and the indenter surface during each IES-elicited contraction. In the intact pigs, the muscle contraction restored muscle thickness to  $61\% \pm 14\%$ ,  $55\% \pm 14\%$ , and  $53\% \pm 14\%$  of its original thickness for the 25%, 50%, and 75% BW loading levels, respectively. Comparable changes were seen in the pigs with SCI, here the contraction restored muscle thickness to 77% and 62% at the 25% BW loading level, to 70% and 49% at the 50% BW loading level, and to 55% and 45% at the 75% BW loading levels, respectively.

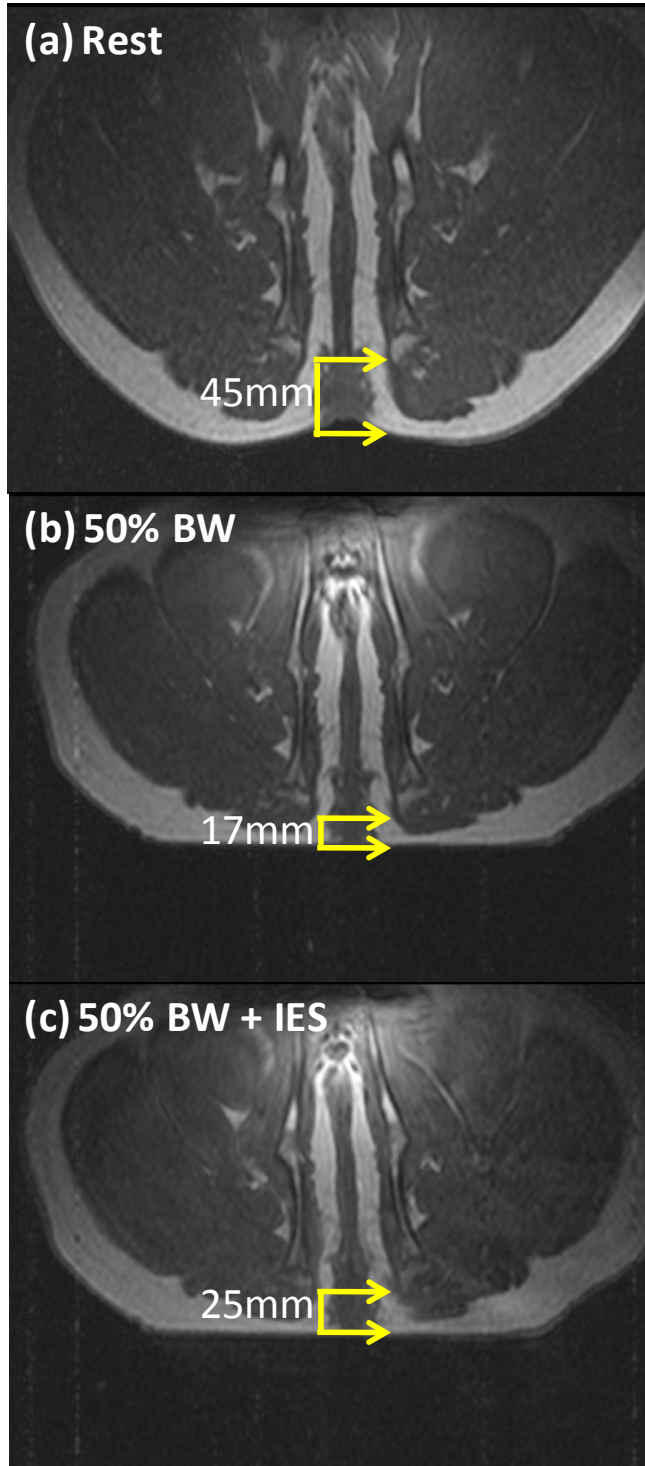


**Figure 11.** Tissue thickness between apex of ischial tuberosity and edge of skin utilized to assess the effectiveness of IES. (a) Thickness of the unloaded tissue in an intact pig. (b) Thickness of tissue externally loaded to 50% BW. (c) Thickness of the tissue externally loaded to 50% BW during IES-elicited contraction.

The loading level (25%, 50%, 75% BW) did not have a significant effect on tissue thickness. This further demonstrated that the tissue compression caused by the 25% BW loading level was already near its maximal limit. Contractions produced by IES did produce significant increases in tissue thickness ( $p = 0.026$ ). This indicated that each IES-elicited contraction significantly reduced the extent of tissue compression, regardless of the level of external loading (25%, 50% or 75% BW).

### **3.5 Discussion**

#### *3.5.1 Overview*

The main goal of this pre-clinical study was to quantify the levels of strain in pig muscles externally loaded to levels comparable to those experienced by individuals at risk of developing DTI. Secondary to this goal, we were interested in assessing the effectiveness of IES in counteracting muscle compression observed in loaded muscles. Strain measurements were conducted not only at the center of the ischial tuberosities, but also in regions dorsal and ventral to the ischial tuberosity. A general trend towards an increase in peak strain magnitudes was seen at locations up to 2 cm ventrally from the center of the ischial tuberosities (furthest measured). The use of IES was capable of partially counteracting muscle compression during the IES-elicited contractions.

### 3.5.2 *Strain measurements*

In the study of DTI etiology, it has been recognized that high strain and stress magnitudes within loaded tissue can lead to the onset of DTI. High deformation levels in particular have been associated with faster or more severe onset of injury[46, 55]. Previous studies have attempted to quantify strains in loaded muscles through the use of either MRI or numerical models that for the most part, focused on a single 2 dimensional plane centered on the ischial tuberosities[21, 46, 56]. For this study, we included measurements from slices 1 cm dorsally and up to 2 cm ventrally from the center of the bony prominence.

Peak magnitudes of strain in the slice centered on the ischial tuberosities obtained in this study were in agreement with those previously measured in rat muscles by Stekelenburg et al [35]. In their study, external loading of the muscles equivalent to ~50% of body weight (150 kPa using a 3 mm indenter) caused peak minimal principal strain values of 0.37. In the present study this value was  $0.34 \pm 0.04$ . However, maximal principal strain magnitudes in Stekelenburg et al [35] were lower (between 1 and 1.17 vs.  $1.30 \pm 0.16$ ) and peak maximal shear strains were higher (1.0 vs.  $0.66 \pm 0.06$ ). Interestingly, a different study by the same group above (van Nierop et al [57]) reported maximal shear strains of  $0.67 \pm 0.03$  in rats. These differences may be due to inconsistencies in tissue loading in the very small muscles of the rat model (Stekelenburg et al vs. van Nierop et al) or differences in the animal models used (rat vs. pig as is the case in this study).

More importantly, the results of the present study highlighted the importance of investigating the magnitudes of strain induced by different levels of loading and in regions away from the ischial tuberosities. The results showed that tissue compression (minimal principal strain) at the center and ventrally to the ischial tuberosity is already near its maximal level when the muscle is loaded to only 25% of BW. This was also evidenced in the measurements of tissue thickness, where most of the compression occurred at the 25% BW level. These results were observed in both intact pigs and the pig with SCI and no DTI. Nonetheless, the magnitude of the strain levels was higher in the pig with SCI likely as a result of atrophy in the muscles, which emphasizes the higher risk of DTI in people with reduced mobility. Moreover, the 25% BW loading level is lower than the level of loading experienced by wheelchair users while sitting[48-49]. In studies conducted in rats comparable external loading levels (28% BW) induced extensive DTI[58]. That such a relatively low level of loading is capable of nearly maximally compressing muscle between a bony prominence and an external surface, and induce severe muscle injury is indicative of the susceptibility of immobilized individuals to the development of DTI.

Peak levels of tensile, and shear strain (maximal principal strain and maximal shear strain, respectively) were found in the region encompassing the centre of the ischial tuberosity and up to 2 cm ventrally. Surprisingly, there was an upward trend in these values as the distance from the centre of the tuberosity increased ventrally, suggesting that higher strain magnitudes may be found further

away from the bone than previously thought. This result could have important implications in the understanding of DTI etiology; namely, strain (especially, tensile and shear) in the tissue may not be the main cause of mechanical damage in muscle leading to DTI. In a companion study in pigs[50], we demonstrated that the highest levels of internal pressure were indeed located in the slice centered on the bony prominence, coinciding with the location where DTI is expected to develop. Collectively, the results from these two studies suggest that high internal pressure and compressive strain play a large role in the development of DTI.

In one of the pigs that underwent a hemisection surgery of the spinal cord, a DTI developed unbeknownst to the researchers. In this pig, no visible skin signs or behavioural changes suggested the presence of the DTI, and the DTI was revealed only in MR images acquired on the day of the terminal experiment which took place 4 weeks after spinalization surgery. This case shares some similarities with the difficulties that clinicians undergo in the daily care of people at risk of developing pressure ulcers, where in some situations, even where utmost care is given, DTI can still develop. The exact mechanism that triggered the onset of this particular DTI is hard to determine. One possibility is that the level of pressure relief provided by the padded floor was not adequate for the degree of mobility of this particular pig. Work by Shabshin et al[59] evaluating wheelchair cushions showed that the reduction in soft tissue deformation provided by different cushions only acts as a time buffer, delaying the onset of cell death by some degree. It is possible that this time threshold for cell death was exceeded

with this particular pig at one point during the period of paralysis. Cases like this are commonly found clinically, where it has been shown that the use of specialized mattresses or cushions does not guarantee that a pressure ulcer will not form[60-61].

In this pig with SCI and DTI, the overall distribution of strain within the various slices analyzed was altered, with less compression and more tensile and shear relative to intact pigs and the pig with SCI and no DTI. Nonetheless, the magnitude of all strain levels was lower. From a mechanical standpoint, exposure to prolonged deformation can cause changes in the mechanical properties of skeletal muscle cells, which could explain the difference in the strain magnitudes measured in the pig with DTI. Single cell studies[62-64] have shown that under excessive compressive strains, cell membranes initially form blebs followed by complete failure and rupture of the membrane. In-vivo testing in rats[65] showed that after prolonged loading loss of muscle fiber cross-striation is encountered as well as infiltration of inflammatory cells as necrosis ensues. Necrosis in turn affects the overall composition of the muscle, modifying its stiffness[66]. Similarly, as DTI develops, tissue stiffness increases[67]. This increase in stiffness could reduce the degree of deformation a muscle undergoes, thus reducing the magnitudes of the principal strains measured. The case study of the pig with SCI and DTI supports this notion.

### 3.5.3 *Effects of IES*

Given the substantial physical, psychological and economical costs associated with DTIs, we believe that interventions for prophylactically preventing their formation are needed. Electrical stimulation for the prevention of pressure ulcers was first proposed by Levine et al in 1989[68]. Since then, studies by Levine et al[69-70], Bogie et al[71], Liu et al[72-73], van Londen et al[74], and Rischbieth et al[16], have shown its benefits in reducing superficial pressure levels, reshaping the muscle, increasing skin oxygenation levels, as well as causing an increase in muscle mass due to long-term application of electrical stimulation. All of these studies suggest electrical stimulation could be an effective preventative intervention against DTI formation. Our approach to the use electrical stimulation to prevent DTI differs from these previous studies in the manner in which electrical stimulation is applied. Intermittent electrical stimulation is intended to mimic the subconscious postural adjustments (“fidgeting”) performed by able-bodied individuals in response to discomfort while sitting or lying down. Therefore, IES only needs to be applied for short durations of time (~10 - 15 sec) every several minutes (~10 – 15 min). This ON-OFF pattern allows its use throughout the hours of sitting or lying down without appreciably fatiguing the target muscle. In addition, the effectiveness of IES is independent of muscle mass and does not require muscle conditioning prior to its use as an intervention for preventing the formation of pressure ulcers.

In previous studies, we demonstrated that IES-induced contractions reduce superficial pressure, increase tissue oxygenation[48-49], as well as reduce the levels of pressure in deep tissue[50]. More importantly, in animal studies we have demonstrated that the use of IES can significantly reduce the extent of DTI in loaded muscles[47, 58]. Moreover, we demonstrated that IES is more effective than current interventions (e.g., wheelchair push-ups) in preventing DTI<sup>11</sup>. To the best of our knowledge, these studies are the only ones where the effectiveness of any type of electrical stimulation has been tested directly for preventing the formation of DTI. In the present study we assessed the effect of muscle contractions produced by IES on compressive strain in loaded muscles, by comparing the thickness of the muscle before and during each IES-elicited contraction. IES-elicited contractions increased tissue thickness for all levels of loading, effectively reducing the level of compression in the muscle. Importantly, our results indicate that IES can generate strong contractions even in pigs with SCI and muscles externally loaded by up to 75% BW. This suggests that even under extreme circumstances of external loading and atrophied muscles, IES may still be effective in generating contractions, and in turn alleviating the levels of internal strain. In a companion study, we also demonstrated that IES-produced contractions can redistribute internal pressure[50], moving it away from high risk areas around the bone, even in severely atrophied muscles. Moreover, we previously demonstrated that IES can increase tissue oxygenation[48-49]. These beneficial outcomes, combined with the results from animal studies in which IES effectively prevented DTI formation, suggest that that IES could become a viable

intervention for preventing the formation of DTI in immobilized individuals.

#### 3.5.4 *Study Limitations*

In this study we utilized an MRI tagging technique that allowed the measurement of strain in two dimensional slices throughout the muscle. This provided detailed quantification of compressive, tensile and shear strains in the soft tissue surrounding the ischial tuberosities. To the best of our knowledge, this is the first use of multi-direction tagging for assessing strain in skeletal muscles. Nonetheless, this technique presents three limitations: 1) the degree of deformation experienced by the tissue between MRI image acquisitions has to be of a certain level. If the deformation is too large the tag lines become too distorted and cannot be reconstructed, as shown in **Figure 4a**. If the deformation is too small compared to the spacing between the tag lines, it becomes unquantifiable since the tag lines do not deform even if the tissue located between the tag lines does. 2) Deformations are assumed to occur in the imaged  $x$  and  $y$  plane. This means that deformations in the  $z$  direction cannot be measured. If during loading some of the tissue is pushed either dorsally or ventrally from the imaging slice, the degree of deformation obtained will have some degree of error.

3) Another limitation relates to changes in tissue visco-elastic properties due to repeated loading during the course of the experiment. To assess these changes, measurements of strain in the slice centered on the ischial tuberosities were periodically repeated and compared. No detectable changes were observed,

suggesting that minimal to no changes in the visco-elastic properties occurred throughout the course of the experiment.

Despite these limitations, we believe that this approach is the best available option for studies investigating large deformations in skeletal muscles. To the best of our knowledge, this is the first study that used a stepped tagging approach to quantify such large deformations and could open the field for a wider range of studies in the future.

### *3.5.5 Conclusions*

In this study, we demonstrated that relatively low levels of external loads are capable of generating near maximal magnitudes of strain in the loaded muscles, particularly in atrophied muscles. We also provided evidence, for the first time, that the highest magnitudes of strain do not occur in the muscle around the bony prominence, but at locations ventral to the bone. This information could help re-evaluate the notion that high magnitudes of strain in the muscle are the main contributors to the onset of DTI. Finally, we demonstrated that the IES-elicited contractions are strong enough to alleviate the compression experienced by the muscles during external loading as high as 75% of BW. This finding explains one mechanism by which contractions due to electrical stimulation are able to prevent the formation for DTI as demonstrated in Solis et al[47] and Curtis et al[58], which suggests that IES could be an effective intervention for preventing the formation of DTI in immobilized individuals.

### 3.5.6 *Acknowledgements*

Mr. Robert Lederer designed and built the MR-compatible pig carrier. This work was funded by the Alberta Heritage Foundation for Medical Research (AHFMR), the Canadian Institutes of Health Research (CIHR), and the Spinal Cord Injury Treatment Centre Society (SCITCS). VKM is an AHFMR Senior Scholar.

### 3.6 References

- [1] S. Bergquist-Beringer and B. J. Gajewski, "Outcome and assessment information set data that predict pressure ulcer development in older adult home health patients.," *Advances in Skin and Wound Care*, vol. 24, pp. 404 - 414, 2011.
- [2] B. Pham, L. Teaguem, J. Mahoney, L. Goodman, M. Paulden, J. Poss, J. Li, L. Ieraci, S. Carcone, and M. Krahn, "Early Prevention of Pressure Ulcers Among Elderly Patients Admitted Through Emergency Departments: A Cost-effectiveness Analysis.," *Annals of Emergency Medicine*, vol. 58, pp. 468 - 478, 2011.
- [3] E. Jaul, "Assessment and management of pressure ulcers in the elderly: current strategies.," *Drugs and Aging*, vol. 27, pp. 311 - 325, 2010.
- [4] N. Nijs, A. Toppets, T. Defloor, K. Bernaerts, K. Milisen, and G. Van Den Berghe, "Incidence and risk factors for pressure ulcers in the intensive care unit.," *Journal of CLinical Nursing*, vol. 18, pp. 1258 - 1266, 2009.
- [5] J. A. O'Brien and S. Cowman, "An exploration of nursing documentation of pressure ulcer care in an acute setting in Ireland.," *Journal of Wound Care*, vol. 20, pp. 197 - 198, 200, 202-203, 2011.
- [6] Y. Li, J. Yin, X. Cai, J. Temkin-Greener, and D. B. Mukamel, "Association of race and sites of care with pressure ulcers in high-risk nursing home residents.," *JAMA*, vol. 306, pp. 179 - 186, 2011.
- [7] B. Pham, L. Teague, J. Mahoney, L. Goodman, M. Paulden, J. Poss, J. Li, N. J. Sikich, R. Lourenco, L. Ieraci, S. Carcone, and M. Krahn, "Support surfaces for intraoperative prevention of pressure ulcers in patients undergoing surgery: a cost-effectiveness analysis.," *Surgery*, vol. 150, pp. 122 - 132, 2011.
- [8] A. Vaishampayan, F. Clark, M. Carlson, and E. Blanche, "Preventing pressure ulcers in people with spinal cord injury: targeting risky life circumstances through community-based interventions.," *Advances in Skin and Wound Care*, vol. 24, pp. 275 - 284, 2011.
- [9] J. M. Zanca, D. M. Brienza, D. Berlowitz, R. G. Bennett, C. H. Lyder, and N. P. U. A. Panel., "Pressure ulcer research funding in America: creation and analysis of an on-line database," *Advances in Skin & Wound Care*, vol. 16, pp. 190-7, 2003.
- [10] T. A. Conine, A. K. Choi, and R. Lim, "The user-friendliness of protective support surfaces in prevention of pressure sores," *Rehabilitation Nursing*, vol. 14, pp. 261-3, 1989.
- [11] R. F. Edlich, K. L. Winters, C. R. Woodard, R. M. Buschbacher, W. B. Long, J. H. Gebhart, and E. K. Ma, "Pressure ulcer prevention," *Journal of Long-term Effects of Medical Implants*, vol. 14, pp. 285-304, 2004.
- [12] C. A. Salzberg, D. W. Byrne, C. G. Cayten, P. van Niewerburgh, J. G. Murphy, and M. Viehbeck, "A new pressure ulcer risk assessment scale for individuals with spinal cord injury," *American Journal of Physical Medicine & Rehabilitation*, vol. 75, pp. 96-104, 1996.
- [13] S. L. Garber and D. H. Rintala, "Pressure ulcers in veterans with spinal cord injury: a retrospective study," *Journal of Rehabilitation Research & Development*, vol. 40, pp. 433-41, 2003.
- [14] A. Gefen, "Risk factors for a pressure-related deep tissue injury: a theoretical model.," *Medical and Biological Engineering and Computing*, vol. 45, pp. 563 - 573, 2007.
- [15] T. A. Krouskop, P. C. Noble, S. L. Garber, and W. A. Spencer, "The effectiveness of preventive management in reducing the occurrence of pressure sores," *Journal of Rehabilitation Research & Development*, vol. 20, pp. 74-83, 1983.
- [16] H. Rischbieth, M. Jelbart, and R. Marshall, "Neuromuscular electrical stimulation keeps a tetraplegic subject in his chair: a case study," *Spinal Cord.*, vol. 36, pp. 443-5, 1998.
- [17] J. C. Grip and C. T. Merbitz, "Wheelchair-based mobile measurement of behavior for pressure sore prevention," *Computer Methods & Programs in Biomedicine*, vol. 22, pp. 137-44, 1986.

- [18] Z. B. Niazi, C. A. Salzberg, D. W. Byrne, and M. Viehbeck, "Recurrence of initial pressure ulcer in persons with spinal cord injuries," *Advances in Wound Care*, vol. 10, pp. 38-42, 1997.
- [19] C. V. Bouten, C. W. Oomens, F. P. Baaijens, and D. L. Bader, "The etiology of pressure ulcers: skin deep or muscle bound?," *Archives of Physical Medicine and Rehabilitation*, vol. 84, pp. 616-619, 2003.
- [20] A. Stekelenburg, D. Gawlitta, D. L. Bader, and C. W. Oomens, "Deep tissue injury: how deep is our understanding?," *Archives of Physical Medicine and Rehabilitation*, vol. 89, pp. 1410 - 1413, 2008.
- [21] K. K. Ceelen, A. Stekelenburg, S. Loerakker, G. J. Strijkers, D. L. Bader, K. Nicolay, F. P. Baaijens, and C. W. Oomens, "Compression-induced damage and internal tissue strains are related.," *Journal of Biomechanics*, vol. 41, pp. 3399 - 3404, 2008.
- [22] L. Agam and A. Gefen, "Pressure ulcers and deep tissue injury: a bioengineering perspective," *Journal of Wound Care*, vol. 16, pp. 336 - 342, 2007.
- [23] R. K. Daniel, D. L. Priest, and D. C. Wheatley, "Etiologic factors in pressure sores: an experimental model," *Archives of Physical Medicine & Rehabilitation*, vol. 62, pp. 492-8, 1981.
- [24] N. A. Lahmann and J. Kottner, "Relation between pressure, friction and pressure ulcer categories: A secondary data analysis of hospital patients using CHAID methods.," *International Journal of Nursing Studies*, vol. 48, pp. 1487 - 1494, 2011.
- [25] R. M. Woolsey and J. D. McGarry, "The cause, prevention, and treatment of pressure sores," *Neurologic Clinics.*, vol. 9, pp. 797-808, 1991.
- [26] R. H. Guthrie and D. Goulian, "Decubitus ulcers: Prevention and Treatment," *Geriatrics*, vol. 28, pp. 67-71, 1973.
- [27] R. Salcido, S. B. Fisher, J. C. Donofrio, M. Bieschke, C. Knapp, R. Liang, E. K. LeGrand, and J. M. Carney, "An animal model and computer-controlled surface pressure delivery system for the production of pressure ulcers," *Journal of Rehabilitation Research & Development*, vol. 32, pp. 149-61, 1995.
- [28] D. R. Berlowitz and D. M. Brienza, "Are all pressure ulcers the result of deep tissue injury? A review of literature.," *Ostomy Wound Management*, vol. 53, pp. 34 - 38, 2007.
- [29] J. Black, M. M. Baharestani, J. Cuddigan, B. Dorner, L. Edsberg, D. Langemo, M. E. Posthauer, C. Ratliff, G. Taler, and T. N. P. U. A. P. (NPUAP). "National Pressure Ulcer Advisory Panel's Updated Pressure Ulcer Staging System.," *Advances in Skin & Wound Care*, vol. 20, pp. 269-274, 2007.
- [30] E. A. Peeters, C. V. Bouten, C. W. Oomens, D. L. Bader, L. H. Snoeckx, and F. P. Baaijens, "Anisotropic, three-dimensional deformation of single attached cells under compression.," *Annals of Biomedical Engineering*, vol. 32, pp. 1443 - 1452, 2004.
- [31] C. W. Oomens, O. F. Bressers, E. M. Bosboom, C. V. Bouten, and D. L. Blader, "Can loaded interface characteristics influence strain distributions in muscle adjacent to bony prominences?," *Computer Methods in Biomechanics & Biomedical Engineering*, vol. 6, pp. 171-80, 2003.
- [32] M. Kosiak, W. G. Kubicek, M. Olson, J. N. Danz, and F. J. Kottke, "Evaluation of pressure as factor in production of ischial ulcers," *Archives of Physical Medicine & Rehabilitation*, vol. 39, pp. 623-629, 1958.
- [33] M. Kosiak, "Etiology and pathology of ischemic ulcers," *Archives of Physical Medicine & Rehabilitation*, vol. 40, pp. 62-9, 1959.
- [34] M. Kosiak, "Etiology of decubitus ulcers," *Archives of Physical Medicine & Rehabilitation*, vol. 42, pp. 19-29, 1961.
- [35] A. Stekelenburg, G. J. Strijkers, H. Parusel, D. L. Bader, K. Nicolay, and C. W. Oomens, "Role of ischemia and deformation in the onset of compression-induced deep tissue injury: MRI-based studies in a rat model.," *Journal of Applied Physiology*, vol. 102, pp. 2002-2011, 2007.
- [36] P. A. Grace, "Ischaemia-reperfusion injury," *British Journal of Surgery*, vol. 81, pp. 637-47, 1994.

- [37] D. C. Gute, T. Ishida, K. Yarimizu, and R. J. Korthuis, "Inflammatory responses to ischemia and reperfusion in skeletal muscle," *Molecular & Cellular Biochemistry*, vol. 179, pp. 169-87, 1998.
- [38] S. Tsuji, S. Ichioka, N. Sekiya, and T. Nakatsuka, "Analysis of ischemia-reperfusion injury in a microcirculatory model of pressure ulcers," *Wound Repair and Regeneration*, vol. 13, pp. 209-215, 2005.
- [39] S. Loerakker, E. Manders, G. J. Strijkers, K. Nicolay, F. P. Baaijens, D. L. Bader, and C. W. Oomens, "The effects of deformation, ischemia, and reperfusion on the development of muscle damage during prolonged loading.," *Journal of Applied Physiology*, vol. Ahead of print, 2011.
- [40] R. G. Breuls, C. V. Bouten, C. W. Oomens, D. L. Bader, and F. P. Baaijens, "Compression induced cell damage in engineered muscle tissue: an in vitro model to study pressure ulcer aetiology.," *Annals of Biomedical Engineering*, vol. 31, pp. 1357 - 1364, 2003.
- [41] T. Nagel, S. Loerakker, and C. W. Oomens, "A theoretical model to study the effects of cellular stiffening on the damage evolution in deep tissue injury.," *Computer Methods in Biomechanics and Biomedical Engineering*, vol. 12, pp. 585 - 597, 2009.
- [42] A. Gefen, B. van Nierop, D. L. Bader, and C. W. Oomens, "Strain-time cell-death threshold for skeletal muscle in a tissue-engineered model system for deep tissue injury.," *Journal of Biomechanics*, vol. 41, pp. 2003 - 2012, 2008.
- [43] R. Sopher, J. Nixon, C. Gorecki, and A. Gefen, "Exposure to internal muscle tissue loads under the ischial tuberosities during sitting is elevated at abnormally high or low body mass indices.," *Journal of Biomechanics*, vol. 43, pp. 280 - 286, 2010.
- [44] N. Shabshin, V. Ougortsin, G. Zoizner, and A. Gefen, "Evaluation of the effect of trunk tilt on compressive soft tissue deformations under the ischial tuberosities using weight-bearing MRI," *Clinical Biomechanics*, vol. 25, pp. 402 - 408, 2010.
- [45] M. Makhsous, D. Lim, R. Hendrix, J. Bankard, W. Z. Rymer, and F. Lin, "Finite element analysis for evaluation of pressure ulcer on the buttock: development and validation," *IEEE Transactions on Neural Systems and Rehabilitation Engineering*, vol. 15, pp. 517 - 525, 2007.
- [46] S. Loerakker, A. Stekelenburg, G. J. Strijkers, J. J. Rijpkema, F. P. Baaijens, D. L. Bader, K. Nicolay, and C. W. Oomens, "Temporal effects of mechanical loading on deformation-induced damage in skeletal muscle tissue.," *Annals of Biomedical Engineering*, vol. 38, pp. 2577 - 2587, 2010.
- [47] L. R. Solis, D. P. Hallihan, R. R. Uwiera, R. B. Thompson, E. D. Pehowich, and V. K. Mushahwar, "Prevention of pressure-induced deep tissue injury using intermittent electrical stimulation.," *Journal of Applied Physiology*, vol. 102, pp. 1992-2001, 2007.
- [48] S. Gyawali, L. R. Solis, S. L. Chong, C. A. Curtis, P. Seres, I. Kornelsen, R. B. Thompson, and V. K. Mushahwar, "Intermittent electrical stimulation redistributes pressure and promotes tissue oxygenation in loaded muscles of individuals with spinal cord injury," *Journal of Applied Physiology*, vol. 110, pp. 246 - 255, 2011.
- [49] L. R. Solis, S. Gyawali, P. Seres, C. A. Curtis, S. L. Chong, R. B. Thompson, and V. K. Mushahwar, "Effects of intermittent electrical stimulation on superficial pressure, tissue oxygenation, and discomfort levels for the prevention of deep tissue injury.," *Annals of Biomedical Engineering*, vol. 39, pp. 649 - 663, 2011.
- [50] L. R. Solis, A. Liggins, R. E. Uwiera, N. Poppe, E. Pehowich, P. Seres, R. B. Thompson, and V. K. Mushahwar, "Distribution of Internal Pressure around Bony Prominences: Implications to Deep Tissue Injury and Effectiveness of Intermittent Electrical Stimulation," *Annals of Biomedical Engineering (submitted)*, 2011.
- [51] D. Gagnon, S. Nadeau, L. Noreau, P. Dehail, and D. Gravel, "Quantification of reaction forces during sitting pivot transfers performed by individuals with spinal cord injury.," *Journal of Rehabilitation Medicine*, vol. 40, pp. 468 - 476, 2008.
- [52] P. Gilsdorf, R. Patterson, and S. Fisher, "Thirty-minute continuous sitting force measurements with different support surfaces in the spinal cord injured and able-bodied," *Journal of Rehabilitation Research & Development*, vol. 28, pp. 33-8, 1991.

- [53] P. Gilsdorf, R. Patterson, S. Fisher, and N. Appel, "Sitting forces and wheelchair mechanics," *Journal of Rehabilitation Research & Development.*, vol. 27, pp. 239-46, 1990.
- [54] M. G. D. GEERS, R. DE BORSTS, and W. A. M. BREKELMANS, "Computing strain fields from discrete displacement fields in 2D-Solids," *International Journal of Solid Structures*, vol. 33, pp. 4293 - 4307, 1996.
- [55] C. W. Oomens, S. Loerakker, and D. L. Bader, "The importance of internal strain as opposed to interface pressure in the prevention of pressure related deep tissue injury.," *Journal of Tissue Viability*, 2009.
- [56] E. Linder-Ganz, N. Shabshin, Y. Itzchak, and A. Gefen, "Assessment of mechanical conditions in sub-dermal tissues during sitting: A combined experimental-MRI and finite element approach.," *Journal of Biomechanics*, vol. 40, pp. 1443 - 1454, 2007.
- [57] B. J. van Nierop, A. Stekelenburg, S. Loerakker, C. W. Oomens, D. Bader, G. J. Strijkers, and K. Nicolay, "Diffusion of water in skeletal muscle tissue is not influenced by compression in a rat model of deep tissue injury.," *Journal of Biomechanics*, vol. 43, pp. 570 - 575, 2010.
- [58] C. A. Curtis, S. L. Chong, I. Kornelsen, R. R. Uwiera, P. Seres, and V. K. Mushahwar, "The effects of intermittent electrical stimulation on the prevention of deep tissue injury: varying loads and stimulation paradigms.," *Artificial Organs*, vol. 35, pp. 226 - 236, 2011.
- [59] N. Shabshin, G. Zoizner, A. Herman, V. Ougortsin, and A. Gefen, "Use of weight-bearing MRI for evaluating wheelchair cushions based on internal soft-tissue deformations under ischial tuberosities.," *Journal of Rehabilitation Research and Development*, vol. 47, pp. 31 - 42, 2010.
- [60] L. Rafter, "Evaluation of patient outcomes: pressure ulcer prevention mattresses.," *British Journal of Nursing*, vol. 20, pp. S32, S34 - S38, 2011.
- [61] E. McInnes, S. E. Bell-Syer, J. C. Dumville, R. Legood, and N. A. Cullum, "Support surfaces for pressure ulcer prevention.," *Cochrane Database of Systematic Reviews*, pp. CD001735, 2008.
- [62] E. A. Peeters, C. W. Oomens, C. V. Bouten, D. L. Bader, and F. P. Baaijens, "Viscoelastic properties of single attached cells under compression.," *Journal of Biomechanical Engineering*, vol. 127, pp. 237 - 243, 2005.
- [63] E. A. Peeters, C. V. Bouten, C. W. Oomens, and F. P. Baaijens, "Monitoring the biomechanical response of individual cells under compression: a new compression device," *Medical & Biological Engineering & Computing*, vol. 41, pp. 498-503, 2003.
- [64] Y. N. Wang, C. V. Bouten, D. A. Lee, and D. L. Bader, "Compression-induced damage in a muscle cell model in vitro," *Proceedings of the Institution of Mechanical Engineers. Part H Journal of Engineering in Medicine*, vol. 219, pp. 1 - 12, 2005.
- [65] E. M. H. Bosboom, C. V. Bouten, C. W. Oomens, H. W. M. van Straaten, F. P. Baaijens, and H. Kuipers, "Quantification and localization of damage in rat muscles after controlled loading; a new approach to study the etiology of pressure sores," *Medical Engineering & Physics*, vol. 23, pp. 195-200, 2001.
- [66] E. Linder-Ganz and A. Gefen, "Mechanical compression-induced pressure sores in rat hindlimb: muscle stiffness, histology, and computational models," *Journal of Applied Physiology*, vol. 96, pp. 2034-49, 2004.
- [67] A. Gefen, N. Gefen, E. Linder-Ganz, and S. S. Margulies, "In vivo muscle stiffening under bone compression promotes deep pressure sores," *Journal of Biomechanical Engineering*, vol. 127, pp. 512-524, 2005.
- [68] S. P. Levine, R. L. Kett, P. S. Cederna, L. D. Bowers, and S. V. Brooks, "Electrical muscle stimulation for pressure variation at the seating interface," *Journal of Rehabilitation Research & Development*, vol. 26, pp. 1-8, 1989.
- [69] S. P. Levine, R. L. Kett, M. D. Gross, B. A. Wilson, P. S. Cederna, and J. E. Juni, "Blood flow in the gluteus maximus of seated individuals during electrical muscle stimulation," *Archives of Physical Medicine & Rehabilitation*, vol. 71, pp. 682-6, 1990.

- [70] S. P. Levine, R. L. Kett, P. S. Cederna, and S. V. Brooks, "Electric muscle stimulation for pressure sore prevention: tissue shape variation," *Archives of Physical Medicine & Rehabilitation*, vol. 71, pp. 210-5, 1990.
- [71] K. M. Bogie, X. Wang, and R. J. Triolo, "Long-term prevention of pressure ulcers in high-risk patients: a single case study of the use of gluteal neuromuscular electric stimulation," *Archives of Physical Medicine & Rehabilitation*, vol. 87, pp. 585-591, 2006.
- [72] L. Q. Liu, G. P. Nicholson, S. L. Knight, R. Chelvarajah, A. Gall, F. R. Middleton, M. W. Ferguson-Pell, and M. D. Craggs, "Interface pressure and cutaneous hemoglobin and oxygenation changes under ischial tuberosities during sacral nerve root stimulation in spinal cord injury.," *Journal of Rehabilitation Research & Development*, vol. 43, pp. 553 - 564, 2006.
- [73] L. Q. Liu, G. P. Nicholson, S. L. Knight, R. Chelvarajah, A. Gall, F. R. Middleton, M. W. Ferguson-Pell, and M. D. Craggs, "Pressure changes under the ischial tuberosities of seated individuals during sacral nerve root stimulation.," *Journal of Rehabilitation Research & Development*, vol. 43, pp. 209 - 218, 2006.
- [74] A. van Londen, M. Herwegh, C. H. van der Zee, A. Daffertshofer, C. A. Smit, A. Niezen, and T. W. Janssen, "The effect of surface electric stimulation of the gluteal muscles on the interface pressure in seated people with spinal cord injury.," *Archives of Physical Medicine and Rehabilitation*, vol. 89, pp. 1724 - 1732, 2008.

## **CHAPTER 4**

# **Prevention of Deep Tissue Injury by inducing muscle contractions using Intermittent Electrical Stimulation after Spinal Cord Injury in Pigs**

### **4.2 INTRODUCTION**

Pressure-related deep tissue injury (DTI) is a type of pressure ulcer that is commonly prevalent in people with reduced mobility and sensation such as individuals with spinal cord injury [1-3]. It develops in muscles entrapped for prolonged durations between a bony prominence and a surface [4-7]. The entrapment causes muscle breakdown due to sustained mechanical deformation [8-13], ischemia [9, 14-17], and reperfusion injury [9, 18-19]. Because DTI develops deep in the tissue and without exhibiting early skin signs, it cannot be detected using routine skin inspections. Once skin signs become evident extensive damage in the soft tissue underlying the skin would have already occurred. The resulting lesions often require surgical intervention and several months to heal. In the United States more than \$11 billion dollars are spent annually on treating pressure ulcers [20-21].

Current interventions for the prevention of DTI consist of performing frequent repositioning movements to alleviate pressure from regions at risk [22-23], the use of specialized wheelchair cushions and mattresses to reduce interfacial (skin-surface) pressures [24-26], and a general improvement in nursing

care, including better nutrition [27]. Nonetheless, despite the advancements in clinical care and support surface technology, the incidence rates of pressure ulcers have not significantly changed since the 1940s [28].

Electrical stimulation for the prevention of pressure ulcers was previously suggested by Levine et al [29-31]. In their work, they found that muscle contractions produced by electrical stimulation reduce superficial pressure and increase blood flow. Bogie et al [32-34], Liu et al [35-36] and Van Londen et al [37] also reported similar results. Nonetheless, these studies had two limitations: 1) testing the effectiveness of electrical stimulation in preventing the formation of pressure ulcers was not conducted, and 2) all advocated the use of continuous or near continuous generation of muscle contractions to be effective, which limits the duration of deployment of electrical stimulation due to muscle fatigue.

Intermittent electrical stimulation (IES) is a novel electrical stimulation approach for the prevention of pressure ulcers. Electrical stimulation is applied for short durations (~10 sec) every few minutes (~10 min) to loaded muscles (e.g., gluteus maximus muscles of the buttocks) to induce periodical contractions. These contractions produce postural shifts that mimic the subconscious shifts (fidgeting movements) performed by able-bodied individuals in response to discomfort while sitting or lying down. The brief contractions every few minutes greatly reduce the rate of muscle fatigue, allowing the use of the intervention throughout the day or night. We demonstrated in previous studies that each IES-

elicited contraction significantly increases the level of oxygenation in a loaded muscle [38], reduces and redistributes the levels of internal stress around bony prominences, and counteracts compression in the muscle [39-40]. In studies with human volunteers with and without spinal cord injury, we also showed that each IES-elicited contraction reduces superficial (skin-surface) pressure around bony prominences and increases oxygenation in the muscle for up to 15 minutes after each brief contraction [38, 41]. Most importantly, in studies in rats, IES significantly reduced the extent of deep tissue damage caused by externally loading a muscle for 2 hours [42-43]. IES was more effective in reducing the extent of DTI than periodical muscle unloading which emulated the wheelchair push-up exercises prescribed to wheelchair users for preventing pressure ulcer formation [43].

The goal of this study was to test the effectiveness of IES in preventing DTI formation in an animal model of spinal cord injury subjected to realistic levels of prolonged muscle loading. The hypothesis was that the use of IES in the loaded muscle would effectively prevent the formation of DTI in said muscle. Studies were conducted in adult pigs with partial spinal cord injury leading to paralysis of one hind leg. Atrophied muscles in the paralyzed limb were loaded for 4 hours every day for 1 month, and the effect of IES in preventing the formation of DTI in the loaded muscles was assessed.

## 4.3 METHODS

### *Overview*

Experiments were conducted in six adult Yucatan miniature pigs (weight  $58.5 \pm 7.4$  kg, mean  $\pm$  standard deviation) with approval from the University of Alberta Animal Care and Use Committee. The miniature pig was selected as the animal model given that its muscle size and weight are similar to those of humans. In addition, pigs have skin that closely resembles that of humans, and historically, pigs have been a widely used animal model for studies involving pressure ulcers and wounds in general. All animals underwent a surgical procedure that hemisected the spinal cord at the second lumbar level (L-2), leading to paralysis of the left hind leg. The animals recovered from surgery for a period of two weeks after which an external load was applied over the superficial and middle gluteal muscles and biceps femoris muscle for 4 hours every day, 4 days a week, for one month. The animals were divided in two groups (N =3/group), one received IES to the loaded muscles during the loading hours, while the other did not receive IES. The effectiveness of IES in preventing the formation of DTI was assessed weekly through the use of magnetic resonance imaging (MRI).

### *4.3.1 Spinalization surgery*

Sedation was induced through intramuscular administration of a mix of Ketamine (22mg/kg), Glycopyrrolate (0.01mg/kg), and Xylazine (2.2mg/kg). Anaesthesia was induced and maintained through the use of isoflurane (2% - 3%).

A 15 – 20 cm incision was made in the skin of the back, and the muscles covering the spinal column at the level of the L-2 vertebra were carefully separated to expose the spinal column. A laminectomy was then performed to expose the dorsal surface of the spinal cord. The dura mater was carefully opened using iridectomy scissors and a medio-lateral hemisection of the spinal cord was performed. The cord was then covered with a thin plastic film and the muscles and skin were sutured shut in layers.

#### *4.3.2 Post-surgical recovery and palliative care*

The animals recovered individually in cages with padded flooring to prevent the formation of uncontrolled DTI or superficial pressure ulcers. Analgesia was maintained for the first 4-5 days post-surgery using Hydromorphone (0.075mg/kg) administered intravenously three times per day for the first 4-5 days. Hydromorphone was subsequently replaced by the oral analgesic Tramadol (2mg/kg), which was administered twice daily for another week. Antibiotics (Cefazolin, 15mg/kg) were also administered intravenously twice a day for the first week post-surgery. The oral antibiotic, Cephalexin (20mg/kg), was subsequently administered for an additional week. The change from intravenous to oral medications in the post-operative care was due to the difficulty in maintaining a viable intravenous catheter in place beyond one week post surgery. The pigs were fed a slurry of dry pellets mixed in water through a syringe for the first 3-4 days post-surgery, and fluids (Plasma-Lyte, 180ml/hr) were administered intravenously as needed (2 – 3 L/day). The intravenous fluids

were stopped as soon as the pigs resumed eating on their own, typically by the 4<sup>th</sup> or 5<sup>th</sup> day post-surgery.

As part of the recovery protocol, all pigs were placed in a suspension sling every day starting the first day after the surgery. The sling allowed the pigs to stand in place by supporting most of the animal's body weight, particularly the weight from the distal half of the body. The rostral part of the sling, which supported the weight from the shoulders and head, was set slightly lower than the distal part. This allowed each pig to support itself with its front limbs. The time the pigs spent in the sling each day was gradually increased, starting with 1 hour on the first day, and up to 4 hours by the end of the first week. All pigs tolerated this procedure very well, remaining in place calmly and with minimal movement for the required time. Occasionally, the pigs would fall asleep, relaxing their front limbs and allowing the sling to support their weight fully.

#### *4.3.3 Daily loading procedure*

Two weeks after the spinalization surgery, the behaviour (appetite and mood) of each animal returned to pre-surgery norms. During these two weeks, most pigs learned how to move around their kennel by utilizing their three intact limbs. The daily loading protocol entailed placing the pigs in the suspension sling for 4 hours. To minimize the chance of random movements while in the sling, straps were used to attach the sling to the frame holding the sling, fixing the sling's position in place (**Figure 1A**). This constrained the pig's body movement

except for the head.

Loading was applied to the paralyzed limb through a 12in x 10in acrylic indenter (**Figure 1A, 1B**) over the superficial and middle gluteal muscles, as well as part of the biceps femoris muscle of the paralyzed limb, pushing the muscles against the iliac crest. To monitor discomfort or pain during the loading periods, close attention was given to each animal's behaviour, particularly loud vocalizations, which are very common when pigs are in pain or stressful situations. The level of loading corresponded to 25% of each animal's body weight (**Figure 2A and 2C**). With 61% and 70% of body weight carried by the ischial tuberosities and thighs while sitting in people with intact and injured spinal cords, respectively [38-39, 41], the applied loading on the paralyzed limb represented the average level of loading experienced by the tissue around each ischial tuberosity. The indenter was attached to a computer controlled servo-motor (Danaher AKM23D, Danaher Motion, Washington, DC, USA) mounted on the post of a drill press (**Figure 1A**). The loading level was monitored through a force transducer (Interface SMT2-225, Interface, Arizona, USA) placed in-line with the servo-motor and indenter, and through a thin pressure sensing pad (PX200:36:36, XSensor Technology Corporation, Calgary, Alberta, Canada) placed between the indenter and the skin of the pig. Loading was applied for 4 hrs/day, 4 consecutive days/week, for 4 weeks. A piece of 4 inch-thick Tempur-Pedic mattress was placed between the contralateral limb and the wall of the metal frame supporting the sling during the loading to prevent DTI formation in

that limb.

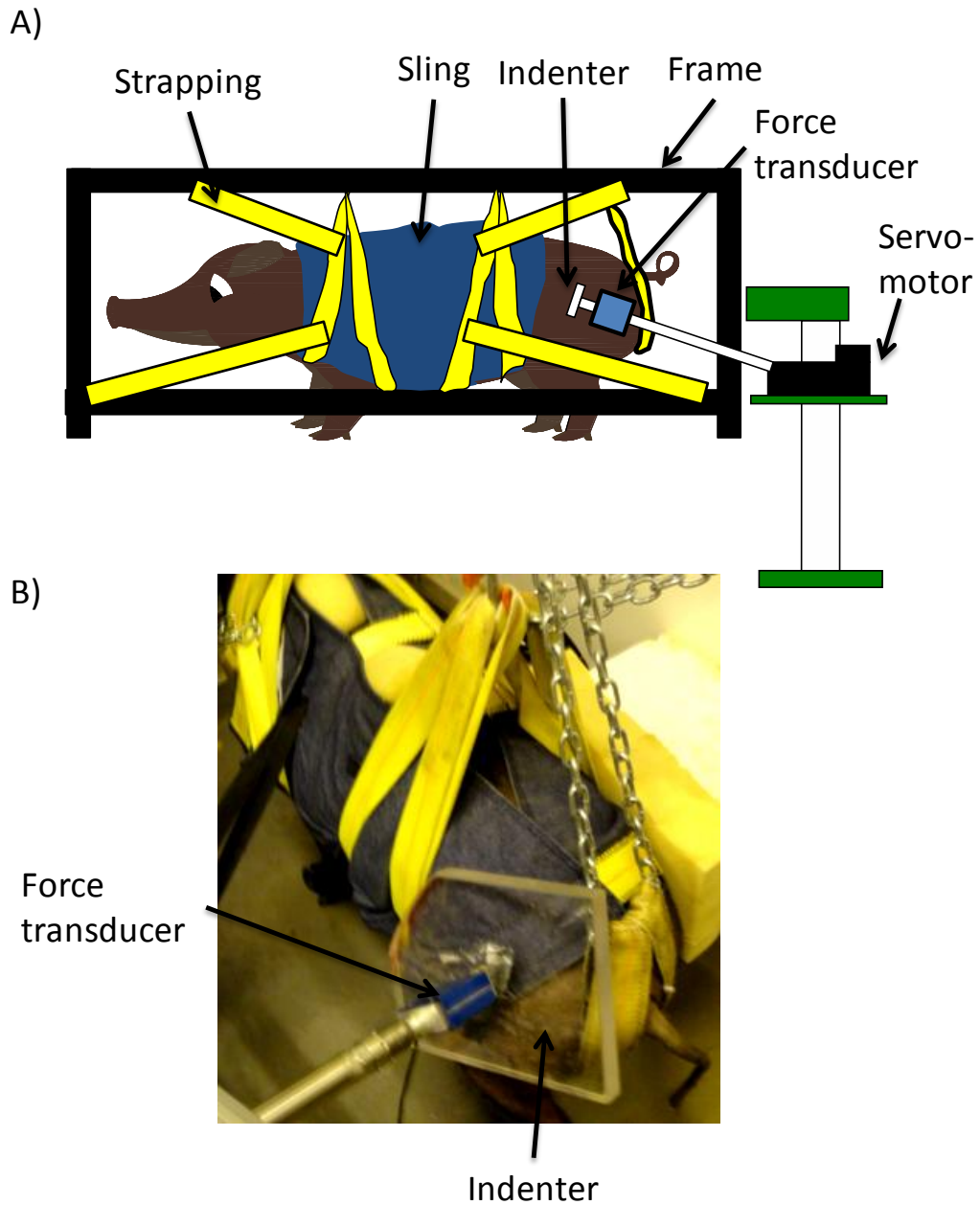


**Figure 1: Daily loading setup. A) Diagram of suspension sling used to support the pigs and to apply the external load to the superficial gluteus, middle gluteus, and biceps femoris muscles. B) A photograph of the indenter during daily external loading of the pig muscles.**

#### *4.3.4 Application of IES*

Three of the six pigs were randomly assigned to receive IES throughout the duration of daily loading. Stimulation was delivered through a pair of electrodes placed on the skin (5cm x 10cm, Pure Care, Sherwood Park, Alberta, Canada) and a hand-held stimulator (BioStim NMS+ stimulator, Biomedical Life Systems, California, USA). The active electrode was placed over the motor point of the superficial gluteus muscle, while the return electrode was placed over the middle gluteus muscle. Stimulation consisted of trains of biphasic, square pulses. Pulse width was 250 $\mu$ s and pulse frequency 35 Hz. Pulse amplitude was adjusted individually for each pig in order to generate a visible fused contraction in the targeted muscle. The IES cycle consisted of 10 sec of stimulation (ON period) followed by a 10 min period of no stimulation (OFF period). Force recordings were used to monitor the quality of the contraction and assess muscle fatigue resulting from the use of IES over the 4 hours of loading (**Figure 2B, 2D, and 2E**).

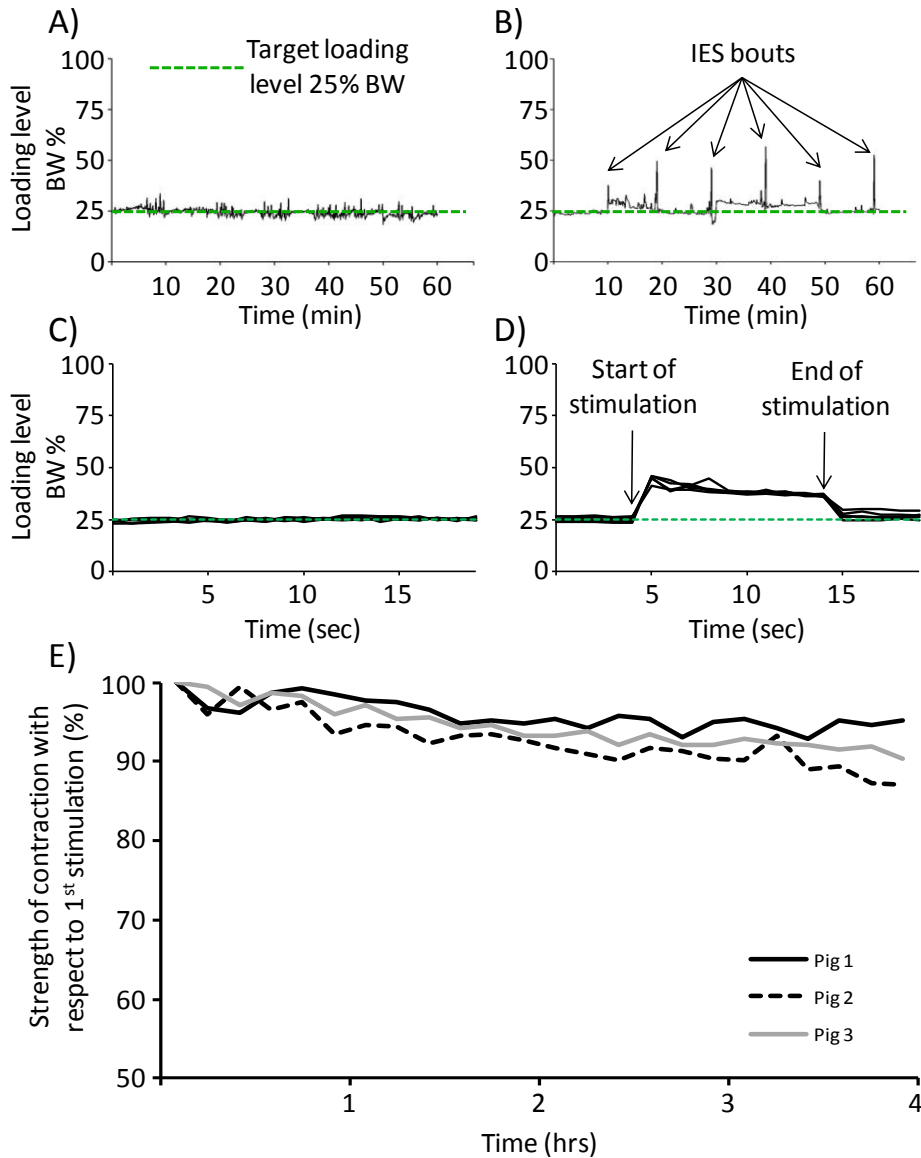


**Figure 2: Force measurements during external loading. A) One hour of external loading from 1 pig in the No IES group. B) One hour of external loading from 1 pig in the IES group. C) Segments of 20 second time windows from 1 pig in the No IES group. D) Segments of 20 second time windows centered on IES bouts from 1 pig in the IES group. E) Comparison of force generated between 1<sup>st</sup> IES bout and last 6 IES bouts for all three pigs in the IES group.**

#### 4.3.5 Assessment of DTI through MRI

The effectiveness of IES was evaluated weekly through MRI assessments of the hip region. Two assessments were acquired prior to the application of

external loading, the first one week prior to the spinalization surgery and the second two weeks post-surgery. The two assessments allowed for comparisons of muscle mass before and after spinal cord injury, and were compared to ensure that no muscle injury developed unbeknownst to the researchers during the two weeks of surgical recovery. The assessment acquired two weeks post-surgery also served as a baseline measure for subsequent assessments. Once the loading protocol was initiated, MRI assessments were obtained weekly (after 4 days of consecutive loading each week).

On the day of the MRI assessment, the animals were sedated using the same cocktail described in the surgical methods. A tracheal tube was then inserted to allow proper air flow, and intravenous catheters were inserted in both ears. Anaesthesia was maintained through bolus intravenous injections of Propofol (2.5mg/kg), which were administered at a rate of 10ml every 10 minutes. The animals were transported to the Peter S Allen MR Research Centre at the University of Alberta. Three different MRI sequences were utilized. Muscle morphology was assessed with a high resolution 3D-gradient echo sequence with the following parameters: number of slices = 104; slice thickness = 2.5mm; echo time (TE) = 2.33ms; repetition time (TR) = 4.92ms; field of view (FOV) = 400\*400mm; acquisition matrix = 640\*640 pixels; in-plane resolution = 0.625\*0.625mm; and flip angle = 12°. T<sub>2</sub>-weighted imaging was used to determine the presence of indicators of DTI in the muscle, such as edema and cell death, and provide a measurement of the extent of tissue injury [42-44]. A T<sub>2</sub>-

weighted spin echo sequence with fat suppression was used with the following parameters: number of slices = 10; slice thickness = 8mm; TE = 70ms; TR = 3000ms; FOV = 283\*400mm; acquisition matrix 272\*384 pixels; and in-plane resolution = 1.04\*1.04mm. Additionally, a multi-echo T<sub>2</sub>-weighted sequence was utilized to quantify the short and long transverse relaxation (T<sub>2</sub>) times of the middle gluteus muscle, as well as their respective weightings contributing to the overall T<sub>2</sub> signal. These short and long components have been associated with cellular and extracellular compartments, respectively [45-46]. The short T<sub>2</sub> components are associated with the reduced mobility of water within the cells, while the long components are associated with relatively larger mobility of water in the vascular and interstitial spaces. The short and long T<sub>2</sub>-time components, and their relative weightings, which reflect the different water pool volumes, were measured throughout the experimental protocol in all animals, including baseline (post-surgical assessment), prior to the initiation of the loading regime. The parameters for this sequence were as follows: number of slices = 20; slice thickness = 8mm; 12 echo times with TE's ranging from 23ms to 353ms in 30ms increments; TR = 1000; FOV = 266\*400mm; acquisition matrix = 256\*384 pixels; and in-plane resolution = 1.04\*1.04mm.

#### *4.3.6 Analysis of MR images*

##### 1) Quantification of muscle atrophy

Muscle atrophy was determined by comparing the volume of the middle gluteus and biceps femoris muscles in the paralyzed leg before and 6 weeks after

spinalization. These 6 weeks include the 4 weeks of IES application and the 2 weeks prior allowed for the pig to recover from surgery. The muscles of interest were manually delineated in each of the slices obtained from the 3D-gradient echo MRI sequence and the volume was calculated by summing the volume within the delineated region in each slice.

## 2) Detection of Injury

MRI and histological injury detection analyses were performed by a researcher blinded to the treatment groups. Quantification of the extent of tissue injury in the middle gluteus muscle was performed through the analysis of the T<sub>2</sub>-weighted MR images using custom written Matlab (Mathworks, Cambridge, USA) scripts. The T<sub>2</sub>-weighted MR sequence is sensitive to the increase of more freely moving water in the tissue, serving as a good indicator of the formation of edema or scar resulting from cell death. For each MRI slice two regions of interest were selected (**Figure 3**): one delineated the middle gluteus muscle on the intact side of the pig (contralateral control limb), and the other delineated the muscle that received the daily loading on the paralyzed side (loaded limb). The signal intensity of each pixel in the region of interest of the loaded limb was compared to the average signal intensity of the region of interest in the contralateral control side. If the pixel had a signal intensity greater than the mean + 2\*standard deviation of the signal intensity on the contralateral control side, the pixel was considered to be injured tissue. The number of pixels with increased signal intensity from the loaded side was then calculated for each slice and a

measure of total muscle volume exhibiting signs of DTI was obtained.

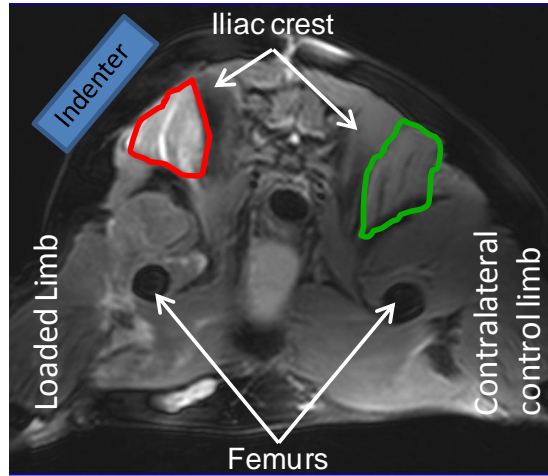


**Figure 3: T<sub>2</sub>-weighted MR image from one pig. To assess the amount of DTI two regions of interest were selected around the middle gluteus muscle in both the loaded and contralateral control limbs. Blue indenter rectangle represents the angle at which the external loading would occur daily.**

### 3) Bi-exponential fitting of multi-echo MR images

Using custom written scripts in Matlab, a region of interest was selected around the middle gluteus muscles on both the loaded and contralateral control limbs. A bi-exponential function was fitted to the MR signal from each pixel within these regions to quantify both the short and long T<sub>2</sub>-time components of the signal, as well as their respective contributions (weightings) to the T<sub>2</sub> times. The decaying MRI signal sampled over the 12 echoes, S(TE), can be represented as:

$$S(TE_i) = c_1 e^{(-T_{2(1)}/TE_i)} + c_2 e^{(-T_{2(2)}/TE_i)},$$

where, TE<sub>i</sub> are the echo times, c<sub>1</sub> and c<sub>2</sub> are the weightings of the short and long T<sub>2</sub> components, T<sub>2(1)</sub> and T<sub>2(2)</sub>. Data were fitted with this equation using a non-

negative least squares method, using custom written code in Matlab. Regions of interest were adjusted to avoid the inclusion of confounding tissues such as fat or fascia. The short and long  $T_2$ -time components within the adjusted regions, as well as their respective weightings, were calculated for all individual pixels, and the results were averaged over the region of interest.

#### *4.3.7 Histological assessment of tissue*

Following the final MRI assessment, and under continued anaesthesia (isoflurane 2 – 3%), muscle samples from the gluteus and biceps femoris muscles from both the loaded and contralateral control limbs were extracted. In addition, a muscle sample from the shoulder region was also extracted to serve as a naive, unaffected control sample (naive control). This additional sample was collected to ensure that the results from the contralateral control limb, used as the reference for MR analyses, were indeed indicative of healthy, undamaged muscle. All muscle samples were stored in 10% buffered paraformaldehyde fixative for processing at a later time. The animals were then euthanized with an intra-cardiac injection of Euthanyl (Sodium Pentobarbital 107mg/kg). Muscle samples were histologically processed for hematoxylin and eosin staining. The stained slides were analyzed under a light microscope at 10x and 20x magnification and given a score from 0 to 4 based on the degree of cellular damage present in each slide, with 0 representing no signs of damage and 4 the most severely damaged. The histological assessment was done by a person blinded to all treatments of the study. The slides were assessed according to cell shape, number of neutrophils,

and amount of necrosis. Each slide was assessed three times to ensure an accurate rating. The assessment scale was not validated against other scales utilized in different studies.

#### *4.3.8 Statistical analyses*

The main hypothesis of this study was that the use of IES would reduce the amount of DTI formed in the loaded muscles in comparison to the no IES group. Deep tissue injury was assessed with three different techniques, which were T<sub>2</sub>-weighted MR imaging, MRI multi-exponential T<sub>2</sub> analysis, and a histological assessment of muscle samples. The specific null hypothesis for each technique was that there would be no statistical difference between the IES and no IES groups.

Reductions in muscle volume due to atrophy were assessed by comparing the muscle volume (middle gluteus and biceps femoris muscles) from each pig prior to spinalization surgery with the volumes from the same muscles 2 and 6 weeks post surgery. A repeated measures ANOVA was utilized to assess statistical significance. Time (pre surgery, 2wks post surgery, 6wks post surgery) was defined as the within subjects factor, and the use or no use of IES was designated as the between subjects factor. Post mortem, muscle fiber cross-sectional area measurements were assessed from histological samples. A one-way ANOVA was used to compare reductions in cross-sectional area in the paralyzed limb compared to the control limb within each group (IES and no IES).

Statistical comparisons of the muscle volume demonstrating increased signal, indicating injury, in T<sub>2</sub>-weighted images in the loaded legs of all pigs were conducted using repeated measures ANOVA. Time was used as the within-subjects factor, and IES/no IES as the between subjects factor.

For the multi-exponential T<sub>2</sub> analysis, the relative weighting of the T<sub>2</sub> components, c<sub>1</sub> and c<sub>2</sub>, were assessed using a one-way ANOVA with three levels (contralateral limb, loaded limb with IES, and loaded limb without IES). The test was repeated for each time point and Tukey's Honest Significant Difference (HSD) post-hoc test was used to identify which level(s) experienced significant differences. Only c<sub>2</sub>, the weighting of the long T<sub>2</sub> component (i.e., the relative size of the extracellular volume), was considered in the analysis because the weighting of the short component, c<sub>1</sub>, is determined by the long component,  $c_1 = 1 - c_2$ . Contralateral limb data from the IES and No IES groups were grouped because the conditions experienced by the contralateral limb in both groups were the same at all times.

Statistical comparisons between the different histological samples were conducted using a one-factor, four levels Kruskal-Wallis non-parametric test. The levels were considered to be the following four muscle groups: 1) naive control (samples from the shoulder), contralateral control (samples from contralateral leg), loaded No-IES (samples from loaded muscles that did not receive IES), and loaded IES (samples from loaded muscles that received IES). A

standard  $\alpha$  of 0.05 was utilized for all statistical tests. A multiple comparison test (Wilcoxon's Signed Rank Test with a Bonferroni Correction) was then performed to identify the specific group(s) with significant differences. A standard  $\alpha$  of 0.05 was utilized for all statistical tests.

#### **4.4 RESULTS**

At the study end point for all pigs, none of them had regained any motor function in the paralyzed hind-limb. All pigs underwent noticeable atrophy in the middle gluteus and biceps femoris muscles from the paralyzed limb as a function of time post-spinalization surgery. Two weeks after surgery and prior to the initiation of the external loading regime, the volume of these muscles was  $7\% \pm 3\%$  (mean  $\pm$  SD,  $n = 6$ ) smaller than that prior to surgery; however, the reduction was not statistically significant. By the time of the terminal MRI assessment (6 wks post-surgery), the loss of muscle volume had increased in all pigs to  $19 \pm 6\%$  (mean  $\pm$  SD,  $n = 6$ ) of the pre-surgery volume. This reduction was statistically significant ( $p = 0.006$ ). There was no significant difference in the degree of atrophy between the pigs that received IES and those that did not ( $p = 0.33$ ), although this was not unexpected, as the treatment time was only one month. A comparison between the cross sectional area of the muscle fibers from each group showed that in the pigs from the IES group, muscle fiber size was 14% smaller in the paralyzed limb in comparison to the muscle fiber size in the control limb. Although this reduction approached significance, it was not statistically significant ( $p = 0.081$ ). In the No IES group, muscle fiber size had been reduced

by 15% in the paralyzed limb in comparison to the control limb. Similar to the IES group, this reduction in size approached statistical significance ( $p = 0.078$ ) but did not reach it.

External loading was equivalent to 25% of each pig's body weight. Averaged over the entire contact area, this load was equivalent to  $11.97 \pm 2.57$  kPa for all pigs.

After the 4 hours of loading, in the pigs that received the application of IES there was a decrease of ~10% in the force generated by each stimulation bout compared to the force generated during the initial stimulation bout (Figure 2E)

#### *4.4.1 Assessment of muscle injury*

Examples of regions showing increased  $T_2$  signal intensity in the loaded muscles of the paralyzed limb in a pig that received IES during the period of loading and a pig that did not receive IES are shown in **Figure 4** for 2 and 4 weeks of loading. The use of IES significantly reduced the amount of injured tissue measured in the loaded muscles at all time points ( $p=0.019$ ; **Figure 6A**). In the pigs that received IES, the extent of  $T_2$ -hyperintensity was ~5 times less than the amount measured in the pigs that did not receive IES at all assessment points. In the pigs that did not receive IES,  $23 \pm 5\%$  of the middle gluteus muscle volume in the loaded limb had measureable injury by the 2<sup>nd</sup> week of loading. By the 4<sup>th</sup> week of loading, this amount had increased to  $49 \pm 11\%$  (**Figure 6A**); although

there were no statistical differences between the volumes of T<sub>2</sub>-hyperintensity measured between weeks 2-4, the result was approaching significance ( $p = 0.07$ ). In comparison, the extent of injury measured in the pigs receiving IES was  $5 \pm 4\%$  after 2 weeks of loading and  $8 \pm 9\%$ , after 4 weeks of loading (**Figure 6A**). There were no statistical differences between measurements at any time point of loading (baseline, 2 and 4 weeks) in this group ( $p = 0.63$ ).

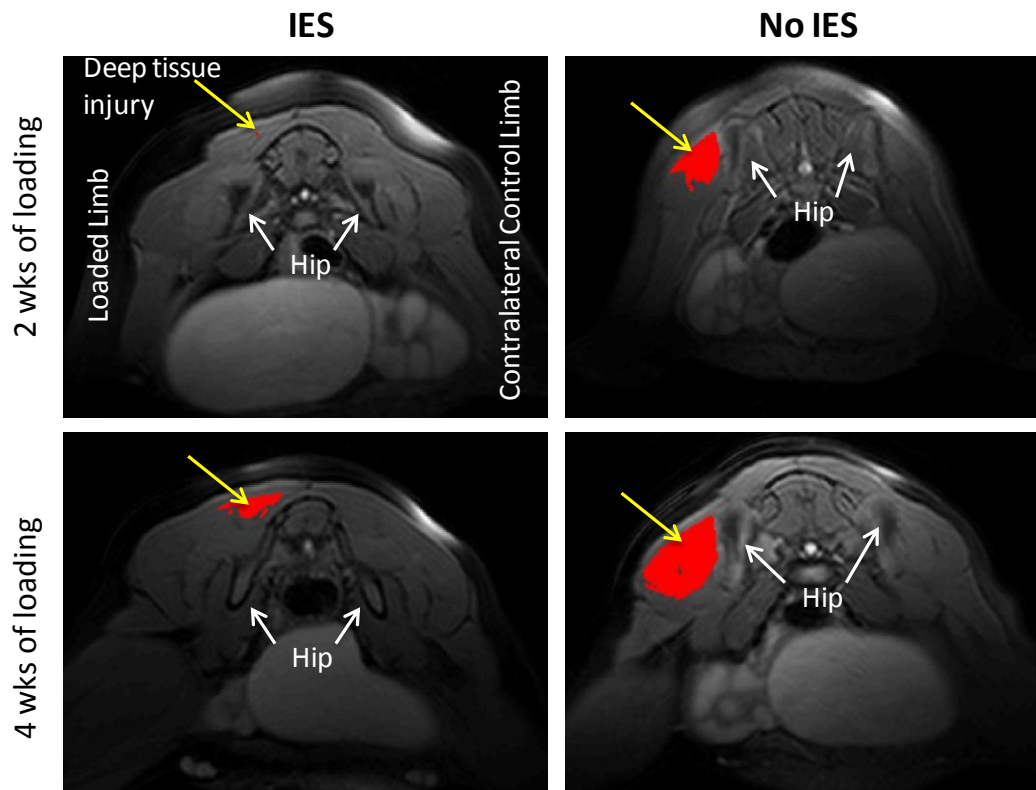


**Figure 4: Comparison of the amount of DTI estimated in one pig from each group after 2 and 4 weeks of daily loading. Yellow arrows indicate the location of muscle regions considered to contain DTI (red regions).**

#### 4.4.2 Changes to intracellular and extracellular muscle components by DTI

**Figure 5** shows examples of the distribution of the long  $T_2$  component weighting at baseline (post-surgical, pre-loading assessment) and 4 weeks post-loading in a animal that received IES (left) and one that did not receive IES (right) during the period of loading. At baseline, there were no significant differences ( $p = 0.527$ ) in the weighting of the long  $T_2$  component between the middle gluteus muscles of both hind limbs in the IES ( $0.08 \pm 0.02$ , mean  $\pm$  standard error) and no IES groups ( $0.1 \pm 0.02$ ). Moreover, the baseline weighting values of the long  $T_2$  component were similar (no statistical difference) in both groups (**Figure 6B**).

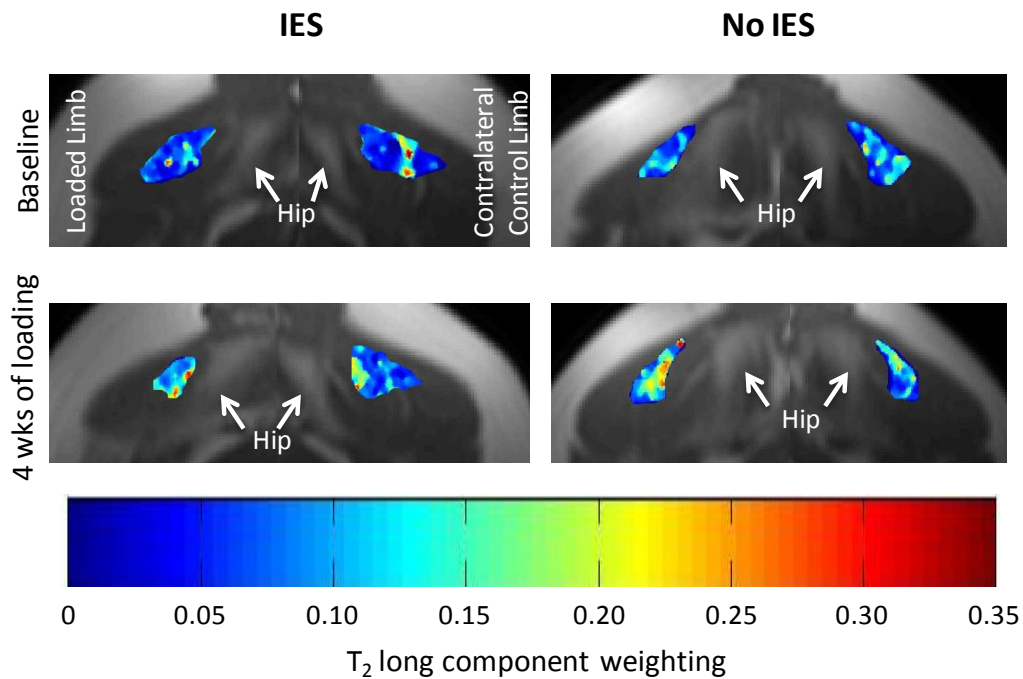
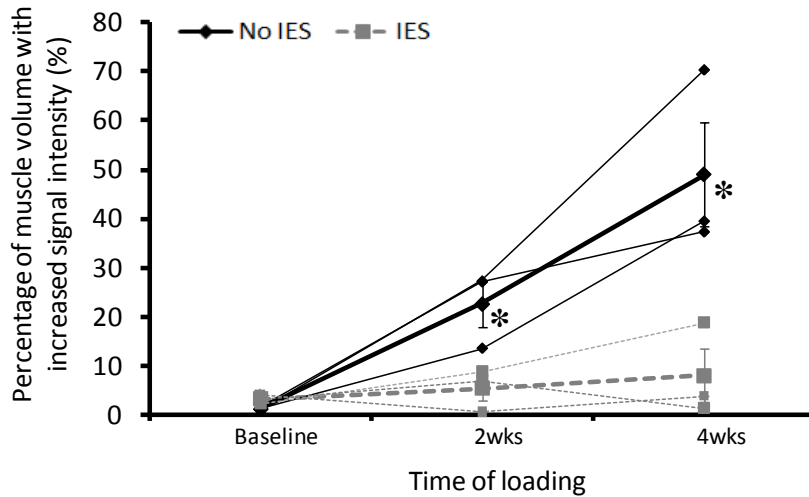


**Figure 5:** Comparison of the weighting of the long  $T_2$  component in one pig from each group for both the loaded and contra-lateral control limbs. Color maps indicate the weighting for each pixel in the selected muscle regions. Long  $T_2$  component =  $1 - T_2$  short component weighting.

Two weeks after the onset of the loading regime, the weighting of the long T<sub>2</sub> component doubled to  $0.22 \pm 0.07$  in the loaded middle gluteus muscle of the group that did not receive IES, while only a small increase was seen in the contralateral control limb ( $0.13 \pm 0.02$ ). In comparison, in the group that received IES, both legs maintained similar weighting values for the long T<sub>2</sub> component, increasing only slightly to  $0.11 \pm 0.02$  and  $0.12 \pm 0.03$ , in the loaded and contralateral control limbs, respectively (**Figure 6B**). The weighting of the long T<sub>2</sub> component at this time point significantly increased in the loaded muscle of the group that did not receive IES compared to the same muscle in the contralateral limb ( $p = 0.05$ ). This increase also neared significance relative to the loaded muscle in the pigs that received IES ( $p = 0.059$ ). In the pigs receiving IES, there was no statistical difference between the long T<sub>2</sub> component in the loaded and contralateral muscles ( $p = 0.946$ ).

A)



B)

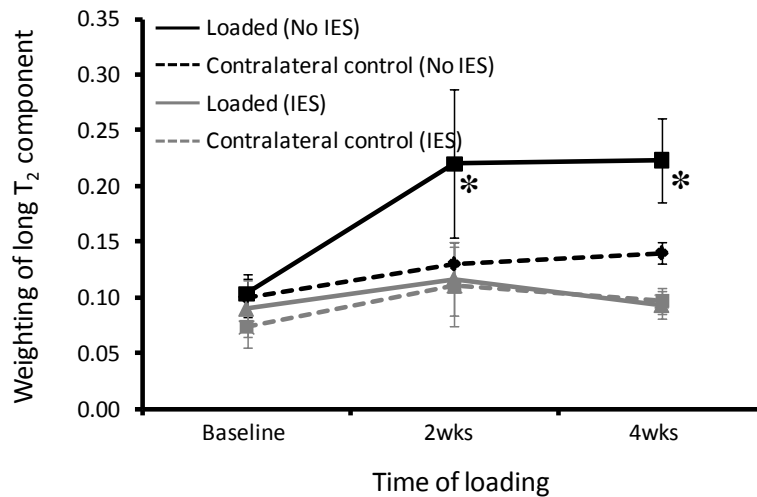


**Figure 6: Extent of DTI measured in pigs over time. A) Results from individual pigs (thin lines) and group results (mean  $\pm$  standard error, thick lines) of the quantification of T<sub>2</sub>-weighted images in the IES and no IES groups (n=3 per group) showing the percent of muscle exhibiting signs of injury. B) Weighting of the T<sub>2</sub>-long component at different assessment time points for each limb (loaded and contralateral control), for each group. Results show mean  $\pm$  standard error values.**

After 4 weeks of loading, the weighting of the long T<sub>2</sub> component in the middle gluteus muscle of the pigs that did not receive IES remained elevated (0.22  $\pm$  0.04). This elevation was again statistically significant (p = 0.01)

compared to measurement in the middle gluteus muscle of the contralateral limb ( $0.14 \pm 0.01$ ). It was also statistically significant ( $p = 0.009$ ) relative to the loaded middle gluteus muscle in the pigs that received IES ( $0.10 \pm 0.01$ ). In contrast, there was no statistical difference between the weightings of the long  $T_2$  component in the loaded and contralateral muscles of the pigs that received IES ( $p = 0.761$ ).

#### *4.4.3 Assessment of cellular necrosis*

Samples collected from the contralateral control limb in the groups with or without IES exhibited minimal signs of cellular damage (**Figure 7**, top row). In a majority of these samples (10 out of 12) no damage was seen and normal cellular features were maintained, with no inflammatory cell infiltration into the interstitial space or within the cells. The same result was observed in the samples collected from the shoulder (naive control, not shown).

In the group that received IES, the majority of histological slides were very similar to those from the contralateral control limb (**Figure 7**, bottom left). The highest score given to any of the samples in this group was 3, given to a single slide in the group. In these slides, the affected areas demonstrated some infiltration of inflammatory cells into the interstitial space. There were also a few gaps in the cellular structure, with inflammatory cells in the space that used to be occupied by a muscle cell. Nonetheless, the median score for this group was zero (**Figure 8**). In the group that did not receive IES, some degree of damage was

seen across a majority of samples (10 out of 12) from the entire group, with damage more pronounced in these samples compared to the other groups. These samples exhibited a larger number of neutrophil infiltration into the extra and intra cellular space, and larger gaps in the interstitial space between the cells (**Figure 7**, bottom right). The highest score for samples in this group was the maximum of 4, indicating severe cellular damage, with a median score of 3 for the entire group (**Figure 8**). The scores from the No IES group were statistically higher than those from the control group ( $p = 0.005$ ), as well as those from the IES group ( $p = 0.001$ ). In contrast, there was no statistical difference between the IES and control groups ( $p = 0.13$ ).

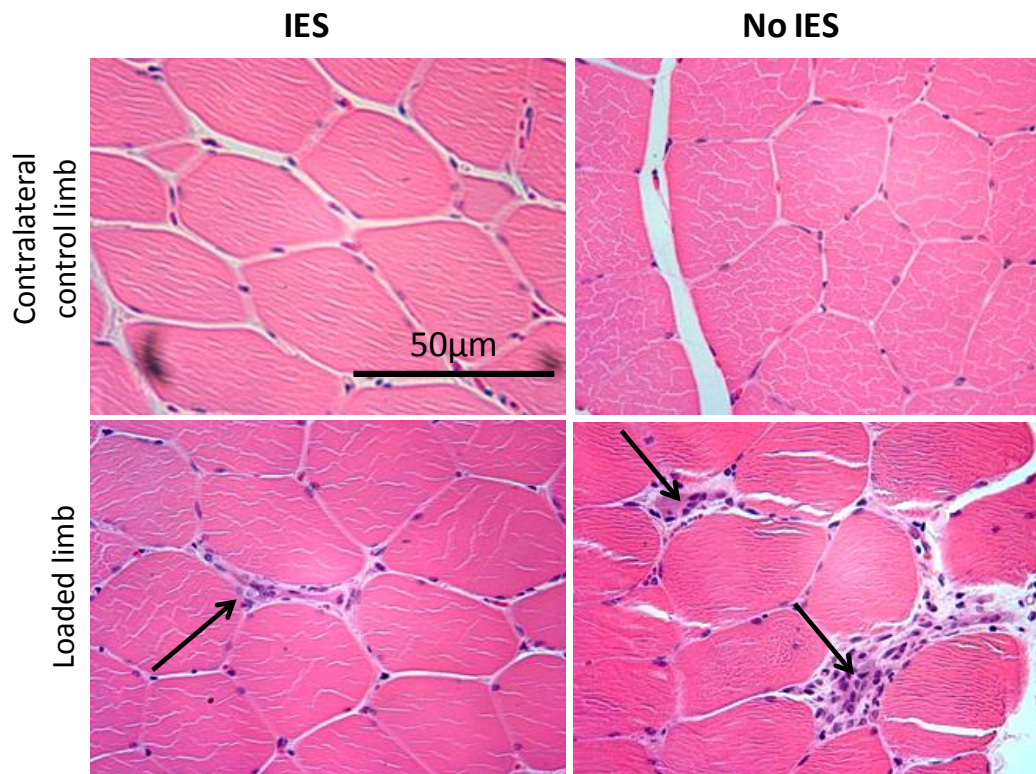


**Figure 7: Muscle samples from the contralateral control and loaded muscles from one pig in the IES and no IES groups stained with hematoxylin and eosin. Arrows indicate location of high infiltration of inflammatory cells into the muscle tissue.**

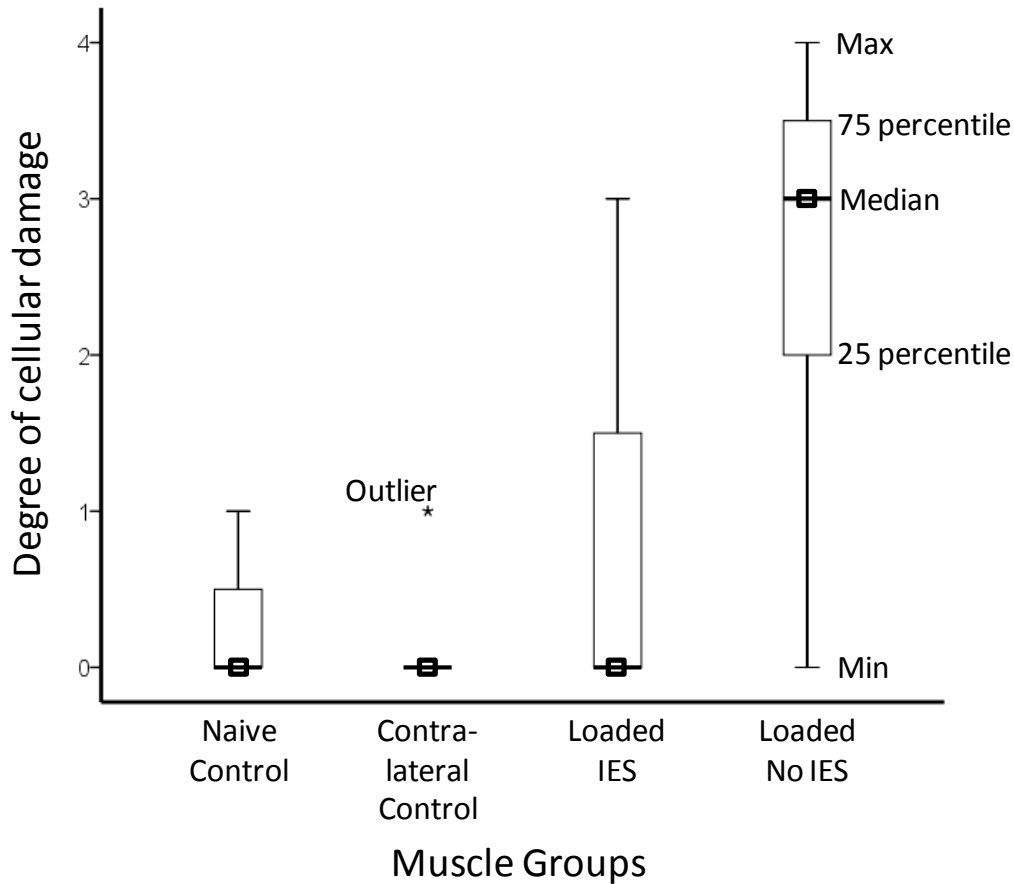


**Figure 8: Group results from tissue histological assessment. Results show median (square marker), 25% and 75% percentiles (box), maximum and minimum values (error bars), and outliers (star, 2 slices out of 12 in the group).**

Throughout the study the skin of all pigs was closely inspected on a daily basis. Within 2 to 3 days after the spinal hemi-sectioning surgery, 5 out of the 6 pigs developed small (1 – 2 cm diameter) circular surface ulcers directly under the ischial tuberosities. These ulcers were caused by the dragging against the support surface as the pigs moved in their kennel. Once the pigs adapted to moving by using their 3 intact limbs (7 – 10 days post surgery) the ulcers began to heal and were completely healed by the third week post-surgery.

The skin overlying the middle gluteus muscle in the paralyzed limb, which was the area loaded for 4 hrs every day, 4 successive days a week, remained intact for the duration of the study in all pigs. By the experimental endpoint (6 wks post-surgery), this region of skin continued to exhibit no signs of damage, even in those animals with extensive muscle injury caused by the external loading.

#### *4.4.4 Summary of results*

The use of IES significantly reduced the extent of DTI. By the 4<sup>th</sup> week of loading, T<sub>2</sub>-weighted MR imaging showed that the volumetric extent of injury in the loaded legs of the pigs that did not receive IES was 7 times larger than in the pigs that received IES. The multi-echo T<sub>2</sub>-weighted MR analysis showed an increase in the weighting of the long T<sub>2</sub> component in the loaded muscle of the pigs that did not receive IES, while in the pigs that received IES, the weighting between the short and long T<sub>2</sub> components did not show significant changes over time compared to the measurements in the contralateral control muscles. This test provided a more direct measure of the microscopic origin of the increase in the signal in the T<sub>2</sub>-weighted images, indicating that the extracellular volume fraction was increased in the injured tissue, which is consistent with edema or cell death. The loaded middle gluteus muscle of the pigs that did not receive IES showed a doubling of the extracellular volume fraction, from 10% to 22%, which agreed with the trends shown in the histological assessment of the muscle samples. Histology showed that the degree of cellular damage, with visible large increases in extracellular volume fraction, was high in the pigs that did not receive IES. In

the pigs that received IES, cellular damage was comparable to that from muscle samples from the contralateral control limbs.

## **4.5 DISCUSSION**

The goal of this study was to test the effectiveness of the novel IES approach in preventing the formation of DTI due to daily external loading of paralyzed muscles in animals with SCI. DTI was assessed using MRI techniques as well as through post-mortem histological assessments.

### *4.5.1 Skin is a poor indicator of DTI*

In the present study none of the pigs from either group exhibited visual signs of damage in the skin nor signs of tenderness upon palpation in the area surrounding the iliac crest, the bony prominence against which the external load was applied for the duration of the study. Despite the absence of damage at the skin level, significant muscle injury developed during the 4 weeks of external loading in the pigs that did not receive IES. Currently, the primary method for detecting pressure ulcers is periodical skin inspections. Nonetheless, as demonstrated in this and other studies [7, 39, 42, 47], skin is a poor indicator of deep tissue health.

The difficulty in detecting DTI soon after its onset and during its stages of development compromises the effective deployment of early interventions and allows extensive tissue damage to develop untreated. Alternative techniques to

skin inspection have been suggested to better detect and/or quantify the extent of a suspected DTI. These include the use of biomarkers measured from blood tests [48-49] or sweat [50-52], or the use of imaging techniques such as MRI [17, 42, 44, 47] and ultrasound [53-54]. Results to date have been promising in controlled research laboratory environments; nonetheless, limitations including accuracy, specificity, availability, or cost have prevented their clinical implementation for this purpose. In the present study, two different MRI sequences were successfully used to assess the development of DTI in the pigs. While the current cost and availability of MRI scans may be prohibitive as an early detection and assessment technique of DTI in the immediate future, its high spatial resolution and ability to differentiate between different types of soft tissue make it an ideal tool for assessing DTI progression in small studies.

#### *4.5.2 MRI techniques are sensitive measures of edema formation and associated DTI*

The development of a DTI in the muscle is associated with cellular death and the accumulation of fluid (edema). This leads to changes in the volume of freely moving water in the tissue, the extent of which we assessed using a T<sub>2</sub>-weighted MRI sequence. An increase in the signal intensity of T<sub>2</sub>-weighted MR images has been associated with the formation of acute edema in skeletal muscle, one of the earliest signs of an inflammatory response due to cellular damage in the tissue [42-44]. Increased intensity in these images has also been associated with the amount of tissue injury (i.e., cell death) measured through post-mortem

histological assessments [42, 44]. We further explored the tissue injury with bi-exponential  $T_2$  quantification to estimate the extracellular volume fraction, which can provide an indication of edema accumulation as the muscle's cellular matrix breaks down due to injury. Such multi-echo imaging has been used to identify short and long components in the signal from skeletal muscle, with the short component thought to be associated with cellular structures in the tissue, and the long component associated with the extracellular space [45-46, 55-56]. We showed a baseline weighting of  $\sim 0.1$  for the longer  $T_2$  component, suggesting an extracellular volume fraction of 10% in uninjured muscle. Previous bi-exponential studies have shown similar weighting of the long  $T_2$  component in skeletal muscle [56-59], which is also in general agreement with extracellular volumes measured with other methods, such as using extra-vascular contrast agents [60]. The increase in the weighting of the long  $T_2$  component to over 20% with DTI in the limbs with no IES is consistent with the histological results, where much larger extracellular volumes are directly visualized.

#### *4.5.3 IES may be effective in preventing the formation of DTI*

The use of IES significantly reduced the formation of DTI in the muscles entrapped against the iliac crest due to repeated external loading in all pigs that received IES compared to the pigs that did not receive IES. In all animals receiving IES, the amount of DTI measured through the  $T_2$ -weighted images was significantly smaller than that measured in the animals that did not received IES, and was not different from measurements obtained at baseline. The multi-echo

imaging yielded similar results. In the pigs that received IES, there were no changes in the ratios between the weighting of the short and long  $T_2$  components of the muscle in the treated leg throughout the study, indicating that no changes occurred between the volumes of cellular and extracellular water content. Significant cellular death leads to the formation of edema, characterized by a more homogenous cellular environment (less differentiation in the water content and mobility between the two cellular spaces), and an increase in the weighting of the long  $T_2$ -component. Therefore, the consistency in the ratio of cellular/extracellular water content suggests that in the IES group, no detectable changes cellular compartmentalization developed in the tissue during the study. Moreover, the ratio of the cellular/extracellular water content was similar to that obtained from the contralateral limb used for control. In comparison, in the pigs that did not receive IES, there was a significant increase in the weighting of the long  $T_2$  component as early as the second week of loading.

The mechanisms underlying the effectiveness of IES in preventing the formation of DTI rely on the manner in which the stimulation is applied, generating muscle contractions that last a few seconds (~10 sec) every few minutes (~10 minutes). This pattern mimics the effects of natural repositioning that able bodied individuals perform subconsciously when exposed to periods of prolonged sitting or lying down. In previous studies we have shown that IES works by effectively counteracting both mechanical [38-41] and vascular [38, 41] factors which can lead to DTI development.

The degree of muscle atrophy experienced by the pigs during this study as a result of the spinal cord injury was less than the degree observed in our previous studies involving pigs with one paralyzed limb [39-40]. This difference could be due to the difference in the original mass of the pigs before the spinal surgery, as the pigs used in this study were on average 10kg smaller than those utilized in our previous studies. A higher degree of atrophy (of approximately 50%) similar to the one encountered in humans with spinal cord injury and in our previous pig studies would be conducive to increased levels of strain and stress affecting the loaded muscle if similar magnitudes of external load are used in both scenarios (more atrophy vs less atrophy), as shown in Solis et al [40] and Solis et al [39]. Increased levels of strain and stress could in turn have lead to greater extents of DTI in this study at each respective time point in the pigs in the control group (No IES). As for the pigs that received IES, in our previous studies [39-40] we showed that the effects of IES induced contractions can still effectively counteract the negative effects of external loading levels of up to 50 and 75% of BW, which are 2 and 3 times higher than the loading levels used in this study. These results would make us expect that the extent of DTI in the IES group could have remained similar to the extent observed in this study.

Interestingly, the effects of IES are not dependent on muscle bulk [38-39]; thus are not limited to those individuals who have undergone muscle build-up training after prolonged atrophy. Moreover, muscle fatigue was minimal throughout the duration of IES application in any loading session as shown by the

force recordings of muscle contractions throughout the IES sessions. This suggests that IES could be used throughout the hours of sitting or lying down without diminished effectiveness.

One potential problem that could affect the application of IES is the skinfold thickness. If a thicker layer of fat is covering the target muscles as seen in people who have obesity problems, this increase in the thickness of the adipose layer would require the use of higher amplitudes of electrical stimulation to induce a muscle contraction, which may become uncomfortable or even unbearable for some individuals if they maintain sensation in the region. If a problem like this were to arise in practice, surface electrodes may not be the best way to apply IES, and alternatives like the use of implantable electrodes may need to be explored.

#### *4.5.4 Comparison of IES to other interventions for preventing pressure ulcers*

In a previous study, we demonstrated that the active IES-induced muscle contractions in loaded muscles may in fact be more effective in reducing the extent of DTI than traditional prevention techniques involving complete unloading of the muscle (e.g., wheelchair push-ups) [43]. Loading encountered by a muscle while sitting or lying down deforms the muscles. Because atrophied muscles have reduced stiffness [61], the same level of loading induces larger deformations [8, 39-40, 62]. This increases the susceptibility of atrophied muscles to breakdown due to sustained loading and increases the chances of DTI

formation. Even low levels of strain have been shown to increase the permeability of cell membranes, causing cell swelling which could potentially lead to cell death if not reversed [63]. During the ON-phase of IES, active contractions are produced in the loaded muscle. This in turn periodically increases muscle stiffness which reduce the extent of deformation. In addition to increasing muscle stiffness, the active contractions also periodically change the shape of the muscle; thus redistributing the levels of stress deep into the muscle and reducing their magnitudes in high risk regions close to the bone [39]. Therefore, each IES-contraction is likely capable of “resetting” the mechanical properties in the muscle more effectively than passive unloading alone. The intermittent nature of the IES ON-OFF cycle, repeats these processes throughout the hours of IES use; thus potentially allowing the muscle to remain loaded for long periods of time without triggering the onset of DTI.

#### **4.6 CONCLUSION**

This study demonstrated that IES may be an effective prevention technique of DTI when applied daily to muscles that are subjected to prolonged external loads due to immobility. This paradigm-shifting approach may fill a critical gap in the interventions currently deployed for preventing pressure ulcers. Future studies will focus on identifying the best IES parameters (e.g., durations of ON and OFF periods, stimulation amplitude and frequency during the ON period) for preventing DTI in preparation for clinical trials in human volunteers.

#### *4.6.1 ACKNOWLEDGEMENTS*

The authors thank the staff of the Surgical Medical Research Institute, as well as the staff of the Health Sciences Laboratory and Animal Services for their support during the surgical and post-surgical recovery procedures. The work was funded by the Alberta Heritage Foundation for Medical Research (AHFMR) and the Canadian Institutes of Health Research (CIHR). VKM is an AHFMR Senior Scholar.

#### *4.6.2 CONFLICTS OF INTEREST*

The authors report no conflicts of interest.

## 4.7 REFERENCES

- [1] D. W. Byrne and C. A. Salzberg, "Major risk factors for pressure ulcers in the spinal cord disabled: a literature review," *Spinal Cord*, vol. 34, pp. 255-263, 1996.
- [2] C. A. Salzberg, D. W. Byrne, C. G. Cayten, P. van Niewerburgh, J. G. Murphy, and M. Viehbeck, "A new pressure ulcer risk assessment scale for individuals with spinal cord injury," *American Journal of Physical Medicine & Rehabilitation*, vol. 75, pp. 96-104, 1996.
- [3] M. J. Fuhrer, S. L. Garber, D. H. Rintala, R. Clearman, and K. A. Hart, "Pressure ulcers in community-resident persons with spinal cord injury: prevalence and risk factors," *Archives of Physical Medicine & Rehabilitation*, vol. 74, pp. 1172-7, 1993.
- [4] R. Salcido, S. B. Fisher, J. C. Donofrio, M. Bieschke, C. Knapp, R. Liang, E. K. LeGrand, and J. M. Carney, "An animal model and computer-controlled surface pressure delivery system for the production of pressure ulcers," *Journal of Rehabilitation Research & Development*, vol. 32, pp. 149-61, 1995.
- [5] R. H. Guthrie and D. Goulian, "Decubitus ulcers: Prevention and Treatment," *Geriatrics*, vol. 28, pp. 67-71, 1973.
- [6] R. K. Daniel, D. L. Priest, and D. C. Wheatley, "Etiologic factors in pressure sores: an experimental model," *Archives of Physical Medicine & Rehabilitation*, vol. 62, pp. 492-8, 1981.
- [7] G. T. Nola and L. M. Vistnes, "Differential response of skin and muscle in the experimental production of pressure sores.," *Plastic and Reconstructive Surgery*, vol. 66, pp. 728 - 733, 1980.
- [8] E. Linder-Ganz, N. Shabshin, Y. Itzhak, Z. Yizhar, I. Siev-Ner, and A. Gefen, "Strains and stresses in sub-dermal tissues of the buttocks are greater in paraplegics than in healthy during sitting," *Journal of Biomechanics*, vol. 41, pp. 567 - 580, 2008.
- [9] S. Loerakker, E. Manders, G. J. Strijkers, K. Nicolay, F. P. Baaijens, D. L. Bader, and C. W. Oomens, "The effects of deformation, ischemia, and reperfusion on the development of muscle damage during prolonged loading.," *Journal of Applied Physiology*, vol. Ahead of print, 2011.
- [10] C. W. Oomens, S. Loerakker, and D. L. Bader, "The importance of internal strain as opposed to interface pressure in the prevention of pressure related deep tissue injury.," *Journal of Tissue Viability*, 2009.
- [11] C. V. Bouten, R. G. Breuls, E. A. Peeters, C. W. Oomens, and F. P. Baaijens, "In vitro models to study compressive strain-induced muscle cell damage," *Biorheology*, vol. 40, pp. 383-8, 2003.
- [12] S. Loerakker, A. Stekelenburg, G. J. Strijkers, J. J. Rijkema, F. P. Baaijens, D. L. Bader, K. Nicolay, and C. W. Oomens, "Temporal effects of mechanical loading on deformation-induced damage in skeletal muscle tissue.," *Annals of Biomedical Engineering*, vol. 38, pp. 2577 - 2587, 2010.
- [13] E. Linder-Ganz, N. Shabshin, Y. Itzhak, and A. Gefen, "Assessment of mechanical conditions in sub-dermal tissues during sitting: A combined experimental-MRI and finite element approach.," *Journal of Biomechanics*, vol. 40, pp. 1443 - 1454, 2007.
- [14] M. Kosiak, "Etiology and pathology of ischemic ulcers," *Archives of Physical Medicine & Rehabilitation*, vol. 40, pp. 62-9, 1959.
- [15] M. Kosiak, "Etiology of decubitus ulcers," *Archives of Physical Medicine & Rehabilitation*, vol. 42, pp. 19-29, 1961.
- [16] M. Kosiak, W. G. Kubicek, M. Olson, J. N. Danz, and F. J. Kottke, "Evaluation of pressure as factor in production of ischial ulcers," *Archives of Physical Medicine & Rehabilitation*, vol. 39, pp. 623-629, 1958.
- [17] A. Stekelenburg, G. J. Strijkers, H. Parusel, D. L. Bader, K. Nicolay, and C. W. Oomens, "Role of ischemia and deformation in the onset of compression-induced deep tissue injury: MRI-based studies in a rat model.," *Journal of Applied Physiology*, vol. 102, pp. 2002-2011, 2007.

- [18] P. A. Grace, "Ischaemia-reperfusion injury," *British Journal of Surgery*, vol. 81, pp. 637-47, 1994.
- [19] S. Tsuji, S. Ichioka, N. Sekiya, and T. Nakatsuka, "Analysis of ischemia-reperfusion injury in a microcirculatory model of pressure ulcers," *Wound Repair and Regeneration*, vol. 13, pp. 209-215, 2005.
- [20] I. Bales and A. Padwojski, "Reaching for the moon: achieving zero pressure ulcer prevalence.," *Journal of Wound Care*, vol. 18, pp. 137 - 144, 2009.
- [21] C. A. Russo, C. Steiner, and W. Spector, "Statistical Brief #64: Hospitalizations Related to Pressure Ulcers among Adults 18 Years and Older, 2006," Agency for Healthcare Research and Quality: Healthcare Cost and Utilization Project (HCUP), 2008.
- [22] S. E. Rich, D. Margolis, M. Shardell, W. G. Hawkes, R. R. Miller, S. Amr, and M. Baumgarten, "Frequent manual repositioning and incidence of pressure ulcers among bed-bound elderly hip fracture patients.," *Wound Repair and Regeneration*, vol. 19, pp. 10 - 18, 2011.
- [23] K. Vanderwee, M. H. Grypdonck, D. De Bacquer, and T. Defloor, "Effectiveness of turning with unequal time intervals on the incidence of pressure ulcer lesions.," *Journal of Advanced Nursing*, vol. 57, pp. 59-68, 2007.
- [24] L. Rafter, "Evaluation of patient outcomes: pressure ulcer prevention mattresses.," *British Journal of Nursing*, vol. 20, pp. S32, S34 - S38, 2011.
- [25] T. A. Krouskop, P. S. Noble, J. Brown, and R. Marburger, "Factors affecting the pressure-distributing properties of foam mattress overlays," *Journal of Rehabilitation Research & Development*, vol. 23, pp. 33-9, 1986.
- [26] B. Pham, L. Teaguem, J. Mahoney, L. Goodman, M. Paulden, J. Poss, J. Li, L. Ieraci, S. Carcone, and M. Krahn, "Early Prevention of Pressure Ulcers Among Elderly Patients Admitted Through Emergency Departments: A Cost-effectiveness Analysis.," *Annals of Emergency Medicine*, vol. 58, pp. 468 - 478, 2011.
- [27] R. H. Houwing, M. Rozendaal, W. Wouters-Wesseling, J. W. Beulens, E. Buskens, and J. R. Haalboom, "A randomised, double-blind assessment of the effect of nutritional supplementation on the prevention of pressure ulcers in hip-fracture patients.," *Clinical Nutrition*, vol. 22, pp. 401 - 405, 2003.
- [28] E. S. Marks and C. L. Cogbill, "Surgical therapy of decubitus ulcers in the paraplegic patient.," *Annals of Surgery*, vol. 132, pp. 994 - 1002, 1950.
- [29] S. P. Levine, R. L. Kett, P. S. Cederna, L. D. Bowers, and S. V. Brooks, "Electrical muscle stimulation for pressure variation at the seating interface," *Journal of Rehabilitation Research & Development*, vol. 26, pp. 1-8, 1989.
- [30] S. P. Levine, R. L. Kett, P. S. Cederna, and S. V. Brooks, "Electric muscle stimulation for pressure sore prevention: tissue shape variation," *Archives of Physical Medicine & Rehabilitation*, vol. 71, pp. 210-5, 1990.
- [31] S. P. Levine, R. L. Kett, M. D. Gross, B. A. Wilson, P. S. Cederna, and J. E. Juni, "Blood flow in the gluteus maximus of seated individuals during electrical muscle stimulation," *Archives of Physical Medicine & Rehabilitation*, vol. 71, pp. 682-6, 1990.
- [32] K. M. Bogie, X. Wang, and R. J. Triolo, "Long-term prevention of pressure ulcers in high-risk patients: a single case study of the use of gluteal neuromuscular electric stimulation," *Archives of Physical Medicine & Rehabilitation*, vol. 87, pp. 585-591, 2006.
- [33] K. Bogie, R. Triolo, and J. Chae, "Dynamic pressure relief for the wheelchair user with long-term therapeutic neuromuscular electrical stimulation.," presented at RESNA Annual Conf., Minneapolis, MN, 2002.
- [34] K. Bogie, R. Triolo, and J. Chae, "Dynamic pressure relief using therapeutic neuromuscular electrical stimulation," presented at American Spinal Injuries Association/ International Medical Society of Paraplegia, 1st Joint Meeting, Vancouver, BC, 2002.
- [35] L. Q. Liu, G. P. Nicholson, S. L. Knight, R. Chelvarajah, A. Gall, F. R. Middleton, M. W. Ferguson-Pell, and M. D. Craggs, "Interface pressure and cutaneous hemoglobin and oxygenation changes under ischial tuberosities during sacral nerve root stimulation in spinal cord injury.," *Journal of Rehabilitation Research & Development*, vol. 43, pp. 553 - 564, 2006.

- [36] L. Q. Liu, G. P. Nicholson, S. L. Knight, R. Chelvarajah, A. Gall, F. R. Middleton, M. W. Ferguson-Pell, and M. D. Craggs, "Pressure changes under the ischial tuberosities of seated individuals during sacral nerve root stimulation.," *Journal of Rehabilitation Research & Development*, vol. 43, pp. 209 - 218, 2006.
- [37] A. van Londen, M. Herwegh, C. H. van der Zee, A. Daffertshofer, C. A. Smit, A. Niezen, and T. W. Janssen, "The effect of surface electric stimulation of the gluteal muscles on the interface pressure in seated people with spinal cord injury.," *Archives of Physical Medicine and Rehabilitation*, vol. 89, pp. 1724 - 1732, 2008.
- [38] S. Gyawali, L. R. Solis, S. L. Chong, C. A. Curtis, P. Seres, I. Kornelsen, R. B. Thompson, and V. K. Mushahwar, "Intermittent electrical stimulation redistributes pressure and promotes tissue oxygenation in loaded muscles of individuals with spinal cord injury," *Journal of Applied Physiology*, vol. 110, pp. 246 - 255, 2011.
- [39] L. R. Solis, A. Liggins, R. E. Uwiera, N. Poppe, E. Pehowich, P. Seres, R. B. Thompson, and V. K. Mushahwar, "Distribution of Internal Pressure around Bony Prominences: Implications to Deep Tissue Injury and Effectiveness of Intermittent Electrical Stimulation," *Annals of Biomedical Engineering*, vol. 40, pp. 1740 - 1759, 2012.
- [40] L. R. Solis, A. Liggins, P. Seres, R. E. Uwiera, N. Poppe, E. Pehowich, R. B. Thompson, and V. K. Mushahwar, "Distribution of Internal Strains around Bony Prominences in pigs," *Annals of Biomedical Engineering*, vol. 40, pp. 1721 - 1739, 2012.
- [41] L. R. Solis, S. Gyawali, P. Seres, C. A. Curtis, S. L. Chong, R. B. Thompson, and V. K. Mushahwar, "Effects of intermittent electrical stimulation on superficial pressure, tissue oxygenation, and discomfort levels for the prevention of deep tissue injury.," *Annals of Biomedical Engineering*, vol. 39, pp. 649 - 663, 2011.
- [42] L. R. Solis, D. P. Hallihan, R. R. Uwiera, R. B. Thompson, E. D. Pehowich, and V. K. Mushahwar, "Prevention of pressure-induced deep tissue injury using intermittent electrical stimulation.," *Journal of Applied Physiology*, vol. 102, pp. 1992-2001, 2007.
- [43] C. A. Curtis, S. L. Chong, I. Kornelsen, R. R. Uwiera, P. Seres, and V. K. Mushahwar, "The effects of intermittent electrical stimulation on the prevention of deep tissue injury: varying loads and stimulation paradigms.," *Artificial Organs*, vol. 35, pp. 226 - 236, 2011.
- [44] A. Stekelenburg, C. W. Oomens, G. J. Strijkers, K. Nicolay, and D. L. Bader, "Compression-induced deep tissue injury examined with magnetic resonance imaging and histology.," *Journal of Applied Physiology*, vol. 100, pp. 1946-1954, 2006.
- [45] G. Saab, R. T. Thompson, and G. D. Marsh, "Effects of exercise on muscle transverse relaxation determined by MR imaging and in vivo relaxometry.," *Journal of Applied Physiology*, vol. 88, pp. 226 - 233, 2000.
- [46] G. Saab, R. T. Thompson, and G. D. Marsh, "Multicomponent T2 relaxation of in vivo skeletal muscle.," *Magnetic Resonance in Medicine*, vol. 42, pp. 150 - 157, 1999.
- [47] A. Stekelenburg, C. W. Oomens, G. J. Strijkers, L. de Graaf, D. L. Bader, and K. Nicolay, "A new MR-compatible loading device to study in vivo muscle damage development in rats due to compressive loading," *Medical Engineering & Physics*, vol. 28, pp. 331-8, 2006.
- [48] S. Hagsisawa, M. W. Ferguson-Pell, V. R. Palmieri, and G. V. Cochran, "Pressure sores: a biochemical test for early detection of tissue damage," *Archives of Physical Medicine & Rehabilitation*, vol. 69, pp. 668-71, 1988.
- [49] Y. Saito, M. Hasegawa, M. Fujimoto, T. Matsushita, M. Horikawa, M. Takenaka, F. Ogawa, J. Sugama, D. A. Steeber, S. Sato, and K. Takehara, "The loss of MCP-1 attenuates cutaneous ischemia-reperfusion injury in a mouse model of pressure ulcer.," *The Journal of Investigative Dermatology*, vol. 128, pp. 1838 - 1851, 2008.
- [50] A. Polliack, R. Taylor, and D. Bader, "Sweat analysis following pressure ischaemia in a group of debilitated subjects.," *Journal of Rehabilitation Research & Development*, vol. 34, pp. 303-308, 1997.
- [51] A. Polliack, R. Taylor, and D. Bader, "Analysis of sweat during soft tissue breakdown following pressure ischaemia.," *Journal of Rehabilitation Research & Development*, vol. 30, pp. 250-259, 1993.

- [52] M. Ferguson-Pell and S. Hagsawa, "Biochemical changes in sweat following prolonged ischemia," *Journal of Rehabilitation Research & Development*, vol. 25, pp. 57-62, 1988.
- [53] J. F. Deprez, E. Brusseau, J. Fromageau, G. Cloutier, and O. Basset, "On the potential of ultrasound elastography for pressure ulcer early detection.," *Medical Physics*, vol. 38, pp. 1943 - 1950, 2011.
- [54] S. Moghimi, M. H. Miran Baygi, G. Torkaman, and A. Mahloojifar, "Quantitative assessment of pressure sore generation and healing through numerical analysis of high-frequency ultrasound images.," *Journal of Rehabilitation Research and Development*, vol. 47, pp. 99 - 108, 2010.
- [55] G. Saab, R. T. Thompson, G. D. Marsh, P. A. Picot, and G. R. Moran, "Two-dimensional time correlation relaxometry of skeletal muscle in vivo at 3 Tesla," *Magnetic Resonance in Medicine*, vol. 46, pp. 1093-8, 2001.
- [56] E. Le Rumeur, J. De Certaines, P. Toulouse, and P. Rochcongar, "Water phases in rat striated muscles as determined by T2 proton NMR relaxation times," *Magnetic Resonance Imaging*, vol. 5, pp. 267-72, 1987.
- [57] Z. Ababneh, H. Beloeil, C. B. Berde, G. Gambarota, S. E. Maier, and R. V. Mulkern, "Biexponential parameterization of diffusion and T2 relaxation decay curves in a rat muscle edema model: decay curve components and water compartments.," *Magnetic Resonance in Medicine*, vol. 54, pp. 524 - 531, 2005.
- [58] R. Harrison, M. J. Bronskill, and R. M. Henkelman, "Magnetization transfer and T2 relaxation components in tissue," *Magnetic Resonance in Medicine*, vol. 33, pp. 490-6, 1995.
- [59] M. D. Noseworthy, J. K. Kim, J. A. Stainsby, G. J. Stanisz, and G. A. Wright, "Tracking oxygen effects on MR signal in blood and skeletal muscle during hyperoxia exposure," *Journal of Magnetic Resonance Imaging*, vol. 9, pp. 814-20, 1999.
- [60] R. B. Thompson, R. J. Aviles, A. Z. Faranesh, V. K. Raman, V. Wright, R. S. Balaban, E. R. McVeigh, and R. J. Lederman, "Measurement of skeletal muscle perfusion during postischemic reactive hyperemia using contrast-enhanced MRI with a step-input function.," *Magnetic Resonance in Medicine*, vol. 54, pp. 289 - 298, 2005.
- [61] S. Loerakker, L. R. Solis, D. L. Bader, F. P. Baaijens, V. K. Mushahwar, and C. W. Oomens, "How does muscle stiffness affect the internal deformations within the soft tissue layers of the buttocks under constant loading?," *Computer Methods in Biomechanics and Biomedical Engineering*, vol. Epub ahead of print, 2012.
- [62] E. Linder-Ganz, G. Yarnitzky, Z. Yizhar, I. Siev-Ner, and A. Gefen, "Real-time finite element monitoring of sub-dermal tissue stresses in individuals with spinal cord injury: toward prevention of pressure ulcers.," *Annals of Biomedical Engineering*, vol. 37, pp. 387 - 400, 2009.
- [63] N. Slomka and A. Gefen, "Relationship Between Strain Levels and Permeability of the Plasma Membrane in Statically Stretched Myoblasts.," *Annals of Biomedical Engineering*, vol. Epub ahead of print, 2011.

## CHAPTER 5

### CONCLUSIONS AND FUTURE DIRECTIONS

#### *Summary*

In spite of advances in the understanding of pressure ulcer etiology, prevention, and treatment over the past 30 years, they still remain a prevalent medical concern for individuals with reduced mobility and/or sensation. The findings of this thesis have helped to improve the understanding of DTI etiology, by providing direct measurements of changes in internal levels of stress and strain in loaded muscles. This information can prove valuable in the design of new detection, assessment, and prevention interventions. Some of the findings have already been utilized in finite element models to better understand changes in muscle stiffness under loaded conditions. In addition, this work has also provided evidence that the daily use of IES can significantly reduce the development of DTI in pigs. Furthermore, this work provided an insight into the mechanisms through which IES works to reduce DTI formation. These findings set the stage for future human testing in individuals at risk with the goal of developing a commercially available system.

#### *Intermittent Electrical Stimulation parameters*

At its core, IES consists of relatively short bouts (~10sec) of electrical stimulation applied intermittently between longer periods of inactivity (~10min). This thesis compared four different IES paradigms to assess which one provided the best surface pressure redistribution and reduction in sitting discomfort

perception, and two different IES paradigms to assess changes in deep tissue oxygenation. In addition, these IES paradigms were compared against the traditional pressure ulcer prevention technique of voluntary repositioning, as well as against voluntary muscle contractions. The results demonstrated that IES applied bilaterally to both gluteus maximus muscles in bouts of 10 seconds provided the best benefits. This paradigm proved to be more effective at redistributing superficial pressure, increasing tissue oxygenation, and reducing sitting discomfort, than the alternative IES paradigms that were tested. It also proved to be similarly effective to or better than the current standard interventions with regards to tissue oxygenation and sitting discomfort.

Although these findings guide the possible ways in which to apply IES, the number of variables tested was relatively small. It is yet to be determined if maximal contractions as used in this thesis are truly required or if contractions of less strength could be adequate. In addition, the time windows for both the ON and OFF periods of IES could also be expanded or reduced in varying magnitudes to identify an optimal ON-OFF duty cycle. Moving forward, more exhaustive testing will be required to identify the variables that could be modified in the application of IES and potentially improve its effectiveness.

#### *Internal stress and strain distributions*

It has been shown in the past that in the etiology of DTI both internal stress and strain levels play a crucial role in the onset and extent of DTI

development. The work presented in this thesis is the first to show empirical measurements of internal stress around the ischial tuberosities of pigs under external loading. These measurements were correlated not only to levels of superficial pressure, but also to deep muscle strain levels. This provided a unique perspective into the different mechanical forces taking effect within the muscle during external muscle loading. The measurements of internal stress indicated an approximate two-fold difference between levels of internal stress and the peak superficial pressure. Although the difference was substantial and in agreement with previous data estimated from computer models, it was less than what had been previously estimated using only finite element computer modeling, suggesting an overestimation of peak internal stress by computer simulations. The location of peak stress matched the expected location of DTI onset, corresponding to the region immediately surrounding the bony prominence. In contrast, peak strain levels were not found in this location, but rather up to 2 cm ventrally from the ischial tuberosity, suggesting that perhaps internal stress levels play a bigger role than strain levels in the onset of deep tissue injury. In addition, compressive strain levels were found to be already at their maximal level with external loading levels as low as 25% BW, with nearly no increases in compressive strain beyond that level external loading level. In comparison, both tensile and shear strain significantly increased as the external level increased.

These findings could provide a better understanding of how DTI develops in immobilized individuals and if incorporated into already available or future

finite element models, could improve their accuracy to assess those individuals at risk of developing DTI. The pig MRI data and strain results of this thesis have already helped to further scientific knowledge, having been shared with a research team in Eindhoven in the Netherlands to evaluate their most recent finite element model of a loaded muscle to assess changes in muscle stiffness due to loading.

### *Effectiveness of Intermittent Electrical Stimulation*

The main goal of my PhD work was to develop the intervention of IES to prevent the formation of DTI caused by daily loading. The final step to accomplish this goal was to test the efficacy of IES in paralyzed pig muscles subjected to daily loading. The results from this study indicate that the daily use of IES can effectively reduce the extent of DTI caused by up to four hours of continuous external loading applied daily over a one-month period. This finding is crucial because it demonstrates the efficacy of a prophylactic intervention for DTI against a control model for the first time. In addition, the results elucidate that the use of IES does not cause any significant fatigue in paralyzed muscles for the durations tested in this thesis. This last point is especially important because previous attempts at using electrical stimulation applied continuous or near continuous trains of stimulation but found that muscle fatigue appeared rapidly in the muscle, especially if the muscle had not undergone a training regime prior to the use of electrical stimulation.

The overall findings of this PhD work have led to a patent application and commercial interest in IES technology from a private company. Currently, working prototypes of garments designed to deliver IES to immobilized individuals have already been tested at three clinical settings in Edmonton and Calgary, Canada, with the goal of testing its clinical feasibility; results so far have been very promising. These findings, combined with the efficacy demonstrated in the animal work presented in this thesis, have set the stage for the next phase of testing for IES in preventing the development of DTI; clinical efficacy. Although there are still several steps that need to be taken, the results so far suggest that a working product that can benefit those at risk of developing DTI is not far into the future.